

Archiv EURO MEDICA

2^a 2022



WISSENSCHAFTLICHE
GESELLSCHAFT

Editor-in-Chief

Dr. Georg Tyminski
EWG e.V., Hannover, Germany

Prof. Dr. Jörg Schulz
Geriatric Clinics Berlin-Buch, Germany

Publishing Director

Prof. Aleksei Zhidovinov
Astrakhan State Medical University, Astrakhan, Russia

Executive Editor

Prof. Dmitry Domenyuk
Stavropol State Medical University, Stavropol, Russia

Managing Editor

Prof. Maya Dgebuadze
Tbilisi State Medical University, Tbilisi, Georgia

Ethics Manager

Prof. Gayane Khachatryan
Erivan State Medical University, Erivan, Armenia

Associate Editors

Prof. Sergey Kolbasnikov
Tver State Medical Academy, Tver, Russia

Dr. rer. Nat. Stephan Heymann
Noventalis – Institut für systemische BioKorrektur,
Berlin-Buch, Germany

ARCHIV EUROMEDICA

ISSN 2193-3863

Disclaimer

Europäische Wissenschaftliche Gesellschaft e.V. Hannover
Sutelstr. 50A, 30659 Hannover, Deutschland

Tel. 49(0)511 3908088
Fax 49(0)511 3906454

Vorstand Dr. G. Tyminski, Vorsitzender
Eingetragen ins Vereinsregister
am Amtsgericht Hannover: VR 7957

Design & layout by
Tří barvy, s.r.o.
Mariánské Lázně, Česká Republika

Editorial Advisory Board

Prof. Vadim Astashov
Peoples' Friendship University of Russia, Moscow, Russia

Prof. Tatiana Belousova
Privolzhsky Research Medical University, Nizhny Novgorod, Russia

Prof. Eduard Batkaev
Peoples' Friendship University of Russia, Moscow, Russia

Prof. Sergey Dmitrienko
Pyatigorsk Medical and Pharmaceutical Institute, Pyatigorsk, Russia

Dr. Elena Drabkin
Ophthalmology Department, Shaare Zedek Medical Center, Jerusalem, Israel

Prof. Carlos Kusano Bucalen Ferrari
Federal University of Mato Grosso, Barra do Garças, Brazil

Prof. Iryna Khozhlyo
Dnipropetrovsk Regional Institute for Public Administration Dnipro, Ukraine

Prof. Liana Gogiashvili
Ivane Javakhishvili Tbilisi State University, Tbilisi, Georgia

Prof. Habibulo Ibodov
Institute of Postgraduate Medical Studies, Dushanbe, Tajikistan

Prof. Vladimir Izranov
Immanuel Kant Baltic Federal University, Kaliningrad, Russia

Prof. Igor V. Kastyro
Moscow S.U. Witte University, Moscow, Russia

Prof. Gulnara Kapanova
Al Farabi Kazakh National University, Almaty, Kazakhstan

Prof. Semen Kireev
Tula State Medical University, Tula, Russia

Prof. Vladimir Krestyashin
Pirogov Russian National Research Medical University, Moscow, Russia

Dr. Abdulkasym Kuzibaev
National Center for Endocrinology, Dushanbe, Tajikistan

Prof. Naimakhon Kuzibaeva
Khatlon National State Medical University, Dushanbe, Tajikistan

Prof. Sergey Levakov
I.M. Sechenov First Moscow State Medical University, Moscow, Russia

Prof. Oral Ospanov
Medical University "Astana", Astana, Kazakhstan

Prof. Ants Peetsalu
Tartu University Clinics, Tartu, Estonia

Prof. Maura Pelle
School of Science and Technology, University of Camerino, Italy

Prof. Urij Peresta
Uzhhorod National University, Uzhhorod, Ukraine

Dr. Olga Pitirimova
MD, Bakulev Scientific Center of Cardiovascular Surgery, Moscow, Russia

Dr. Joerg Poetzsch
Satina Medical UG, Berlin, Germany

Prof. Vladimir Protsenko
Institute of Traumatology and Orthopedics NAMS of Ukraine, Kiev, Ukraine

Prof. Galina Reva
Biomedicine School FEFU, Vladivostok, Russia

Prof. Stefan Antonio Sandu
Stefan cel Mare University of Suceava, Iasi, Romania

Prof. Carlo Santini
School of Science and Technology, University of Camerino, Italy

Prof. Vaqif Bilas oğlu Shadlinskiy
Azerbaijan Medical University, Baku, Azerbaijan

Prof. Natalia Shnayder
Krasnoyarsk State Medical University, Krasnoyarsk, Russia

Prof. Rudolf Yuy Tsun-Shu
Kazakh National Medical University, Almaty, Kazakhstan

Dr. Will Nelson Vance
Beelitz-Heilstätten Hospital for Neurological Rehabilitation, Beelitz, Germany

Dr. Mayank Vats
Rashid Hospital, Dubai Health Authority, Dubai, UAE

CONTENTS

MORPHOLOGY, PATHOLOGY, PHYSIOLOGY

*Anzhela Brago, Svetlana Razumova,
Vadim Astashov, Yuliya Kozlova
Natalia Zolotova*

PULP TISSUE MORPHOLOGY IN EXPERIMENTAL PULPITIS BY USING DIFFERENT MATERIALS FOR DIRECT PULP CAPPING.....4

*Andrew Martusevich, Lida Kovaleva,
Konstantin Karuzin, Maria Feofilova,
Ivan Bocharin, Alexandra Surovegina,
Vladimir Nazarov, Anastasia Kashirina*

DIGITAL TECHNOLOGY FOR PROCESSING DRIED DROPS OF BIOFLUIDS9

*Andrew Martusevich, Kristina Kishoyan,
Alexandra Surovegina, Elena Golygina,
Ivan Bocharin I, Vladimir Nazarov*

CHARACTERISTICS OF SKIN DIELECTRIC PROPERTIES IN PREGNANCY (EXPERIMENTAL STUDY) 12

*Anna Sindireva, Oleg Zayko
Vadim Astashov, Inna Borodina,
Elizaveta Guseva, Polina Zaytseva*

ANALYSIS OF THE COMPLETE BLOOD COUNT IN MALE WISTAR RATS EXPOSED TO DIFFERENT DOSES OF ORALLY ADMINISTERED SODIUM SELENITE 15

*Aleksandr Naumov, Dmitry Nikitjuk,
Ekaterina Zadneprovskaya, Aleksei Zhidovinov,
Tatyana Shishkina, Lyubov Naumova*

DISTRIBUTION OF S100-POSITIVE CELLS IN THE STRUCTURES OF THE SPLEEN IN THE SIMULATION OF CHRONIC NORMOBARIC HYPOXIC HYPOXIA IN THE EXPERIMENT 17

*Polina Krivonogova, Andrew Martusevich,
Oxana Bitkina, Lida Kovaleva,
Alexandra Surovegina*

CRYSTALLOSCOPIC MONITORING OF THE EFFECTIVENESS OF SYSTEMIC RETINOLIDS IN PATIENTS WITH SEVERE ACNE.....21

*Ivan Reva, Tatsuo Yamamoto,
Kirill Stegni, Ellada Slabenko,
Viktoria Emiglasova, Igor Sementsov,
Olga Lebed'ko, Marina Fleishman,
Aleksey Kudelya, Mariya Tuchina,
Viktor Usov, Yuriy Krasnikov,
Ekaterina Mozhibevskaya, Tatiana Lemesko,
Aleksey Novikov, Valeriy Tolmachev,
Galina Reva*

RED BONE MARROW DAMAGE IN COVID-19 PATHOGENESIS CAUSED BY SARS-COV-224

Vadim Brin, Vladlen Zemlianov

THE EFFECT OF MELATONIN ON ELECTROLYTE AND WATER-RETENTION RENAL DYSFUNCTION IN CHRONIC ALCOHOL INTOXICATION ASSOCIATED WITH AUTOIMMUNE NEPHRITIS: AN EXPERIMENTAL RAT MODEL29

Gulnara Kerimzade

AGE-RELATED CHANGES IN THE SECOND KNEE AREA OF THE FACIAL CANAL35

MICROBIOLOGY

*Oksana Boiko, Rushaniya Mukhamedzyanova,
Yurii Dotsenko, Anzhela Ramaeva,
Surkhai Akhadov, Nadezhda Zaporozhets,
Vera Dmitrieva, Ilfat Karimov*

SYNTHESIS OF A PROTEIN THAT IS IMMUNOCHEMICALLY SIMILAR TO HUMAN LACTOFERRIN BY KLEBSIELLA PNEUMONIAE38

CLINICAL MICROBIOLOGY

*Valeh Jafarov, Konstantin Horak,
Artem Morozov, Elizaveta Sobol,
Anastasia Domracheva, Anastasia Romanova,
Sofia Zinkovskaia*

ANALYSIS OF THE SENSITIVITY OF STAPHYLOCOCCUS AUREUS TO ANTIBIOTICS IN PATIENTS WITH PURULENT-SEPTIC DISEASES42

CONTENTS

PHARMACOLOGICAL STUDIES

Natalia Shabanova, Anastasia Gerashchenko
**COMPREHENSIVE ASSESSMENT OF NEUROLOGICAL DEFICIT
 AND ITS CORRECTION WITH PIR-10 COMPOUND
 IN EXPERIMENTAL FOCAL CEREBRAL ISCHEMIA OF RATS**45

Anastasia Gerashchenko, Natalia Shabanova
**STUDY OF THE ANTIOXIDANT ACTIVITY OF HESPERIDIN
 UNDER DEBILITATING PHYSICAL EXERTION IN RATS**.....48

INTENSIVE THERAPY: CLINICAL RESEARCH

*Mikhail Turovets, Alexander Popov,
 Andrej Ekstrem, Anastasia Streltsova*
**VALIDITY OF USING THE SpO_2/FiO_2 RATIO
 TO DETERMINE THE DYNAMICS AND CORRECTION
 METHODS OF OXEMIA IN ACUTE LUNG INJURY
 AND ACUTE RESPIRATORY DISTRESS SYNDROME**51

OPHTHALMOLOGY

Elena Drabkin, Aleza Andron
**SURGICAL APPROACH TO THE TREATMENT
 OF UPPER EYELID RETRACTION CAUSED
 BY PROMINENT FILTRATION BLEB**55

PSYCHIATRY

*Alexey Gorbunov, Svetlana Krasnianskaya,
 Dmitry Parshin, Egor Dolgov,
 Zhanna Shishkina, Aleksey Loktev*
**MONITORING OF PSYCHOTHERAPEUTIC PATIENTS
 BY ASSESSING MOTOR ACTIVITY DURING NIGHT SLEEP**60

*Alexey Gorbunov, Svetlana Krasnianskaya,
 Dmitry Parshin, Egor Dolgov, Zhanna Shishkina,
 Aleksey Loktev*
**NOSOLOGICAL SPECIFICITY OF MOTOR ACTIVITY
 IN THE PSYCHIATRIC CLINIC DURING NIGHT SLEEP**63

*Polina Pozdnyakova, Lesya Chichanovskaia,
 Tatiana Sorokovikova, Artem Morozov,
 Olga Peltikhina*

**CLINICAL CHARACTERISTICS IN CORNELIA DE LANGE
 SYNDROME OF THE FIRST TYPE ON THE EXAMPLE
 OF A CLINICAL CASE**66

CARDIOLOGY

*Saeed Abkhiz, Mojgan Hajahmadi-Pourrafsanjani,
 Alireza Rostamzade, Soma Elhami,
 Roghaiyeh Afsargharehbagh*
**EVALUATION OF THE PROGNOSTIC VALUE
 OF URINARY CREATININE LEVEL IN PATIENTS HOSPITALIZED
 WITH THE DIAGNOSIS OF CHRONIC SYSTOLIC
 HEART FAILURE IN SEYED AL-SHOHADA
 HOSPITAL IN URMIA, IRAN**70

SURGERY: EXPERIMENTAL RESEARCH

*Sergey Konovalev, Volodymyr Protsenko,
 Yevgen Solonitsyn, Taras Osadchuk,
 Volodymyr Konovalev, Taras Omelchenko*
**EFFECT OF BIOACTIVE GLASS-BASED COMPOSITE
 AND LOW ENERGY LASER ON BONE REGENERATION
 IN AN EXPERIMENTALLY INDUCED BONE DEFECT**75

*Itay Chen, Attal Pierr, Daria Kozlova,
 Jean-Yves Sichel*
**A UNIQUE CASE OF NODULAR FASCIITIS
 IN THE SUBMANDIBULAR GLAND MIMICKING
 PLEOMORPHIC ADENOMA**81

*Stanislav Romanenko, Yuriy Kostyamin,
 Gleb Malgin, Elena Kurochka,
 Vyacheslav Mykbaylichenko*
**ESTIMATION OF THE POSSIBILITY FOR LEFT
 VENTRICULAR REMODELLING AFTER RESTORATION
 OF THE SINUS RHYTHM IN PATIENTS WITH PERSISTENT
 FORM OF ATRIAL FIBRILLATION**85

*Lina Ancupova, Artem Morozov,
 Elshad Askerov, Alexey Sergeev,
 Maria Belyak, Lydia Pototskaya*
**RARE INTRAOPERATIVE FIND — ADENOCARCINOMA
 OF THE APPENDIX: CLINICAL CASE**88

CONTENTS

*Mikhail Topchiev, Dmitry Parshin,
Misrikhan Misrikhanov, Stanislav Pyatakov,
Lev Brusnev, Marat Chotchaev*

**INTESTINAL ALKALINE PHOSPHATASE — A BIOMARKER
OF THE DEGREE OF ACUTE ENTERAL INSUFFICIENCY
IN URGENT SURGERY91**

*Yulia Artemova, Anna Plotnikova, Danil Naumov,
Daria Asatryan, Zinfira Kaitova, Sergey Ryzhakin*

**SURGICAL OPTIONS FOR THE TREATMENT
OF PATIENTS WITH CENTRAL DIABETES INSIPIDUS.....94**

ONCOLOGY

*Oleg Krashenkov, Igor Ivanikov, Oleg Kononov,
Mikhail Ryabov, Ruslan Absalyamov, Asan Kashurnikov,
Nikolai Sturov, Alexander Tolkachev, Sergej Ryzhakin*

**THE STRUCTURE OF SYNCHRONOUS
MULTIPLE PRIMARY COLORECTAL CANCER.....97**

OBSTETRICS

*Nart Faruk Kunesbko, Vasilina Golomazova,
Olga Pitirimova*

**THE ASSOCIATION BETWEEN INTRAUTERINE
GROWTH RETARDATION AND MATERNAL
THROMBOPHILIA 100**

DENTISTRY

*Ekaterina Gorbatova, Marina Kozlova,
Larisa Dzikovitskaya, Tamara Glybina*

**IMPROVEMENT OF AUTOFLUORESCENCE IMAGING METHOD
IN DETECTION OF CANCEROUS LESIONS
OF THE ORAL MUCOSA..... 104**

*Dmitry Domenyuk, Taisiya Kochkonyan,
Maria Rozhkova, Sergey Fischev,
Alexandr Lepilin, Arkady Sevastyanov,
Irina Orlova, Margarita Puzdyreva,
Roman Subbotin, Sergei Dmitrienko,
Stanislav Domenyuk*

**IMPLEMENTATION OF NEUROMUSCULAR DENTISTRY PRINCIPLES
IN REHABILITATION OF PATIENTS
WITH COMPLETE ADENTIA 108**

*Alexandr Lepilin, Maria Shalina,
Nadezhda Erokina, Natalia Zakharova,
Sergey Fischev, Arkady Sevastyanov,
Yana Chernenko, Dmitry Domenyuk*

**EFFECTIVENESS OF DENTAL IMPLANTATION
WITH IMMEDIATE LOADING WHEN REPLACING
FRONTAL DENTITION DEFECTS..... 118**

*Zurab Khabadze, Sergey Ivanov,
Aleksandra Kotelnikova, Mikhail Protsky,
Ekaterina Shylyeva, Darya Nazarova*

**THE EFFECT OF SILICA GEL TO THE ADHESIVE PROTOCOL
STAGES IN THE TREATMENT OF CARIES
AND ITS COMPLICATIONS 124**

*Taisiya Kochkonyan, Dmitry Domenyuk,
Vladimir Shkarin, Sergei Dmitrienko,
Stanislav Domenyuk*

**VARIANT ANATOMY OF TRANSITIONAL OCCLUSION
DENTAL ARCH AT OPTIMAL OCCLUSAL RELATIONSHIPS 128**

*Vladimir Tlustenko, Elena Golovina,
Valentina Tlustenko, Sergey Komlev,
Vladimir Koshelev*

**MATHEMATICAL ANALYSIS BASED STUDY
OF DENTAL IMPLANT BIOMECHANICS
WITH OCCLUSAL LOAD ON BONE TISSUE 134**

<http://dx.doi.org/10.35630/2199-885X/2022/12/2.1>

PULP TISSUE MORPHOLOGY IN EXPERIMENTAL PULPITIS BY USING DIFFERENT MATERIALS FOR DIRECT PULP CAPPING

Received 18 January 2022;
Received in revised form 22 February 2022;
Accepted 25 February 2022

Anzhela Brago¹ , Svetlana Razumova¹ ,
Vadim Astashov³ , Yuliya Kozlova¹ ,
Natalia Zolotova² 

¹ Department of Propaedeutics of Dental Diseases, Medical Institute, Peoples' Friendship University of Russia, Moscow;

² Research Institute of Human Morphology, Moscow;

³ Department of Human Anatomy, Medical Institute, Peoples' Friendship University of Russia, Moscow, Russia

✉ anzhela_bogdan@mail.ru

ABSTRACT — The minimally invasive concept of treatment in clinical medicine and, in particular, in dentistry is associated with the introduction of pulp-saving treatment technologies into clinical practice. The aim of the study was to identify the reaction of the structure of pulp tissues in traumatic pulpitis in the experiment using various means and techniques of direct pulp capping. The experiment was carried out on male minipigs aged 4–5 months with deciduous dentition. Milk molars were selected for trepanation. After teeth preparation under anesthesia, the crowns of the first and second milk premolars were trepanned on the vestibular surface in the cervical region with pulp probing until bleeding. After bleeding has been stopped, the trepanation hole was closed with various preparations. For direct pulp capping we used mineral trioxide aggregate (MTA) — containing silicate material and glass ionomer cement (GIC). All samples of teeth with experimental pulpitis using MTA-containing materials (Rutdent), tricalcium silicate materials (Biodentin) and even GIC (Vitremmer) did not reveal inflammatory changes in the pulp tissues when they were directly covered with various materials. Of all the experimental samples of pulpitis, inflammation was detected with a sample of the Rutdent material with fragment damage to the pulp. With traumatic pulpitis and the use of various materials for direct pulp capping, active reparative regeneration of pulp tissue was revealed. All studied materials contribute to the reparation of the pulp after damage and reduction of pulp inflammation.

KEYWORDS — pulp morphology, pulpitis, treatment of initial and reversible pulpitis, MTA-containing materials, direct pulp capping

BACKGROUND

The minimally invasive concept of treatment in clinical medicine and, in particular, in dentistry is associated with the introduction of pulp-saving treatment

technologies into clinical practice. For the treatment of reversible forms of pulpitis, along with calcium hydroxide material, calcium salicylates, materials based on the mineral aggregate trioxide (MTA), tricalcium silicate cements are used. In a review of publications on the effectiveness of the use of various materials Paula A.B., Laranjo M. et al. (2018), using a meta-analysis method, found that MTA cements showed a significantly higher success rate in all parameters compared to calcium hydroxide cements. However, when compared with tricalcium silicate cements, there were no statistically significant differences. Adhesive systems showed significantly lower success rates in all respects compared to calcium hydroxide cements. The authors concluded that MTA and tricalcium silicate cements have a higher success rate, with a lower inflammatory response and more predictable formation of a hard dentinal barrier than calcium hydroxide cements [1].

A high success rate of pulp-saving treatment methods, comparable to the success of extirpation methods, will allow avoiding invasive intervention and resource-intensive endodontic procedures. However, different success rates of pulp-saving methods make it necessary to search for new methods of treating pulpitis.

Dhar V., Marghalani A.A., et al. (2017) published an evidence-based review of recommendations for the use of pulp treatments in primary teeth: indirect pulp capping, direct pulp capping, and pulpotomy. The group of authors was unable to recommend the benefit of any particular type of pulp therapy due to the lack of studies directly comparing these interventions. The authors recommended the use of MTA and formocresol for pulpotomy; these recommendations are based on moderate quality evidence over 24 months. The same recommendations apply to direct pulp capping. Researchers considered the use of tricalcium silicate cement, ferrous sulfate, sodium hypochlorite, and a laser as evidence of poor quality [6]. Thus, the issues of minimally invasive interventions on the dental pulp are relevant in modern endodontics.

The aim of the study

is to detect structural changes in the dental pulp enabling to identify responses of pulp tissues in traumatic pulpitis; and to test various materials and techniques for direct pulp capping.

MATERIALS AND METHODS

To determine the responses of pulp tissues when using various materials for direct pulp capping, an experiment was carried out on 10 male laboratory pigs (mini-pigs), aged 4–5 months (Kennel LLC “Krolinfo”, Russia), weighing not less than 20 kg, deciduous dentition (Decision of the Ethics Committee of MI Peoples’ Friendship University of Russia, Protocol No. 1, 20 September 2018). All experiments were carried out in accordance with the principles of humanity set out in the European Community directive (86/609 / EC).

For premedication, Atropine 0.02–0.04 mg/kg subcutaneously was used, Meditin 0.1 — 0.2 ml/5 kg. Then, chloral hydrate anesthesia was performed by intravenous administration. A 10% solution of chloral hydrate in isotonic solution with the addition of 5% glucose at the rate of 1 ml per kg was injected into the large ear vein of the auricle. Induction: Propofol 7 mg/kg, if necessary, maintenance dose 0.2–0.5 mg/kg/min. Maintenance of anesthesia: Isoflurane 5% (induction and deepening), with an oxygen flow of 0.1 l/kg/min, Isoflurane 1.5–2% (maintenance of anesthesia), with an oxygen flow of 0.1 l/kg/min. Antimedon 0.1 — 0.2 ml/5 kg was used for induction. The animals were divided into two groups: intact animals (5 individuals) and animals that underwent trepanation of their teeth with further closure of the trepanation hole with various medications (5 individuals). For trepanation milk molars were selected: 5.4, 6.4, 6.5, 7.5, 7.4, 8.5 in each animal. After cleaning the teeth with a toothbrush, the crowns of the first and second milk molars were trepanned on the vestibular surface in the cervical region. The direction of the bur is perpendicular to the vestibular surface of the tooth with an apical inclination of 6–9 degrees. Preparation under water cooling until a sinking sensation, spraying the surface with saline. Probing the pulp before bleeding, after stopping the bleeding in each tooth, the trepanation hole was closed with various preparations (6 teeth each): materials based on MTA – Rootdent (Technodent, Russia), materials based on tricalcium silicate — Biodentin (Biodentine, Septodont, France) and glass ionomer cement (GIC, Vitremer, 3M, USA).

After withdrawal from anesthesia, during the first day, the animals were injected with non-steroidal anti-inflammatory drugs (Meloxicam 250 mg/kg). The animals were withdrawn from the experiment on the 28th day by an overdose of ether anesthesia, the teeth were extracted with the adjacent alveolar ridge and placed in a 2% formalin solution. The teeth were fixed during the day in 10% buffered formalin. The teeth were fixed within 24 hours in 10% buffered formalin. Then decalcification was carried out using an electrolytic decalcifier Medax Mod. 33.000 (Germany)

in Electrolytic decalcifying solution (05–03004E, Bio Optica, Italy) within 3 weeks; then washed in 70% ethyl alcohol for 24 hours. After histological processing in the device Tissue-Tek VIP5Jr (Sakura, USA), teeth were enclosed in a histomix in the device Tissue-Tek TEC (Sakura, USA), sections with a thickness of 5–8 microns on a microtome Microm HM340E (Thermo Scientific, USA) were made. The obtained preparations were stained with hematoxylin and eosin. Using the method of light microscopy (Microscope Axioplan 2 imaging (Carl Zeiss, Germany)) we studied exudative-inflammatory changes in the dental pulp, such as the severity of infiltration, cellular composition, edema, changes in the histology of the pulp with the use of photofixation.

RESULTS

The results of histological examination showed absence of inflammatory changes in the samples of teeth treated with MTA. Morphological examination of dentin and pulp of intact teeth showed a clear striation of dentin.

On the micrograph of the histological section of the tooth 8.5 after trepanation using Rootdent material to close the hole, the pulp has a normal structure, no inflammatory changes were detected. A strip of predentin or uncalcified dentin is determined between dentin and odontoblasts. Rows of odontoblasts with long narrow nuclei are oriented perpendicular to the inner surface of the dentin layer, forming a peripheral layer of pulp. The central layer of the pulp consists of loosely arranged mesenchymal cells, fibers and blood vessels (Fig. 1). In the preparation of the tooth 5.4 (tangentially cut tooth crown), when using Rutdent after trepanation we noticed inflammatory changes around the dentin fragment associated with the presence of foreign bodies in the pulp. (Fig. 2). In the pulp of the tooth, focal inflammatory infiltration around a foreign body (a fragment of hard tooth tissues) was revealed - pulpitis (stasis, plethora, edema, plasmolymphocytic infiltration, disruption of the pulp structure) caused by the intrusion of a foreign body into the pulp.

Outside this zone, the pulp has a normal structure: it is represented by loose fibrous connective tissue with many thin-walled, unevenly plethoric blood vessels; a layer of odontoblasts is located on the border with dentin. Thus, the use of the MTA-containing material after crown trepanation showed a pulp-saving effect, the revealed inflammatory changes in the pulp are associated with the penetration of a foreign body into the pulp tissue.

In the preparations of teeth, the trepanation holes of which were closed with Biodentin, no histological changes characteristic of pulpitis were found (Fig. 3).

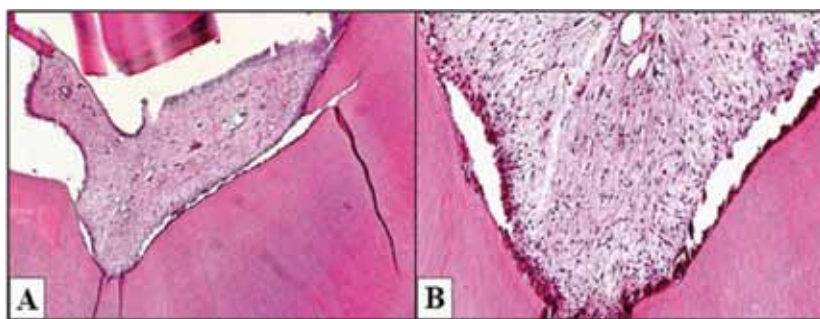


Fig. 1. Longitudinal section of the premolar 8.5 in laboratory pigs after trepanation with MTA closure: A — general view of the crown of the tooth, magnification $\times 50$. B — tooth pulp without damage, multicellular, normal odontoblast row, magnification. $\times 200$. Staining with hematoxylin and eosin

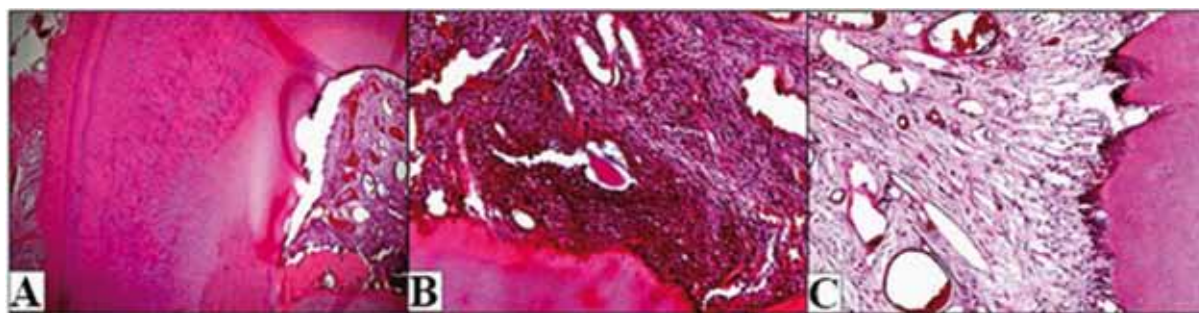


Fig. 2. Tooth preparation 5.4 (Rootdent). A — general view of the tooth, magnification $\times 50$. B — focal inflammation around a foreign body, magnification $\times 200$. C — normal pulp of the tooth, magnification $\times 200$. Staining with hematoxylin and eosin

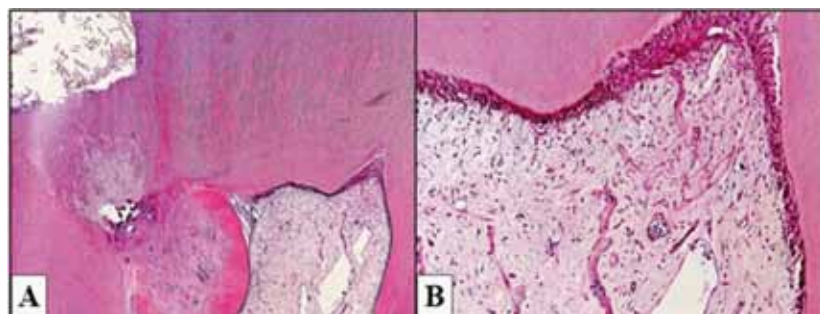


Fig. 3. Pulp of the tooth 6.4 (Biodentin). A — general view of the crown of the tooth, fragments of the filling material are visible, magnification $\times 50$ B — normal pulp of the tooth, magnification $\times 200$. Staining with hematoxylin and eosin

In the preparation of tooth 6.4 (Biodentin) a longitudinally cut tooth with fragments of the pulp, crown and two roots with fragments of filling material in the pulp tissues. In all areas, the pulp has a normal structure, no inflammatory changes were found.

In preparation of tooth 6.5, Vitremer glass ionomer cement was used to close the trepanation hole (Fig. 4). In the preparation of tooth 6.5 (Vitremer), the coronal part of the tooth and the orifice of the root canals are cut tangentially.

In one canal, the pulp has a normal structure, there are no inflammatory changes. In the second canal the pulp cells have a mesenchymal morphology, their number is increased, but there is no inflammatory infiltration, which indicates the development of physiological repair in the pulp.

DISCUSSION

High reparative properties of the pulp were shown by Giraud T., Jeanneau C. et al. (2019). When using various models of pulpitis to study the effect of materials on the pulp, it was shown that the pulp has an innate anti-inflammatory potential and a high ability to regenerate in all teeth and at any age [3].

In research of Ricucci D., Siqueira J.F. Jr, Li Y. et al. (2019) on 264 carious teeth, histological and histobacteriological analysis carried out on the extirpated pulp showed a localized inflammatory reaction that usually occurs in the adjacent pulp tissue as soon as the enamel was affected by caries. If softened and infected dentin was completely excised and the cavity repaired, pulpal inflammation was often relieved. In teeth with a carious process, the degree of penetration of bacteria

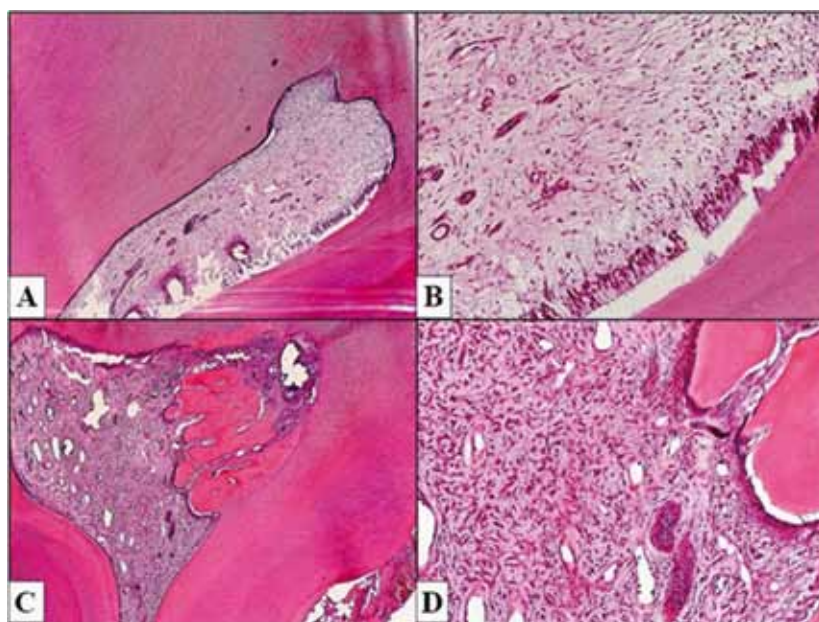


Fig.4. Tooth pulp 6.5 (Vitremar). A, B — canal of the tooth with normal pulp. C, D — cellular reaction in the pulp in the second canal. A, B — magnification $\times 50$; C, D — magnification $\times 200$.

varied, and the areas of infection were pulp inflammation, including micro-abscesses. However, the pulp tissue in the root canals was usually non-inflamed and normal [4].

In experimental samples, simulated pulpitis, inflammation was detected in samples containing Rudent material (tooth 5.4). The cause of inflammation in sample 5.4 is associated with the presence of a foreign body (dentin fragment) in the pulp chamber. In the sample (tooth 8.5) containing the MTA-based materials, no inflammatory changes were detected. In all other samples of teeth with experimental pulpitis, where MTA-containing material (Rootdent), tricalcium silicate materials (Biodentin) were used for direct pulp capping there were no inflammatory changes in the pulp tissues. The high efficiency of MTA material and tricalcium silicate cements has been confirmed by numerous clinical studies in the treatment of pulpitis in young patients with an unformed and uncovered root apex. Brizuela C., Ormeño A. et al. (2017) published the results of a study on 169 patients using MTA, calcium silicate cements and calcium hydroxide. After a year of follow-up, no significant differences were found between Biodentin and MTA. The authors noted some of the advantages of these cements over classical calcium hydroxide. [5].

Hegde S., Sowmya B., et al. (2017) treated reversible pulpitis in 24 permanent molars with carious lesions. There were two groups, group I - MTA and group II - Biodentin. Patients were seen at 3 weeks, 3 months, and 6 months for clinical and radiographic evaluation. The authors found that over 6 months

MTA and Biodentin showed 91.7% and 83.3% success, respectively, based on subjective symptoms, pulp sensitivity tests, and radiographic control [6].

The results of our study showed that the reaction of the pulp to GIC (Vitremar), according to histological analysis, did not differ from the reaction to tricalcium silicate cement (Biodentin). Lipski M., Nowicka A., et al. (2018) published the results of predictive value of factors in relation to the results of direct pulp capping treatment with Biodentine (Septodont, Saint-Maur-de-Fosse, France). The overall success rate was 82,6%. The authors noted that age had a significant effect on pulp survival: the success rate was 90.9% of patients under 40 years and 73.8% of patients 40 years and older [7]. Ricucci D., Siqueira J.F. Jr, Li Y., et al. (2019) conducted observation of 757 clinical cases with a long follow-up period of 30 years. The authors found that direct pulp capping was successful in 73.2%, partial pulpotomy in 96.4% and complete pulpotomy in 77.8% of cases [4].

CONCLUSION

Thus, on the basis of our data, we can conclude:

1. In traumatic pulpitis and the use of various materials for direct pulp capping, active reparative regeneration of pulp tissue was revealed. All researched covering materials contribute to the restoration of the pulp structure after damage, relief of the symptoms of pulp inflammation.
2. In case of damage to the pulp by fragments of a tooth during the modeling of pulpitis and the use of Rootdent material to cover the defect, incomplete regeneration of the pulp along the periphery of the inflammatory focus was revealed.

For the final decision on treatment methods – the methods that ensure the healing of the pulp and the formation of replacement dentin, further studies of the humoral and cellular factors of the inflammatory response in the pulp are required.

REFERENCES

1. **PAULA AB, LARANJO M, MARTO CM, PAULO S, ABRANTES AM, CASALTA-LOPES J, MARQUES-FERREIRA M, BOTELHO MF, CARRILHO E.** Direct Pulp Capping: What is the Most Effective Therapy-Systematic Review and Meta-Analysis. *J Evid Based Dent Pract.* 2018 Dec;18(4):298–314. doi: 10.1016/j.jebdp.2018.02.002. Epub 2018 Feb 15. PMID: 30514444.
2. **DHAR V, MARGHALANI AA, CRYSTAL YO, KUMAR A, RITWIK P, TULUNOGLU O, GRAHAM L.** Use of Vital Pulp Therapies in Primary Teeth with Deep Caries Lesions. *Pediatr Dent.* 2017 Sep 15;39(5):146–159. Erratum in: *Pediatr Dent.* 2020 Jan 15;42(1):12–15. PMID: 29070150.
3. **GIRAUD T, JEANNEAU C, ROMBOUTS C, BAKHTIAR H, LAURENT P, ABOUT I.** Pulp capping materials modulate the balance between inflammation and regeneration. *Dent Mater.* 2019 Jan;35(1):24–35. doi: 10.1016/j.dental.2018.09.008. Epub 2018 Sep 27. PMID: 30269862.
4. **RICUCCI D, SIQUEIRA JF JR, LI Y, TAY FR.** Vital pulp therapy: histopathology and histobacteriology-based guidelines to treat teeth with deep caries and pulp exposure. *J Dent.* 2019 Jul; 86:41–52. doi: 10.1016/j.jdent.2019.05.022. Epub 2019 May 21. PMID: 31121241.
5. **BRIZUELA C, ORMEÑO A, CABRERA C, CABEZAS R, SILVA CI, RAMÍREZ V, MERCADE M.** Direct Pulp Capping with Calcium Hydroxide, Mineral Trioxide Aggregate, and Biodentine in Permanent Young Teeth with Caries: A Randomized Clinical Trial. *J Endod.* 2017 Nov;43(11):1776–1780. doi: 10.1016/j.joen.2017.06.031. Epub 2017 Sep 14. PMID: 28917577.
6. **HEGDE S, SOWMYA B, MATHEW S, BHANDI SH, NAGARAJA S, DINESH K.** Clinical evaluation of mineral trioxide aggregate and biodentine as direct pulp capping agents in carious teeth. *J Conserv Dent.* 2017 Mar-Apr;20(2):91–95. doi: 10.4103/0972-0707.212243. PMID: 28855754; PMCID: PMC5564251
7. **LIPSKI M, NOWICKA A, KOT K, POSTEK-STEFAŃSKA L, WYSOCZAŃSKA-JANKOWICZ I, BORKOWSKI L, ANDERSZ P, JARZĄBEK A, GROCHOLEWICZ K, SOBOLEWSKA E, WOŹNIAK K, DROŹDZIK A.** Factors affecting the outcomes of direct pulp capping using Biodentine. *Clin Oral Investig.* 2018 Jun;22(5):2021–2029. doi: 10.1007/s00784-017-2296-7
8. Epub 2017 Dec 12. PMID: 29234957; PMCID: PMC5945752

<http://dx.doi.org/10.35630/2199-885X/2022/12/2.2>

DIGITAL TECHNOLOGY FOR PROCESSING DRIED DROPS OF BIOFLUIDS

Received 23 January 2022;
Received in revised form 19 February 2022;
Accepted 21 February 2022

Andrew Martusevich^{1,3} , **Lida Kovaleva⁴** ,
Konstantin Karuzin² , **Maria Feofilova⁶**,
Ivan Bocharin^{1,3} , **Alexandra Surovegina^{1,3}**,
Vladimir Nazarov^{1,5} , **Anastasia Kashirina**

¹ Privolzhsky Research Medical University, Nizhny Novgorod, Russia

² Bioniq Health-Tech Solutions, London, United Kingdom

³ Nizhny Novgorod State Agricultural Academy, Nizhny Novgorod, Russia

⁴ Kuban State Medical University, Krasnodar, Russia

⁵ Institute of Applied Physics of Russian Academy, Nizhny Novgorod, Russia

⁶ Tula State University, Tula, Russia

✉ cryst-mart@yandex.ru

ABSTRACT — Attempts to digitize samples and apply artificial intelligence and machine learning methods to analyze crystalloscopic (dried drops of biological fluids) and tesigraphic (dried drops of biological fluids with crystallogenic substance) facies have not yet been successful. In this regard, there is a need to develop a simplified algorithm for describing the facies of biological fluids, which can be used for a unified computer study of the results of crystallization of biological objects, which served as the purpose of the work. To develop and test the method presented in this paper, we used more than 16,000 images of dried biological fluids of the human and animal body, including both crystalloscopic and tesigraphic facies. The algorithm is based on determination of 4 main parameters (crystallizability, structure index, facies destruction degree and clarity of the marginal zone), graded on three-point scales. In addition, a facies integral parameter combining the values of all criteria is proposed.

KEYWORDS — biocrystallogics, facies, digital analysis, crystallization

INTRODUCTION

Currently, there are numerous studies devoted to the study of the crystallogenic properties of biological fluids in humans and animals [1–4, 7]. It is shown that the application of biocrystallogics as a new discipline that comprehensively considers the processes of crystallization and structuring in biological systems has broad prospects [5, 6]. They are associated with the diagnosis and differentiation of diseases of various profiles, personification of the appointment and monitoring of the effectiveness of treatment, prediction of the further course of pathology [1–7]. The fundamental basis for the diagnostic informativeness of the technology is the specificity of the dehydration structuring of the

components of biological fluids in the form of a set of organo-mineral aggregates [3, 5, 6]. In conditions of pathology, the component composition and physico-chemical properties of the biological media are significantly transformed, which is recorded in shifts in the morphology of their dried samples (facies) [1–3, 5–7].

To date, two main options for assessing the crystallogenic properties of liquid media have been identified: the study of their own crystallogenic activity (crystalloscopy) and the study of co-dehydration with a crystal-forming agent (tesigraphic), which is performed by various salts (most often isotonic sodium chloride solution and copper sulfate) [6]. On the other hand, the greatest difficulties are caused by the correct description of the crystallization result, for which numerous methods have been proposed (from a morphological approach involving the search and manual counting of the number of individual structures to the application of various quantitative and semi-quantitative parameters). For a long period, we have been developing and testing on various biological objects a system of multiparametric description of crystallograms (result of dehydration of biofluid drops) and tesigrams (result of co-dehydration of biofluid drops with special inducer of crystallization), which is independent of the type of biological fluid and the morphology of the elements formed from it during drying [5, 6]. However, the attempts made by us and other specialists to digitize samples and apply artificial intelligence and machine learning methods to analyze crystalloscopic and tesigraphic facies have not yet been successful [3, 4]. This is primarily due to the multiplicity of criteria, the complex and wide gradation of their values, the presence of direct and inverse scales for various parameters and other factors [3–5]. In this regard, there is a need to develop a simplified algorithm for describing the facies of dried samples of liquid biological media, which can be used for a unified computer study of the results of crystallization of biological objects.

The purpose of this work

was to create a unified algorithm for evaluating crystalloscopic and tesigraphic facies based on basic criteria.

MATERIAL AND METHODS

To develop and test the method presented in the work, we used more than 16,000 images of dried

biological fluids of the human and animal body (blood serum and plasma, saliva, urine, sweat and tear fluids, etc.) obtained over the past 14 years [5, 6]. The specified volume of the material included both crystalloscopic facies, which are the result of their own dehydration of biosubstrates, and tesigrams, in which 0.9%; 0.1%, 3% and 10% solutions of sodium chloride, 0.1N solutions of hydrochloric acid, sodium hydroxide and other compounds were used as crystal-forming agents (crystallization inducers). In micro-preparations of dried biological media, the most informative features were identified, which were used to develop a substrate-independent, compact (in terms of the number of indicators) parameter system based on the minimum number of gradations of each evaluation feature.

RESULTS

In-depth analysis of a large array of crystalloscopic and tesigraphic facies made it possible to form the most compact and simple algorithm for describing dried microsampling of biological fluids. It includes 4 main indicators, graded on three-point straight scales:

I. **Crystallizability** (Cr) is a parameter characterizing the density of crystalline and amorphous elements in facies; the main quantitative criterion for the intensity of crystallogenesis. Composition of the scale:

— 0 points — no signs of crystallization (less than 5 structures in the field of vision) or hypercrystallogenesis (more than 30 structures in the field of vision);

— 1 point — moderately suboptimal crystal density (5–10 or 20–30 elements in the field of view);

— 2 points — optimal intensity of crystallization (10–20 crystals in the field of view).

II. **The structure index** (SI) is an indicator that characterizes the complexity of the structure of the facies. Gradations of the parameter:

— 0 points — only amorphous bodies or numerous branched dendrites filling the entire field of view;

— 1 point — single crystals (it is possible to include single polycrystalline structures);

— 2 points — dendritic and single-crystalline elements are present in facies in almost equal proportions.

III. **The facies destruction degree** (FDD) is a criterion for the correctness of the processes of crystallogenesis. It includes 2 evaluation options:

— 0 points — total destruction of structural elements in the dried microsamples of biological fluid;

— 1 point — pronounced changes in crystal morphology while preserving the possibility of identifying their type;

— 2 points — there are no signs of structural destruction or are fleeting, morphology and interac-

tion with other elements can be determined for all elements.

IV. **The clarity of the marginal protein zone** (Mz) is an indicator describing the state of the proteome of a biological fluid. Gradations of the parameter:

— 0 points — the marginal belt is absent or has an excessive size (more than $\frac{2}{3}$ of the facies radius), numerous, randomly located faults are found in it;

— 1 point — the radius of the marginal zone from $\frac{1}{3}$ to $\frac{2}{3}$ of the radius of the dried sample, there are moderately chaotic faults;

— 2 points — the marginal zone occupies less than $\frac{1}{3}$ of the facies radius, contains evenly distributed, centripetal faults.

For the tasks of digitizing the result of own and initiated crystallization of biological fluids and obtaining a single value for each sample in order to form a conclusion on it, a facies integral parameter (FIP) was additionally proposed, calculated by the formula:

$$FIP = Cr + SI + FDD + Mz,$$

where Cr is crystallizability; SI is the structure index; FDD is the facies destruction degree; Mz is the clarity of the marginal zone.

Based on subsequent studies, the informativeness of the created algorithm for describing crystalloscopic and tesigraphic facies was confirmed.

CONCLUSION

A detailed analysis of an extensive array of crystallograms and tesigrams of biological fluids in humans and animals (blood serum and plasma, saliva, urine, sweat and tear fluids, etc.) has been created and we tested a comprehensive unified algorithm for their evaluation. It is based on the determination of 4 main parameters (crystallizability, structure index, facies destruction degree and clarity of the marginal zone), graded on three-point scales. In addition, a facies integral parameter combining the values of all criteria is proposed. It should be noted that the developed approach for the first time makes it possible to describe both crystalloscopic and tesigraphic facies according to uniform criteria.

FUNDING

This work was financially supported by the Ministry of the Health of Russian Federation (№AAAA-A20-121030100012-9).

REFERENCES

DENISOV A.B., PUSHKAR' D.Y., DENISOV S.A. Use of saliva crystallogenic properties for early diagnostics of

prostate cancer // Bull. Exp. Biol. Med. – 2006. – Vol. 142, no. 2. – P. 242-245. DOI: 10.1007/s10517-006-0338-2

JORDANISHVILI A.K. Oral liquid adult: age peculiarities of the physicochemical properties and micro crystallization // Adv. Gerontol. – 2019. – Vol.32, N3. – P. 477-482.

KOKORNACZYK M.O., BODROVA N.B., BAUMGARTNER S. Diagnostic tests based on pattern formation in drying body fluids - A mapping review // Colloids Surf B Biointerfaces. – 2021. – Vol. 208. - 112092. doi: 10.1016/j.colsurfb.2021.112092

LI Z.X., ZHA Y.M., JIANG G.Y., HUANG Y.X. AI aided analysis on saliva crystallization of pregnant women for accurate estimation of delivery date and fetal status // IEEE J Biomed Health Inform. – 2021. - Dec 15. doi: 10.1109/JBHI.2021.3135534

MARTUSEVICH A.K., KAMAKIN N.F. Crystallography of biological fluid as a method for evaluating its physicochemical characteristics // Bull. Exp. Biol. Med. – 2007. – Vol. 143, no. 3. – P. 385-388. doi: 10.1007/s10517-007-0118-7.

MARTUSEVICH A.K., KAMAKIN N.F. Unified algorithm for the study of free and initiated crystallogenesis of biological fluids // Clinical laboratory diagnostics. - 2007. - No. 6. - P. 21-24.

PANCU G., LĂCĂTUȘU S., CĂRUNTU I.D., IOVAN G., GHIORGHE A. Evaluation of caries activity using the micro-crystallization saliva index (IMK) // Rev. Med. Chir. Soc. Med. Nat. Iasi. – 2006. – Vol. 110, no. 1. – P. 206–211.

<http://dx.doi.org/10.35630/2199-885X/2022/12/2.3>

CHARACTERISTICS OF SKIN DIELECTRIC PROPERTIES IN PREGNANCY (EXPERIMENTAL STUDY)

Received 11 February 2022;
Received in revised form 10 March 2022;
Accepted 14 March 2022

**Andrew Martusevich^{1,2} , Kristina Kishoyan,
Alexandra Surovegina^{1,2}, Elena Golygina¹ ,
Ivan Bocharin^{1,2} , Vladimir Nazarov^{1,3} **

¹ Privolzhsky Research Medical University, Nizhny Novgorod;

² Nizhny Novgorod State Agricultural Academy, Nizhny Novgorod;

³ Institute of Applied Physics, Nizhny Novgorod, Russia

✉ cryst-mart@yandex.ru

ABSTRACT — The purpose of our study was to evaluate the dielectric characteristics of the skin that occur during pregnancy in an experiment. The study included 60 Wistar rats, 30 of which were pregnant (in the 3rd trimester; parturition took place 2–3 days after the study). Once, on a pre-epilated area of the skin of the back, the dielectric properties were studied using the method of near-field resonant microwave sensing. The diagnostic software and hardware complex for microwave sensing allows calculating the level of dielectric permittivity of the medium and conductivity based on the shift of the resonant frequency. Based on the conducted studies, it was found that the integumentary tissues of pregnant rats have a significantly higher level of dielectric permittivity and conductivity compared to non-pregnant animals. Such shifts are caused by the formation of edematous syndrome associated with pregnancy, and predispose to the development of postpartum skin changes.

KEYWORDS — dielectric properties, skin, permittivity, conductivity, pregnancy.

INTRODUCTION

It is known that pregnancy is accompanied by significant structural and functional changes in the mother's body [1, 3, 7]. At the same time, the main attention of researchers is focused on assessing the condition of the fetus itself, the placenta and the regulatory (neuro-immune-endocrine) mechanisms of the latter's activity [1, 3]. In addition, pathological conditions directly associated with pregnancy (the classic triumvirate *edema* — *proteinuria* — *hypertension*, gestational diabetes, etc.) are considered in detail [2, 7], while changes occurring in other organs and tissues are monitored less carefully.

On the other hand, dermatological manifestations are one of the important functional and cosmetic shifts that form during pregnancy [1, 7].

They can consist of the development of initially non-manifested allergic reactions, the formation of *stretch marks* in the abdominal region, as well as systemic changes in the structure of the skin, even in anatomically remote areas [1, 3, 7]. It should be noted that these consequences and *side effects* of gestation have not been fully studied.

Currently, the study of the skin condition can be carried out in various ways, and the most informative is its histological examination, however, it is invasive, long-term, requires a specialized laboratory and can be performed only in case of suspicion of pronounced pathological processes (primarily neoplasms). A common alternative to this is dermatoscopy, based on the reflection of a light beam from the surface layers of the skin, but this method allows you to evaluate only their and trichological status [8]. Another diagnostic instrumental approach is optical coherence tomography, but it also makes it possible to detect changes only at a shallow depth (up to 100–120 microns), and the equipment for its implementation is exclusive and has a high cost.

In this regard, an innovative technology based on near-field microwave sensing of biological tissues attracts attention [4–6]. Unlike ultrasound, this technology does not require reflection of the probed signal from biostructures, which makes it universal and applicable for assessing the morphostructure of surface tissues [4, 5]. Sufficient depth of probing (up to 10 mm or more) provides an opportunity to study the condition of not only the nearest, but also more distant layers of the skin from the surface [5, 6]. The most indicative microwave tomographic assessment of the structure of the integumentary tissues in laboratory animals, in which the study in question allows us to study both the morphological features of the epidermis and the dermis (in some cases, even subcutaneous fat) [4, 5]. In our previous studies performed on healthy Wistar rats, the features of spatial variability of the distribution of dielectric parameters of the skin in different regions of the body (abdomen, back, forehead, lumbar region) were established [6]. The heterogeneity of the considered regions according to the studied indicators is shown. At the same time, the dielectric properties of rat skin during pregnancy have not been evaluated before.

In connection with all of the above, the purpose of the study was to evaluate the dielectric characteristics of the skin that occur during pregnancy in an experiment.

MATERIAL AND METHODS

The study included 60 Wistar rats, 30 of which were pregnant (in the late stages, in the 3rd trimester; childbirth took place 2–3 days after the study). Once, on a pre-epilated area of the skin of the back, the dielectric properties were studied using the method of near-field resonant microwave sensing [4–6]. The diagnostic software and hardware complex for microwave sensing allows calculating the level of dielectric permittivity of the medium and conductivity based on the shift of the resonant frequency [5, 6]. Probing was carried out using an integrative sensor evaluating the dielectric properties of tissues at a depth of 5 mm.

Experiments with animals were provided in accordance with the rules of the European Convention ET/S 129, 1986 and Directives 86/609 EEC.

Statistical processing of the results was performed using Statistica 6.1 program.

RESULTS

It was found that in pregnant rats, the dielectric parameters of the integumentary tissues differ significantly from those in non-pregnant individuals (Fig. 1, 2). In particular, animals in the third trimester of pregnancy showed a marked increase in dielectric permittivity relative to rats of the control group (by 2.49 times; $p < 0.05$). Taking into account the biophysical meaning of the shifts in the indicator level, we can assume a significant increase in the degree of tissue hydration due to edematous syndrome associated with gestation (Fig. 1).

A similar trend was registered for the dielectric permittivity of the skin and subcutaneous tissues (Fig. 2). It was found that in pregnant rats the indicator level is 1.94 times higher than the values characteristic of non-pregnant individuals ($p < 0.05$). Such dynamics also indicates an increase in the proportion of the liquid component in the tissues, which further confirms the formation of systemic edematous syndrome in various regions of the rat body [2].

CONCLUSION

Based on the conducted studies, it was found that the integumentary tissues of pregnant rats have a significantly higher level of dielectric permittivity and conductivity compared to non-pregnant animals. Such shifts are caused by the formation of edematous syndrome associated with pregnancy, and predispose to the development of postpartum skin changes.

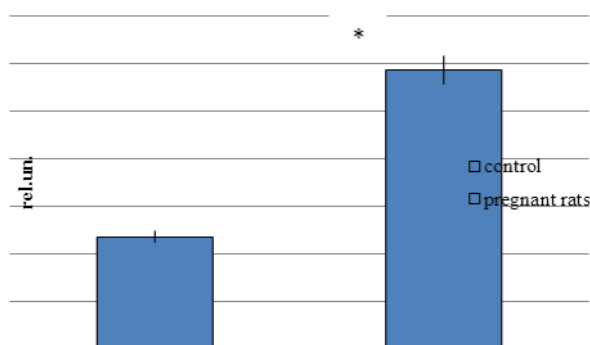


Fig. 1. The level of dielectric permittivity of integumentary tissues in pregnant and non-pregnant Wistar rats (* — statistical significance of differences relative to non-pregnant animals $p < 0.05$)

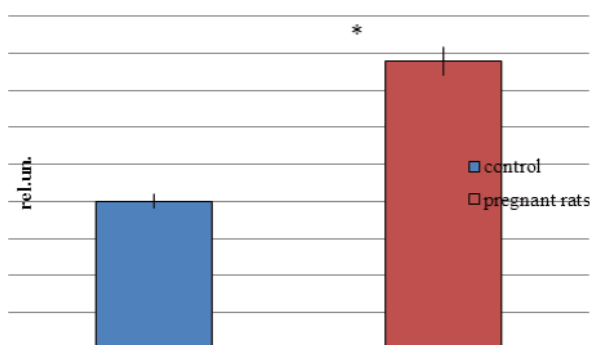


Fig. 2. The level of dielectric conductivity of integumentary tissues in pregnant and non-pregnant Wistar rats (* — $p < 0.05$ to non-pregnant animals)

REFERENCES






1. CARLIN A., ALFIREVIC Z. Physiological changes of pregnancy and monitoring // Best Pract Res Clin Obstet Gynaecol. – 2008. – Vol. 22, N 5. – P. 801–823. doi: <https://doi.org/10.1016/j.bpobgyn.2008.06.005>
2. FILIPEK A., JUREWICZ E. Preeclampsia - a disease of pregnant women // Postepy Biochem. – 2018. – Vol. 64, N 4. – P. 232–229. Polish. doi: 10.18388/pb.2018_146
3. KOHLHEPP L.M., HOLLERICH G., VO L., HOFMANN-KIEFER K., REHM M., LOUWEN F., ZACHAROWSKI K., WEBER C.F. Physiological changes during pregnancy // Anaesthesist. – 2018. – Vol. 67, N 5. – P. 383–396. German. doi: DOI: 10.1007/s00101-018-0437-2.
4. MARTUSEVICH A., GOLYGINA E., ANUCHIN A., GALK A., TUZHILKIN A., FEDOTOVA A., EPISHKINA A. Microwave detection of skin dielectric properties in some laboratory animals // Archiv Euromedica. – 2020. – Vol. 10, N 1. – P. 46. doi: 10.35630/2199-885X/2020/10/10
5. MARTUSEVICH A.K., GALK A.G., KRASNOVA S.YU., YANIN D.V., KOSTROV A.V. Comparative study

- of dielectric properties of the skin of human and laboratory animals // EPJ Web of Conferences. – 2018. – Vol. 195. – 08004. doi: <https://doi.org/10.1051/epjconf/201819508004>
6. **MARTUSEVICH A.K., EPISHKINA A.A., GOLYGINA E.S., TUZHILKIN A.N., FEDOTOVA A.S., GALKA A.G.** Near-Field Resonance Microwave Sounding to Study Dielectric Properties of Different Skin Areas (Experimental Study) // Modern Technologies in Medicine – 2020. – Vol. 12, No 5. – P. 57–61. doi: [10.17691/stm2020.12.5.06](https://doi.org/10.17691/stm2020.12.5.06)
7. **TAN E.K., TAN E.L.** Alterations in physiology and anatomy during pregnancy // Best Pract Res Clin Obstet Gynaecol. – 2013. – Vol. 27, N 6. – P. 791–802. doi: <https://doi.org/10.1016/j.bpobgyn.2013.08.001>
8. **WEBER P., TSCHANDL P., SINZ C., KITTLER H.** Dermatoscopy of Neoplastic Skin Lesions: Recent Advances, Updates, and Revisions // Curr Treat Options Oncol. – 2018. – Vol. 19, N 11. – 56. [10.1007/s11864-018-0573-6](https://doi.org/10.1007/s11864-018-0573-6)

<http://dx.doi.org/10.35630/2199-885X/2022/12/2.4>

ANALYSIS OF THE COMPLETE BLOOD COUNT IN MALE WISTAR RATS EXPOSED TO DIFFERENT DOSES OF ORALLY ADMINISTERED SODIUM SELENITE

Received 13 December 2021;
Received in revised form 23 January 2022;
Accepted 25 January 2022

Anna Sindireva¹ , Oleg Zayko² ,
Vadim Astashov² , Inna Borodina²,
Elizaveta Guseva² , Polina Zaytseva³ 

¹ Tyumen State University, Tyumen;

² Peoples' Friendship University of Russia, Moscow;

³ Sechenov First Moscow State Medical University (Sechenov University),
Moscow Russia

✉ vastashov3@gmail.com

ABSTRACT — AIMS: To compare the structure of the formula and morphological characteristics of the blood cells after an acute experiment in laboratory rats with oral administration of sodium selenite at a concentration of selenium (Se) 0.5, 1 and 2 maximum permissible concentration (MPC).

METHODS: Four groups of Wistar rats weighing 260–300 g (a control group and three experimental ones: Se group of 0.5 MPC, 1 MPC and 2 MPC) were given sodium selenite in the respective concentrations for 5 days (except for the control group). After the rats were removed from the experiment, blood was taken from the caudal artery and a biochemical blood test was performed and the data obtained were evaluated and compared with the norm.

RESULTS: Changes in the cell composition of rat blood were determined by the dose of selenium. There were no changes in the "Se 0.5 MPC" group compared to the control group. In the Se 1 MPC group, the main difference was a decrease in the number and morphological changes in red blood cells, as well as an increase in the number of eosinophils. Hypochromic anemia and lymphocytopenia were found in the Se 2 MPC group.

CONCLUSION: During an acute experiment, when selenium is given to rats at a dosage equal to the maximum permissible concentration and more, changes in the blood formula are observed, reflecting the pathological processes related to selenium poisoning: anemia, eosinophilia, lymphocytopenia.

KEYWORDS — sodium selenite, maximum permissible concentration, red blood cells, anemia, eosinophilia, lymphocytopenia.

INTRODUCTION

The huge and still growing market of biologically active supplements has product groups aimed

at correcting function of metabolism, antioxidant and cardiovascular systems. They even claim to have antitumor activities. Some of them may contain compounds of selenium. [1, 2] However, due to a relatively narrow therapeutic index of selenium, a person with a normal level of selenium (13 to 30 mg), who takes such a supplement, may easily exceed the therapeutic dose and receive a toxic dose.

In many ways, the effect of high doses of selenium on the body has not been observed. [1] In our work we investigated the effect of selenium at different concentrations on the blood of rats to predict its toxic effect in humans.

METHODS

Laboratory male rats of the Wistar line weighing 260–300 g were used in the study. The rats were divided into 4 groups: control group (n=10), group Se 0.5 MPC (n=10), group Se 1 MPC (n=10), group Se 2 MPC (n=10). The rats of the experimental groups (Se) were given a solution of sodium selenite once a day for five days at a dose of 2.5 mg/kg, 5 mg/kg and 10 mg/kg of weight, based on the MPC = 5 mg/kg of weight.

The rats were kept, cared for, fed and removed from the experiment in accordance with the requirements for the provision of human treatment of animals, the rules of clinical trials in the Russian Federation approved by the Ministry of Health of the Russian Federation on December 29, 1998, the provisions of the Helsinki Declaration (2000).

RESULTS

The blood formula of rats of the control and experimental groups is presented in Table 1.

Changes in the blood formula of rat blood correlated with the dose of selenium (Table 1) [5].

It can be stated, that in the experimental group "Se 0.5 MPC" there were no significant differences in the blood formula of animals of the control and experimental groups.

Considerable differences in the group of rats "Se 1 MPC" were observed due to a decrease in the number of red blood cells and an increase in eosinophils

Table 1. Blood formula of control group (K) of rats and test groups exposed to selenium at doses of 0.5, 1, 2 MPC, $X \pm m$, $n=10$, LII — leukocyte intoxication index [3]

Levels	Group of rats			
	control	Se 0,5 MPC	Se 1 MPC	Se 2 MPC
Red blood cell	4,78±0,09		3,76±0,14	
Basophils	0	0	0	0
Eosnophis	1,5±0,21	2,5±0,23	3,0±0,32	5,0±0,34
Neutrophils:				
- young	0	0	0	0
- rod-shaped	3±0,3	3,5±0,2	3,3±0,25	2,0±0,34
- segmented	29±2,7	28±3,5	30±1,9	49±3,7
Arneth count, units	0,10	0,13	0,11	0,04
Lymphocytes	65,3±4,9	65,5±5,1	60,3±4,7	40,6±4,2
Monocytes	1,5±0,12	2±0,12	2±0,14	1±0,09
LII	0,2	0,2	0,2	0,2

compared to the control group. Hypochromasia of erythrocytes was noted in blood smears of animals of this group. Poikilocytosis and anisocytosis are weakly expressed, which indicates the initial signs of anemia. It was also morphologically established that single lymphomonocytic cells were in a state of dystrophy and lysis. Besides, the obtained data indicate a weakening of humoral immunity.

In the "Se 2 MPC" group of our studies the development of lymphocytopenia in rats was observed. This can be considered as a result of a decrease in the immune response. At the same time, the leukocyte intoxication index does not differ from the control one. Blood smears of animals of the "Se 2 MPC" group are characterized by the aggregation of erythrocytes. Most smears showed poikilocytosis and hypochromasia, which indicates hypochromic anemia. It is confirmed by a decrease in their number and a decrease in hemoglobin levels in rats of this experimental group.

CONCLUSION

After oral administration of sodium selenite at a dose of "Se 1 MPC", a toxic effect on the body of laboratory animals was revealed: slight deviations in the leukocyte count and morphology of blood cells were noticed. The rats received "Se 2 MPC" showed a more significant toxic effect of selenium, which is manifested by leukopenia and hypochromic anemia and indicates acute selenium poisoning.

REFERENCES

1. BLEYS J, NAVAS-ACIEN A, STRANGES S, MENKE A, MILLER ER 3RD, GUALLAR E. Serum selenium and serum lipids in US adults. *Am J Clin Nutr.* 2008 Aug;88(2):416–23. doi: 10.1093/ajcn/88.2.416. PMID: 18689378; PMCID: PMC2553708.
2. RAYMAN MP. Selenium and human health. *Lancet.* 2012 Mar 31;379(9822):1256–68. doi: 10.1016/S0140-6736(11)61452-9. Epub 2012 Feb 29. PMID: 22381456.
3. LOMAKO VV. [Blood leukocyte indices in male rats of different ages.]. *Adv Gerontol.* 2019;32(6):923–929. Russian. PMID: 32160430.
4. JELIŃSKA M, SKRAJNOWSKA D, WRZOSEK M, DOMANSKA K, BIELECKI W, ZAWISTOWSKA M, BOBROWSKA KORCZAK B. Inflammation factors and element supplementation in cancer. *J Trace Elem Med Biol.* 2020 May;59:126450. doi: 10.1016/j.jtemb.2019.126450. Epub 2020 Jan 8. PMID: 31931255.
5. KAMPFMANN I, BAUER N, JOHANNES S, MORITZ A. Differences in hematologic variables in rats of the same strain but different origin. *Vet Clin Pathol.* 2012 Jun;41(2):228–34. doi: 10.1111/j.1939-165X.2012.00427.x. Epub 2012 May 2. PMID: 22551195.
6. GUO A. , SRINATH J, FEUERECKER M. ET AL. Immune function testing in sepsis patients receiving sodium selenite. *J Crit Care.* 2019 Aug;52:208–212. 10.1016/j.jcrc.2019.05.001

<http://dx.doi.org/10.35630/2199-885X/2022/12/2.5>

DISTRIBUTION OF S100 -POSITIVE CELLS IN THE STRUCTURES OF THE SPLEEN IN THE SIMULATION OF CHRONIC NORMOBARIC HYPOXIC HYPOXIA IN THE EXPERIMENT

Received 21 December 2021;
Received in revised form 24 January 2022;
Accepted 27 January 2022

Aleksandr Naumov¹ , Dmitry Nikitjuk² ,
Ekaterina Zadneprovskaya¹, Aleksei Zhidovinov¹ ,
Tatyana Shishkina¹ , Lyubov Naumova¹ 

¹ Astrakhan State medical University, Astrakhan;

² Federal Research Centre of Nutrition and Biotechnology, Moscow, Russia

✉ zhidovinov.aleksey2014@yandex.ru

ABSTRACT — The aim of the research was to study the behavior of S100-positive cells in the structures of the spleen of laboratory animals in normal conditions and against the background of chronic hypoxic hypoxia. S100-positive cells are professional antigen-presenting cells and at the same time create a microenvironment for B-lymphocytes in the corresponding B-dependent areas of the spleen. Along with this, the expression of markers such as Ki67 and p53 was defined as determining the relationship between the processes of cell regeneration and apoptosis. Chronic isolated normobaric hypoxic hypoxia was simulated on 86 white outbred male rats in special priming chambers with controlled air supply for four hours a day, five days a week for 4 months. The analysis of the data showed that as the duration of the chronic experiment increased, the expression of the p53 marker increased mainly in the B-dependent zones, while the expression of Ki67 in the analogous zones decreased. Also, as the period of chronic hypoxia increased, a significant increase in the expression of the S100 marker in the lymphoid nodules of the white pulp of the spleen was noted. In parallel with this, there is an increase in the relative volume of the T-dependent zone and a decrease in the marginal zone of the white pulp. Thus, an increase in the volume fraction of stromal components along with an increase in the expression of an apoptosis marker in lymphoid nodules of the white pulp of the spleen may indicate the formation of tension in humoral immunity and subsequent depletion of compensatory-adaptive cellular elements of the corresponding zones by the end of the experiment.

KEYWORDS — hypoxic hypoxia, spleen, macrophages, S100 marker, apoptosis, proliferation, white pulp.

INTRODUCTION

The immunological foundations of the study of the mechanisms and cellular foundations of the adaptation process in the conditions of the forma-

tion of acute and chronic hypoxia have become one of the main tasks of ecological immunology, the subject of which is the study of changes in the body's immunoreactivity under the influence of environmental factors [3, 5, 6]. The information available today about the effect of prolonged exposure to hypoxia on the state of the immune system is ambiguous [4]. This is most likely due to the lack of standardized models of hypoxic exposure, as well as the difference in methodological approaches for the quantitative and qualitative characteristics of the parameters of the body's immune status and, possibly, insufficient coverage of this issue.

The hematopoietic system, which combines myeloid and lymphoid tissues, is the supplier of all types of cellular elements of the body's immune defense and is recognized as one of the most sensitive systems to the action of external damaging factors. The processes of proliferation and subsequent differentiation of immunocompetent cells require a specific hematopoietic microenvironment with special structural, anatomical and functional characteristics. The stromal components of hematopoietic tissue are capable not only of recognizing and retaining antigen, but also providing the factors necessary for the regulation of proliferation, differentiation, maturation, and in some cases the death of immunocompetent cells. The stroma of the hematopoietic organs consists of various cell populations that make a specific contribution to the organization of the hematopoietic microenvironment. So, there are two populations of dendritic cells - follicular and interdigitating, located, respectively, in the B- and T-dependent compartments of the white pulp of the spleen. It is believed that they have a different origin: follicular cells are cellular elements of stromal origin, and interdigitating ones are of bone marrow origin [7]. Follicular dendritic cells form a three-dimensional network in the cells of which B-lymphocytes are located. They are believed to be responsible for the survival of B-lymphocytes and stimulate the process of their proliferation and differentiation. The S100 protein, which is a group of calcium-binding proteins with low molecular weight, acts as a marker for these cells [2].

MATERIALS AND METHODS

Modeling of chronic normobaric hypoxic hypoxia was performed on 86 white outbred male rats. The animals were kept in the appropriate rooms of the vivarium, where they were cared for in accordance with the rules and regulations for handling laboratory animals [8]. The experiment was carried out in accordance with the standards of the Declaration of Helsinki (2000). Removal of animals from the experiment was carried out by decapitation under chloroform anesthesia in accordance with the Rules of laboratory practice in the Russian Federation (order of the Ministry of Health of the Russian Federation of June 19, 2003 No. 267), in accordance with the International Recommendations for Biomedical Research Using Animals (1985), and also in accordance with the regulations of the law "On the protection of animals from cruelty" [1]. The model of normobaric hypoxia was reproduced using special priming chambers manufactured at the F.F. Erisman Moscow Institute of Occupational Diseases and Occupational Hygiene (Russia) with a volume of 200 liters with a controlled composition of the air-gas mixture. An "Ankat" gas analyzer was used as a control device. The animals were kept under experimental conditions for four hours a day for five days a week. In the experimental group, four subgroups were formed in accordance with the duration of the experiment (30, 60, 90 and 120 days). A control group was also allocated ($n = 14$). Animals of the control group were placed in the chamber in a similar time regime, but with the usual air composition. We studied histological sections, stained with hematoxylin and eosin, according to Van Gieson for connective tissue. For immunohistochemical studies, paraffin histological sections were prepared on a LEICA RM 2255 microtome (Germany) with a thickness of $4\ \mu\text{m}$ and stained using a Leica Microsystems Bond™ immunohisto-stainer (Germany). The following panel of monoclonal antibodies was used as primary: Ki-67 (Ready-to-Use, clone Mib 1, Daco, Denmark); P53 (Ready-to-Use, clone 7JUL, Leica Biosystems Bond™, Germany); S100 (Ready-to-Use, clone 4C4.9, Diagnostic Biosystems, The Netherlands).

An indirect streptavidin-biotin detection system Leica BOND (Novocastra™, Germany) was used for staining. The specificity of the reaction was assessed by staining sections without primary antibodies. The study and visualization of the preparations was carried out using a Zeiss Axio Scope A1 microscope (Germany) and a Leica Aperio CS2 digital slide scanner with specialized software for controlling the settings and image capture.

To assess the results of the immunohistochemical reaction, the expression indices of S100 and P53

were calculated as a percentage per 1000 cells (or their nuclei for Ki-67) in 10 randomly selected fields of view (magnification of the microscope $\times 400$). Moderate and pronounced immunohistochemical staining was taken into account.

RESULTS AND DISCUSSION

The analyze of preparations from the control group stained with hematoxylin and eosin in animals showed that the spleen has a characteristic structure of the parenchymal organ, covered with a capsule of dense fibrous connective tissue, in which smooth myocytes, individual or lying in groups, are observed. Connective tissue trabeculae extend from the capsule into the organ, and two morphofunctional compartments are clearly delimited from each other — white and red pulp, the ratio of which relative to each other was $26, 39 \pm 1.02\%$ and $73.61 \pm 0.86\%$. Clear boundaries are determined between the compartments; in the compartments themselves, a different density of arrangement of cellular elements is revealed. In the composition of the white pulp, two main areas of B-dependent zones are revealed — the germinal center and the mantle of the lymphoid nodule; as well as the periarterial lymphoid sheath — the T-dependent zone. A marginal zone is located along the periphery of the white pulp, which passes into the red pulp and differs from the latter also in the density of the population of cellular elements. The relative area of the B-dependent zone was about a third of the entire area of the white pulp — $32.84 \pm 0.92\%$, half of the area was occupied by the marginal zone — about $51.36 \pm 1.04\%$, and the rest fell on the T-dependent zone — about $15.8 \pm 0.82\%$. In the red pulp of the spleen of the control group of animals, a significant number of blood vessels with a relatively straight course are determined. In the lumen of the vessels, isolated or small groups of shaped elements are revealed.

Immunohistochemical analysis of the S100 marker content in the structural components of the spleen in the control group of animals showed the predominant localization of the studied marker in the white pulp in the B-dependent zone; we did not find S100-positive cells in the T-dependent periarterial sheath (Fig. 1a).

The analyze of preparations stained with hematoxylin and eosin obtained from the group of animals of stimulated hypoxic normobaric hypoxia revealed certain changes. When the time of the experiment was prolonged, the organ capsule thickened and became fragmented with symptoms of edema. On the part of the trabeculae arising from the stroma of the organ, similar changes were found — thickening due to the phenomena of collagen formation and edema.

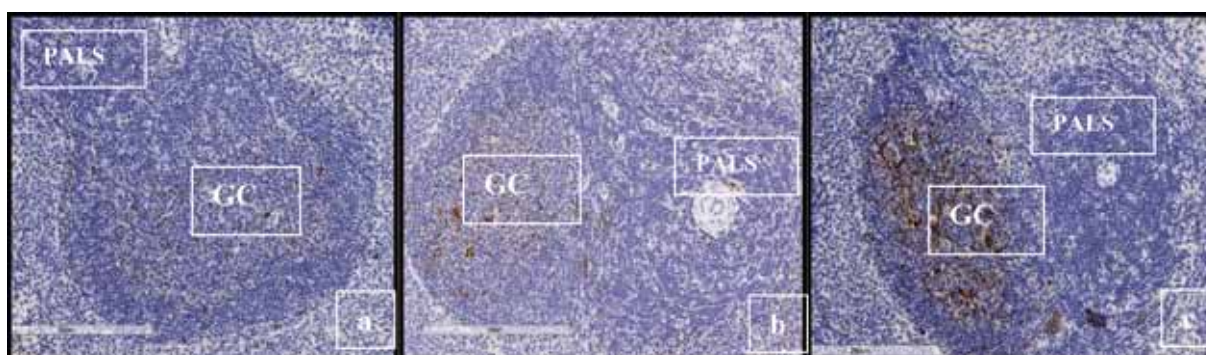


Fig. 1. Distribution of S100-positive cells in the structures of the white pulp of the spleen in the control group (a), in the group after 60 days of the experiment (b) and after 120 days (c); GS — germinal center, PALS — periarterial lymphoid sheath. Immunohistochemical staining with antibodies to the S100 follicular dendritic cell marker. Indirect streptavidin-biotin detection system. Zoom $\times 400$

In the subgroup of animals exposed to isolated hypoxic hypoxia, there is an increase in the total volume of the white pulp by the end of the third month of the experiment to 36.03 ± 0.82 , after which, by the end of 120 days of the experimental exposure, a decrease in the volume of the white pulp was revealed in comparison with the previous period and control and amounted to $23.4 \pm 0.76\%$ (Table 1).

the volume of the periarterial sheath gradually increased, while the marginal zone not only decreased in volume, but also the number of cellular elements in it decreased. So, by the 90th day of the experiment, the T-dependent zone increased by 6.52%, and by the 120th day, more than three times relative to the control values. Also, the volume of the marginal zone by the end of the 4th month of the experiment

Table 1. The relative area of the structural components of the white pulp of the spleen in the control group and the group exposed to chronic normobaric hypoxic hypoxia

Duration of the experiment	B-dependent zone	T-dependent zone	Marginal zone
Control	$32,84 \pm 0,92$	$15,8 \pm 0,82$	$51,36 \pm 1,04$
30 days	$39,6 \pm 1,2^*$	$17,44 \pm 1,08$	$42,96 \pm 0,83^*$
60 days	$47,41 \pm 0,95^*$	$20,7 \pm 0,74^*$	$31,89 \pm 0,7^*$
90 days	$52,7 \pm 1,07^*$	$22,32 \pm 0,82^*$	$24,98 \pm 0,88^*$
120 days	$35,42 \pm 0,74$	$48,63 \pm 0,97^*$	$15,95 \pm 0,67$

Note: * — statistically significant differences compared with the control group ($p < 0.05$)

In the composition of the white pulp, changes were also determined from the side of its components. So, the main changes affected the lymphoid follicles: there was a gradual increase in their volume in the structure of the white pulp up to 90 days to $52.7 \pm 1.07\%$, after which, by the 120th day of the experiment, a sharp decrease to $35.42 \pm 0.74\%$. In the lymphoid nodule itself, the ratio of zones changed in favor of an increase in the volume of germinal centers and a relative decrease in cellular elements in the entire B-dependent zone.

As for the T-dependent and marginal zones, as the duration of the chronic hypoxic state increased,

decreased by more than three times and amounted to $15.95 \pm 0.67\%$.

The analyze of distribution of the marker of follicular dendritic cells S100 revealed that in the setting of chronic hypoxic hypoxia there was an increase in the number of S100-positive cells in the structures of the white pulp, especially by 90 and 120 days of the exposure. A statistically significant increase in S100-positive cells in the areas of the white pulp occurs in the germinal center of the lymphoid nodule. As for the proliferation marker Ki-67, we observed an increase in lymphoid nodules within two months of modeling chronic hypoxia, after which a significant decrease in

its expression by 120 days of the experiment in B-dependent zones. At the same time, the expression of the apoptosis marker p53, on the contrary, was detected mainly in the B-dependent zones of the white pulp, especially by 90th and 120th days of chronic development of normobaric hypoxia, which may indicate death processes, mainly among immunocompetent cells.

CONCLUSION

Thus, chronic normobaric hypoxic hypoxia that develops during a long time in the first months of exposure leads to activation of adaptive capabilities from the immunological components of the spleen. This is manifested by an increase in the relative volume of B-dependent zones and an increase in them not only S100-positive cells, but also the expression of the marker Ki67, however, by the end of the experiment, adaptation was disrupted and the expression of the proliferation marker decreased. In this case, the expression of markers of follicular dendritic cells and apoptosis, on the contrary, increases.

REFERENCES

1. Guide for the Care and Use of Laboratory Animals. Washington, D.C. : The national academies press. 243 p. URL: <http://www.nap.edu/catalog/12910.html> (accessed: 05.07.18).
2. KAPITONOVA M.YU., MOROZOVA Z.CH., SIDORKINA A.V., NESTEROVA A.A., MURAEVA N.A., FOMINA N.G., DEMIDOVICH I.L. The distribution of s100-positive cells in the white pulp of the spleen of rats in the age aspect // Successes of modern natural science. – 2006. – No. 1. – P. 83–84; URL: <https://natural-sciences.ru/ru/article/view?id=14171> (date of access: 12/13/2021).
3. KVARATSKHELIA A.G., KLOCHKOVA S.V., NIKITYUK D.B., ALEKSEEVA N.T. Morphological characteristics of the thymus and spleen under the influence of factors of various origins. Journal of Anatomy and Histopathology. – 2016. – V 5. – No. 3. – P.77–83.
4. MOHYELDIN A, GARZON-MUVDI T, QUINONES-HINOJOSA A (2010) Oxygen in stem cell biology: a critical component of the stem cell niche // Cell Stem Cell. – 2010. – No. 7. – P.150–161. 10.1016/j.stem.2010.07.007
5. NIKITYUK D.B., KLOCHKOVA S.V., ALEKSEEVA N.T., KVARATSKHELIA A.G. Modern ideas about the general laws of the macromicroscopic anatomy of lymphoid organs. Journal of Anatomy and Histopathology. – 2015. – V 4. – No. 2. – P.9–13.
6. ROZHKOVA I.S., WARM D.L. Antioxidants in the regulation of the functional activity of the spleen under conditions of intoxication // Modern problems of science and education. – 2020. – No. 3. – P.124.
7. TAKAHASHI K, ASAGOE K, ZAISHUN J ET AL. Heterogeneity of dendritic cells in human superficial lymph node in vitro maturation of immature dendritic cells into mature or activate. Am J Pathol. 1998 Sep; 153 (3): 745–55. doi: 10.1016/S0002-9440(10)65618-0
8. ZAPADNYUK V.I. Laboratory animals / V.I. Zapadnyuk, I.P. Zapadnyuk, E.A. Zakharia. - Kiev: Vishcha school, 1983. – 383 p.

<http://dx.doi.org/10.35630/2199-885X/2022/12/2.6>

CRYSTALLOSCOPIC MONITORING OF THE EFFECTIVENESS OF SYSTEMIC RETINOIDS IN PATIENTS WITH SEVERE ACNE

Received 23 January 2022;
Received in revised form 19 February 2022;
Accepted 21 February 2022

Polina Krivonogova¹ , Andrew Martusevich^{1,2✉} ,
Oxana Bitkina¹ , Lida Kovaleva³ ,
Alexandra Surovegina^{1,2} 

¹ Privolzhsky Research Medical University, Nizhny Novgorod;

² Nizhny Novgorod State Agricultural Academy, Nizhny Novgorod;

³ Kuban State Medical University, Krasnodar, Russia

✉ cryst-mart@yandex.ru

ABSTRACT — The aim of the work was to study the effect of isotretinoin preparations with different bioavailability (acnecutane and roaccutane) on blood and saliva crystallization in patients with severe forms of acne. The studies were conducted in two main groups: 25 patients used the drug Acnecutan in the treatment, 10 patients used the usual isotretinoin (Roaccutane). A study of the nature of own and initiated crystallization of blood serum and saliva was carried out by our techniques. The results of the study allow us to conclude that the tescrystalloscopic "pattern" of the biological environment of patients with acne differs significantly from that characteristic of practically healthy people. Based on biocrystalloscopic testing, it was found that in the course of treatment with isotretinoin drugs, a partial normalization of indicators was observed, which occurs mainly when using Acnecutan.

KEYWORDS — biocrystallogics, blood serum, acne, acnecutane, roaccutane

INTRODUCTION

Currently, the issue of selecting the optimal drug for treatment of severe forms of acne is relevant [1, 3-7]. The drugs of choice are often antibiotics: tetracycline, doxycycline [7]. The dominant role is assigned to isotretinoin preparations, used in a dosage of 0.4-0.8 mg / kg (Acnecutan) and 0.5-1 mg / kg (Roaccutane, Erase) during a 4-months course. In the most severe forms of the disease, systemic steroids (prednisone 1 mg/kg/day for 2-4 weeks) can be used simultaneously [3]. Data on the use of Dapsone at a dose of 50-150 mg/day have been published [5]. Successful treatment of Perifolliculitis capitis abscedens et suffodiens accompanied by acne conglobata with a combination of dapsone and isotretinoin has been reported [3]. Interleukin- β -blockers are used in the treatment of the PASH triad [4]; Etanercept, a combination of

isotretinoin and adalimumab – in the treatment of SAPHO syndrome [5]. The literature also provides information on the effectiveness of other methods of treatment: carbon dioxide laser in combination with local use of tretinoin with fractional grinding [3, 5]; cryotherapy; intra-focal administration of triamcinolone.

The crystallogenic properties, are inherent in any biosubstrate and being an integral parameter of its homeostasis [2, 8, 9], can indirectly reflect the state of the proteome of the biological medium, since the crystallogenic potential of the latter, realized due to its mineral components, directly depends on the conformational features and the degree of hydration of proteins [8, 9]. We have previously shown that the nature of dehydration structuring of blood serum in dermatological pathology (in particular, During's herpetiform dermatitis) differs significantly from that characteristic of healthy people [1]. This makes it possible, according to the theory of biocrystallogics analysis [8, 9], to evaluate the effectiveness of treatment by the crystallogenic properties of biofluids, primarily blood serum [9], as well as to compare various drugs by the effect on this indicator of homeostasis of the biological medium.

The aim of the work

was to study the effect of isotretinoin preparations with different bioavailability (acnecutane and roaccutane) on blood and saliva crystallization in patients with severe forms of acne.

MATERIAL AND METHODS

35 patients with severe forms of acne were under observation, including 22 men and 13 women aged 15 to 35 years (average age 21.33 years), duration of the disease: up to 3 years — 9 people (25.7%), 4–7 years in 19 people (54.3%), 8–11 years — 7 people (20%). The comparison group consisted of 23 people.

The studies were conducted in two main groups: 25 patients used the drug Acnecutan in the treatment, 10 patients used the usual isotretinoin (Roaccutane). The daily dose of Acnecutan averaged 0.45 mg/kg of weight (31.4 ± 8.6 mg), the course dose was 104.3 mg/kg of weight (7.1 ± 1.4 g) with an average patient weight of 63.8 ± 10.62 kg. According to Roaccutane, the daily dosage was taken at the rate of 0.6

mg/kg of weight (43 ± 10.37 mg), 126.4 mg/kg per course (8.85 ± 1.19 g) with an average patient weight of 68.9 ± 10.1 kg.

A study of the nature of own and initiated crystallization of blood serum and saliva was carried out by our techniques [2, 8, 9]. The basic substance for tesigraphy was 0.9% sodium chloride solution. The crystallograms and tesigrams were evaluated using a system of parameters [8, 9]. The study of these indicators was carried out before the start of treatment (1st examination), a month later (2nd examination) and 3 months after the start of therapy (3rd examination).

The data obtained were processed using the Statistica 6.0 program.

RESULTS

It was found that the tesicrystalloscopic "pattern" of the biological environment of acne patients differed significantly from the physiological one [2, 8]. Analysis of the facies of blood serum and saliva of acne patients before treatment revealed the features of the structuring of these biofluids (Fig. 1 and 2). Thus, the facies of the latter are characterized by high crystallogenic activity with a predominance of single crystal structures in the samples. It should be emphasized that the structural elements in microsamples of patients with acne are characterized by the presence of pronounced signs of destruction. The marginal zone of blood serum and saliva facies is quite clear, can be traced along the entire perimeter of the sample.

By the time of the 2nd examination (end of 1 month of treatment), the normalization of the crystallogenic properties of biofluids was variable. At the same time, changes in the crystallization of biofluids were characterized by a decrease in the density and complexity of the crystal structure, as well as the severity of destruction (Fig. 1a and 2a). Interestingly, the rates of normalization of the initiated crystallogenesis of biosubstrates at this observation point were lower (Figs. 1b and 2b).

By the 3rd examination, various degrees of normalization of the crystallogenic and initiating properties of saliva and blood serum were observed (Fig. 1 and 2). Thus, the maximum approximation of the tesicrystalloscopic "pattern" to the norm was recorded in the blood serum samples of patients treated with Acnecutan (Fig. 1a). At the same time, patients treated with Roaccutane had significant deviations from the norm (a decrease in the density of crystals and the complexity of their construction). In addition, a decrease in the marginal zone size with an increase in destruction degree was noted in microsamples. At the end of the therapy, similar processes of normalization of structure were observed in the facies of blood serum and saliva of patients with acne in both groups receiving Acnecutan and Roaccutane.

CONCLUSION

The results of the study allow us to conclude that the tesicrystalloscopic "pattern" of the biological

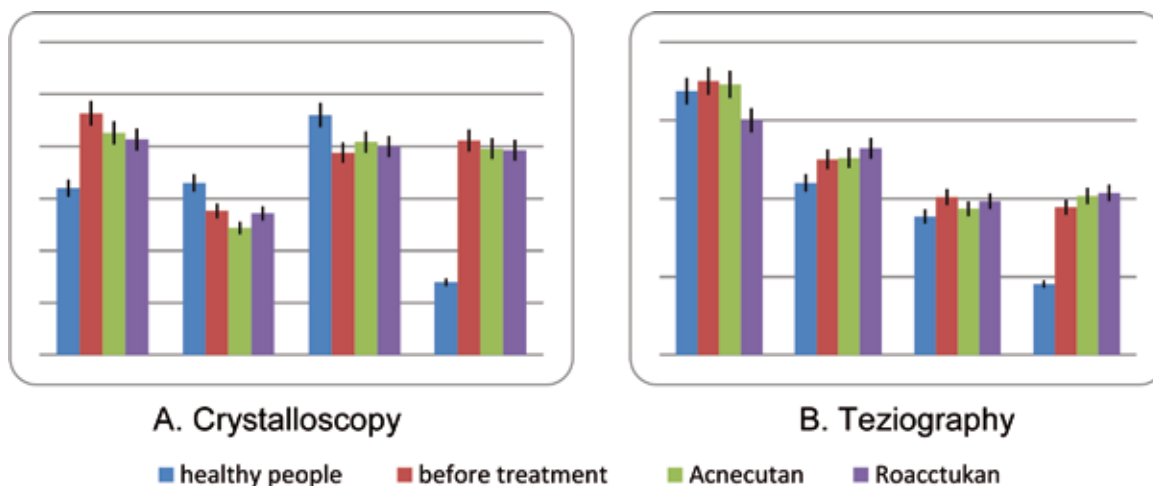


Fig. 1. Dynamics of crystallogenic and initiating properties of blood serum in patients with acne depending on treatment option (Cr — crystallizability, K — crystallinity, TI — tesigraphic index, SI — structure index, Mz — marginal zone, FDD — facies destruction degree)

environment of patients with acne differs significantly from that characteristic of healthy people. Based on biocrystalloscopic testing, it was found that in the course of treatment with isotretinoin drugs, a partial normalization of indicators was found, which occurs mainly when using Acnecutan.

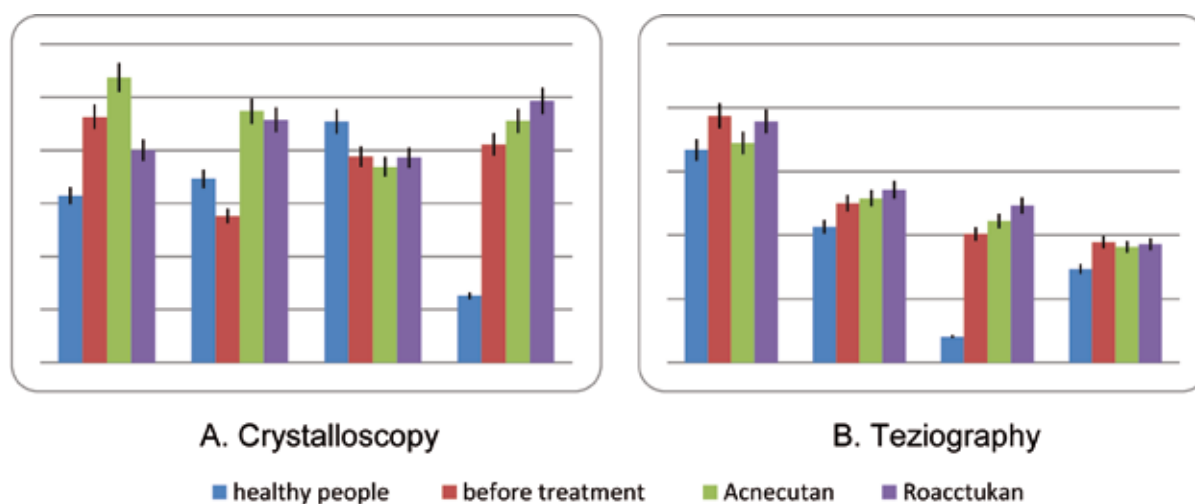


Fig. 2. Dynamics of crystallogenic and initiating properties of saliva in patients with acne depending on the treatment option (Cr — crystallizability, K — crystallinity, TI — tesigraphic index, SI — structure index, Mz — marginal zone, FDD — facies destruction degree)

REFERENCES

1. BITKINA O.A., KOPYTOVA T.V., KONTORSH-CHIKOVA K.N., BAVRINA A.P. The level of oxidative stress in patients with rosacea and the rationale for the therapeutic use of ozone-oxygen mixture // Clinical laboratory diagnostics. – 2010. – N4. – P. 13–16.
2. BITKINA O.A., KRIVONOGOVA P.L., MARTUSEVICH A.K., PANTELEEVA G.A. Physico-chemical parameters of biological fluids in Dering's herpetiform dermatitis // Russian Journal of Skin and Venereal Diseases. – 2012. – N4. – P. 11–15.
3. BOLZ S., JAPPE U., HARTSCHUH W. Successful treatment of perifolliculitis capitis abscedens et suffodiens with combined isotretinoin and dapsone // J. Dtsch. Dermatol. Hes. – 2008. – Vol. 6, N1. – P. 44–47. DOI: 10.1111/j.1610-0387.2007.06399.x
4. BROWN-FALCO M., KOVNERYSTYY O., LOHSE P. ET AL. Pyoderma gangrenosum, acne, and suppurative hidradenitis (PASH)—a new autoinflammatory syndrome distinct from PAPA syndrome // J. Am. Acad. Dermatol. – 2012. – Vol. 66, N3. – P. 409–415. DOI: 10.1016/j.jaad.2010.12.025
5. GARCOVICH S., AMELIA R., MAGARELLI N. ET AL. Long-term treatment of severe SAPPPO syndrome with adalimumab: case report and a review of the literature // Am. J. Clin. Dermatol. – 2012. – Vol. 13, N1. – P. 55–59. DOI: 10.2165/11593250-000000000-00000
6. HASEGAWA T., MATSUKURA T., HIRASAWA YU. ET AL. Conglobate acne successfully treated by fractional laser after CO2 laser abrasion of cysts combined with topical tretinoin // Journal of Dermatology – 2009. – Vol. 36, N2. – P. 118–119. <https://doi.org/10.1111/j.1346-8138.2009.00604.x>
7. MARGOLIS D.J., HOFFSTAD O., BILKER W. Association or lack of association between tetracycline class antibiotics used for acne vulgaris and lupus erythematosus // Br. J. Dermatol. – 2007. – Vol. 157. – P. 540–546. DOI: 10.1111/j.1365-2133.2007.08056.x
8. MARTUSEVICH A.K., KAMAKIN N.F. Crystallography of biological fluid as a method for evaluating its physicochemical characteristics // Bull. Exp. Biol. Med. – 2007. – Vol. 143, N3. – P. 385–388.
9. MARTUSEVICH A.K., KAMAKIN N.F. Unified algorithm for the study of free and initiated crystallogenes of biological fluids // Clinical laboratory diagnostics. – 2007. – N6. – P. 21–24.

<http://dx.doi.org/10.35630/2199-885X/2022/12/2.7>

RED BONE MARROW DAMAGE IN COVID-19 PATHOGENESIS CAUSED BY SARS-COV-2

Received 13 December 2021;
Received in revised form 17 January 2022;
Accepted 20 January 2022

Ivan Reva^{1,2} , Tatsuo Yamamoto² ,
Kirill Stegnyy¹ , Ellada Slabenko¹ ,
Viktoriya Emiglasova¹ , Igor Sementsov¹,
Olga Lebed'ko⁴ , Marina Fleishman⁴ ,
Aleksy Kudelya¹ , Mariya Tuchina¹ ,
Viktor Usov , Yuriy Krasnikov ,
Ekaterina Mozhilevskaya¹ , Tatiana Lemeshko⁵,
Aleksy Novikov¹, Valeriy Tolmachev¹,
Galina Reva^{1,2} 

¹ Far Eastern Federal University, Vladivostok, Russia,

² International Medical Education and Research Center, Niigata, Japan,
Vladivostok, Russia,

³ Far Eastern State Medical University, Khabarovsk, Russia

⁴ Khabarovsk Branch of Far East Scientific Center of Respiratory Physiology
and Pathology, Research Institute of Maternity and Childhood Protection,
Khabarovsk, Russia

⁵ Pacific State Medical University, Vladivostok, Russia

✉ RevaGal@yandex.ru

ABSTRACT — With the emerging of new strains of the SARS-CoV-2 coronavirus (such as B.1.1.529 for example), despite numerous studies to create effective vaccines, it becomes obvious that the relevance of studying the pathomorphology of tissue structures with damaged cellular targets has increased manifold. Most knowledge on genes of pathogenicity loses its importance for the development of antiviral agents since the reservoir for the virus is the cells, in which SARS-CoV-2 then persists. These data are more important for the development of vaccines, and the treatment strategy should be based on damaged cellular targets. The mechanisms of hypoxia in patients infected by SARS-CoV-2 with COVID-19 do not have an exhaustive explanation based only on the acute alveolar damage. Our investigation deals with the data on pathologic red bone marrow in patients with a fatal COVID-19 outcome against the background of various indicators of erythrocytes in clinical blood tests. We found in the structure of the red bone marrow that there is damage to the stroma and parenchyma as well as pathomorphological signs of damage to erythropoiesis in the patients of both groups. The data obtained on the cellular targets of SARS-CoV-2 can serve as a fundamental platform for the development of targeted conservative therapy in the treatment of patients infected with SARS-CoV-2, and should also be taken into account in severe COVID-19 cases with the risk of unfavorable prognosis.

KEYWORDS — COVID-19; SARS-CoV-2, cytokine storm; red bone marrow; erythrocyte; hematopoiesis; hemoglobin; hypoxia; hemophagocytosis; macrophages.

RELEVANCE

The damaging effect on cells when SARS-CoV-2 enters the body has not been fully studied and in some cases is hypothetical [1, 2]. New strains of SARS-CoV-2 turned out to be more aggressive and contagious than the first ones registered, while the strain of coronavirus B.1.1.529, omicron-VOC, contain an unusually high number of mutations in the S-protein gene, which helps it to avoid the protective effect of antibodies. Chisholm S.T., Coaker G., Day B., Staskawicz B.J. (2006), Megahed FAK, Zhou X., Sun P. (2020) argue that monitoring virus-host interactions is critical to understanding the pathogenesis of the disease [3, 4], especially given the global problem of SARS-CoV-2 and COVID-19. It is known that infection or vaccination induces a population of long-lived bone marrow plasma cells (BMPC), which are a persistent and important source of protective antibodies [5]. However, at the present stage, it is not known whether SARS-CoV-2 is capable of inducing this population in patients with developing severe acute respiratory syndrome (SARS-CoV-2). Recent reports suggest that convalescent SARS-CoV-2 patients experience rapid degradation of antigen-specific serum antibodies, raising concerns that humoral immunity against this virus may be short-lived [6, 7, 8]. This puts the study of the pathogenesis of COVID-19 at the forefront of medical problems in terms of relevance [9, 10, 11]. To develop a specific treatment for COVID-19, there is not enough large-scale work on sequencing the genomes of a new pathogen to monitor the genetic variability of the coronavirus, therefore, there is no pathogenetically justified treatment of infected patients with COVID-19 at the present stage, as well as there is no comprehensive information about the reasons for the development of a cascade of body reactions, leading to death [12, 13]. The mechanisms of hypoxia are not always associated with damage to alveolocytes, which requires a scientific search for the reasons for a decrease in oxygenation of blood and tissues [14, 15]. The least studied damage and the role of morphological changes in the red bone marrow in the pathogenesis of COVID-19, which determined the direction of our research.

Aim of the research:

to analyze the role of red bone marrow in the pathogenesis of hypoxia in COVID-19.

MATERIAL AND METHODS

The research was carried out following the fundamental ethical principles of the Declaration of Helsinki, GCP Rules (Good Clinical Practice), and approved by the ethical commission of the Ministry of Education and Science of the Russian Federation. The diagnosis in COVID-19 patients caused by SARS-CoV-2 was confirmed by PCR. The tissue of the red bone marrow was taken from the deceased no later than 24 hours from the onset of death. In total, 67 biopsies of the red bone marrow were studied in the work, of which in 2 patients a clinical blood test showed erythropenia, and in the rest the number of erythrocytes was within normal limits. After separating the soft tissues of the chest and iliac region, using a sectional saw, fragments of the rib and ilium with bone marrow with dimensions of $1 \times 1 \times 0.5$ cm were taken. Biopsies were placed in buffered neutral 10% formalin from BIOVITRUM in a ratio of 1:20. The objects were fixed for 18-24 hours. After that, biopsies of red bone marrow were additionally placed in a decalcifying solution SoftDec (BIOVITRUM) in a ratio of 1:70. The material was kept for no more than 3 days. The decalcifying solution was replaced twice a day. During decalcification, bone fragments were checked with a medical alloy needle. Upon reaching the softness of the bone, it was removed from the decalcifying solution, placed in a container of 300–500 ml, fixed in a stationary state and continuously, with a weak flow of running water, washed for at least 2 hours. Then the material was carried out according to the standard protocol of embedding in paraffin and staining with hematoxylin and eosin. In each case, at least three preparations were observed with the analysis of at least 500 nuclear cells. Analysis of preparation and production of illustrations were carried out using an Olympus Bx52 microscope and a DP25 digital camera.

RESULTS OF RESEARCH AND DISCUSSION

A clinical analysis of the blood of deceased patients only in 2 out of 65 was characterized by erythropenia, the number of erythrocytes reached $1.4 \cdot 10^{12}/l$ and $2 \cdot 10^{12}/l$. The rest of the patients had quantitative parameters of erythrocytes within the normal range. However, the pathomorphological analysis of red bone marrow (BMC) preparations of patients with fatal outcomes showed that BMC is one of the participants in the pathological events in COVID-19 caused by SARS-CoV-2, and plays an important role in the pathogenesis of the cascade of reactions leading to hypoxia and death. infected patients. The bone marrow preparations were characterized by a decrease in the number of stromal elements, as well as qualitative and

quantitative changes in the structure of hematopoietic foci, not only erythrocyte germs but also granulocytic ones (Fig. 1).

For better clarity of the revealed pathomorphological features of the red bone marrow in patients who died as a result of the severe course of COVID-19 caused by SARS-CoV-2, the study results are presented in the form of illustrations performed with high magnification. The observed picture in patients with low erythrocyte counts in the blood was characterized by an almost complete absence of foci of erythropoiesis, in those who died from SARS-CoV-2 and a small number of macrophages containing granules of transferrin-bound iron (Fig. 2).

On preparations of the red bone marrow of this group of patients, 1–2 hypochromic, basophilic and oxyphilic erythrocytes are identified in the field of view, small or large, irregular in shape, as well as 1-2 macrophages in the field of view with iron granules and phagocytosed erythrocytes. Lymphocytes are characterized by brightly basophilic nuclei surrounded by a narrow rim of cytoplasm. Cells with fragmented or annular nuclei are also noted, indicating apoptosis. The blood vessels are identified, but the nuclei are hypertrophied and the cytoplasm is thinned.

In the material of patients who died from COVID-19 disease, against the background of low erythrocyte counts in the blood on the preparations of red bone marrow, there is a complete absence of stromal elements, blood vessels and reticular cells are not identified, macrophages are absent, oxyphilic erythroblasts with a homogeneously expanded cytoplasm are observed in a small amount. Hypochromic and polychromatophilic erythrocytes of irregular shape, eosinophilic granulocytes of varying degrees of maturity, mainly young and stab, are identified. In addition to eosinophils, stab neutrophils are also detected (Fig. 3).

Numerous pathological forms of hypochromic erythrocytes, lymphocytes, eosinophils, a small number of macrophages without granular inclusions in the cytoplasm are identified in the field of view. The presence of polychromatophilic non-nuclear erythrocytes indicates impaired differentiation and specialization of erythrocytes. The wall of the preserved sinusoidal capillaries is represented by the endothelium with intermittent thinned cytoplasm, with hypertrophied nuclei, in the lumen of which polychromatophilic erythrocytes are identified, thinned or destroyed sinusoidal capillaries and the reticular stroma of the CCM are also identified. Single megakaryocytes are found near the capillary wall. There are no normal erythrocytes, poikilo- and anisocytosis are noted, few spherocytes, hypochromic erythrocytes with Howell-Jolly bodies, Conde rings.

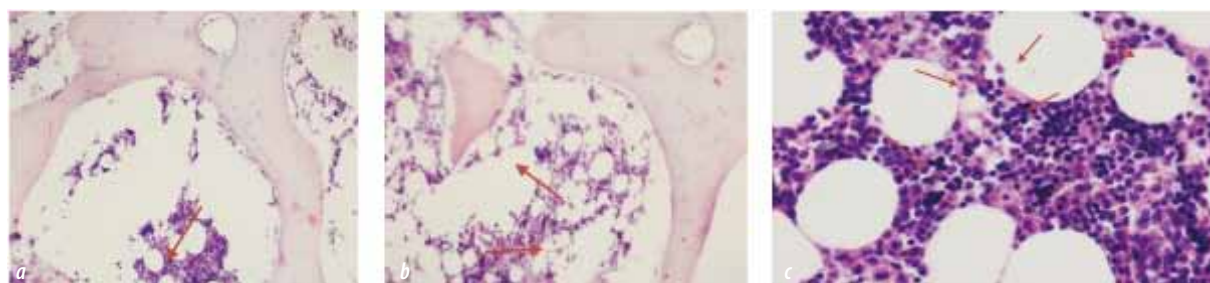
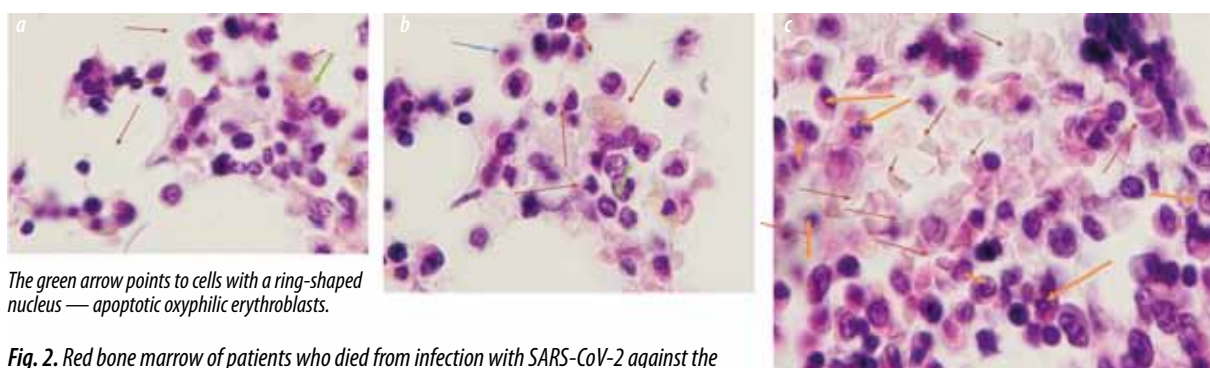


Fig. 1. Red bone marrow of deceased patients infected with SARS-CoV-2. A, b) red bone marrow of the deceased against the background of low erythrocyte counts; c) red bone marrow of a patient who died from infection with SARS-CoV-2 against the background of erythrocyte counts within normal limits. Microphoto. Staining with hematoxylin and eosin. Magnification a, b) $\times 100$; c) $\times 200$



The green arrow points to cells with a ring-shaped nucleus — apoptotic oxyphilic erythroblasts.

Fig. 2. Red bone marrow of patients who died from infection with SARS-CoV-2 against the background of erythrocyte counts within normal limits. Staining with hematoxylin and eosin. Microphoto. Magnification a, b, c) $\times 400$.

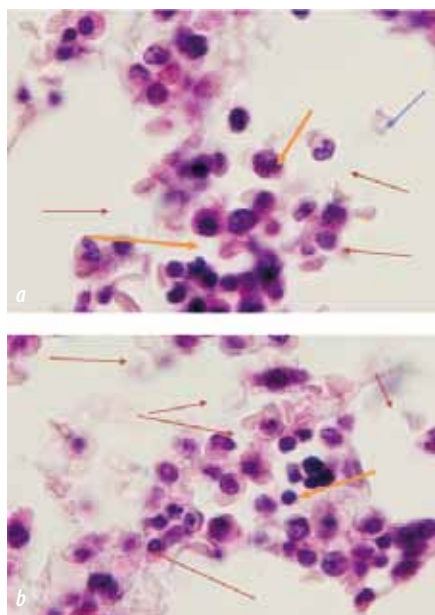


Fig. 3. Red bone marrow of patients infected with SARS-CoV-2 who died against the background of low red blood cell counts in the clinical blood test. Staining with hematoxylin and eosin. Microphoto. Magnification a, b) $\times 400$.

Oxyphilic erythroblasts with annular nuclei, which are signs of apoptosis, surround macrophages.

Formerly H. Chandra, S. Chandra, Rm. Kaushik, Nk. Bhat, V. Shrivastava (2014) in bone marrow aspirates, the phenomena of hemophagocytosis, which is a life-threatening condition, were described based on the identification of macrophages with phagocytosed neutrophils and a large number of plasma cells in pancytopenia and erythroid hyperplasia [16]. Many coronaviruses cause autophagy. Monitoring and analysis of intercellular interactions under the influence of viral cellular behavior are critical for understanding the pathogenesis of the disease for the development of prevention and targeted treatment through the protection and regeneration of damaged targets. These studies are of particular importance because of the global problem of COVID-19 caused by the increasingly aggressive strains of SARS-CoV-2 [18].

CONCLUSION

The red bone marrow of COVID-19 patients who died of multiple organ failure, depending on the clinical parameters of the content of erythrocytes in the blood, morphologically differs from the red bone marrow of patients who died from complications of concomitant diseases, the absence of intact foci of erythropoiesis. With indicators of severe erythropenia in the blood of patients, disruption of erythropoiesis in the red bone marrow should be assumed, which should be taken into account when developing a

treatment strategy for this group of patients. Understanding of spectrum and frequency of histological findings in COVID-19 is essential for a better image of the pathogenetic aspects of the disease mechanisms and the prospects for predicting favorable outcomes. Hemophagocytosis, noted in the red bone marrow of dead patients, even in rare cases, must be taken into account in the study protocols since it is a marker of deep damage not only to the central organ of hematopoiesis, like red bone marrow but also to the systems involved in the regulation of hematopoiesis, leading to hypoxia and death.

Pancytopenia and cell hyperplasia of the erythroid lineage were frequent hematological manifestations. Moderate to severe hemophagocytosis was observed in the red bone marrow of the deceased. The study concluded that hemophagocytosis, even if observed in single cells, should always be documented in bone marrow reports. Bone marrow aspirates should be included in the differential diagnosis of COVID-19 caused by SARS-CoV-2. This may be the only sign of the development of COVID-19 infection caused by SARS-CoV-2, with damage to the red bone marrow and with the prediction of a severe course of COVID-19, as well as for the development of a pathogenetically based strategy. Thus, hypoxia in COVID-19 is associated not only with damage to the alveolar epithelium but also due to damage to the stroma and blood vessels of the BMC, abnormal activity of lymphocytes and macrophages in the tissue of the red bone marrow, as well as disturbances in the regulation system of hemoglobin synthesis and damage to erythrocyte diferon and erythropenia, which leads to impaired cellular respiration and severe damage to organs involved in the synthesis of erythropoietin.

REFERENCES

1. SCOTT MINERS, PATRICK G KEHOE, SETH LOVE. Cognitive impact of COVID-19: looking beyond the short term. // *Alzheimers Res Ther*. 2020 Dec 30;12(1):170. doi: 10.1186/s13195-020-00744-w
2. SEYED HOSSEINI E., RIAHI KASHANI N., NIKZAD H., AZADBAKHT J., HASSANI BAFRANI H., HADDAD KASHANI H.. The novel coronavirus Disease-2019 (COVID-19): Mechanism of action, detection and recent therapeutic strategies. *Virology*. 2020 Dec;551:1-9. doi: 10.1016/j.virol.2020.08.011
3. CHISHOLM S.T., COAKER G., DAY B., STASKAWICZ B.J. Host-microbe interactions: shaping the evolution of the plant immune response. *Cell*. 2006 Feb 24;124(4):803-14. doi: https://doi.org/10.1016/j.cell.2006.02.008
4. MEGAHEH F.A.K., ZHOU X., SUN P. The Interactions between HBV and the Innate Immunity of Hepatocytes. *Viruses*. 2020 Mar 5;12(3):285. doi: 10.3390/v12030285
5. TURNER J.S., KIM W., KALAIIDINA E, GOSS C.W., RAUSEO A.M., SCHMITZ A.J., HANSEN L, HAILE A., KLEBERT M.K., PUSIC I., O'HALLORAN J.A., PRESTI R.M., ELLEBEDY AH. SARS-CoV-2 infection induces long-lived bone marrow plasma cells in humans. *Res Sq* [Preprint]. 2020 Dec 31:rs.3.rs-132821. doi: 10.21203/rs.3.rs-132821/v1.Update in: *Nature*. 2021 May 24:: PMID: 33398264; PMCID: PMC7781328.
6. GAEBLER C., WANG Z., LORENZI J.C.C., MUECKSCH F., FINKIN S., TOKUYAMA M., CHO A., JANKOVIC M., SCHAEFER-BABAJEW D., OLIVEIRA T.Y., CIPOLLA M., VIANI C., BARNES C.O., BRAM Y., BRETON G., HÄGGLÖF T., MENDOZA P., HURLEY A., TURROJA M., GORDON K., MILLARD K.G., RAMOS V., SCHMIDT F., WEISBLUM Y., JHA D., TANKELEVICH M., MARTINEZ-DELGADO G., YEE J., PATEL R., DIZON J, UNSON-O'BRIEN C., SHIMELIOVICH I., ROBBIANI D.F., ZHAO Z., GAZUMYAN A., SCHWARTZ R.E., HATZIOANNOU T., BJORKMAN P.J., MEHANDRU S., BIENIASZ P.D., CASKEY M. NUSSENZWEIG M.C.. Evolution of antibody immunity to SARS-CoV-2. *Nature*. 2021 Mar;591(7851):639-644. doi: 10.1038/s41586-021-03207-w
7. KIRTIPAL N., BHARADWAJ S., KANG S.G. From SARS to SARS-CoV-2, insights on structure, pathogenicity and immunity aspects of pandemic human coronaviruses. *Infect Genet Evol*. 2020 Nov;85:104502. doi: 10.1016/j.meegid.2020.104502
8. LACZKÓ D., HOGAN M.J., TOULMIN S.A., HICKS P., LEDERER K., GAUDETTE B.T., CASTAÑO D., AMANAT F., MURAMATSU H., OGUIN T.H. 3RD, OJHA A., ZHANG L., MU Z., PARKS R., MANZONI T.B., ROPER B., STROHMEIER S., TOMBÁČZ I., ARWOOD L., NACHBAGAUER R., KARIKÓ K., GREENHOUSE J., PESSANT L., PORTO M., PUTMAN-TAYLOR T., STRASBAUGH A., CAMPBELL T.A., LIN P.J.C., TAM Y.K., SEMPOWSKI G.D., FARZAN M., CHOE H., SAUNDERS K.O., HAYNES B.F., ANDERSEN H., EISENLOHR L.C., WEISSMAN D., KRAMMER F., BATES P., ALLMAN D., LOCCI M., PARDI N.. A Single Immunization with Nucleoside-Modified mRNA Vaccines Elicits Strong Cellular and Humoral Immune Responses against SARS-CoV-2 in Mice. *Immunity*. 2020 Oct 13;53(4):724-732.e7. doi: https://doi.org/10.1016/j.immuni.2020.07.019
9. WALSH K.A., JORDAN K., CLYNE B., ROHDE D., DRUMMOND L., BYRNE P., AHERN S., CARTY P.G., O'BRIEN K.K., O'MURCHU E., O'NEILL M., SMITH S.M., RYAN M., HARRINGTON P. SARS-CoV-2 detection, viral load and infectivity over the course of an infection. *J Infect*. 2020 Sep;81(3):357-371. doi: 10.1016/j.jinf.2020.06.067
10. Y. A. MALIK. Properties of Coronavirus and SARS-CoV-2. *Malays J. Pathol*. 2020 Apr;42(1):3-11.
11. RODRÍGUEZ HERNÁNDEZ C., SANZ MORENO L. Inmunidad frente a SARS-CoV-2: caminando hacia la vacunación [Immunity against SARS-CoV-2: walking to the vaccination]. *Rev Esp Quimioter*.

- 2020 Dec;33(6):392–398. Spanish. doi: 10.37201/req/086.2020
12. **KATELYN MILLER, MARISA E. MCGRATH, ZHI-QIANG HU, SOHHA ARIANNEJAD, STUART WESTON, MATTHEW FRIEMAN, WILLIAM T JACKSON.** Coronavirus interactions with the cellular autophagy machinery. *Autophagy*. 2020 Dec;16(12):2131–2139. doi: 10.1080/15548627.2020.1817280
 13. **BELLO-PEREZ M, SOLA I, NOVOA B, KLIONSKY DJ, FALCO A.** Canonical and Noncanonical Autophagy as Potential Targets for COVID-19. *Cells*. 2020 Jul 5;9(7):1619. doi: <https://doi.org/10.3390/cells9071619>
 14. **CAVEZZI A., TROIANI E., CORRAO S..** COVID-19: hemoglobin, iron, and hypoxia beyond inflammation. A narrative review. *Clin Pract*. 2020 May 28;10(2):1271. doi: 10.4081/cp.2020.1271
 15. **HERNÁNDEZ A., VIÑALS M., ISIDORO T., VILÁS F.** Potential Role of Oxygen-Ozone Therapy in Treatment of COVID-19 Pneumonia. *Am J Case Rep*. 2020 Aug 17;21:e925849. doi: 10.12659/AJCR.925849
 16. **H. CHANDRA, S. CHANDRA, RM KAUSHIK, NK BHAT, V SHRIVASTAVA.** Hemophagocytosis on bone marrow aspirate cytology: single center experience in north himalayan region of India. *Ann Med Health Sci Res*. 2014 Sep;4(5):692-6. doi: 10.4103/2141-9248.141515
 17. **GRIESEMER S.B., VAN SLYKE G., EHRLER D., STRLE K., YILDIRIM T., CENTURIONI D.A., WALSH A.C., CHANG A.K., WAXMAN M.J., ST GEORGE K..** Evaluation of Specimen Types and Saliva Stabilization Solutions for SARS-CoV-2 Testing. *J. Clin Microbiol*. 2021 Apr 20;59(5):e01418-20. doi: 10.1128/JCM.01418-20
 18. **NORRIS V, OVÁDI J.** Role of Multifunctional Cytoskeletal Filaments in Coronaviridae Infections: Therapeutic Opportunities for COVID-19 in a Nutshell. *Cells*. 2021 Jul 19;10(7):1818. doi: <https://doi.org/10.3390/cells10071818>

<http://dx.doi.org/10.35630/2199-885X/2022/12/2.24>

THE EFFECT OF MELATONIN ON ELECTROLYTE AND WATER-RETENTION RENAL DYSFUNCTION IN CHRONIC ALCOHOL INTOXICATION ASSOCIATED WITH AUTOIMMUNE NEPHRITIS: AN EXPERIMENTAL RAT MODEL

Received 14 March 2022;
Received in revised form 25 March 2022;
Accepted 26 March 2022

Vadim Brin^{1,2} , Vladlen Zemlianoy¹

¹ North Ossetian State Medical Academy, Vladikavkaz;

² Institute of Biomedical Research, Vladikavkaz Research Center, Russian Academy of Sciences, Vladikavkaz, Russia

✉ vbbrin@yandex.ru

ABSTRACT — Autoimmune nephritis represents one of the frequent types of kidney pathology. With rates of alcohol consumption being on the rise, it is crucial to study the effects of alcohol abuse on the manifestations of nephropathy. Since the activation of lipid peroxidation plays a significant role in the formation of autoimmune and alcoholic nephropathy, it appears relevant to investigate the potential positive effects of a natural antioxidant, melatonin. THE AIM OF THE STUDY was to investigate the effect of melatonin on renal function in chronic alcohol intoxication associated with autoimmune nephritis. MATERIAL AND METHODS. The characteristics of changes in electrolyte and water excretory functions of the kidneys in Wistar rats with chronic alcohol intoxication associated with autoimmune nephritis were examined. Experimental chronic alcohol intoxication was obtained by daily intragastric injection through an atraumatic tube of 40% ethanol solution and the administration of isovaleric acid amide solution for 30 days. The model of autoimmune nephritis was obtained via a single subcutaneous injection of an emulsion of complete Freund's adjuvant with an equal volume of a mixture of kidney cortical homogenate at five points. Melatonin was administered intragastrically at a dose of 10 mg/kg for one month.

RESULTS. Alcohol intoxication was found to increase the degree of renal dysfunction in autoimmune nephritis. The administration of melatonin as a preventative agent led to a significant reduction in manifestations of nephropathy.

CONCLUSIONS. Alcohol intoxication may exacerbate the manifestations of autoimmune nephritis. The administration of melatonin in chronic alcohol intoxication associated with autoimmune nephritis leads to the reduction in the severity of pathological changes in the electrolyte-excretory function of the kidneys.

KEYWORDS — chronic alcohol intoxication, autoimmune nephritis, melatonin, nephrotoxicity.

INTRODUCTION

Previous studies have shown a decline in alcohol consumption in Russia since 2007, as in many other developed countries [1,2]. However, since the second quarter of 2020, when *stay-at-home* restrictions were first introduced to contain the spread of coronavirus infection, self-isolation and unemployment have been the trigger for a sharp rise in per capita ethanol consumption. Chronic alcohol intoxication causes the destruction of the normal renal microstructure, increases the distance between capillaries and renal tubular cells, and damages capillaries that supply oxygen and nutrients to renal tubular cells. Damage to renal tubular cells can lead to renal interstitial fibrosis, which in turn impairs renal function [3]. Thus, due to spread of infectious diseases, which create a favorable environment for autoimmune diseases, the growth of autoimmune disorders, including autoimmune nephritis, has been noticed. Autoimmune disorders are a major cause of chronic kidney disease, accounting for about 10% of all patients on dialysis [4].

Ways of treating multi-organ alcohol-related damage associated with autoimmune nephritis have received little attention in modern experimental studies. The prevention of chronic alcohol intoxication associated with autoimmune nephritis presents a pressing issue. The activation of lipid peroxidation plays a significant role in the pathogenesis of autoimmune nephritis and alcoholic kidney damage. In this regard, it appears relevant to study the effects of the natural antioxidant melatonin. Melatonin as a preventative medication has a positive effect in toxic nephropathies caused by heavy metals, such as those caused by long-term lead intoxication, which was confirmed by significant changes in the parameters of renal functions, systemic haemodynamics and biochemical blood parameters [6].

The aim of the present study

was to investigate the effect of melatonin on renal function in chronic alcohol intoxication associated with autoimmune nephritis.

METHODS

The research was performed in white male Wistar rats weighing 200–300g split into 12 groups (n=120): 1) background (intact) animals; 2) the group subjected to intragastric administration of melatonin at a dose of 10 mg/kg 3) the group subjected to intragastric administration of 40% ethanol at a dose of 3.0 g/kg for a month; 4) the group subjected to intragastric administration of 40% ethanol at a dose of 3.0 g/kg and melatonin at a dose of 10 mg/kg for a month 5) the group subjected to intragastric administration of isovaleric acid amide solution (alcohol dehydrogenase inhibitor) at a dose of 500 mg/kg for a month; 6) the group subjected to intragastric administration of isovaleric acid amide solution at a dose of 500 mg/kg and melatonin at a dose of 10 mg/kg for a month; 7) the group subjected to intragastric administration of isovaleric acid amide solution at a dose of 500 mg/kg together with 40% ethanol at a dose of 3.0 g/kg every day for 30 days (a model of chronic alcohol intoxication) [7]; 8) the group with the model of chronic alcohol intoxication subjected to intragastric administration of melatonin at a dose of 10 mg/kg every day for 30 days 9) the group of rats subjected to subcutaneous injection of Freund's complete adjuvant emulsion with an equal volume of a mixture of kidney cortex homogenate, pre-diluted with saline, at the rate of 1.0 ml of saline per 100.0 mg of tissue. The solution was injected once subcutaneously into five locations: axillary and inguinal areas, intraperitoneally 0.1 ml of the active solution per 100 g of animal weight (a model of autoimmune nephritis) [8]; 10) the model of autoimmune nephritis with intragastric administration of melatonin at a dose of 10 mg/kg for a month; 11) a model of chronic alcohol intoxication against autoimmune nephritis for 30 days; 12) the model of chronic alcohol intoxication associated with autoimmune nephritis subjected to intragastric administration of melatonin at a dose of 10 mg/kg for a month.

During the experiment, the animals were given a standard diet and had free access to water and food throughout the day. Light conditions were natural. The electrolyte- and water-excretory functions of the kidneys during spontaneous diuresis were studied. To assess renal function, animals were placed in exchange cages, where urine was collected for 6 hours. The following parameters were assessed: urine output volume, glomerular filtration rate, relative tubular water reabsorption, cations excretion level (potassium, sodium), protein content in urine. Contents of sodium and potassium in serum and urine were determined by ion-selective method using the electrolyte analyzer AEK-1 ("Kverti-Med").

Functional renal condition was assessed with conventional research methods [9] involving the application of biochemical reagent kits ("Olvex" and "Agat-Med") for the analysis of urine and blood plasma and further sample processing with the "Solar" spectrophotometer.

Experiments were performed in accordance with "International Guiding Principles for Biomedical Research Involving Animals" (1985), the 11th article of the WMA Declaration of Helsinki and the rules of laboratory practice in the Russian Federation (order of 01.04.2016 № 199).

The results obtained were statistically processed with consideration of the features of distribution within the groups using the Shapiro-Wilk criterion. Nonparametric Mann-Whitney U-criterion was applied to compare the data across the groups. Statistical analysis was performed using the standard Microsoft Excel 2016 and Statistica 10.0 software packages. Differences were considered reliable at $p \leq 0.05$.

RESULTS

The study of water-excretory function during 6 hours of spontaneous diuresis revealed no reliable changes in the functional renal condition in the control groups 2–6.

A decrease in spontaneous 6-hour diuresis ($p \leq 0.01$) was observed in Group 7 (a model of chronic alcohol intoxication), which is associated with a decrease in glomerular filtration rate ($p \leq 0.01$), contrary to the trend towards reduction in tubular water reabsorption (Table 1). We also observed an increase in urinary protein concentration ($p \leq 0.001$) (Table 1). In Group 8 (prophylactic administration of melatonin in a model of chronic alcohol intoxication), we observed an increase in spontaneous diuresis and tubular water reabsorption ($p \leq 0.05$) compared to Group 7; as well as a decrease in urinary protein content ($p \leq 0.001$) (Table 1).

In Group 9 (a model of autoimmune nephritis), a decrease in 6-hour spontaneous diuresis ($p \leq 0.05$), and a decrease in tubular water reabsorption ($p \leq 0.05$) and glomerular filtration rate ($p \leq 0.05$) relative to intact values were observed. In the Group 10 (prophylactic administration of melatonin in a model of autoimmune nephritis) we observed an increase in tubular water reabsorption ($p \leq 0.05$), as well as a decrease in urinary protein concentration ($p \leq 0.01$) compared to Group 9.

Group 11 (a model of chronic alcohol intoxication in autoimmune nephritis) revealed a marked decrease in 6-hour spontaneous diuresis ($p \leq 0.01$) relative to baseline values, associated with decreased glomerular filtration rate ($p \leq 0.001$), despite the trend

Table 1. Basic urine formation and urine protein content indicators in rats under conditions of spontaneous diuresis in chronic alcohol intoxication in the setting of autoimmune nephritis

Experimental conditions	Urine output, (ml/h/100 g)	Glomerular filtration rate, (ml/h/100 g)	Relative tubular water reabsorption (%)	Urine protein concentration (mg/ml)
Intact animals	0,092±0,004	19,8±1,41	99,53±0,012	0,137±0,012
Group 2 (melatonin administered at 10 mg/kg)	0,098±0,0031	20,3±1,122	99,54±0,014	0,0987±0,0044
	-	-	-	-
Group 3 (40% ethanol at 3.0g/kg administered for 1 month)	0,087±0,007	17,9±1,5	99,51±0,010	0,156±0,007
	-	-	-	-
Group 4 (40% ethanol at 3.0g/kg and melatonin at 10mg/kg administered for 1 month)	0,090±0,0034	18,422±1,212	99,523±0,012	0,155±0,0086
	-	-	-	-
Group 5 (isovaleric acid amide solution administered at 500 mg/kg for a month)	0,085±0,008	18,6±1,65	99,54±0,011	0,156±0,013
	-	-	-	-
Group 6 (isovaleric acid amide solution at 500 mg/kg and melatonin at 10 mg/kg administered for a month)	0,081±0,0052	18,425±1,322	99,548±0,014	0,114±0,0102
	-	-	-	-
Group 7 (model of chronic alcohol intoxication)	0,073±0,005 (**)	14,3±0,9 (**)	99,49±0,009 (**)	0,401±0,023 (***)
Group 8 (model of chronic alcohol intoxication with daily administration of melatonin at 10 mg/kg for a month)	0,087±0,0021 (#)	16,835±0,873 -	99,517±0,011 (#)	0,221±0,0145 (***)###)
Group 9 (model of autoimmune nephritis)	0,076±0,004 (*)	15,4±1,0 (*)	99,5±0,009 (*)	0,394±0,033 (***)
Group 10 (model of autoimmune nephritis with melatonin administered at 10 mg/kg for a month)	0,086±0,0024 -	17,842±0,755 -	99,527±0,007 (!)	0,266±0,0176 (***)!!!)
Group 10 (model of chronic alcohol intoxication against autoimmune nephritis)	0,061±0,003 (***)	11,6±0,75 (***)	99,46±0,011 (***)	0,647±0,01 (***)
Group 12 (model of chronic alcohol intoxication against autoimmune nephritis with melatonin administered at 10 mg/kg for a month)	0,079±0,0026 (*)♣♣♣) ▲▲)	16,844±0,657 (♣♣♣)	99,513±0,010 (♣♣)	0,343±0,0339 (***)♣♣♣)▲▲▲)

Notes: (*) – $p \leq 0,05$; (**) – $p \leq 0,01$; (***) – $p \leq 0,001$ vs background
 (#) – $p \leq 0,05$; (##) – $p \leq 0,01$; (###) – $p \leq 0,001$ vs Group 7
 (▲) – $p \leq 0,05$; (▲▲) – $p \leq 0,01$; (▲▲▲) – $p \leq 0,001$ vs Group 8
 (!) – $p \leq 0,05$; (!!) – $p \leq 0,01$; (!!!) – $p \leq 0,001$ vs Group 9
 (♣) – $p \leq 0,05$; (♣♣) – $p \leq 0,01$; (♣♣♣) – $p \leq 0,001$ vs Group 13

towards a reduction in tubular water reabsorption ($p \leq 0.001$). Urine protein concentration was significantly increased compared to background (intact animal) values ($p \leq 0.001$).

In Group 12 (prophylactic administration of melatonin in a model of chronic alcohol intoxication in autoimmune nephritis), an increase in spontaneous diuresis ($p \leq 0.001$) and glomerular filtration rate ($p \leq 0.001$) compared to the melatonin-free Group 11 was observed. Tubular reabsorption of water also increased ($p \leq 0.01$; Table 1) compared to Group 11.

The study of electrolyte excretion function under the conditions of 6-hour spontaneous diuresis revealed no reliable changes in renal functions in the control groups 2-6 (see Table 2).

An increase in sodium ($p \leq 0.01$) and potassium excretion ($p \leq 0.001$) compared to background (intact animals) values was observed in Group 7 (a model of chronic alcohol intoxication). Sodium filtration charge ($p \leq 0.001$) and tubular cation reabsorption ($p \leq 0.001$) showed a decrease. Blood sodium concentration ($p \leq 0.05$) decreased, whereas blood potassium concentration significantly increased ($p \leq 0.01$). In Group 8 (prophylactic use of melatonin in a model of chronic alcohol intoxication), we observed an increase in sodium ($p \leq 0.05$) and potassium ($p \leq 0.05$) excretion compared to Group 7. Tubular reabsorption of sodium ($p \leq 0.05$) was shown to increase; there was also an increase in blood sodium concentration ($p \leq 0.05$) and a decrease in plasma potassium concentration

Table 2. Renal electrolyte processing indicators (sodium, potassium) and their concentrations in blood plasma in rats in a model of chronic alcohol intoxication in autoimmune nephritis

Experimental conditions	Sodium excretion ($\mu\text{mol/hr/100g}$)	Sodium filtration charge ($\mu\text{mol/hr/100g}$)	Sodium channel reabsorption (%)	Blood sodium levels (mmol/l)	Potassium excretion ($\mu\text{mol/hr/100g}$)	Potassium filtration charge ($\mu\text{mol/hr/100g}$)	Blood potassium levels (mmol/l)
Intact animals	7,84 \pm 0,37	2696 \pm 164	99,7 \pm 0,032	145 \pm 1,69	4,4 \pm 0,39	85,7 \pm 7,58	4,45 \pm 0,28
Group 2 (melatonin administered at 10 mg/kg)	7,77 \pm 0,6556	2746,44 \pm 142	99,717 \pm 0,028	144,656 \pm 1,53	4,290 \pm 0,41	87,39 \pm 7,15	4,570 \pm 0,31
Group 3 (40% ethanol at 3.0g/kg administered for 1 month)	8,93 \pm 1,09	2420 \pm 202	99,6 \pm 0,035	143 \pm 0,75	5,2 \pm 0,45	80,2 \pm 6,7	4,7 \pm 0,17
Group 4 (40% ethanol at 3.0g/kg and melatonin at 10mg/kg administered for 1 month)	7,81 \pm 0,6435	2610,42 \pm 213	99,701 \pm 0,0312	143,843 \pm 0,523	4,864 \pm 0,3334	84,32 \pm 7,1332	4,622 \pm 0,142
Group 5 (isovaleric acid amide solution administered at 500 mg/kg for a month)	7,83 \pm 0,61	2518 \pm 223	99,7 \pm 0,02	144 \pm 0,8	5,1 \pm 0,5	92,6 \pm 8,2	4,79 \pm 0,1
Group 6 (isovaleric acid amide solution at 500 mg/kg and melatonin at 10 mg/kg administered for a month)	7,92 \pm 0,8051	2575,11 \pm 210	99,692 \pm 0,0267	145,456 \pm 0,643	5,142 \pm 0,4233	94,85 \pm 7,3340	4,335 \pm 0,213
Group 7 (model of chronic alcohol intoxication)	9,24 \pm 0,31 **)	1891 \pm 118 ***)	99,5 \pm 0,03 ***)	140 \pm 1,28 *)	6,4 \pm 0,34 ***)	66,9 \pm 5,9 -	5,44 \pm 0,25 **)
Group 8 (model of chronic alcohol intoxication with daily administration of melatonin at 10 mg/kg for a month)	8,11 \pm 0,4340 #)	2247,14 \pm 104 -	99,639 \pm 0,0264 *)#)	143,755 \pm 0,835 #)	5,414 \pm 0,3022 #)	82,46 \pm 4,5330 -	4,327 \pm 0,266 ##)
Group 9 (model of autoimmune nephritis)	9,09 \pm 0,43 *)	2074 \pm 132 **)	99,6 \pm 0,032 **)	141 \pm 1,09 *)	5,9 \pm 0,48 **)	67,7 \pm 4,3 *)	5,2 \pm 0,15 **)
Group 10 (model of autoimmune nephritis with melatonin administered at 10 mg/kg for a month)	7,89 \pm 0,4055 -	2534,12 \pm 185 -	99,689 \pm 0,0232 !)	144,344 \pm 1,134 !)	4,456 \pm 0,4253 !)	78,59 \pm 3,3430 -	4,533 \pm 0,185 !)
Group 10 (model of chronic alcohol intoxication against autoimmune nephritis)	10,22 \pm 0,35 ***)	1530 \pm 139 ***)	99,3 \pm 0,054 ***)	139 \pm 1,2 **)	7,5 \pm 0,34 ***)	53,4 \pm 5,2 **)	5,7 \pm 0,13 ***)
Group 12 (model of chronic alcohol intoxication against autoimmune nephritis with melatonin administered at 10 mg/kg for a month)	8,58 \pm 0,4013 ♣♣)	2136,76 \pm 154 ♣♣)	99,599 \pm 0,0425 ♣♣♣)	142,235 \pm 0,755 ♣♣)	5,653 \pm 0,2554 *)♣♣♣)	69,66 \pm 4,7440 *)♣♣)	4,752 \pm 0,135 ♣♣♣)

Notes: see Table 1.

($p \leq 0.01$; Table 2). Obtained results are consistent with previously published literature [12].

In Group 9 (a model of autoimmune nephritis), we observed an increase in sodium ($p \leq 0.05$) and potassium ($p \leq 0.01$) excretion compared to baseline values. Sodium filtration charge ($p \leq 0.01$) and tubular cation reabsorption ($p \leq 0.001$) decreased. Blood sodium concentration ($p \leq 0.05$) decreased, whereas blood potassium concentration significantly increased

($p \leq 0.01$) (Table 2). We observed a decrease in potassium excretion ($p \leq 0.05$) in Group 10 (prophylactic administration of melatonin in autoimmune nephritis) compared to Group 9, as well as an increase in blood sodium concentration ($p \leq 0.05$) and a decrease in plasma potassium concentration ($p \leq 0.05$; Table 2).

In Group 11 (chronic alcohol intoxication in autoimmune nephritis), we observed an increase in urine excretion of sodium ($p \leq 0.01$) and potassium

($p \leq 0.001$). The decrease in sodium levels ($p \leq 0.05$) was associated with high urinary sodium losses due to renal tubular damage and decreased tubular cation reabsorption ($p \leq 0.001$; Table 2), despite a significant decrease in cation filtration charge. Potassium filtration charge tended to decrease due to decreased glomerular water filtration rate ($p \leq 0.01$), but cation excretion was still higher than that in controls ($p \leq 0.001$), probably due to changes in tubular cation processing under hyperpotasemia ($p \leq 0.05$). In the Group 12 (prophylactic use of melatonin in a model of chronic alcohol intoxication in autoimmune nephritis), we observed a decrease in sodium ($p \leq 0.01$) and potassium excretion ($p \leq 0.001$). Filtration charge of potassium ($p \leq 0.01$) and sodium ($p \leq 0.01$; Table 2) showed an increase compared to the group without prophylactic administration of melatonin.

DISCUSSION

Thus, it was found that chronic alcohol intoxication against the background of autoimmune nephritis was associated with a more pronounced decrease in the volume of 6-hour spontaneous diuresis than alcohol intoxication without concomitant renal pathology. This is probably due to dystrophic changes in the tubular epithelium and linear deposits of IgG and complement component C3 along the glomerular basal membranes, which occurs in autoimmune renal damage [10]. The increase in protein concentration in urine was also more pronounced than in chronic alcohol intoxication without concomitant pathology. In the experimental group with simulated chronic alcohol intoxication in autoimmune nephritis, we observed a decrease in sodium levels related to high urinary sodium losses due to renal tubular apparatus damage and decreased tubular reabsorption of cations. Potassium filtration charge was significantly decreased due to decreased glomerular water filtration rate, but cation excretion was still higher than in controls, probably due to changes in tubular cation processing under the conditions of hyperpotasemia. These changes are most likely related to the deposition of circulating immune complexes in renal structures, which is accompanied by the activation of monocytes and macrophages, resulting in increased damage to the endothelium of the glomerular vessels, apoptosis and disruption of blood flow in the microcirculatory channel [11]. Administration of melatonin as a preventative agent in chronic alcohol intoxication associated with autoimmune nephritis contributed to the restoration of spontaneous diuresis indicators and glomerular filtration rate compared to the melatonin-free group; we also observed an increase in tubular water reabsorption, which is probably associated with one of the

main preventive effects of melatonin manifesting in the increased sensitivity of the renal tubular apparatus to endogenous regulators. The positive effect of melatonin in toxic nephropathies has also been confirmed in the literature, where it is reported that it may reduce the severity of lipid peroxidation processes in renal cellular structures and the amount of reactive oxygen species, and also may exert immunomodulatory effects [12].

CONCLUSIONS AND KEY POINTS

1. Alcohol intoxication intensifies the manifestations of autoallergic nephritis. 2. The use of melatonin in chronic alcohol intoxication associated with autoimmune nephritis leads to a decrease in the severity of pathological changes in renal function.

Contributors

The aim, the objectives and planning of research — V.Brin; the experiments — V.Zemlianoy.

REFERENCES

1. MENG Y, HOLMES J, HILL-MCMANUS D, BRENNAN A, MEIER PS. Trend analysis and modelling of gender-specific age, period and birth cohort effects on alcohol abstinence and consumption level for drinkers in Great Britain using the general lifestyle survey 1984–2009. *Addiction* 2014; 109:206–15.
2. LASOTA, D., PAWŁOWSKI, W., MIROWSKA-GUZEL, D., GONIEWICZ, K., & GONIEWICZ, M. Ethanol as a stimulus to risky and auto-aggressive behaviour. *Annals of agricultural and environmental medicine* : AAEM, 2021. 28(2), 220–223. <https://doi.org/10.26444/aaem/118861>
3. J. S. FARIAS, K. M. SANTOS, N. K. S. LIMA ET AL. Maternal endotoxemia induces renal collagen deposition in adult offspring: role of NADPH oxidase/TGF- β 1/MMP-2 signaling pathway. *Archives of Biochemistry and Biophysics*, 2020. vol. 684, no. 5, pp. 306–312.
4. C. F. KREBS, T. SCHMIDT, J. H. RIEDEL, U. PANZER, T helper type 17 cells in immune-mediated glomerular disease. *Nat. Rev. Nephrol.* 2017. V.13, P.647–659.
5. V. B. BRIN, A. K. MITTSIEV & K. G. MITTSIEV. Method of correction of nephrotoxic action of cadmium in experiment. *Journal of New Medical Technologies*, 2011. XVIII (2), 194–195. (in Rus.)
6. M.R. BUZOEVA. Effect of melaxen on the functional state of the kidneys, lipid peroxidation and metal accumulation in rats in the presence of combined application of cadmium, lead and zinc salts. *East European Scientific Journal*, 2021. 4-3 (68), p.25–30. (in Rus.)
7. V.B. BRIN, V.M. ZEMLIANOY, N.V. SOKOLOVSKY, E.M. GAGLOEVA. Method of chronic alcohol intoxication modeling in rats in experiment. Patent RU № 2740569 C1, 15.01.2021. Bulletin number 2. (in Rus)

8. **PUSEY C.D., HOLLAND M.J., CASHMAN S.J. SINICO R.A., LLOVERAS J.J., EVANS D.J., LOCKWOOD C.M.** Experimental autoimmune glomerulonephritis induced by homologous and isologous glomerular basement membrane in Brown-Norway rats. *Nephrol Dial Transplant.* 1991;6(7):57–65.
9. **Y.V. NATOCHIN**, Physiology of the Kidney: Formulas and Calculations. L. Nauka. 1974. – 56 p. (in Rus.)
10. **T.H. LATYPOV, I.A. CHEKMAREVA, G.P. KAZANTSEVA, R. V. DEEV**, Structure and ultrastructure of kidney tissues in Goodpasture syndrome: a clinical case. *Nauka molodikh – Eruditio Juvenium*, 2018. 6 (3), 405–413 pp (in Rus.)
11. **I.T. MURKAMILOV, K.A., V.V., A.I. FOMIN, F.A. YUSUPOV**, Systemic lupus erythematosus and renal lesions: clinical and pathogenetic aspects. *The Scientific Heritage*, 2021. (58-2), 37–43. doi: 10.24412/9215-0365-2021-58-2-37-43 pp
12. **M.R. BUZOEVA, V.B. BRIN**, Effect of melaxen on the functional state of the kidneys in conditions of cadmium intoxication associated with hypercalcemia. *Journal of New Medical Technologies*, 2019. 26 (3), 64–67. doi: 10.24411/1609-2163-2019-16433 (in Rus.)
13. **HAKIM, E. M., SIVAK, K. V., & KAUKHOVA, I. E.** Evaluation of the diuretic effect of crude ethanol and saponin-rich extracts of *Herniaria glabra* L. in rats. *Journal of ethnopharmacology*, 2021. 273, 113942. <https://doi.org/10.1016/j.jep.2021.113942>

<http://dx.doi.org/10.35630/2199-885X/2022/12/2.17>

AGE-RELATED CHANGES IN THE SECOND KNEE AREA OF THE FACIAL CANAL

Received 03 March 2022;
Received in revised form 25 March 2022;
Accepted 26 March 2022

Gulnara Kerimzade 

Azerbaijan Medical University, Baku, Azerbaijan

✉ kerimzade73@list.ru

ABSTRACT — The aim of the study was to measure the cross-sectional area near the second knee of the facial canal and to estimate the dependence of their values on age. Our data is of relevance for practical neuropathology, and may be one of the factors explaining the occurrence of paralysis and paresis of the facial nerve as a result of its compression in the facial canal (Bell's syndrome).

MATERIAL AND RESEARCH METHODS: The material for the study was tomograms of 28 patients (11 women, 17 men) of different ages, taken from the archives of the Department of Radiation Diagnostics and Radiation Therapy, Azerbaijan Medical University (Baku, Azerbaijan). The studies were carried out on a computer tomograph "Toshiba aquilion 128 ct scanner". Computed tomography made it possible to measure the bone canal in the axial and coronal planes. Images with insufficient image quality were not included in the study.

RESULTS: This study confirmed an anatomical difference in facial canal cross-sectional area in patients of different ages. The measurements showed that with age there is an increase in the cross-sectional area of the facial canal. However, in patients aged 46–69 years, there is a noticeable decrease in this indicator. This can be attributed to a decrease in the width of the mastoid segment of the facial canal in this age group.

KEYWORDS — cross-sectional area, second knee angle, facial canal.

INTRODUCTION

The facial nerve canal refers to the bony canal through which the facial nerve passes through the petrous part of the temporal bone from the internal auditory meatus to the stylomastoid foramen. There are three segments of the canal: labyrinthic, tympanic, mastoid. The course of the facial nerve in a narrow bone canal is one of the main adverse developmental factors. The frequent vulnerability of the facial nerve in the same name canal is due to the fact that it occupies from 40 to 70% of its cross-sectional area [1]. A limited number of studies are available related to the study of the cross-sectional area of the facial canal. At the same time, no studies have been conducted on the relationship between the cross-sectional area of the facial canal in different age periods of postnatal

development. In a number of works, the course and various morphometric parameters of the facial canal were carried out by the method of canal dissection at different levels [2]. Due to the tortuosity of the canal, such a method (sections in the frontal and sagittal planes) sometimes does not always reliably determine the topographic position of the study area. In recent years, methods of radiological research, in particular, computed tomography, have been widely used [3]. This method allows you to accurately determine the area of the study area and importantly to take measurements in a living person. In this work, we present morphometric data obtained from the analysis of tomograms. In particular, in these images, we studied the cross-sectional area of the facial canal at a certain level, near the knee of the facial canal, which is of practical importance for the surgery of this canal.

The aim of the study

was to measure the cross-sectional area near the second knee of the facial canal and compare this indicator in patients of different ages.

MATERIALS AND METHODS

The material for the study was tomograms of 28 patients (11 women, 17 men) of different ages, taken from the archives of the Department of Radiation Diagnostics and Radiation Therapy, Azerbaijan Medical University (Baku, Azerbaijan). The studies were carried out on a computer tomograph "Toshiba aquilion 128 ct scanner". Computed tomography made it possible to measure the bone canal in the axial and coronal planes. Images with insufficient image quality were not included in the study. Using a computer method, the cross-sectional area of the facial canal was measured near its second knee. The patients were divided into age groups, so that 5 patients belonged to the age group of 7–16 years, 5 patients — 17–25 years, 5 patients — 26–35 years, 4 patients — 36–45 years, 9 patients — 46–69 years. For comparison, both bone canals (right and left sides) of each patient were measured.

RESEARCH RESULTS

This study demonstrated an anatomical difference in facial canal cross-sectional area depending on age. In patients belonging to the age group from 7 to 16 years, the minimum values of the cross-sectional

area of the facial canal at the level of the second knee were 0.97 mm² on the right, 1.00 mm² on the left, the maximum values were respectively 1.65 mm² on the right, 2.27 mm² left. In patients belonging to the age group of 17–25 years, the range of fluctuations of this indicator on the right was 0.93–2.74 mm², on the left 0.56–4.45 mm². The minimum and maximum values in patients of the age group of 26–35 years on the right were 1.82 mm² and 2.94 mm², on the left 1.04 mm² and 4.48 mm², in patients aged 36–45 years these figures were 1.86 mm² and 7.05 mm² on the right, 1.12 mm² and 8.47 mm² on the left. In patients aged 46–69 years, the cross-sectional area has a minimum value of 1.05 mm² on the right and 1.04 mm² on the left, the maximum values were 3.82 mm² and 5.36 mm².

The measurement results are presented in the Table, which shows the values of the cross-sectional area of the facial canal. As can be seen from the table, with age, there is an increase in the cross-sectional area of the facial canal, however, in patients aged 46–69 years, there is a noticeable decrease in this indicator. This is due to a decrease in the width of the mastoid segment of the facial canal in this age group (Table 1).

When analyzing the tomograms, we also found that the shape of the second knee of the canal can be round, elliptical, or kidney-shaped. In this regard, the measurement of the cross-sectional area is more accurate than the measurement of the diameter. These data are consistent with the opinion of other authors (7), who thus determined a possible anatomical predisposition to Bell's palsy.

According to [8], a significant relationship was found between the degree of development of facial nerve palsy and the area of the facial canal at the level of the second knee.

Considering the parameters on the right and left, we found some asymmetry. So the parameters were somewhat larger on the right side, which corresponds to the generally accepted dominance of the right side than the left. Researchers studying possible factors leading to Bell's palsy [9, 10] have focused on measurements related to the tortuous course of the bony facial canal. Various anatomical variations in this canal can lead to compression of the facial nerve, culminating in Bell's syndrome [11,12].

Table 1. Minimum and maximum values of the cross-sectional area near the knee of the facial canal in patients of different age groups

Age	Number of cases	Cross-sectional area near the knee of the facial canal			
		Right		Left	
		Min	Max	Min	Max
7–16	5	0.97	1,65	1,00	2,27
17–25	5	0,93	2,74	0,56	4,45
26–35	5	1,82	2,94	1,24	4,48
36–45	4	1,86	7,05	1,12	8,47
46–69	9	1,05	3,82	1,04	5,36
Total: 7–69	28	M±m			
		2,05± 0,24		2,19± 0,32	

DISCUSSION

According to Saito et al., [4], the ratio of the cross-sectional area of the facial nerve to the area of the facial canal in children was 0.31±0.08, 0.35±0.10, and 0.18±0.12, respectively, in the labyrinth, tympanic and mastoid segments, and in adults these figures were 0.4±0.07, 0.52±0.17 and 0.37±0.04, respectively. As a result, the authors concluded that children are less likely to have a pinched facial nerve in the facial canal. However, our studies show that this parameter in the area of the facial knee increases up to 36–45 years, and then sharply decreases towards the old age. This can be explained with a decrease in the mastoid segment closer to its outlet (stylomastoid foramen) with age, which are indicated in the works of other authors [5, 6].

CONCLUSION

Analysis of tomograms of the facial canal, in particular the second knee, showed that it has various shapes (round, elliptical and kidney-shaped). In this regard, the study of its cross section is more informative. We found that when considering the dynamics of age-related changes, this indicator tends to increase at 36–45 years. In people older than 46 years, this figure slightly decreased. Keeping the same trend, a certain predominance of these indicators was found on the right side, than to the left. The obtained results are of practical importance for practical neuropathology, and may be one of the factors explaining the occurrence of paralysis and paresis of the facial nerve as a result of its compression in the facial canal (Bell's syndrome).

REFERENCES

1. **CELIK O, ESKIZMIR G, PABUSCU Y, ET AL.** The role of facial canal diameter in the pathogenesis and grade of Bell's palsy: a study by high resolution computed tomography // *Braz J Otorhinolaryngol.* 2017; 83(3): 261–268 <https://doi.org/10.1016/j.bjorl.2016.03.016>
2. **ORHAN BEGER, OSMAN ERDOĞAN, ENGİN KARA.** Morphometric properties of the facial canal in children: A retrospective computed tomography study // *Int J Pediatr Otorhinolaryngol.* 2019, Sep;124: p.59–67. doi: 10.1016/j.ijporl.2019.05.039
3. **PHILLIPS CD, BUBASH LA.** The facial nerve: anatomy and common pathology. *Semin Ultrasound CT MR.* 2002; 23(3): 202–217 DOI: 10.1016/s0887-2171(02)90047-8
4. **SAITO H., TAKEDA T., KISHIMOTO S.** Vulnerability of the Facial Nerve in Entrapment Palsy: Comparative Study in Guinea Pigs and Humans, *The Facial Nerve*, 10.1007/978-3-642-85090-5, (163–164), (1994).
5. **SHADLINSKI V.B.** Anthropology with the basics of morphology / V.B. Shadlinski, A.S. Abdullayev – Baku: Shahhahchi Printing Polygraphy, – 2019. – 413 p.
6. **VIANNA M, ADAMS M, SCHACHERN P, ET AL.** Differences in the diameter of facial nerve and facial canal in bell's palsy: a 3-dimensional temporal bone study // *Otol Neurotol.* 2014; 35(3): 514–518 doi: 10.1097/MAO.0000000000000240
7. **YETISER S, KAZKAYAS M, ALTINOK D, ET AL.** Magnetic resonance imaging of the intratemporal facial nerve in idiopathic peripheral facial palsy // *Clin Imag.* 2003; 27(2): 77–81 DOI: 10.1016/s0899-7071(02)00485-0
8. **ZHANG W, XU L, LUO T, ET AL.** The etiology of Bell's palsy: a review // *J Neurol.* 2020; 267(7): 1896–1905 DOI: 10.1007/s00415-019-09282-4
9. **M.K. SCHWABER, T.C. LARSON III, D.L. ZEAL-
EAR, J. CREASY.** Gadolinium-enhanced magnetic resonance imaging in Bell's palsy // *Laryngoscope*, 100 (1990), pp. 1264–1269 DOI: 10.1288/00005537-199012000-00003
10. **M. ENGSTROM, K.A. THUOMAS, P. NAESER, JONSSON.** Facial nerve enhancement in Bell's palsy demonstrated by different gadolinium-enhanced magnetic resonance imaging techniques // *Arch Otolaryngol Head Neck Surg*, 119 (1993), pp. 221–225 doi: 10.1001/archotol.1993.01880140111017
11. **ASLI TANRIVERMIS SAYIT, PINAR GUNBEY HEDIYE, SAĞLAM DİLEK** Association between facial nerve second genu angle and facial canal dehiscence in patients with cholesteatoma: evaluation with temporal multi-detector computed tomography and surgical findings // *Braz J Otorhinolaryngol.* 2019; 85(3): p. 365–370. doi: 10.1016/j.bjorl.2018.03.005
12. **KOZERSKA M.** 3D visualization of the intratemporal course of the facial canal using computed micro-tomography / M Kozerska, J Skrzat, A Spulber, [et al.] // *Folia Med Cracov.* 2016; 56(3): p. 11–19.

<http://dx.doi.org/10.35630/2199-885X/2022/12/2.8>

SYNTHESIS OF A PROTEIN THAT IS IMMUNOCHEMICALLY SIMILAR TO HUMAN LACTOFERRIN BY *KLEBSIELLA PNEUMONIAE*

Received 24 January 2022;
Received in revised form 25 February 2022;
Accepted 27 February 2022

Oksana Boiko¹ , Rushaniya Mukhamedzyanova¹ ,
Yurii Dotsenko¹ , Anzhela Ramaeva² ,
Surkhai Akhadov⁴, Nadezhda Zaporozhets³,
Vera Dmitrieva³ , Ilfat Karimov¹

¹ Astrakhan State Medical University, Astrakhan;

² Alexandro-Mariinsky Regional Clinical Hospital, Astrakhan;

³ Railway Clinical Hospital, Astrakhan;

⁴ Municipal Out-patient Clinic No.5, Astrakhan Region, Russia

✉ oboyko08@mail.ru

ABSTRACT — Nowadays, great importance is attached to the role of iron in infection processes, since pathogenic bacteria produce Fe^{3+} chelating compounds with the ability to absorb Fe^{3+} and remove it from the siderophores of the host. This ability is considered as a pathogenicity factor, enabling the pathogen to propagate in the macroorganism. Many bacterial species are known to increase virulence with iron ions present. Therefore, the siderophore system of bacteria can influence the disease severity by binding Fe^{3+} ions and reducing their content in tissues. **THE STUDY PURPOSE** was to determine the ability of *K. pneumoniae* to synthesize a protein, immunochemically similar to human lactoferrin (hereinafter — microbial-derived lactoferrin, MdLF), and the resistance of these microorganisms to the damaging effect of human lactoferrin (LF). **METHODS.** The study was conducted on archival strains of *K. pneumoniae*, formerly isolated from patients with intestinal bacterial overgrowth syndrome ($n=140$), and from the control group ($n=70$). The supposed presence of MdLF in the samples was confirmed through an ELISA assay using *Hycult Biotech* test kits (Netherlands). **RESULTS.** The ability to synthesize MdLF, which directly depends on the presence of lactoferrin in the culture medium, was revealed in 100% of the strains. MdLF synthesis significantly decreased if LF was present. The patient strains synthesized MdLF less than those taken from the healthy people, but they were more resistant to human lactoferrin, which suggests that the criterion of microbial resistance to LF, taken at 400 ng/ml, should be used as a diagnostic criterion. *Klebsiellae* bacteria that formed single colonies after beef-extract agar inoculation synthesized MdLF the most and had the highest resistance to LF, which increases their epidemiological importance. **CONCLUSION.** The study established the diagnostic value of the human LF — microorganism MdLF system for predicting infectious process development and assessing the epidemiological danger from particular strains.

KEYWORDS — siderophores; protein immunochemically similar to human lactoferrin; *K. pneumoniae*; chromatography; electrophoresis.

INTRODUCTION

Bacteria that are capable of propagating in vivo are entangled in a complex competitive relationship both with the human organism and with other microorganisms at the metabolic level. Modern research suggests that iron is a universal growth factor for microorganisms; all microorganisms need iron to a different extent, depending on their taxonomy. Iron is exposed to oxidation and hydrolysis processes in the environment, which results in a decrease in the concentration of free Fe^{2+} and Fe^{3+} ions to 10^{-9} – 10^{-18} M, which is not enough for adequate life activity of most microorganisms. Similarly, iron is bound to iron-binding proteins in mammals and is unavailable to microorganisms. Therefore, microorganisms have evolved ways of getting iron under iron-deficiency conditions. Synthesis of siderophores is one of the best-studied ways [1, 2, 3, 5, 12].

Siderophores are low-molecular substances that chelate Fe^{3+} ions released by microorganisms and plants under iron-deficiency conditions in the environment. The key function of siderophores is to convert iron that is bound to proteins or water-insoluble compounds into the Fe^{3+} ionic form available to microorganisms. Most of aerobic and facultative anaerobic microorganisms synthesize at least one siderophore. A relationship of siderophores to the virulence of microorganisms has been proven, and approaches for their clinical usage are being developed. Indeed, the loss of the ability to synthesize siderophores correlates with the loss of virulence, which is seen in many bacterial species — *Erwinia chrysanthemi*, *Pseudomonas aeruginosa*, *Vibrio anguillarum*, *Yersinia enterocolitica*, *Escherichia coli*, etc. [7, 11].

Active studies of siderophores started in the 1990s; since then, siderophores of different groups of microorganisms have been isolated and described. Siderophores can be divided into five classes depending on their chemical nature — catecholates and phenolates (aryl caps), hydroxamates (α -oxycarboxylic acids), carboxylates (dicarboxylic and tricarboxylic acids) and siderophores of mixed type. Mixed-type siderophores correspond to two classes by their structure, that is why they were classified separately [5].

At the same time, there are bacteria that are classified as non-siderophore-forming microorganisms.

These include, for example, *Neisseria* and *Moraxella*. They do not synthesize siderophores to utilize iron from the medium but utilize iron by means of special protein receptors on the surface of the outer membrane. Iron regulatory proteins are supposed to be such receptors. Enhanced expression of these proteins *in vitro* is observed under conditions of a limited amount of iron in the culture medium, in particular when chemical compounds (chelators) that form strong chelating complexes with iron are introduced into the medium. In particular, eleven iron regulatory proteins are known for *Neisseria meningitidis*, whereas only five have been reported for *Moraxella* so far. Basically, the iron regulatory proteins of *Neisseria meningitidis* are minor proteins under normal laboratory culture conditions and begin to express intensively only when the medium is iron-deficient. Cop B, which is one of the major proteins of *Moraxella catarrhalis* with a molecular mass of 81 kD, is quite sensitive to the iron content in the culture medium: its expression sharply increased under the conditions of limited iron content in the medium and, on the contrary, decreased in case of an increase in the Fe^{3+} ion content in the medium. For *in vitro* growth, the mentioned Cop B is able to utilize iron from different sources — iron citrate, transferrin, lactoferrin and heme-containing proteins. It was found that increased expression of iron regulatory proteins, capable of specific binding of transferrin and human lactoferrin, was observed once the iron chelator EDDA was introduced into the *Moraxella* culture medium. Other studies have shown that a 37-kD iron regulatory protein that is typical of most *Neisseria* but is not expressed by *Moraxella* and non-pathogenic *Neisseria*, is localized mainly in the periplasmic space and is involved into the iron transfer from transferrin to the cytoplasmic membrane through the periplasm. An analogy has also been established between the active centre of this protein and the one of invertebrate transferrin [6, 12].

Lactoferrin belongs to the transferrin family and is capable of active binding and transporting of Fe^{3+} and other mixed-valent metals. Previously examined lactoferrins are glycoproteins with the molecular masses within the range of 75–80 kDa, containing intramolecular disulfide bonds. A polypeptide chain of lactoferrin forms two globular domains called M- and C-lobes, connected with an alpha helix. Each lobe has an iron-binding centre. The tertiary structures of apo-lactoferrin (iron-free lactoferrin) and iron-binding lactoferrin differ [5, 7, 8, 9, 10]. For example, it is found that Fe^{3+} binding plays an essential role in implementing the antioxidant and bacteriostatic function of lactoferrin. Along with antimicrobial activity, lactoferrin also has other biological properties — it

can act as an immunomodulatory agent, antioxidant and anti-inflammatory agent and transcriptional factor and definitely participates in iron metabolism [2, 4, 8, 9, 10].

The purpose

of the study is to determine the ability of *K. pneumoniae* bacteria to synthesize protein, immunochemically similar to human lactoferrin, and the resistance of these microorganisms to the damaging effect of human lactoferrin (LF).

MATERIALS AND METHODS

The culture under study was taken from a local centre for culture collection of microorganisms *Klebsiella pneumoniae*, isolated from the patients with the small intestinal bacterial overgrowth syndrome (n=140) and from the control group (n=70) and were identified as *Klebsiella pneumoniae* after performing standard microbiological tests and using the polymerase chain reaction (PCR) method. Later on, they were kept in a semisolid agar for microorganism cultures.

Determining the production of the protein immunochemically similar to human lactoferrin

The production of the protein that is immunochemically similar to human lactoferrin was determined in the following steps:

Lactoferrin solution (400 ng/ml concentration in the nutrient (beef-extract) broth) was poured into 0.2 ml tubes. Then a bacteriological loop was used to inoculate *K. pneumoniae* in the agar culture tubes.

At the same time, the authors took control samples with the beef-extract broth that did not contain lactoferrin, with *K. pneumoniae* being inoculated, as it was done with the test samples.

Once all the tubes were incubated at $t=37^{\circ}\text{C}$ for 24 hours, their content was centrifuged (5,000 rpm for 45 min). The supposed presence of MdLF in the samples was confirmed through an ELISA assay using *Hycult Biotech* test kits (Netherlands).

Determining K.pneumoniae resistance to human lactoferrin

The microbial number of *K. pneumoniae* culture in normal saline was adjusted to a concentration of 10^{20} CFU/ml by the turbidity standard (Scientific Centre for Expert Evaluation of Medicinal Products named after L.A. Tarasevich). After that, 0.3-ml suspension of *Klebsiellae* was added to two tubes; there were two tubes per strain.

Then 0.2 ml of lactoferrin apoform solution were added to the test sample (so that its final concentration was 400 ng/ml).

0.2 ml of normal saline were added to the control sample instead of lactoferrin.

Once the samples were incubated ($t=37^{\circ}\text{C}$ for 30 min), the reaction was stopped by adding 5 ml of broth to all the samples with subsequent measurement of optical density (OD1).

The samples were again incubated at $t=37^{\circ}\text{C}$ for one hour to propagate lactoferrin-resistant *Klebsiellae*, and the optical density of the solutions was measured again (OD2).

The bactericidal effect of lactoferrin was calculated by the formula:

$\Delta\text{ODt} - \Delta\text{ODc} / \Delta\text{ODt}$, where

ΔODc is the changes in the optical density of the control samples;

ΔODt is the changes in the optical density of the test samples.

The authors made an attempt to isolate and purify the protein that is immunologically similar to human lactoferrin (MdLF) from *Klebsiella* culture. MdLF presence in the samples of the pre-centrifuged (5,000 rpm during 45 minutes) liquid culture of *K.pneumoniae* (meat-peptone broth, incubation time — 24 hours at $t=37^{\circ}\text{C}$) was assumed on the basis of EIA results with the use of *Hycult biotech* test kits (Netherlands) [3].

STATISTICAL ANALYSIS

The results were processed with standard variance statistics methods using Statistica 12 software. The statistical significance was assessed with the Wilcoxon–Mann–Whitney test at a significance level of $p < 0.05$.

RESULTS

The intensity of MdLF synthesis by *Klebsiellae* directly depended on the presence of lactoferrin in the medium ($p < 0.05$). Interestingly, all *K.pneumoniae* cultures produced MdLF both in the presence of human LF in the culture medium and in its absence. However, the average concentration ($M \pm m$) of MdLF in the non-lactoferrin medium was 24.6 ± 2.34 ng/ml, while it was 37.5% lower in the medium containing lactoferrin (only 15.35 ± 1.7 ng/ml).

K.pneumoniae that were isolated from the patients and the healthy group also demonstrated different levels of MdLF production: MdLF synthesis in the strains taken from the patients with SIBO averaged 9.62 ± 1.1 ng/ml, which is $p < 0.05$ reliably lower than in the strains isolated from the healthy group (17.98 ± 2.21 ng/ml).

Binding iron ions, lactoferrin largely provides the bactericidal activity of serum and many other biological fluids. *K.pneumoniae* isolated from the patients and the healthy group differed in their resistance to it. The

number of the survived microorganisms (in %) after their contact with lactoferrin at a concentration of 400 ng/ml was 98.03 ± 7.2 in the strains isolated from the patients with SIBO and 69.31 ± 4.91 ($p < 0.05$) in the healthy group, which allows to recommend the lactoferrin resistance criterion as a prognostic one.

Therefore, one can speak of the existence of a kind of a human LF — microorganism MdLF system. The authors also revealed significant differences (Table 1) when considering this system among *Klebsiellae* with different growth rates on dense nutrient agar after inoculation with 1 ml of broth culture of *K.pneumoniae*.

The least significant production of MdLF was in the *Klebsiellae* with pronounced growth. At the same time, the lawn-growing *Klebsiellae*, i.e. suppressing all other bacteria most successfully, produced MdLF significantly higher ($p < 0.05$). The lawn-growing *Klebsiellae* also had higher resistance to lactoferrin.

However, the most active synthesis of MdLF was noted in the *Klebsiellae* forming single colonies on dense medium ($p < 0.05$ compared with the first group). The very representatives of this *Klebsiella* group proved to be the most resistant to lactoferrin — almost 100% of the cells remained viable.

DISCUSSION

Microorganisms have evolved ways of getting iron in iron-deficiency conditions, which is important for optimal development in the environment and, in certain cases, may be critical for survival of the population. In this case, microbial strategies for getting iron can be considered as one of the factors that determine the formation and stability of microbial associations, playing an important role in the functioning of normal and pathological microbiocenoses in the host.

Interpreting the results obtained in the first part of the study, in particular the increased content of MdLF in the control samples against the test samples, the authors found that LF and MdLF had much in common in their structure and are similar in immunochemical terms. Therefore, it seems clear that synthesis of MdLF by *Klebsiellae* in the nutrient media containing human LF is inhibited on the principle of negative feedback. The same negative feedback mechanism also explains the reduced production of MdLF by strains isolated from the patients with the small intestinal bacterial overgrowth syndrome against the strains obtained from the healthy group, which was identified by the authors in further studies, since an increase in the concentration of LF in bacterial infections has been proven and described in numerous articles and reviews.

Parasites constantly face problems of survival in the adaptively changing environment of the host where they parasitize and where humans control the infec-

Table 1. MdLF synthesis by microorganisms and their resistance to human LF ($M \pm m$)

<i>K. pneumoniae</i> growth rate	n	MdLF concentration in culture medium (ng/ml)	Number of <i>K. pneumoniae</i> bacteria (in %) survived after LF incubation (concentration – 400 ng/ml)
1. Lawn growth	30	33.942 \pm 2.4	78.0 \pm 3.6
2. Pronounced growth; <i>Klebsiellae</i> form isolated colonies	80	15.612 \pm 6.3	62.0 \pm 3.1
3. Single colonies when inoculated with beef-extract agar	100	42.810 \pm 7.1	98.0 \pm 4.4

tion; in this regard, the increased resistance to LF of the patient strains identified by the authors also seems quite logical.

Analyzing the production of MdLF and the resistance to LF depending on the intensity of growth, it is safe to say that in terms of predicting the infection development and determining the potential danger of inoculated microorganisms, it is important to evaluate not only their number but also the pathogenic potential of individual strains. These were *Klebsiellae*, forming single colonies in the authors' studies, that not only had almost 100% resistance to human LF but also actively produced MdLF themselves, which allows them both to successfully survive in the host organism and to compete with microorganisms of other taxonomic groups. It seems clear that such bacteria are most often the cause of bacteria carrying and pose a serious epidemiological danger.

CONCLUSION

The study established the existence of a system that includes synthesis of the protein immunochemically similar to human lactoferrin by microorganisms and, consequently, of microorganisms' resistance to the antibacterial action of human lactoferrin. This confirms the significance of both iron itself and biomolecules determining its level in the human organism under the pathogen persistence.

The study established the diagnostic value of the human LF — microorganism MdLF system for predicting infectious process development and assessing the epidemiological danger from particular strains.




REFERENCES

1. BOIKO O.V., TERENTIEV A.A., BOIKO V.I. Molecular mechanisms of bacteria carrying (characteristics and detailed analysis) / Saarbrücken, 2012.
2. BOIKO O.V., DOTSENKO YU.I., GUDINSKAYA N.I., BOIKO V.I., MUKHAMEDZYANOVA R.I., KOZAK D.M., STENKIN F.S. Effect of pollutants on biochemical properties of microorganisms. Hygiene and Sanitation. 2020; 99 (4): 368–378. doi: <https://doi.org/10.33029/0016-9900-2020-99-4-368-378>.
3. BOIKO O.V., NIKOLAEV A.A., KOZAK D.M., GUDINSKAYA N.I., SAKHAROV M., GUDINSKAYA P., DOTSENKO YU.I. Isolation and purification of protein that is immunologically similar to human lactoferrin. Archiv EuroMedica. 2021. Vol. 11, No. 2, p. 10–12. DOI: 10.35630/2199-885X/2021/11/2.2
4. DRAGO-SERRANO ME, CAMPOS-RODRÍGUEZ R, CARRERO JC, DE LA GARZA M. Lactoferrin: Balancing ups and downs of inflammation due to microbial infections. Int J Mol Sci. 2017 Mar 1;18(3):501. doi: 10.3390/ijms18030501
5. CHALLIS, G. L. A widely distributed bacterial pathway for siderophore biosynthesis independent of nonribosomal peptide synthetases / G. L. Challis // Chem. biochem. – 2005. – Vol. 6. – P. 601–611.
6. COBESSI, D. Crystal structure at high resolution of ferric-pyochelin and its membrane receptor FptA from *Pseudomonas aeruginosa* / D. Cobessi, H. Celia, F. Patrus // J. Mol. Biol. – 2005. – Vol. 352. – P. 893–904.
7. DERTZ, E. A. Siderophores and transferrins / E. A. Dertz, K. N. Raymond // In Comprehensive coordination chemistry II, vol. 8 / L. Que, Jr., and W. B. Tolman (ed.). – Philadelphia, PA : Elsevier, Ltd., 2003. – P. 141–168.
8. GONZÁLEZ-CHÁVEZ SA, ARÉVALO-GALLEGOS S, RASCÓN-CRUZ Q. Lactoferrin: structure, function and applications. Int J Antimicrob Agents. 2009 Apr;33(4):301.e1–8. doi: 10.1007/s00005-021-00637-2
9. HASSOUN LA, SIVAMANI RK. A systematic review of lactoferrin use in dermatology. Crit Rev Food Sci Nutr. 2017 Nov 22;57(17):3632–3639. doi: 10.1080/10408398.2015.1137859.
10. KELL DB, HEYDEN EL, PRETORIUS E. The biology of lactoferrin, an iron-binding protein that can help defend against viruses and bacteria. Front Immunol. 2020 May 28;11:1221. doi: 10.3389/fimmu.2020.01221
11. MORGENTHAU A, POGOUTSE A, ADAMIAK P, MORAES TF, SCHRYVERS AB. Bacterial receptors for host transferrin and lactoferrin: molecular mechanisms and role in host-microbe interactions. Future Microbiol. 2013 Dec;8(12):1575–85. doi: 10.2217/fmb.13.125
12. NEUMANN W, HADLEY RC, NOLAN EM. Transition metals at the host-pathogen interface: how *Neisseria* exploit human metalloproteins for acquiring iron and zinc. Essays Biochem. 2017 May 9;61(2):211–223. doi: 10.1042/EBC20160084

<http://dx.doi.org/10.35630/2199-885X/2022/12/2.9>

ANALYSIS OF THE SENSITIVITY OF STAPHYLOCOCCUS AUREUS TO ANTIBIOTICS IN PATIENTS WITH PURULENT-SEPTIC DISEASES

Received 29 January 2022;
Received in revised form 3 March 2022;
Accepted 7 March 2022

Valeh Jafarov, Konstantin Horak ,
Artem Morozov , Elizaveta Sobol,
Anastasia Domracheva , Anastasia Romanova ,
Sofia Zinkovskaia 

Tver State Medical University, Tver

✉ ammorozovv@gmail.com

RELEVANCE

The purulent-septic infection caused by *Staphylococcus aureus* is one of the biggest problems of modern medicine.

There are some strategies to control the increasing antibiotic resistance of bacteria. They are the development and introduction of new antibacterial drugs into surgical practice, the improvement of antimicrobial therapy methods and the rotation of antibacterial drugs [1, 2, 3].

Staphylococcus aureus is one of the most common causative agents of infections of various localizations. The development of mechanisms of antibiotic resistance of bacteria is more often determined by genes located on the bacterial chromosome or R-plasmids. Particular attention is paid to methicillin-resistant staphylococci (MRS strains). They are registered in nosocomial or out-of-hospital infections. The resistance of staphylococci to β -lactam antibiotics is due to the presence of the *mec A* gene. It encodes the penicillin-binding protein (PBP). The *mec A* gene is located on a mobile genetic element. This element is called the staphylococcal chromosome cassette (SCCmec). Methicillin-resistant *Staphylococcus aureus* is resistant to all β -lactam antibiotics. Currently, it is necessary to use combinations of antibacterial drugs for the treatment of infections caused by methicillin-resistant staphylococci [4, 5, 6, 7].

Purpose:

to analyze the sensitivity of *Staphylococcus aureus* detected in patients with various purulent-inflammatory diseases to antibacterial drugs of different classes.

MATERIALS

The present study provided a statistical analysis of 300 registration forms of the microbiological study re-

ABSTRACT — RELEVANCE: The study of microflora speciation is one of the important aspects of surgical practice. The gram-positive microorganisms are the most common causative agents of surgical infection. *Staphylococcus aureus* is the most pathogenic species of staphylococci. It is the causative agent of purulent-inflammatory human diseases. Of particular importance is the increase in the frequency with which hospital strains adapted to hospital conditions are released.

PURPOSE: to analyze the sensitivity of *Staphylococcus aureus* detected in patients with various purulent-inflammatory diseases to antibacterial drugs of different classes.

MATERIALS: The present study provided a statistical analysis of 300 registration forms of the microbiological study results of the microbiological landscape of purulent-septic diseases. The study was conducted on the basis of the surgical department of the City Clinical Hospital No. 7 (Tver, Russia) for the period 2020-2021. Statistical data processing was carried out using Microsoft Excel 2020 licensed software.

RESULTS: The study identified *Staphylococcus aureus* as the most common causative agent of purulent-septic diseases. It was found that this pathogen was detected in 99 out of 300 patients. The study included patients with phlegmon of the lower extremities (23.8%), phlegmon of the upper extremities (16.09%), festering atheromas (50%), gangrene of the lower extremities (28.6%), osteomyelitis (14.4%), soft tissue abscesses (33.3%). It was found that ciprofloxacin was one of the most common antibiotics, to which *Staphylococcus aureus* showed the greatest sensitivity in case of phlegmon of the upper and lower extremities, festering atheromas, gangrene of the lower extremities and osteomyelitis. *Staphylococcus* showed the greatest sensitivity to gentamicin (21.6%) and amikacin (8.1%) in case of soft tissue abscesses. This pathogen also showed sensitivity to tetracycline (8.1%) and doxycycline (5.4%) in patients with abscesses. *Staphylococcus aureus* showed identical sensitivity to fosfomicin, ofloxacin, vancomycin, meronem, imipenem and clindamycin in various nosologies. **CONCLUSION:** *Staphylococcus aureus* showed the greatest sensitivity to antibiotics of the cephalosporin class. The second most common were representatives of the class of aminoglycosides — gentamicin and amikacin. The sensitivity of *Staphylococcus aureus* to vancomycin and clindamycin was manifested only in patients with suppurated atheromas. The sensitivity to erythromycin was observed in *Staphylococcus aureus* only in patients with soft tissue abscesses. The results of this study showed that *Staphylococcus aureus* exhibits different sensitivity to antibacterial drugs depending on the specific purulent-inflammatory disease. It must be taken into account when starting etiotropic therapy until the sensitivity is determined in each specific situation.

KEYWORDS — *Staphylococcus aureus*, antibiotic resistance, antibacterial drugs.

sults of the microbiological landscape of purulent-septic diseases. The study was conducted on the basis of the surgical department of the City Clinical Hospital No. 7 of Tver (Russia) for the period 2020–2021. The clinical material was taken with a sterile tampon probe, which was placed in a tube containing Ames' transport environment with coal. The obtained samples were stored at a temperature not lower than + 5° C and not higher than +30. They were delivered to the laboratory within half an hour after taking them. The bacteriological study of clinical material was carried out on Endo selective and differential diagnostic media, yolk-salt agar, blood agar. It used the classical bacteriological method in aerobiosis at 37° C. The morphological and biochemical identification was carried out after the isolation of the pure culture. It used the clinical recommendations "Determination of the sensitivity of microorganisms to antimicrobials" (2018) to establish the category of sensitivity of microorganisms, according to the international European system EUCAST. The sensitivity of the isolated strains was determined by the disk diffusion method using OXOID disks. Then it was determined by degree of sensitivity according to the diameter of the lysis area. Statistical data processing was carried out using Microsoft Excel 2020 licensed software.

RESULTS AND DISCUSSION

In the present study we evaluated the clinical samples of wound discharge from patients with phlegmon of the upper and lower extremities, soft tissue abscesses, wet gangrene of the lower extremities, osteomyelitis and suppurated atheromas. It was found that a Gram-positive pathogen (*Staphylococcus aureus*) was detected in 99 out of 300 patients (33%).

The investigated pathogenic microorganism shows different sensitivity to antibacterial drugs depending on the nosology.

In the study of Tokaeva B.T. (2014) it was found that *Staphylococcus aureus* is sensitive to the following antibacterial drugs: glycopeptides, carboxypenicillins, macrolides, aminoglycosides and cephalosporins. In the course of this clinical study, it was found that *Staphylococcus aureus* is sensitive to antibiotics of the penicillin, tetracycline, aminoglycoside, cephalosporin, oxazolidinone, and sulfonamide classes.

84 cases of the clinical specimens received from patients with phlegmon of the lower extremities were studied. *Staphylococcus aureus* was isolated in 20 cases (23.8%). This pathogen in vitro showed the highest sensitivity to the group of cephalosporins (30%), in particular to ceftriaxone (20%). The sensitivity to cefepime (5%) was manifested only in the pathogen obtained from patients with this nosology. The sen-

sitivity to aminoglycosides was manifested in 25% of cases (Table 1).

Staphylococcus aureus was isolated in 14 cases out of 87 patients with phlegmon of the upper extremities (16.09%). This pathogen was found to be sensitive to cephalosporins in 35.7%. The sensitivity to antibiotics of the aminoglycoside class was 21.4%. The representatives of this drugs group were amikacin (7.1%) and gentamicin (14.3%). *Staphylococcus aureus* also showed sensitivity to tetracycline (14.3%) (Table 1).

Based on the research of Naumkina E.V. (2018) it can be noted that strains of *Staphylococcus aureus* are sensitive to fluoroquinolone antibiotics at 39%. They were isolated from patients in the department of purulent surgery. In the present study, the pathogen showed sensitivity to a representative of the fluoroquinolone class (ofloxacin) only in 14.7% of cases.

Staphylococcus aureus was isolated in 24 cases out of 48 patients with suppurated atheromas (50%). The greatest sensitivity of this pathogen was manifested to antibiotics of the cephalosporin class (33.3%). Only *Staphylococcus aureus*, isolated from patients with suppurated atheromas, showed a sensitivity of 4.3% to vancomycin and meropenem (Table 1).

According to the study of Lipatov K.V. (2019), the isolated strains of *Staphylococcus aureus* in patients with purulent-septic diseases are characterised by high sensitivity to vancomycin and linezolid. However, the present study showed the least sensitivity to these antibiotics. The sensitivity to linezolid was manifested only by *Staphylococcus aureus*, isolated from patients with phlegmon of the upper extremities, soft tissue abscesses. The sensitivity to vancomycin was observed only in patients with suppurated atheromas.

Staphylococcus aureus was isolated in 8 cases out of 28 patients with gangrene of the lower extremities (28.6%). This pathogen showed the highest sensitivity to antibiotics of the cephalosporin class (44.5%). The lowest sensitivity (11.1%) was found to imipenem, tetracycline and norfloxacin (Table 1).

Staphylococcus aureus was detected in 27 cases out of 37 patients with soft tissue abscesses (72.9%). This pathogen showed little sensitivity to antibiotics of the aminoglycoside class: to gentamicin (21.6%) and to amikacin (8.1%). *Staphylococcus aureus* showed sensitivity to amoxicillin in 19% of cases. The sensitivity of *Staphylococcus aureus* to the tetracycline class was manifested in 13.5% of cases. *Staphylococcus aureus* was sensitive to doxycycline in 5.4% (Table 1).

Staphylococcus aureus was isolated in 6 cases out of 16 patients with osteomyelitis (37.5%). This pathogen showed the greatest sensitivity to antibiotics of the cephalosporin class (41%). *Staphylococcus aureus*

Table 1. Sensitivity of *Staphylococcus aureus* in various purulent-septic diseases

Antibiotic	Phlegmon of the upper extremities	Phlegmon of the lower extremities	Soft tissue abscesses	Festering atheromas	Gangrene of the lower extremities	Osteomyelitis
Ceftriaxone	30%	28,6%	20%	20,8%	22,2%	20,5%
Gentamicin	20%	14,3%	21,6%	11,7%	11,1%	20,5%
Amoxicillin	15%	0%	19%	8,3%	0%	9%
Tetracycline	10%	14,3%	8,1%	0%	11,1%	0%
Cefepime	5%	0%	0%	0%	0%	0%
Cefazolin	5%	0%	0%	8,3%	11,1%	20,5%
Amikacin	5%	7,1%	8,1%	20,8%	11,1%	20,5%
Imipenem	5%	0%	2,48%	4,3%	11,1%	0%
Ofloxacin	5%	0%	5,4%	4,3%	0%	0%
Clindamycin	5%	7,15%	0%	4,3%	0%	0%
Co-Trimoxazole	5%	0%	2,48%	0%	0%	0%
Norfloxacin	0%	7,15%	0%	0%	11,1%	0%
Linezolid	0%	7,15%	2,48%	0%	0%	0%
Ciprofloxacin	0%	7,1%	0%	4,2%	11,1%	0%
Doxycycline	0%	0%	5,4%	0%	0%	9%
Fosfomycin	0%	0%	2,48%	4,3%	0%	0%
Erythromycin	0%	0%	2,48%	0%	0%	0%
Vancomycin	0%	0%	0%	4,3%	0%	0%
Meropenem	0%	0%	0%	4,3%	0%	0%

showed sensitivity to ceftriaxone in 20.5% of cases. The sensitivity to amikacin and gentamicin is 41%. *Staphylococcus aureus* is sensitive to amoxicillin and doxycycline in 9% of cases using the method of determining the sensitivity to antibacterial drugs using OXOID discs. The sensitivity to doxycycline was observed only in patients with soft tissue abscesses and osteomyelitis.

CONCLUSION

Staphylococcus aureus showed the greatest sensitivity to antibiotics of the cephalosporin class. The second most common were representatives of the class of aminoglycosides — gentamicin and amikacin. The sensitivity of *Staphylococcus aureus* to vancomycin and clindamycin was manifested only in patients with suppurated atheromas. Sensitivity to erythromycin was observed in *Staphylococcus aureus* only in patients with soft tissue abscesses. The results of this study showed that *Staphylococcus aureus* exhibits different sensitivity to antibacterial drugs depending on the specific purulent-inflammatory disease. Therefore, etiotropic therapy may only be started after the sensitivity for each specific situation is determined.

REFERENCES

1. MISHYNA M. M. Microbiological characterization of pathogenicity factors of candida albicans and staphylococcus aureus association affecting neutrophil phagocytic activity / M.M. Mishyna, O.V. Kochneva, O.V. Kotsar // West Kazakhstan Medical Journal. – 2021. – № 2(63). – P. 70–76. – DOI 10.24412/2707-6180-2021-63-70-76
2. Fluorescence detection of *Staphylococcus aureus* using vancomycin functionalized magnetic beads combined with rolling circle amplification in fruit juice / Y. Wang, Z. Wang, Z. Zhan [et al.] // Analytica Chimica Acta. – 2022. – Vol. 1189. – P. 339213. – DOI 10.1016/j.aca.2021.339213
3. Bioactive glass particles as multi-functional therapeutic carriers against antibiotic-resistant bacteria / N. Pajares-Chamorro, X. Chatzistavrou, Y. Wagley [et al.] // Journal of the American Ceramic Society. – 2021. – DOI <https://doi.org/10.1111/jace.17923>
4. Antibiotic sensitivity of clinical isolates at outpatient unit in Tver, Russia: a comparative / K. Horak, K. Gorodnichen, A. Morozov [et al.] // Archiv EuroMedica. – 2020. – Vol. 10. – No 4. – P. 77–79. – DOI 10.35630/2199-885X/2020/10/4.17
5. Development of antibiotic resistance in the aspect of outpatient services / A. M. Morozov, A. N. Sergeev, V. A. Kadykov [et al.] // Vestnik sovremennoy klinicheskoy meditsiny. – 2021. – T. 14. – No 5. – P. 43–50. – DOI 10.20969/VSKM.2021.14(5).43–50
6. Interaction of the antimicrobial peptide $\Delta M3$ with the *Staphylococcus aureus* membrane and molecular models / M. Manrique-Moreno, E. Patiño-González, E. Fandiño-Devia [et al.] // Biochimica et Biophysica Acta (BBA) – Biomembranes. – 2021. – Vol. 1863. – No 2. – P. 183498. – DOI <https://doi.org/10.1016/j.bbame.2020.183498>
7. DIAS, T. A computer-driven approach to discover natural product leads for methicillin-resistant staphylococcus aureus infection therapy † / T. Dias, S. P. Gaudêncio, F. Pereira // Marine Drugs. – 2019. – Vol. 17. – No 1. – P. 16. – DOI 10.3390/md17010016

<http://dx.doi.org/10.35630/2199-885X/2022/12/2.10>

COMPREHENSIVE ASSESSMENT OF NEUROLOGICAL DEFICIT AND ITS CORRECTION WITH PIR-10 COMPOUND IN EXPERIMENTAL FOCAL CEREBRAL ISCHEMIA OF RATS

Received 08 February 2022;
Received in revised form 02 March 2022;
Accepted 04 March 2022

Natalia Shabanova[✉] , Anastasia Gerashchenko 

Pyatigorsk Medical and Pharmaceutical Institute —
Branch of Volgograd State Medical Pyatigorsk, Russia

✉ vahlushina@mail.ru

ABSTRACT — **INTRODUCTION:** Correction of motor dysfunction resulting from focal cerebral ischemia is one of the significant problems of pharmacology and experimental therapy. Pyrimidine derivatives in the experiment on rats previously showed cerebroprotective activity, as a result of which it was decided to test the PIR-10 compound for the ability to reduce neurological deficit. **METHODS:** A study was conducted to assess the effect of pyrimidine derivative (PIR-10 50 mg/kg) on neurological deficiency in the conditions of focal cerebral ischemia in rats. The study used mature male Wistar rats weighing 220–240 g (n=40). Focal cerebral ischemia was reproduced by coagulation of the left middle cerebral artery (anesthesia chloralhydrate 350 mg/kg). Neurological deficits were assessed using the McGraw, Combs and D'alecy, Garcia scales. **RESULTS:** The studied compound PIR-10 contributes to the reduction of neurological deficits in all selected schools in comparison with the control group of animals (McGraw by 68% ($p<0,05$), Combs and D'alecy by 4,3 times ($p<0,05$), Garcia by 84% ($p<0,05$)). In addition, the results obtained after administration of PIR-10 to rats showed a statistically significantly difference from the group of rats receiving a reference drug cavinton. However, complete recovery of motor functions after modeling focal cerebral ischemia was not observed in any group of rats. **CONCLUSION:** The PIR-10 compound is able to partially correct the neurological deficit that occurs in conditions of cerebral circulatory insufficiency, surpassing the activity of the reference drug cavinton.

KEYWORDS — focal cerebral ischemia, pyrimidine derivatives, neurological deficit.

INTRODUCTION

Focal cerebral ischemia occupies one of the leading places among the causes of disability due to the development of cognitive and neurological disorders [1, 2]. Motor dysfunction is the main cause of high disability in patients with impaired cerebral hemodynamics [3]. In this regard, compounds exhibiting

cerebroprotective properties are of particular interest for the correction of emerging neurological deficits. In previous studies, the ability of pyrimidine derivatives to improve behavioral, mnestic and cognitive functions in the setting of global cerebral ischemia has been proven [4], which makes these compounds promising for further study for the ability to restore impaired musculoskeletal and neurological functions in cerebrovascular pathology.

Objective:

To assess neurological deficiency and correct it with PIR-10 compound in experimental global cerebral ischemia of rats

MATERIALS AND METHODS

The study was conducted in accordance with the "Guidelines for Preclinical Trials of Drug Products" ed. by A.N. Mironov (a 2012 edition.) [5]. The animals were maintained in compliance with current best practices and standards of care in laboratory animals. The experiment was performed on 40 male Wistar rats $m=200-220$ g, divided into 4 groups (n=10). Rats were kept on a standard vivarium diet, with a natural succession of light and darkness. The first group was represented by falsely operated rats (FO), the second one — by negative control animals (NC). The both groups received an intraperitoneal suspension of Tween-80 in purified water. The third groups received reference drugs: Cavinton (3,2 mg/kg, LLC «Gedeon Richter Pharma» [6]. The fourth group was administered the pyrimidine derivative PIR-10 (50 mg/kg), synthesized at the department of organic chemistry of the Pyatigorsk Medical and Pharmaceutical Institute [7]. The second and subsequent groups modeled focal cerebral ischemia, by occlusion of the left middle cerebral artery (OLMCA) (under chloral hydrate anesthesia, 350 mg/kg) [8,9]. All objects were injected intraperitoneally immediately after the surgery and then once daily for three days. 24 hours after pathology modeling, neurological deficiency of animals according to the McGraw [10], Combs and D'alecy [11], Garcia [12] scales. The results were processed by the method of variational statistics using the STATISTICA 6.0 application program. The normality of

the distribution was evaluated by the Shapiro-Wilk criterion. In the case of normal data distribution, the parametric Student t-test was used. In the case of abnormal data distribution, statistical processing was carried out using the Man-Whitney U-test. Differences with a significance level of more than 95% ($p < 0,05$) were considered reliable.

RESULTS

Focal cerebral ischemia in untreated animals contributed to inactivity, lethargy, half-ptosis and ptosis of the eyelids, paresis, and in some cases paralysis, in most cases the contralateral side of the injury. The neurological deficit of the NC group of rats reached $3,85 \pm 0,21$ points, which corresponds to the average severity of violations on the McGraw scale in the modification of Gannushkina (Fig. 1). Due to administration of the reference drug cavinton, rare cases of paresis were noted in animals, no limb paralysis was observed, the neurological status was 52% lower ($p < 0,05$) relative to the animals of the negative control group. The introduction of the PIR-10 compound led to a significant decrease in the McGraw index compared with untreated animals and the group of rats treated with cavinton by 68% ($p < 0,05$) and 32% ($p < 0,05$), respectively.

Assessment of neurological deficits using the Combs and D'alecy scale enables to determine tenacity, balance and muscle strength in motor tests, which indicates the functional state of the extrapyramidal system. Coagulation of the left medial artery led to impaired motor skills and balance of the animals, which manifested itself in the inability to hold most of the muscles on a nylon rope, rod and screen-mesh. In the group of animals of negative control, a decrease in Combs and D'alecy scores was noted to $1,6 \pm 0,16$, which was 79,7% ($p < 0,05$) lower than in the group of rats (Fig. 2). Against the background of cavinton administration, motor function deficiency was 3,9 times ($p < 0,05$) less pronounced in comparison with the group of rats without pharmacotherapy. Nevertheless, no complete recovery of motor disorders was observed. The introduction of the PIR-10 compound contributed to a decrease in motor deficit by 4,3 times ($p < 0,05$) relative to untreated rats. In addition, the indicators of the groups of rats receiving PIR-10 and cavinton were statistically significantly different by 10,1% ($p < 0,05$). Thus, in animals that were injected with PIR-10, the maximum improvement in motor functions was noted.

To assess the reaction of animals and the asymmetry of their movements, the Garsia neurological deficit score scale was used. OLMCA led to pronounced violations of asymmetry, motor skills and proprioception, manifested in a significant decrease in the neu-

rological status in rats of the NC group on the Garsia scale by 2,8 times ($p < 0,05$) relative to falsely operated individuals ($17,7 \pm 0,15$). The introduction of cavinton partially contributed to the improvement of motor functions (by 51% relative to untreated individuals). This indicator significantly differed from the values of the FO group, which indicates incomplete restoration of impaired functions. In the group of rats treated with PIR-10, the neurological index was $11,6 \pm 0,45$, which was 84% ($p < 0,05$) higher than in rats not treated with therapy, but 34% ($p < 0,05$) lower than in the FO group. At the same time, despite the fact that this indicator exceeded that of Cavinton (by 22% ($p < 0,05$)), a complete restoration of asymmetry was not observed.

CONCLUSION

The pyrimidine derivative under the laboratory code PIR-10 made it possible to partially correct the neurological deficit that occurs in conditions of cerebral circulatory insufficiency, and showed an effect in its strength superior to the reference drug cavinton.

REFERENCES

1. FAROKHI-SISAKHT F., FARHOUDI M., SADIGH-ETEGHAD S., MAHMOUDI J., MOHADDES G. Cognitive rehabilitation improves ischemic stroke-induced cognitive impairment: role of growth factors // *Journal of Stroke and Cerebrovascular Diseases*. – 2019. – Vol. 28. – № 10. – P. 104299. DOI: <https://doi.org/10.1016/j.jstrokecerebrovasdis.2019.07.015>. Epub 2019 Jul 30.
2. RAJPUT S.K. SHARMA, A.K., MEENA, C. L., PANT, A.B., JAIN, R., SHARMA, S.S. Effect of L-pGlu-(1-benzyl)-l-His-l-Pro-NH₂ against in-vitro and in-vivo models of cerebral ischemia and associated neurological disorders // *Biomedicine & Pharmacotherapy*. – 2016. – Vol. 84. – P. 1256–1265. DOI: 10.1016/j.biopha.2016.10.059
3. DEFEBVRE L., KRSTKOWIAK P. Movement disorders and stroke // *Revue neurologique*. – 2016. – Vol. 172. – №. 8–9. – P. 483–487. DOI: 10.1016/j.neurol.2016.07.006
4. VORONKOV A.V., SHABANOVA N.B., KODONIDI I.P., SHATALOV I.S. Cerebroprotective activity of new derivatives of pirimidine-4-(1H)-one PIR-9 and PIR-10 in irreversible occlusion of the common carotid artery. *Pharmacy & Pharmacology*. 2018;6(2):167–181. (In Russ.) DOI: <https://doi.org/10.19163/2307-9266-2018-6-2-167-181>
5. MIRONOV A.N. The guidelines for preclinical studies of pharmaceuticals. Part one. – M.: Grif and K, 2012. – 944 p. (In Russ.)
6. NAZAROVA L.E., DYAKOVA I.N. Influence of ferulic acid on the necrosis zone resulting from occlusion of the middle cerebral artery // *medical Bulletin of Bashkortostan* – 2011. – №. 3. – P. 133–135. (In Russ.)
7. VORONKOV A.V., SHABANOVA N.B., VORONKOVA M.P., LYSENKO T.A. Study of cerebrotropic dose-

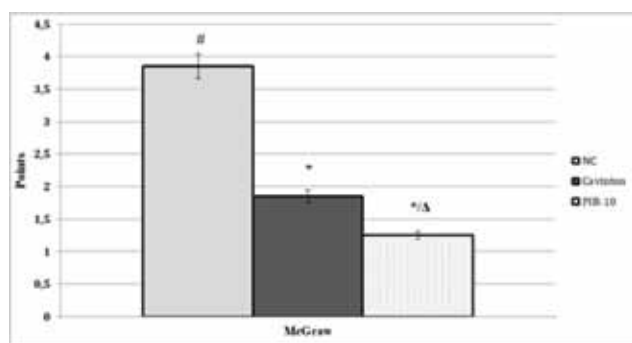


Fig. 1. Assessment of neurological deficit on the McGraw scale while taking the studied compound and the reference drug in focal of cerebral ischemia

Note: FO — falsely operated rats ; NC — negative control rats; Cavinton — a group rats treated with Cavinton; PIR-10 — a group of rats treated with PIR-10; # — statistically significant as compared to the FO rats ($p < 0,05$); * — statistically significant as compared to the NC rats ($p < 0,05$); Δ — statistically significant as compared to rats treated with Cavinton ($p < 0,05$).

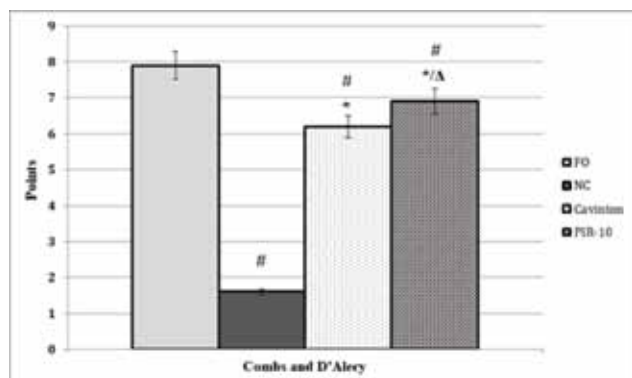


Fig. 2. Assessment of neurological deficit on the Combs and D'Alecy scale while taking the studied compound and the reference drug in focal of cerebral ischemia

Note: FO — falsely operated rats ; NC — negative control rats; Cavinton — a group rats treated with Cavinton; PIR-10 — a group of rats treated with PIR-10; # — statistically significant as compared to the FO rats ($p < 0,05$); * — statistically significant as compared to the NC rats ($p < 0,05$); Δ — statistically significant as compared to rats treated with Cavinton ($p < 0,05$).

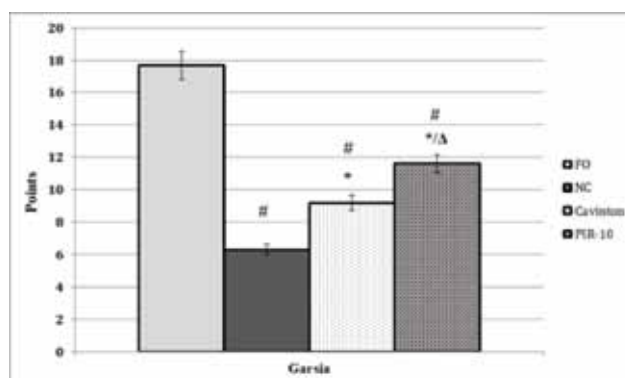


Fig. 3. Assessment of neurological deficit on the Garsia scale while taking the studied compound and the reference drug in focal of cerebral ischemia

Note: FO — falsely operated rats; NC — negative control rats; Cavinton — a group rats treated with Cavinton; PIR-10 — a group of rats treated with PIR-10; # — statistically significant as compared to the FO rats ($p < 0,05$); * — statistically significant as compared to the NC rats ($p < 0,05$); Δ — statistically significant as compared to rats treated with Cavinton ($p < 0,05$).

dependent effect of pyrimidine derivative under pir-9 code against the background of experimental cerebral ischemia in rats. *Pharmacy & Pharmacology*. 2018;6(6):548–567. (In Russ.) DOI: <https://doi.org/10.19163/2307-9266-2018-6-6-548-567>

8. TROFIMENKO A.I., KADE A.A., LEBEDEV V.P., ZANIN S.A., MYASNKOVA V.V. Modeling cerebral ischemia by coagulation of the middle cerebral artery in rats // *Fundamental research* – 2012. – №2. – P. 215–218.
9. Manual of stroke models in rats / ed. by Y. Wang-Fischer. – [S. l.] : CRC Press : Taylor& Francis Group, 2009. – XIII, 332 p.
10. GANNUSHKINA I. V. Cerebral circulation in different types of circulatory hypoxia of the brain // *Bulletin of the Russian Academy of Sciences*. – 2000. – Vol. 9. – P. 22–27.
11. COMBS D. J., D'ALECY L. G. Motor performance in rats exposed to severe forebrain ischemia: effect of fasting and 1, 3-butanediol // *Stroke*. – 1987. – Vol. 18. – №. 2. – P. 503–511. DOI: <https://doi.org/10.1161/01.STR.18.2.503>
12. GARCIA J. H., WAGNER, S., LIU, K. F., & HU, X. J. Neurological deficit and extent of neuronal necrosis attributable to middle cerebral artery occlusion in rats: statistical validation // *Stroke*. – 1995. – Vol. 26. – №. 4. – P. 627–635. DOI: [10.1161/01.str.26.4.627](https://doi.org/10.1161/01.str.26.4.627)

<http://dx.doi.org/10.35630/2199-885X/2022/12/2.11>

STUDY OF THE ANTIOXIDANT ACTIVITY OF HESPERIDIN UNDER DEBILITATING PHYSICAL EXERTION IN RATS

Received 08 February 2022;
Received in revised form 02 March 2022;
Accepted 04 March 2022

Anastasia Gerashchenko[✉] , Natalia Shabanova 

Pyatigorsk Medical and Pharmaceutical Institute —
Branch of Volgograd State Medical Pyatigorsk, Russia

✉ gerashchenko@mail.ru

ABSTRACT — **INTRODUCTION:** The antioxidant activity of hesperidin was studied against the background of debilitating physical activity. **MATERIALS AND METHODS:** Exhausting physical activity was reproduced in rats in the «Forced Swimming» test. A compound used in the study was administered at a dose of 100 mg/kg for 10 days of swimming. **RESULTS AND DISCUSSIONS.** In rats of the negative control group after 10 days of forced swimming, compared with intact animals, there was an increase in the activity of lipid peroxidation products in the blood: malondialdehyde and diene conjugates by 282.2% ($p < 0.05$) and 41.3% ($p < 0.05$). In turn, there was a decrease in the activity of antioxidant defense enzymes: superoxide dismutase by 44.8% ($p < 0.05$), catalase by 53.8% ($p < 0.05$), GP by 34.5% ($p < 0.05$) relative to the parameters of the intact group of rats. The use of hesperidin made it possible to correct these disorders — there was a significant increase in the activity of SOD, catalase and GP by 77.8% ($p < 0.05$), 172.7% ($p < 0.05$) and 153.5% ($p < 0.05$), respectively, and a decrease in the level of TBA-active products and DC in muscle tissue by 57.5% and 43.1% ($p < 0.05$) relative to the negative control group. Against the background of the introduction of the comparison drug Mexidol, a significant decrease in the level of endogenous pro- and an increase in antioxidants was observed. **CONCLUSION:** The results of the study allow us to recommend this compound as a corrector for biochemical shifts that may occur during exhausting loads.

KEYWORDS — physical overload, antioxidant activity, hesperidin, Mexidol, rats.

INTRODUCTION

The balance shift towards the activation of lipid peroxidation processes with a simultaneous weakening of the body's antioxidant defense system is called oxidative stress (OS) [1]. The cascade of reactions that triggers OS is one of the key links in the pathogenesis of nerve tissue damage in various pathological processes [2].

A high level of physical activity, characteristic of sports, has a significant impact on the system of

reactive oxygen species (ROS), causing a complex of changes in the functioning of enzyme systems [3]. These changes can both be positive, compensatory in nature and, in some cases, lead to inhibition of the activity of antioxidant mechanisms, accumulation of ROS in tissues with the development of damage [4].

In view of this, the search for means to reduce the consequences of stress reactions is an urgent and important task of experimental medicine.

Objective:

To study the antioxidant activity of hesperidin against the background of debilitating physical activity.

MATERIALS AND METHODS

The experiment was performed in accordance with the «Guidelines for conducting preclinical studies of drugs, ed. A.N. Mironov (2012 ed.)» [5]. The animals were kept in the vivarium of the Volgograd State Medical University (Russia). The study was carried out on 40 Wistar male rats ($m = 220\text{--}240$ g). Animals were divided into 4 groups ($n = 10$). All experimental animals, during the experiment, were kept under standard vivarium conditions (natural light change, temperature, relative humidity, standard diet of laboratory animals, weekly change of bedding and cages, fixed times for feeding and drinking) in compliance with the International recommendations of the European Convention on protection of vertebrate animals used in experimental studies. Animals were preliminarily randomized by weight and swimming time in the forced swimming test. After that, we formed 4 equal experimental groups. The group of positive control rats (PC) was subjected to physical activity with days of rest, the second group — negative control (NC) received 0.9% sodium chloride solution throughout the experiment. The third group of animals received hesperidin at a dosage of 100 mg/kg [6]. The fourth group received the reference drug Mexidol at a dosage of 150 mg/kg [7]. All test compounds were administered intragastrically 30 min prior to testing.

Exhausting physical activity was reproduced in the «Forced swimming» test with a load of 10% of the animal's body weight for 10 days. On the 11th day of the experiment, the animals were subjected to decapi-

tation under chloral hydrate anesthesia (350 mg/kg), followed by sampling of the gastrocnemius muscle.

In the postnuclear fraction, the content of diene conjugates (DC), TBA-active products in terms of malondialdehyde (MDA), and the activity of endogenous antioxidant defense enzymes: superoxide dismutase (SOD), catalase, and glutathione peroxidase (GP) were determined. The results of the experiments were processed by the method of variation statistics.

RESULTS

During debilitating physical activity in the group of NC rats, an increase in the content of MDA in intact animals by 282.2% and DC by 41.3% ($p < 0.05$), respectively, was observed (Fig. 1). In turn, a decrease in the activity of AOD enzymes was observed: SOD was by 44.8%, catalase by 53.8%, GP by 34.5% (all $p < 0.05$) in the parameters of the rats of the intact group (Fig. 2).

The data obtained during the experiment suggest that under conditions of prolonged debilitating physical overload, rats develop the phenomenon of oxidative stress in muscle tissue, with an increase in the amount of prooxidants and a decrease in the activity of AOD enzymes, which is consistent with the literature data [8].

The administration throughout the experiment of the reference drug Mexidol contributed to a decrease in peroxidation, which was lower than MDA by 72.8% and DC by 30.4% ($p < 0.05$) in comparison with the NC group.

The use of the studied plant flavonoid hesperidin led to the fact that the activity of TBA-active products was lower in the negative control group by 57.5% ($p < 0.05$) and DC by 43.1% ($p < 0.05$).

Daily use of the reference drug contributed to an increase in the activity of antioxidant defense enzymes: SOD-120% ($p < 0.05$), catalase-187.9 ($p < 0.05$) and GP-175% ($p < 0.05$) into the group of negative control (Fig.3).

Against the background of physical overload, the natural test compound significantly increased the activity of endogenous antioxidant defense enzymes, which was manifested in an increase in the activity of SOD, catalase and GP, respectively, by 77.8% ($p < 0.05$), 172.7% ($p < 0.05$) and 153.5% ($p < 0.05$).

At the same time, there were no statistically significant differences between the groups of rats treated with the reference drug Mexidol and hesperidin in terms of antioxidant protection.

CONCLUSION

Oxidative stress that occurs during exercise leads to significant shifts in the work of the pro- and

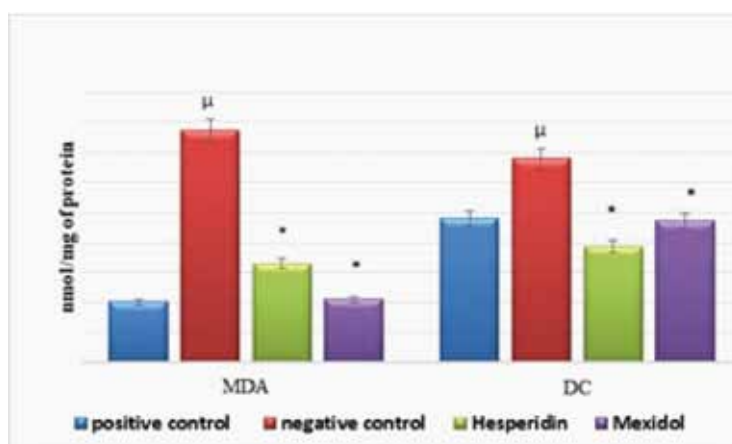


Fig. 1. Influence of hesperidin on the activity of Malondialdehyde (MDA) and conjugated dienes (CD) in rat muscle tissue homogenate during exhausting physical activity

Note: μ — significant relative to intact rats ($p < 0.05$); * — significant relative to negative control rats ($p < 0.05$).

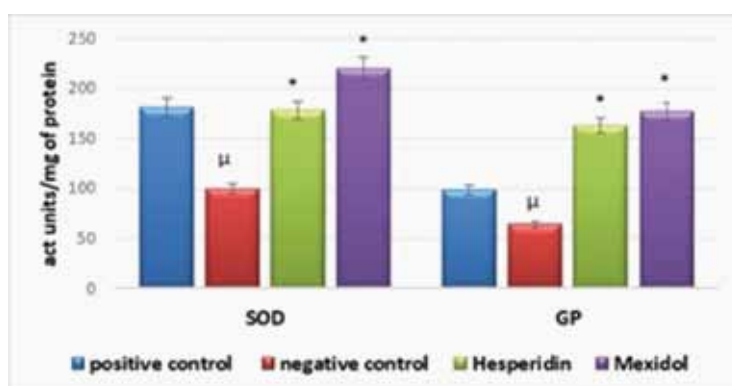


Fig. 2. The effect of hesperidin on the activity of superoxide dismutase and glutathione peroxidase in rat muscle tissue homogenate during exhausting physical activity.

Note: μ — significant relative to intact rats ($p < 0.05$); * — significant relative to negative control rats ($p < 0.05$).

antioxidant system. During the course of administration of hesperidin, a significant decrease in TBA-active products was observed, relative to the negative control group by 57.5% ($p < 0.05$) and DC by 43.1% ($p < 0.05$). At the same time, an increase in the activity of endogenous enzymes of antioxidant protection was noted: SOD — 77.8% ($p < 0.05$), catalase — 172.7% ($p < 0.05$) and GP — 153.5% ($p < 0.05$). It was found that there were no statistically significant differences between the groups of rats treated with the reference drug Mexidol and hesperidin in terms of antioxidant protection.

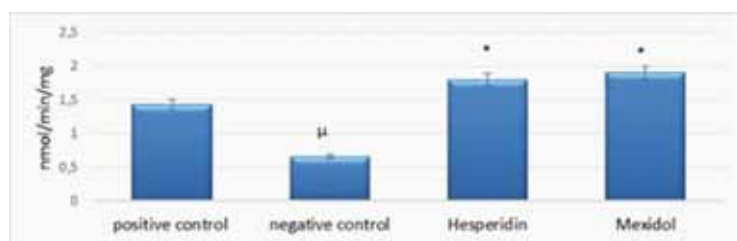


Fig. 3. The effect of hesperidin on catalase activity in rat muscle tissue homogenate against the background of debilitating physical activity

Note: μ — significant relative to intact rats ($p < 0.05$); * — significant relative to negative control rats ($p < 0.05$).

The results of the experiment allow us to recommend hesperidin for correction of biochemical shifts that may occur due to exhausting loads.

REFERENCES

1. **BARRIOS C.** Metabolic muscle damage and oxidative stress markers in an America's Cup yachting crew // *Eur. J. Appl. Physiol.* – 2011. – Vol. 111. – №.7. – P. 1341–1350. doi: 10.1007/s00421-010-1762-6
2. **DJORDJEVIC D., CUBRILO D., MACURA M.** The influence of training status on oxidative stress in young male handball players // *Mol. Cell. Biochem.* – 2011. – Vol. 351.- №.1–2. – P. 251–259. doi: 10.1007/s11010-011-0732-6
3. **FALONE S., MIRABILIO A., PASSERINI A.** Aerobic performance and antioxidant protection in runners // *Int. J. Sports Med.* – 2009. – Vol. 30. – №.11. – P. 782–788. doi: 10.1055/s-0029-1233464
4. **BAZARIN K. P., TITOVA N. M.** Dynamic changes in the activity of enzymes of the antioxidant defense system in blood plasma in professional rugby players // *Acta Biomedica Scientifica.* – 2014. – No 3 (97). – P. 9–13.
5. **MIRONOV A.N.** Guidelines for conducting preclinical studies of drugs. Part one. - M.: Grif and K, 2012. – 944 p.
6. **VORONKOV A.V., OGANESYAN E.T., POZDNYAKOV D.I., SIVTSEVA O.S., CHERVONNAYA N.M., ANDREEVA O.A.** Influence of flavonoids: hesperidin and patuletin on the vasodilating function of the endothelium of the cerebral vessels of experimental animals against the background of its focal ischemia. *Actual problems of medicine.* – 2017. – Vol. 39. – No 19 (268). – P. 186–194.
7. **VORONINA, T. A. KAPITSA I. G., IVANOVA E. A.** Comparative study of the effect of mexidol and mildronate on physical performance in the experiment // *Journal of Neurology and Psychiatry. SS Korsakov.* – 2017. – Vol. 117. – №. 4. – P. 71–74. doi: 10.17116/jnevro20171174171-74
8. **MARGONIS K., FATOUROS G., JAMURTAS Z., NIKOLAIDIS G., DOUROUDOS I., CHATZINIKOLAOU A. [ET AL].** Oxidative stress biomarkers responses to physical overtraining: implications for diagnosis // *Free Radical Biology and Medicine.* - 2007. - T. 43. - No 6. – P. 901-910. doi: <https://doi.org/10.1016/j.freeradbiomed.2007.05.022>

<http://dx.doi.org/10.35630/2199-885X/2022/12/2.12>

VALIDITY OF USING THE $\text{SpO}_2/\text{FiO}_2$ RATIO TO DETERMINE THE DYNAMICS AND CORRECTION METHODS OF OXEMIA IN ACUTE LUNG INJURY AND ACUTE RESPIRATORY DISTRESS SYNDROME

Received 01 February 2022;
Received in revised form 02 March 2022;
Accepted 03 March 2022

Mikhail Turovets[✉] , Alexander Popov ,
Andrey Ekstrem, Anastasia Streltsova 

Volgograd State Medical University, Volgograd, Russia

✉ turovets_aro@mail.ru

ABSTRACT — Continuous monitoring of oxemia in patients with acute lung injury (ALI) and acute respiratory distress syndrome (ARDS) is essential for successful therapy. AIM: To substantiate the validity of the use of pulse oximetry to determine the dynamics of oxemia in patients with ALI and ARDS and approbation of the «Mechanical Ventilation Expert» (MV Expert) smartphone application in a clinical setting.

MATERIALS AND METHODS: The study included 588 patients with ALI and ARDS. The interdependence of 1188 data pairs (SpO_2 and PaO_2) was analyzed. In case of hypoxemia, the parameters of respiratory support were corrected with and without the use of the «MV Expert» application. ROC curves and linear regression analysis were used for data processing.

RESULTS: The prognostic value of SpO_2 and PaO_2 in this group of patients was almost equivalent. At SpO_2 values from 91% to 93%, hypoxemia ($\text{PaO}_2 < 60$ mmHg) was noted in 11.9% (142/1189) of data pairs, and at SpO_2 from 94% to 96% this condition was confirmed in 1.3% (16/1189) of data pairs. In cases where the recommendations of the «MV Expert» application were followed, oxemia indicators increased significantly more often ($p = 0.002$) and by more significant values (with $p = 0.007$ for SpO_2 and $p = 0.001$ for PaO_2) than in cases when doctors adjusted settings based on their own experience.

CONCLUSION: With a high degree of probability, SpO_2 dynamics shows significant changes in oxemia in patients with ALI and ARDS. At SpO_2 from 94% to 96%, the development of hypoxemia ($\text{PaO}_2 < 60$ mmHg) was observed in 1.3% of cases. The use of the «MV Expert» application increases the effectiveness of respiratory support.

KEYWORDS — oxygenation index, acute lung injury, acute respiratory distress syndrome.

INTRODUCTION

Respiratory support is one of the main components of the treatment of patients with acute lung

injury (ALI) and acute respiratory distress syndrome (ARDS) [1, 2].

At the same time, both hypoxia and hyperoxia have a negative effect on mortality rates in severely ill patients [1, 2, 3]. Therefore, an urgent task for the attending physician is to constantly monitor the level of oxemia, especially when using of invasive and non-invasive mechanical ventilation (MV).

Objectively, the most accurate indicator of blood oxygen saturation is the partial oxygen pressure (PaO_2). This indicator is also used in the calculation of the hypoxemia index ($\text{PaO}_2/\text{FiO}_2$) to assess external respiration dysfunction in most scales of severity and physical condition of the patient (SOFA, APACHE II–III, etc.). Measurement of arterial blood gas (ABG) is an invasive and costly procedure that requires both time and consumables, making it difficult to continuously monitor patients for oxemia. Moreover, multiple sampling of arterial blood entails certain risks for patients in terms of the development of adverse consequences (bleeding and thrombotic complications) [4].

A routine method for monitoring oxemia, which is used in most hospitals, is the non-invasive measurement of oxygen saturation (SpO_2) using pulse oximetry. However, there is no direct linear relationship between SpO_2 and PaO_2 [5, 8, 9]. SpO_2 parameters are influenced by hemoglobin and acid-base status, changes in body temperature and cardiac output [6], the level of perfusion of peripheral tissues and the use of vasoactive drugs [7, 9].

The second, but not the last, problem in the treatment of patients with ALI and ARDS is the choice of the ventilation parameter to be adjusted (positive end-expiratory pressure, respiratory rate, inspiratory pressure, etc.) to more effectively correct hypoxemia. Based on numerous publications and extensive practical experience, we have created an application for smartphones called «Mechanical Ventilation Expert» (MV Expert) to help doctors in solving these problems [10].

The objectives of this study were to substantiate the validity of the use of pulse oximetry to determine the dynamics of oxemia in patients with ALI and

ARDS and approbation of the «Mechanical Ventilation Expert» (MV Expert) application in a clinical setting.

MATERIALS AND METHODS

Between January 2019 and December 2021, a prospective comparative study was conducted, which included 637 patients aged 18 to 65 years with ALI and ARDS. All patients were treated in intensive care units of five clinical hospitals in Volgograd, Russia. The study was approved by the local ethics committee of the Volgograd State Medical University (ref: 127/2019/12/12). All patients signed a voluntary consent to participate in the study and also consented to the publication of the results.

49 patients with hyperbilirubinemia ($n = 38$) and those who underwent extracorporeal membrane oxygenation ($n = 11$) were excluded from the study. The $\text{PaO}_2/\text{FiO}_2$ ratio was used to differentiate between ALI and ARDS (≤ 300 for ALI and ≤ 200 for ARDS). The first cohort ($n = 225$) included patients with ALI, the second cohort ($n = 363$) included patients with ARDS. All patients used non-invasive (low and high flow oxygen therapy, CPAP) and invasive (MV) methods of respiratory support.

In intensive care units, PaO_2 was measured using a combined blood gas analyzer (ABL800 FLEX, Denmark) within 5 minutes after sampling. Simultaneously with blood sampling, SpO_2 was measured using a bedside monitor pulse oximeter (BSM-3763, Nihon Kohden Corporation, Japan). In some patients, up to 5 pairs of data (SpO_2 and PaO_2) were collected at least 2 hours apart.

To evaluate the operation of «MV Expert», we checked changes in SpO_2 values 5–10 minutes after following the application's recommendations to correct respiratory support parameters.

The obtained data were analyzed using the SPSS statistical software package (version 26, IBM, USA). The variables were presented as mean with standard deviation (SD). When comparing unrelated groups, the Mann-Whitney U-test (for quantitative values) and Fisher's exact test (for nominal variables) were used. The Wilcoxon test was used for the analysis of related groups. To determine the interdependence of indicators, ROC analysis and linear regression analysis were used. Significance of differences was confirmed by the value of the two-sided coefficient $p \leq 0.05$.

RESULTS AND DISCUSSION

Demographic and clinical data of the included patients are shown in Table 1. At admission to the intensive care unit, 20.4% (46/225) of patients in the ALI group and 55.4% (201/363) of

patients in the ARDS group had a hypoxic profile ($\text{PaO}_2 < 60$ mmHg).

The study groups were comparable in terms of comorbidity. In patients of the ARDS group, vasopressors were used significantly more often ($p = 0.001$) to stabilize hemodynamics.

ROC analysis was performed to determine the relationship between PaO_2 and SpO_2 in 1189 data pairs (Fig. 1). According to the results of the ROC analysis, the area under the ROC curve corresponding to the relationship between ALI prognosis and PaO_2 and SpO_2 values was 0.648 ± 0.02 with 95% CI: $0.610\text{--}0.686$ ($p = 0.000$) for PaO_2 and 0.615 ± 0.02 with 95% CI: $0.576\text{--}0.654$ ($p = 0.000$) for SpO_2 . Cut-off thresholds for PaO_2 and SpO_2 were 61.5 mmHg for PaO_2 and 91.5% for SpO_2 . With a decrease in indicators below the threshold values, a high risk of developing ARDS was predicted. The sensitivity and specificity of the method were 76.0% and 70.5% for PaO_2 and 73.1% and 68.6% for SpO_2 , respectively. The prognostic value of SpO_2 and PaO_2 in this group of patients was almost equivalent. At SpO_2 values from 91% to 93%, hypoxemia ($\text{PaO}_2 < 60$ mmHg) was noted in 11.9% (142/1189) of data pairs, and at SpO_2 from 94% to 96% this condition was confirmed in 1.3% (16/1189) of data pairs.

Linear regression analysis was performed to identify the dependence of $\text{PaO}_2/\text{FiO}_2$ on $\text{SpO}_2/\text{FiO}_2$ (Table 2).

The observed dependence of $\text{PaO}_2/\text{FiO}_2$ on $\text{SpO}_2/\text{FiO}_2$ is described by the equation: $\text{PaO}_2/\text{FiO}_2 = 1.29 + 0.73 \cdot \text{SpO}_2/\text{FiO}_2$. With an increase in $\text{SpO}_2/\text{FiO}_2$ by 1 unit, an increase in $\text{PaO}_2/\text{FiO}_2$ by 0.73 units is expected (95% CI 0.718–0.749). The significance level of the model (p) was less than 0.001. Based on the value of the coefficient of determination, the factors included in the model determine 88.4% of the $\text{PaO}_2/\text{FiO}_2$ variance.

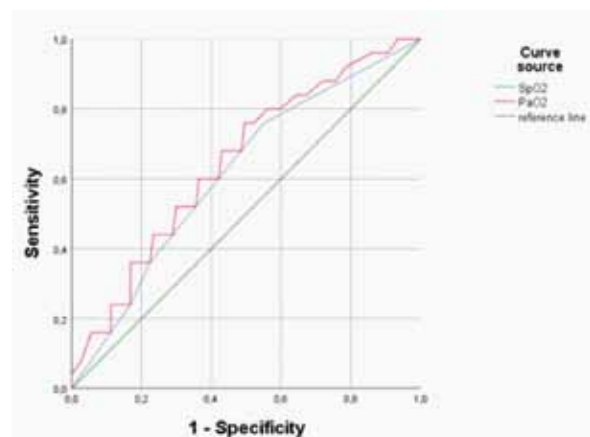
To test the validity of the recommendations given by the «MV Expert» application, we analyzed the dynamics of SpO_2 and PaO_2 after following those recommendations for patients with a decrease in SpO_2 and PaO_2 below the threshold value (Table 3).

In cases where the recommendations of the «MV Expert» application were followed, oxemia indicators increased significantly more often ($p = 0.002$) and by more significant values ($p = 0.007$ for SpO_2 and $p = 0.001$ for PaO_2) than in cases when doctors changed parameters based on their own experience. The use of the «MV Expert» application allowed to increase the effectiveness and validity of changes in respiratory support.

ALI and ARDS are major contributors to morbidity and mortality in intensive care units. The

Table 1. Demographic and clinical characteristics of included patients

Variable	ALI (n=225), M±SD	ARDS (n=363), M±SD	p
Age, years	56.8±7.6	55.9±8.8	0.776
Male, n (%)	132 (58.7)	189 (52.1)	0.118
Comorbidity:			
Obesity, n (%)	64 (28.4)	112 (30.9)	0.535
Arrhythmia, n (%)	24 (10.7)	41 (11.3)	0.813
Hypertension, n (%)	98 (43.6)	161 (44.4)	0.850
Cardiac ischemia, n (%)	37 (16.4)	52 (14.3)	0.486
Diabetes, n (%)	12 (5.3)	27 (7.4)	0.319
Vasopressors, n (%)	67 (40.1)	169 (59.9)	0.001
FiO ₂	0.27±0.01	0.56±0.02	0.000
SpO ₂ , %	93.2±0.27	91.5±0.14	0.000
PaO ₂ , mmHg	74.0±1.05	67.0±0.50	0.000
PaCO ₂ , mmHg	43.6±9.07	43.9±6.12	0.184
pH	7.38±0.04	7.36±0.05	0.281
Arterial Bicarbonate, mmol/l	24.2±5.3	21.8±3.9	0.006
Lactate, mmol/l	2.23±0.17	2.36±0.25	0.012
Hemoglobin, g/l	148.3±7.44	154.6±8.08	0.371
Systolic blood pressure, mmHg	127±9.1	117±8.2	0.034
Diastolic blood pressure, mmHg	72±4.6	87±6.1	0.007

Fig. 1. ROC-curves of the relationship of ALI prediction by SpO₂ and PaO₂ values

routine use of pulse oximetry makes it possible to adequately assess the dynamics of oxemia in patients of this profile and avoid significant costs and possible harm to patients associated with the determination of blood gases.

Several formulas that allow the determination of the oxygenation index ($\text{PaO}_2/\text{FiO}_2$) from SpO₂ have been proposed [11]. This makes it possible to assess the degree of lung damage and the severity of the patient's condition using various scales [12].

This study has its limitations. First, the ABG and pulse oximetry measurements were not simultaneous. Given that changes in SpO₂ and PaO₂ can occur quickly, this may have affected our results. In addition, we did not control body temperature and initial parameters of the ventilator. These factors may also have influenced the relationship between SpO₂ and PaO₂.

CONCLUSION

With a high degree of probability, the dynamics of SpO₂ describes significant changes in oxemia in patients with ALI and ARDS. With an SpO₂ of 94% to 96%, hypoxemia ($\text{PaO}_2 < 60$ mmHg) occurs in 1.3% of cases. Using the «MV Expert» application increases the effectiveness of respiratory support.

CONFLICT OF INTERESTS

The authors state that they have no conflict of interests.

CONTRIBUTORS

MIT and AMS collected, analysed, and interpreted data and made the figures. ASP did the literature review and collected data. AVE collected data and made the figures. MIT and ASP interpreted and analysed the data. MIT, ASP, AVE and AMS prepared the manuscript for submission.

Table 2. PaO_2/FiO_2 versus SpO_2/FiO_2 from linear regression

PaO ₂ /FiO ₂	Model Summary								
	Model	R		R ²		Скоpp. R ²		SD	
	SpO ₂ /FiO ₂	0.940		0.884		0.884		26.9521	
	Coefficients								
	Model	B	SD (B)	β	t	p	95% CL for B		
	Constant	1.287	1.654		0.778	0.436	-1.957	4.531	
	SpO ₂ /FiO ₂	0.733	0.008	0.940	94.942	0.000	0.718	0.749	

Table 3. Results of respiratory support settings adjustments

SpO_2	Adjusting respiratory support settings				
	With «MV Expert» (n = 218)		Without «MV Expert» (n = 223)		p
Increase, n (%)	187 (85.8)		164 (73.5)		0.002
No change, n (%)	24 (11.0)		46 (20.6)		0.006
Decrease, n (%)	7 (3.2)		13 (5.8)		0.253
	Before	After	Before	After	
SpO_2 , M \pm SD	89.7 \pm 1.6	94.7 \pm 1.8	90.2 \pm 1.9	93.4 \pm 2.1	0.007
PaO_2 , M \pm SD	57.7 \pm 0.87	74.9 \pm 1.11	58.3 \pm 0.74	67.3 \pm 0.98	0.001

REFERENCES

- HOCHBERG CH, SEMLER MW, BROWER RG. Oxygen Toxicity in Critically Ill Adults. *Am J Respir Crit Care Med*. 2021 Sep 15;204(6):632-641. doi: 10.1164/rccm.202102-0417CI
- NANCHAL RS, TRUWIT JD. Recent advances in understanding and treating acute respiratory distress syndrome. *F1000Res*. 2018 Aug 20;7:F1000 Faculty Rev-1322. doi: 10.12688/f1000research.15493.1
- WALTER JM, CORBRIDGE TC, SINGER BD. Invasive Mechanical Ventilation. *South Med J*. 2018 Dec;111(12):746-753. doi: 10.14423/SMJ.0000000000000905
- VAPORIDI K, AKOUMIANAKI E, TELIAS I, GOLIGHER EC, BROCHARD L, GEORGOPOULOS D. Respiratory Drive in Critically Ill Patients. Pathophysiology and Clinical Implications. *Am J Respir Crit Care Med*. 2020 Jan 1;201(1):20-32. doi: 10.1164/rccm.201903-0596SO
- VASCONCELOS RS, SALES RP, MELO LHP, MARINHO LS, BASTOS VP, ET AL. Influences of Duration of Inspiratory Effort, Respiratory Mechanics, and Ventilator Type on Asynchrony With Pressure Support and Proportional Assist Ventilation. *Respir Care*. 2017 May;62(5):550-557. doi: 10.4187/respcare.05025
- JONKMAN AH, RAUSEO M, CARTEAUX G, TELIAS I, SKLAR MC, ET AL. Proportional modes of ventilation: technology to assist physiology. *Intensive Care Med*. 2020 Dec;46(12):2301-2313. doi: 10.1007/s00134-020-06206-z
- SCHJØRRING OL, KLITGAARD TL, PERNER A, WETTERSLEV J, LANGE T, ET AL. Lower or Higher Oxygenation Targets for Acute Hypoxemic Respiratory Failure. *N Engl J Med*. 2021 Apr 8;384(14):1301-1311. doi: 10.1056/NEJMoa2032510
- RÖTTGERING JG, DE MAN AME, SCHUURS TC, WILS EJ, DANIELS JM, ET AL. Determining a target SpO_2 to maintain PaO_2 within a physiological range. *PLoS One*. 2021 May 13;16(5):e0250740. doi: 10.1371/journal.pone.0250740
- BROWN SM, DUGGAL A, HOU PC, TIDSWELL M, KHAN A, ET AL. Prevention and Early Treatment of Acute Lung Injury (PETAL) Network. Nonlinear Imputation of PaO_2/FiO_2 From SpO_2/FiO_2 Among Mechanically Ventilated Patients in the ICU: A Prospective, Observational Study. *Crit Care Med*. 2017 Aug;45(8):1317-1324. doi: 10.1097/CCM.0000000000002514
- STRELTsov VO. Mechanical Ventilation Expert. AppStore: <https://apps.apple.com/app/id1591944892?platform=iphone>; GooglePlay: <https://play.google.com/store/apps/details?id=ru.poas.medical.respiratory.support.assistant.sofa.calculator>
- SAUTHIER M, TULI G, JOUVET PA, BROWNSTEIN JS, RANDOLPH AG. Estimated PaO_2 : A Continuous and Noninvasive Method to Estimate PaO_2 and Oxygenation Index. *Crit Care Explor*. 2021 Sep 28;3(10):e0546. doi: 10.1097/CCM.0000000000002514
- BROWN SM, GRISSOM CK, MOSS M, RICE TW, SCHOENFELD D, ET AL. Nonlinear Imputation of PaO_2/FiO_2 From SpO_2/FiO_2 Among Patients With Acute Respiratory Distress Syndrome. *Chest*. 2016 Aug;150(2):307-13. doi: 10.1016/j.chest.2016.01.003

<http://dx.doi.org/10.35630/2199-885X/2022/12/2.13>

SURGICAL APPROACH TO THE TREATMENT OF UPPER EYELID RETRACTION CAUSED BY PROMINENT FILTRATION BLEB

Received 18 December 2021;
Received in revised form 12 January 2022;
Accepted 15 January 2022

Elena Drabkin[✉], Aleza Andron

Oculoplastic Unit, Ophthalmology Department of Shaare Zedek Medical Center, Jerusalem, Israel

✉ dr.drabkin@gmail.com

ABSTRACT — **OBJECTIVE:** To report on the technique of upper eyelid lengthening in patients with upper eyelid retraction not associated with Graves' disease but associated with bleb exposure and exposure keratitis.

CASE SERIES: We present three patients (four eyes) with a history of glaucoma who underwent trabeculectomy with an active bleb with symptoms associated with bleb and corneal exposure due to retraction of the upper eyelid not associated with Graves' disease. All patients underwent surgical treatment to lengthen the upper eyelid by percutaneous complete blepharotomy with complete dissection of the orbicularis muscle, aponeurosis of levator palpebral muscle, Muller's muscle and dissection of nasal and temporal conjunctiva reaching the superior border of the tarsus. In addition, the lateral horns of the levator muscle were resected, while preserving a strip of intact conjunctiva directly above the bulging bleb.

Before and after surgery, the following measurements were made: including, visual acuity, retraction measurement, presence symptoms of dry cornea and bleb, MRD, and upper eyelid contour.

RESULTS: Preoperative upper lid marginal reflex distance (MRD) was measured. In addition, conjunctival staining of the bleb and cornea was recorded. Visual acuity ranged from 6/12 to 6/36. Upper eyelid retraction ranged from 3mm to 7.5mm, this was measured by calculating the marginal reflex distance (MRD) of the upper retracted eyelid minus 4.5 mm, representing the normal MRD. Amounts of lubricating drops used by patients per day was also recorded and quantified.

The following postoperative measurements were recorded: MRD of upper eyelid; specifically including upper eyelid contour and position, present or absence of upper eyelid ptosis. Visual acuity improved by one line in the first postoperative week and maximum up to three lines after a month. A good cosmetic result was achieved.

CONCLUSION: Blepharotomy is a surgical procedure suitable for the treatment of severe eyelid retraction. Preservation of the bridge of the intact conjunctiva over the bleb protects the bleb from traumatization in the postoperative period. This makes possible to use the blepharotomy in cases of eyelid retraction with exposure of the filtration bleb, and also maintain the correct contour of the upper eyelid.

KEYWORDS — eyelid retraction, upper eyelid lengthening, blepharotomy, filtration bleb.

INTRODUCTION

Retraction of the eyelids is defined as an increase in the vertical opening of the palpebral fissure. (1, 2) In this regard, eyelid retraction is both a functional disease and a cosmetic problem. The most commonly seen cause of eyelid retraction is an over-active thyroid gland, a medical condition called Graves' disease. (3, 4, 5) Retraction of the eyelids can be acquired and congenital. (3) Acquired cases are more common. There are several etiologies may cause eyelid retraction. For example, conditions such as autoimmune inflammatory disorder, neurogenic, myogenic and mechanical pathology (3, 4). Mechanical retraction of eyelids the most common cause. Mechanical types of retraction include conditions defined as *bulging or protruding* eyes associated with high myopia, buphthalmos, proptosis, retrobulbar hemorrhage, craniosynostosis. The mechanical etiology of retraction also includes fractures of the lower wall of the orbit, eyelid neoplasia, atopic dermatitis, eyelid skin scars, extended contact lens wear, conditions after irradiation of the orbit or sinuses, after blepharoplasty and surgery to correct ptosis, and also post traumatic or postsurgical or after burn symblepharon and conjunctival scarring of posterior lamella of eyelids. The occurrence of upper eyelid retraction after filtering glaucoma operations is rare but well established. (6, 7) The mechanism by which a bleb is the cause of eyelid retraction remains unclear, but there are several hypotheses are present. The most common hypothesis is mechanical lifting of the eyelid over the underlying bulging superior bulbar conjunctiva (Fig. 1). As a result, the bleb causes retraction of the upper eyelid, and retraction leads to exposure of the bleb and cornea, exposure keratopathy, corneal and bleb erosions, lack of protection of the bleb from external influences, a greater likelihood of infection, followed by the development of blebitis and, in severe cases, endophthalmitis (8, 9). Therefore, the treatment of eyelid retraction in the case of a bare bleb is of primary importance. In these cases, there is no clear indication which surgical method is best for treating eyelid retraction and which surgical technique is superior for performing blepharotomy.

SURGICAL TECHNIQUE

The amount of bleb projection is marked, and the lid crease is marked as well. Local anesthesia is

infiltrated in the upper eyelid with lidocaine HCL 2% and epinephrine 1/100,000. (Fig. 2). The corneal shield is inserted into the palpebral fissure. An incision is made in the skin and orbicularis muscle along the eyelid crease with conjunctival sparing. Dissection is performed reaching a plane superior to the bleb. The levator aponeurosis and Muller's muscle are dissected from the upper edge of the tarsal plate and separating them from the conjunctiva. Dissection is continued to superior conjunctival fornix reaching and incising the lateral horn of the levator muscle. The palpebral conjunctiva is incised on the nasal and temporal sides of the projection (Fig. 3). The incision of the conjunctiva may continue medially, to the medial end of the tarsal plate and laterally, to the lateral canthal ligament. This graded through and through conjunctival incision is done along-side with constant measurement of the lid height to determine how much to incise. (Fig. 4). If necessary, the incision of the conjunctiva is extended from the desired side until the eyelid drops to the planned height (Fig. 5). The orbicularis muscle is sutured with Vicryl 6.0 and an intradermal suture or an external suture with 6.0 nylon suture performed. If non-dissolving sutures are chosen, the sutures are removed in two weeks. Synthomycin ointment 5% is applied in the eye and on the skin of the eyelid. The eye is closed with a tight bandage.

RESULTS:

Case 1. A 60-year-old man with a history of open-angle glaucoma in the right eye. A year prior, he underwent a revision of trabeculectomy. Workup was done and thyroid disease was ruled out. He was treated with lubricants every hour in the right eye. On examination, visual acuity without correction Right Eye — 6/36, MRD — 12mm, eyelid retraction — 7.5 mm, dry bleb, diffuse superficial keratitis. No other pathology of the right eye was found. After surgery on the right eye MRD — 3 mm at check in a month and after half a year, RE vision 6/24 after a 1 week and 6/12 in a month after operation. Post-operative patient was treated with lubricants 6 times a day for one month, then tapering to 4 times a day. Correct eyelid contour. The disappearance of the symptoms of dryness of the bleb and cornea. The filtering function of the bleb has not changed. Patient is satisfied with cosmetics.

Case 2. A 66-year-old man with a history of open-angle glaucoma in both eyes. 3 years prior, trabeculectomy was performed on the right eye. Post operatively, the intraocular pressure decreased well without additional treatment, but his vision deteriorated and he experienced a foreign body sensation. A trial of lubricants yielded not sufficient relief. On workup, there was no evidence of thyroid eye disease.

On examination, visual acuity was 6/12 OD, MRD — 7.5 mm, measuring an eyelid retraction of 3mm; there was dryness and thinning of the raised bleb, and also evidence of superficial keratitis. There was no other pathology in the right eye. Blepharotomy was performed and post-op the MRD was measured — 4 mm, this was preserved 1.5 years post op. There was an improvement as well in the visual acuity OD= 6/9. Post operatively, the eyelid contour significantly improved, there was a significant decrease in corneal and conjunctival signs of dry eye and patient subjectively felt an improvement on sensation. Intraocular pressure remained controlled.

Case 3. 72 year old male with a history of open-angle glaucoma in both eyes. Bilateral trabeculectomy was performed. Post operatively, intraocular pressure decreased well without additional treatment in the first year, but then prostaglandin drops were added. He complained of blurred vision and burning sensation in both eyes and used artificial tears multiple times a day. Upon workup, no evidence of thyroid disease was found. On examination, uncorrected visual acuity was 6/18 OU, MRD OD — 11.5 mm, measuring eyelid retraction at OD 7mm. The MRD OS -8mm with eyelid retraction measuring at 3.5 mm. There was evidence of dryness and thinning of the raised cystic bleb on the right eye, and slightly less raised on the left eye, with superficial keratitis of both corneas. No other eye pathology was found. The patient underwent blepharotomy of both eyes, with an interval of several months between both eyes. Post operatively, eyelid MRD in OD was 4 mm, and 3 mm in OS, with a year half of follow up. Visual acuity in the right eye improved to 6/12 a week postop and 6/9 a month post op, in the left eye vision stayed at 6/12 a week and month post-op. The upper eyelid height and curvature was satisfactory in both eyes. There was a significant decrease in objective and subjective signs of dry eyes, with an absence of complaints. Intraocular pressure is still regulated by the prostaglandin drops. There were no complaints of burning sensation and discomfort in both eyes.

DISCUSSION

Eyelid retraction due to large cystic blebs is a rare entity and not well reported in the literature (6, 7, 8, 9). Eyelid retraction is defined by abnormal elevation of the upper eyelid in primary gaze. Lid retraction is most commonly associated with thyroid eye disease, once excluded, the list of differential diagnoses is complex; including neurological, muscular and mechanical causes (1, 2, 3). Eyelid retraction as a result of a large filtering bleb is a rare mechanical cause and was first described by Putterman in 1975 (10). There



Fig. 1. Retraction of the upper eyelid over the protruding bleb of the right eye.



Fig. 2. Marking of the projection of the bleb and eyelid crease.



Fig. 3. The conjunctival incision is more temporal than the bleb projection



Fig. 4. Intraoperative check of the eyelid height



Fig. 5. The final desired eyelid position



Fig. 6. 2 year post-operative photo

are several types of eyelid retraction surgery, surgical decision is dependent on the anatomical location of the pathology (7). Depending on the disease, there can be vertical shortening of either the anterior lamella, posterior lamella or both; this differentiation determines our surgical approach.

The external or cutaneous approach involves an external skin incision and dissection of the levator and Muller's muscle from the tarsus; this elongates the vertical distance of this structure and with an option

to place a spacer graft (11). The internal approach involves incision through the conjunctiva, dissection of the Muller's muscle and often resection of the Muller's muscle, this creating eyelid recession (11, 12). If eyelid retraction is more significant, through the conjunctival approach, it is also possible to dissect off the levator muscle, creating a greater eyelid recession. In our experience, we can categorize each case based on the severity of the retraction; this enables us to decide on the specific surgical approach.

Usually, for mild lid retraction the internal approach is preferred (12). For more severe cases we tend to use the external approach, and in most severe cases we must elongate both the anterior and posterior lamella with spacer grafts and skin grafts (13).

We presented 3 cases of eyelid retraction secondary to prominent filtering bleb formation. In our opinion, there are multiple possible causes of upper eyelid retraction in patients with large convex upper limbal filtered bleb. The first is a mechanical reason; due to the size and bulge of the bleb, it is difficult for the upper eyelid to close over the bleb and the eyelid remains open above the bleb, creating eyelid retraction (8, 9). Second, enlargement of the bleb increases the surface area of the bulbar conjunctiva, there for necessitating a longer eyelid to cover the eye.

The third suspected mechanism is the contraction of the upper eyelid in response to constant mechanical irritation of Muller's muscle through the conjunctiva and hence, causing Mueller's muscle to retract thus retracting the eyelid (14). A similar mechanism of upper eyelid retraction is observed in some patients wearing rigid contact lenses. Hard contact lenses mechanically irritate the Mueller muscle at the site of its attachment to the eyelid tarsus through the thin conjunctiva. This irritation in the early stages leads to contraction of the Müller muscle and retraction of the upper eyelid (14). Unlike hard contact lenses, a prominent bleb is in contact with a larger area of the Muller's muscle and causes greater eyelid retraction. A fourth proposed mechanism is that long term bleb irritation of conjunctiva and Muller's muscle can cause muscle and conjunctiva fibrosis and shortening of the posterior lamella (14).

The purpose surgery for repair of lid retraction is to increase the length of the eyelids and thereby reduce the size of the palpebral fissure. Unfortunately, there are no surgical algorithms correlating the severity of eyelid retraction with the appropriate surgical approach and the amount of recession needed as we see in ptosis and strabismus repair (15). This fact complicates the possibility of preliminary assessment of the accuracy of the postoperative result.

The result of such an operation may be insufficient drooping of the eyelid or postoperative ptosis, which in either case requires a second operation. An additional complicating factor in the treatment of upper eyelid retraction in glaucomatous patients with prominent filtration blebs is when choosing the internal approach there is increased possibility of bleb damage both during surgery and in the postoperative period by mechanical irritation of sutures and scarring. Blepharotomy with preservation of the bridge of the intact conjunctiva over the filtration bleb is the right choice for surgical treatment of upper eyelid retraction

in glaucomatous patients. The bridge of the preserved conjunctiva protects the bleb from damage, the level of drooping of the eyelid can be adjusted during the operation and the operation can be completed when eyelid is at desired height. We also recommend performing a temporary tarsorrhaphy for one week, continuing the effect of eyelid pulling. The effect of this operation is long lasting and thereby improves the functional and cosmetic condition of the patient.

CONCLUSION

Blepharotomy is a surgical procedure suitable for the treatment of severe eyelid retraction caused by a filtering bleb. Preservation of the bridge of the intact conjunctiva over the whole surface of the bleb protects it from trauma in the postoperative period and makes it possible to use this procedure even in cases of exposure and pathologically thin filtration bleb.

REFERENCES

1. HARVEY JT, ANDERSON RL. The aponeurotic approach to eyelid retraction. *Ophthalmology*. 1981;88:513-524. DOI: 10.1016/s0161-6420(81)34996-3
2. BAYLIS HI, CIES WA, KAMIN DF. Correction of upper eyelid retraction. *Am J Ophthalmol*. 1976;82:790-794. DOI: 10.1016/0002-9394(76)90019-2
3. BARTLEY GB. The differential diagnosis and classification of eyelid retraction. *Ophthalmology*. 1996;103:168-176. DOI: 10.1016/s0161-6420(96)30744-6
4. BARTLEY G. The epidemiologic characteristics and clinical course of ophthalmopathy associated with autoimmune thyroid disease in Olmsted County, Minnesota. *Tr Am Ophth Soc*. 1994;92:477-588.
5. ELNER V ET AL. Graded Full-Thickness Anterior Blepharotomy for Upper Eyelid Retraction. *Arch Ophthalmol*. 2004;122:55-60. PMID: 15083084
6. AWWAD ST, MÁLUF RN, NOUREDDIN B. Upper eyelid retraction after glaucoma filtering surgery and topical application of mitomycin C. *Ophthalm Plast Reconstr Surg*. 2004;20(2):144-149 DOI: 10.1097/01.iop.0000115596.80381.80
7. SALDANA M, ET AL. Lid Retraction Following Glaucoma Filtering Surgery: A Case Series and Literature Review. *Orbit*, 2009; 28:6, 363-367 DOI: 10.3109/01676830903180306
8. BUDENZ DL, HOFFMAN K, ZACCHEI A. Glaucoma filtering bleb dysesthesia. *Am J Ophthalmol*. 2001;131:626-630.
9. BLANCO-AZURA A, KATZ JL. Dysfunctional filtering blebs. *Surv Ophthalmol*. 1998;43:93-126. DOI: 10.1016/s0039-6257(98)00025-3
10. PUTTERMAN AM, FETT DR. Mueller's muscle in the treatment of upper eyelid retraction: a 12-year study. *Ophthalmic Surg*. 1986;17:361-367. PMID: 3737107

11. **KAZIM M, GOLD KG.** A review of surgical techniques to correct upper eyelid retraction associated with thyroid eye disease. *Curr Opin Ophthalmol.* 2011 Sep;22(5):391-3. DOI: 10.1097/ICU.0b013e3283499433
12. **CEISLER EJ, BILYK JR, RUBIN PA, BURKS WR, SHORE JW.** Results of Müllerotomy and levator aponeurosis transposition for the correction of upper eyelid retraction in Graves disease. *Ophthalmology.* 1995;102(3):483–492. DOI: 10.1016/s0161-6420(95)30996-7
13. **GROVE A.** Eyelid retraction treated by levator marginal myotomy. *Ophthalmology.* 1980; 87:1013–1018. DOI: 10.1016/s0161-6420(80)35136-1
14. **AWWAD ST, MÁLUF RN, NOUREDDIN B.** Upper eyelid retraction after glaucoma filtering surgery and topical application of mitomycin C. *Ophthal Plast Reconstr Surg.* 2004;20(2):144–149. 10.1097/01.iop.0000115596.80381.80
15. **CHANG EL, RUBIN PAD.** Upper and lower eyelid retraction. *Int Ophthalmol Clin.* 2002;42:45–59. 10.1097/00004397-200204000-00006

<http://dx.doi.org/10.35630/2199-885X/2022/12/2.14>

MONITORING OF PSYCHOTHERAPEUTIC PATIENTS BY ASSESSING MOTOR ACTIVITY DURING NIGHT SLEEP

Received 24 January 2022;
Received in revised form 20 February 2022;
Accepted 22 February 2022

Alexey Gorbunov¹ , Svetlana Krasnianskaya²,
Dmitry Parshin³ , Egor Dolgov¹,
Zhanna Shishkina⁴ , Aleksey Loktev⁴ 

¹ Tambov State Technical University, Tambov;

² Tambov Psychiatric Clinical Hospital, Tambov;

³ Astrakhan State Medical University, Astrakhan, Russia

⁴ Tambov G.R. Derzhavin State University, Tambov, Russia

✉ parshin.doc@gmail.com

ABSTRACT — In order to monitor the state of patients in the psychotherapy department by assessing motor activity during their night sleep, we examined 16 patients of both sexes with diagnosis of a depressive episode and neurotic, stress-related and somatoform disorders. Data on motor activity during sleep were obtained and processed using a special information-analytical system with the following parameters: the number of movements, the maximum jerk magnitude and the coefficient of motor activity. It showed a high efficiency of monitoring the condition of patients in comparison with healthy people by assessing motor activity during their night sleep.

KEYWORDS — monitoring in psychotherapy, physical activity during sleep, information-analytical system, depressive episode, neurotic, stress-related, and somatoform disorders.

INTRODUCTION

Modern advances in disease monitoring determine the need for *not just monitoring*, but long-term and clinically controlled monitoring of diseases. Despite the fact that traditional methods of diagnosing psychiatric disorders are informative to a certain extent, they are practically not suitable for continuous daily, hourly, minute-to-minute monitoring. Therefore, there is a need for a system capable of continuous monitoring of psychiatric patients [1].

To analyze the effectiveness of treatment and dosage of medications for psychiatric disorders, there is a need for information about a person's health and physical activity. To obtain qualitative and quantitative information about health, there are instrumental methods such as electroencephalography (EEG), video-EEG monitoring and positron emission tomography. These methods are informative, but at the

same time have common drawbacks of impossibility of constant monitoring of the patient, limitations of use at home, high cost and non-absolute verification of the process [2].

From the point of view of metrology, the process of instrumental diagnostics in medical practice is most effective with the largest number of studies carried out under the same conditions [3]. Therefore, in order to increase the reliability of the study, it must be carried out several times under the same conditions. It was demonstrated in the work of University College London, which was dedicated to a new method for measuring blood pressure based on long-term monitoring using a new mobile device. This enabled to increase the reliability of the study by 50% [4].

MATERIALS AND METHODS

At the Tambov Psychiatric Clinical Hospital 16 patients (8 men and 8 women) aged 34 to 73 years were examined. According to the International Classification of Diseases (ICD-10) the patients were diagnosed as follows: F40-48 (neurotic, stress-related, and somatoform disorders) and F32 (depressive episode) [5]. All the patients were monitored before the start of treatment and after the end of treatment according to clinical guidelines.

The study was carried out during the period of night sleep: the information and analytical system (IAS) was working from the moment of going to bed, followed by falling asleep until the moment of awakening when the IAS was switched off. A detailed research methodology was described in our previous works (a study of young healthy people and a study of patients with Parkinson's disease) [6, 7].

To solve the problem of measuring and recording motor activity, we have developed an IAS with a primary measuring transducer based on a 3-D accelerometer and recording the measured values of motor activity on a memory card with their subsequent interpretation using specialized software [8]. Later, using specially developed software [9], the obtained data were processed and presented for further analysis of the following parameters (Fig. 1, 2):

1 — number of movements — the maximum number of hand movements along each axis for the entire study period (dimensionless value);

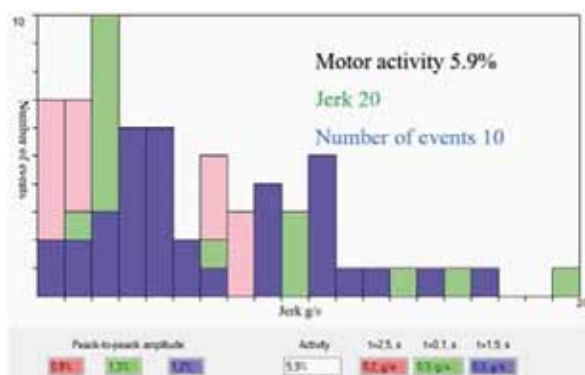


Fig. 1. Monitoring patients with depressive episode before treatment

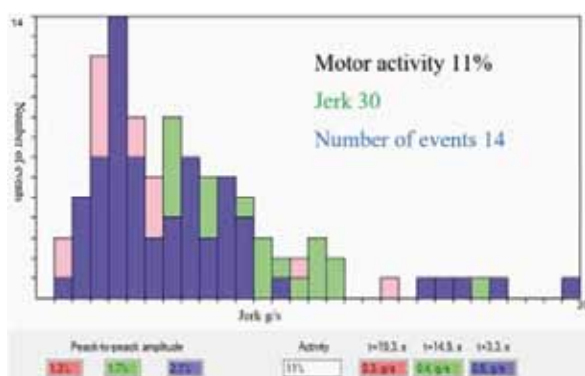


Fig. 2. Monitoring patients with depressive episode after treatment

2 — maximum jerk value — the maximum value of the modules of the rate of acceleration change during data recording (g/s);

3 — coefficient of physical activity — the ratio of the number of files with significant physical activity to the total number of files (%).

RESULTS

As a result of the study, the following data were obtained.

In the group of patients with neurotic and somatoform disorders before treatment, the following results were obtained: the average value for the number of movements was 13.1; the maximum value was 23; the minimum value was 9. The average value of the maximum jerk magnitude was 24.4 g/s; the maximum value was 36 g/s; the minimum value was 10 g/s. The average value of the coefficient of motor activity was 11.4%; the maximum value was 40.8%; the minimum value was 5.9%. After treatment: the average value for the number of movements was 18.2; the maximum value was 29; the minimum value was 11. The average value of the maximum jerk magnitude was 22.9 g/s;

the maximum value was 36 g/s; the minimum value was 17 g/s. The average value of the coefficient of motor activity was 15.8%; the maximum value was 28.1%; the minimum value was 8.5%.

In the group of patients with depressive episodes before treatment, the following results were obtained: the average value for the number of movements was 21.5; the maximum value was 40; the minimum value was 12. The average value of the maximum jerk magnitude was 34.0 g/s; the maximum value was 43.1 g/s; the minimum value was 30.1 g/s. The average value of the coefficient of motor activity was 29.0%; the maximum values was 35.1%; the minimum value was 22.9%. After treatment: the average value for the number of movements was 15.7; the maximum values was 33; the minimum value was 10. The average value of the maximum jerk magnitude was 18.9 g/s; the maximum values was 29 g/s; the minimum value was 13 g/s. The average value of the coefficient of motor activity was 26.9%; the maximum values was 38.4%; the minimum value was 14.5% (Fig. 1, 2).

DISCUSSION

In patients diagnosed with F40-48, the following dynamics of indicators was revealed in comparison with the state before treatment and the state after treatment. The average value of the number of movements increased from 13.1 to 18.2 — by 40.2%. The average value of the maximum jerk magnitude decreased from 24.4 g/s to 22.9 g/s — by 6.1%. The average value of the coefficient of physical activity increased from 11.4% to 15.8% — by 38.6%.

Patients diagnosed with F 32 showed the following dynamics of indicators in comparison with the state before treatment and the state after treatment. The average value of the number of movements decreased from 21.5 to 15.7 — by 26.9%. The average value of the maximum jerk value decreased from 34.0 g/s to 18.9 g/s — by 44.4%. The average value of the coefficient of motor activity decreased from 29.0% to 26.9% — by 0.7% (Fig. 1, 2).

CONCLUSION

When compared with the results in healthy people [6], there are noticeable differences in patients with diagnoses F 40-48 and F 32 in terms of the parameters of the coefficient of motor activity and the number of movements.

REFERENCES

1. ZENKOV L.R. Clinical electroencephalography (with elements of epileptology). MEDpress-inform, 2017, p. 345. (Date of the application: 17.12. 2021. Available from: https://static-eu.insales.ru/files/1/6854/3136198/original/klinich_electroenkefalografija.pdf). (In Russ.).

2. **CALABRESE J, AL KHALILI Y.** Psychosis. [Updated 2021 Jul 19]. In: StatPearls [Internet]. Treasure Island (FL): StatPearls Publishing; 2021 Jan-. Available from: <https://www.ncbi.nlm.nih.gov/books/NBK546579/>
3. **JULIUS S. BENDAT AND ALLAN G.** Piersol. Random Data: Analysis and Measurement Procedures. John Wiley & Sons, 2011, p. 640. ISBN1118210824, 9781118210826.
4. **BANEGAS J.R., RUILOPE L.M., DE LA SIERRA A., VINYOLÉS E., GOROSTIDI M., DE LA CRUZ J.J., RUIZ HURTADO G., SEGURA J., RODRÍGUEZ ARTALEJO F., WILLIAMS B.** Relationship between Clinic and Ambulatory Blood-Pressure Measurements and Mortality. *N Engl J Med* 2018;378:1509–20. doi: 10.1056/NEJMoa1712231
5. International Classification of Diseases, Tenth Revision (ICD-10). 2015. (Date of the application: 17.12. 2021. Available from: <https://www.cdc.gov/nchs/icd/icd10.htm>).
6. **GORBUNOV A., GROMOV YU., PARSHIN D., EGOROV V., DOLGOV E., GRECHUKHA D.** Characteristics of human motor activity during sleep in young adults (18–21 years) using information-analytical system. *Archiv EuroMedica*. 2021;11(1):87–89. doi: 10.35630/2199-885X/2021/11/1.20
7. **GORBUNOV A., PARSHIN D., GROMOV YU., NEPROKIN A., DOLGOV E., GRECHUKHA D.** Capabilities of an information-analytical system for assessing motor activity in Parkinson's disease during sleep *Archiv EuroMedica*. 2021;11(1):84–86. doi: 10.35630/2199-885X/2021/11/1.19
8. **GORBUNOV A.V., EGOROV S.A., EGOROV A.S.** Device for recording human motor activity // Patent of the Russian Federation No. 168584 dated 09.02.2017 (In Russ.).
9. **GORBUNOV A.V., EGOROV S.A., EGOROV A.S.** A method for diagnosing epilepsy and a device for its implementation // Patent of the Russian Federation No. 2640138 dated 26.12.2017 (In Russ.).

<http://dx.doi.org/10.35630/2199-885X/2022/12/2.15>

NOSOLOGICAL SPECIFICITY OF MOTOR ACTIVITY IN THE PSYCHIATRIC CLINIC DURING NIGHT SLEEP

Received 18 December 2021;
Received in revised form 20 January 2022;
Accepted 23 January 2022

Alexey Gorbunov¹ , Svetlana Krasnianskaya²,
Dmitry Parshin³ , Egor Dolgov¹,
Zhanna Shishkina⁴ , Aleksey Loktev⁴ 

¹ Tambov State Technical University, Tambov;

² Regional State Funded Healthcare Facility "Tambov Psychiatric Clinical Hospital", Tambov;

³ Astrakhan State Medical University, Astrakhan;

⁴ Tambov State University named after G.R. Derzhavin, Tambov, Russia

✉ parshin.doc@gmail.com

ABSTRACT — While continuing the cycle of studies on the human motor activity during sleep, we examined 12 male patients with schizophrenia, mental retardation and other mental disorders caused by damage and dysfunction of the brain or somatic illness. Data on motor activity during sleep were obtained using an information-analytical system with registration of the number of movements, the maximum magnitude of jerk and the coefficient of motor activity. The nosological specificity of motor activity during sleep at night in patients with schizophrenia, mental retardation and other mental disorders caused by damage and dysfunction of the brain or somatic illness was revealed.

KEYWORDS — physical activity during sleep, information-analytical system, other mental disorders due to damage and dysfunction of the brain or somatic illness, schizophrenia, mental retardation.

INTRODUCTION

According to the WHO, the prevalence of mental illness in the world is currently about 160 people per 1000 population. 5 out of 10 most serious diseases of all known worldwide are mental [1].

Schizophrenia is widely associated with significant disability, can affect learning and working activity, and limit quality of life. It can also be a severe mental disorder affecting more than 20 million people worldwide. Patients with schizophrenia are 2–3 times more likely to die earlier than the general population [2].

In addition to clinically significant features and complications caused by mental illness, its consequences for social and everyday life are of great importance for the patient. Mental retardation is characterized by developmental impairment, including the cognitive functions and adaptive behavior. Lack

of mental development prevents from coping with everyday household tasks [3].

One of the most difficult problems in modern medical science is the cumulative dynamic analysis of a physiological and/or pathological condition. Among kinematic systems using various algorithms for processing, analysis and interpretation of signals of motor activity, accelerometry is a quite promising one. Although there are a large number of studies of sleep using accelerometry, there have been no studies of motor activity for mental disorders using accelerometry [4].

MATERIALS AND METHODS

We examined 12 patients (12 men) at the Tambov Psychiatric Clinical Hospital aged 20 to 32 years with the following diagnoses according to the international classification of diseases (ICD-10): F06 (Other mental disorders caused by damage and dysfunction of the brain or physical illness), F20 (Schizophrenia) and F70 (Mild mental retardation) [5]. Before the study, all subjects gave informed consent to participate in the study.

The study was carried out during the period of night sleep: the information and analytical system (IAS) was on from the moment of going to bed, followed by falling asleep until the moment of awakening when the IAS was switched off. A detailed research methodology was described in our previous works (a study of young healthy people and a study of patients with Parkinson's disease) [6, 7].

To solve the problem of measuring and recording motor activity, we have developed an IAS with a primary measuring transducer based on a 3-D accelerometer and recording the measured values of motor activity on a memory card with their subsequent interpretation using specialized software [8]. Later, using specially developed software [9], the obtained data were processed and presented for further analysis of the following parameters (Fig. 1, 2):

1 — number of movements — the maximum number of hand movements along each axis for the entire study period (dimensionless value);

2 — maximum jerk value — the maximum value of the modules of the rate of acceleration change during data recording (g/s);

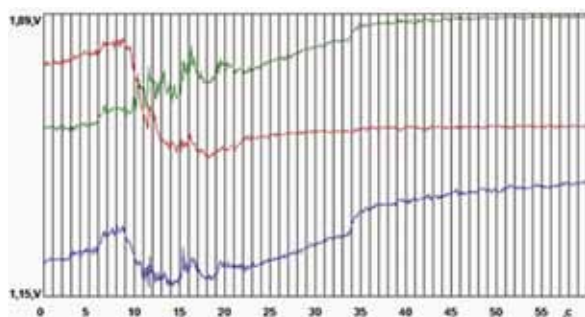


Fig. 1. Graphs of motor activity along three axes

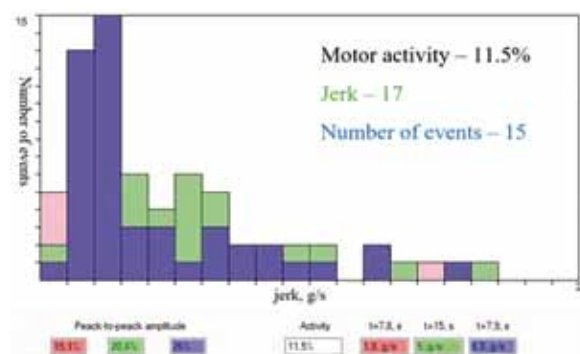


Fig. 2. Histogram of motor activity at night with mental retardation

3 — coefficient of physical activity — the ratio of the number of files with significant physical activity to the total number of files (%).

RESULTS AND DISCUSSION

As a result of the study, the following data were obtained.

In the group of patients with other mental disorders due to brain damage and dysfunction or somatic illness, the average value for the number of movements was 15.5; maximum value — 25; the minimum value - 6. The average value of the maximum jerk magnitude was 25 g/s; the maximum value was 32 g/s; the minimum value was 13 g/s. For the coefficient of motor activity, the average value was 31.7%; the maximum value was 37.9%; the minimum value was 9.8%.

In the group of patients with schizophrenia, the mean for the number of movements was 17.7; the maximum value was 27; the minimum value was 7. The average value of the maximum jerk magnitude 23.5 g/s; the maximum value was 31 g/s the minimum value was 13 g/s. For the coefficient of motor activity, the average value was 15.1%; the maximum value was 26.5%; the minimum value was 12.4%.

In the group of patients with mild mental retardation the average value of the number of movements was 9.9; the maximum value was 14; the minimum value was 6. The average value of the maximum jerk magnitude was 22.8 g/s; the maximum value was 28 g/s; the minimum value was 13 g/s. The average value of the coefficient of motor activity was 6.9%; the maximum value was 13.2%; the minimum value was 5.8% (Fig. 1, 2).

Patients diagnosed with F70 show relatively low rates compared to other patient groups. The F20 group is characterized by a noticeable difference in terms of the maximum jerk magnitude and the coefficient of motor activity. In the F06 group, the indicators are slightly higher than in the F70 group, and at the

same time, the variance in this group is lower than in the rest. All this indicates a difference in the nature of motor activity in patients with various disorders. At the same time, this division is not final and is rather for informational purposes for a specialist doctor.

When compared with the results of healthy people [6], there are noticeable differences in patients with different diagnoses in terms of the parameters of the coefficient of motor activity and the number of movements. These differences will be discussed in detail in one of the following articles.

CONCLUSION

The findings suggest a search for further system upgrades to improve diagnostics and treatment. This will lead to the minimization of technical and technological means, as well as the amount of time spent for the survey, and, consequently, an increase in the accuracy of information and, then, an increase in the quality of future research.

REFERENCES

1. GBD 2015 Neurological Disorders Collaborator Group. Global, regional, and national burden of neurological disorders during 1990-2015: a systematic analysis for the Global Burden of Disease Study 2015. *Lancet Neurol.* 2017;16(11):877-897. doi: [https://doi.org/10.1016/S1474-4422\(17\)30299-5](https://doi.org/10.1016/S1474-4422(17)30299-5)
2. LAURSEN TM, NORDENTOFT M, MORTENSEN PB. Excess early mortality in schizophrenia. *Annu Rev Clin Psychol.* 2014;10:425-48. doi: 10.1146/annurev-clinpsy-032813-153657
3. American Psychiatric Association. Diagnostic and Statistical Manual of Mental Disorders, Fifth Edition (DSM-5). — Arlington, VA: «American Psychiatric Publishing», 2013. 992 p. — ISBN 978-0-89042-554-1. — ISBN 978-0-89042-555-8. — ISBN 0-89042-554-X.
4. JULIUS S. BENDAT AND ALLAN G. PIERSOL. Random Data: Analysis and Measurement Procedures.

- John Wiley & Sons, 2011, p. 640. ISBN1118210824, 9781118210826.
5. International Classification of Diseases, Tenth Revision (ICD-10). 2015. (Date of the application: 17.12. 2021. <https://www.cdc.gov/nchs/icd/icd10.htm>).
 6. **GORBUNOV A., GROMOV YU., PARSHIN D., EGOROV V., DOLGOV E., GRECHUKHA D.** Characteristics of human motor activity during sleep in young adults (18–21 years) using information-analytical system. *Archiv EuroMedica*. 2021;11(1):87–89. <http://dx.doi.org/10.35630/2199-885X/2021/11/1.20>
 7. **GORBUNOV A., PARSHIN D., GROMOV YU., NEPROKIN A., DOLGOV E., GRECHUKHA D.** Capabilities of an information-analytical system for assessing motor activity in Parkinson's disease during sleep *Archiv EuroMedica*. 2021;11(1):84–86. <http://dx.doi.org/10.35630/2199-885X/2021/11/1.19>
 8. **GORBUNOV A.V., EGOROV S.A., EGOROV A.S.** Device for recording human motor activity // Patent of the Russian Federation No. 168584 dated 09.02.2017 (In Russ.).
 9. **GORBUNOV A.V., EGOROV S.A., EGOROV A.S.** A method for diagnosing epilepsy and a device for its implementation // Patent of the Russian Federation No. 2640138 dated 26.12.2017 (In Russ.).

<http://dx.doi.org/10.35630/2199-885X/2022/12/2.16>

CLINICAL CHARACTERISTICS IN CORNELIA DE LANGE SYNDROME OF THE FIRST TYPE ON THE EXAMPLE OF A CLINICAL CASE

Received 10 January 2022;
Received in revised form 21 February 2022;
Accepted 23 February 2022

Polina Pozdnyakova¹, Lesya Chichanovskaia¹ ,
Tatiana Sorokovikova¹, Artem Morozov¹ ,
Olga Peltikhina² 

¹ Tver State Medical University, Tver;

² Pirogov Russian National Research Medical University, Moscow, Russia

✉ ammorozovv@gmail.com

ABSTRACT — **RELEVANCE:** Cornelia de Lange syndrome is a rare congenital disorder associated with orphan diseases and is characterized by multiple stigmas of dysembryogenesis at birth. This syndrome occurs in newborns with a frequency of 1: 30,000 to 1: 10,000; there are no gender differences in the frequency of occurrence. Cornelia de Lange syndrome is a dominantly inherited disease, but most cases are sporadic de novo, therefore, mainly children with Cornelia de Lange syndrome are born from genetically healthy parents.

PURPOSE: Using the example of a clinical case, to demonstrate the characteristic features of the clinical picture, namely the phenotype and deviations of the neurological status in Cornelia de Lange syndrome. **MATERIALS:** Girl M., born in 2018, at the age of 1 year 11 months, together with her mother, was admitted to the Center for Pediatric Neurology and Medical Rehabilitation No. 2 in Tver, Russia. The girl had the following complaints (according to the mother): the child does not walk independently, stands with legs apart, and does not speak. She has obsessive movements ("crossed out" hand movement, waves her arms, puts his right hand behind the body, shakes objects in the mouth area), lags behind in development, does not differentiate significant adults, does not speak, there is no pointing gesture. Inpatient examination and treatment was carried out at the Center for Pediatric Neurology and Medical Rehabilitation.

RESULTS: Based on the examinations, the following diagnosis was established: Cornelia de Lange syndrome, type 1. Delayed physical, static-motor and mental development. Short stature. Congenital kidney anomaly: horseshoe kidney. Sensorineural hearing loss I-II degree. The priority areas in this case are: improving the patient's quality of life, stimulating the development of the mental and motor spheres, socialization with other children.

CONCLUSION: This clinical case demonstrates the need for early diagnosis of genetic disorders in order to build correct social and medical rehabilitation.

KEYWORDS — Orphan diseases, Cornelia de Lange syndrome, Brahman de Lange syndrome.

RELEVANCE

Cornelia de Lange syndrome is a rare congenital disorder associated with orphan diseases and is characterized by multiple stigmas of dysembryogenesis at birth.

The risk factors for the development of Cornelia de Lange syndrome in the fetus do not differ from those for other de novo mutations.

Etiologically, this disease is genetically determined. In the described syndrome, the normal karyotype is most often preserved. However, the genetic heterogeneity of the disease should be considered. Three different variants of genetic disorders have been identified: NIPBL (about 50%), SMC1A (5%), and SMC3. The SMC1A gene is located on the sex X chromosome — with its defects, inheritance is linked to the sex (men are more often sick, women are heterozygous carriers). This gene encodes a subunit of the cohesin protein complex. One case described is associated with a mutation in the SMC3 gene, which also encodes one of the cohesin subunits. In some cases, a cytogenetic study finds microduplication of the q25 — q29 loci of chromosome 3.

From the described violations of protein synthesis, it can be concluded that the pathogenesis of this disease is associated with disruption of the function of cohesin proteins. Cohesins play an important role in the process of cell division, DNA repair, and regulation of gene expression. Due to the dysregulation of these processes, organogenesis is impaired. Significant changes in the brain are revealed (aplasia of the cortex, underdevelopment of the Roland groove, impaired myelination, hypoplasia of the thymus).

Depending on the severity of the impairment of psychomotor development, there are two variants of the course of Cornelia de Lange's syndrome. The first type, classic, is accompanied by a significant delay in physical and intellectual development, with gross defects. The second type, benign, is characterized by facial and minor skeletal anomalies, but borderline retardation of psychomotor development and the absence of gross defects. The final diagnosis is made on the basis of the phenotype, karyotype research and methods of cytogenetic analysis.

Cornelia de Lange syndrome is characterized by features of the phenotype in the form of typical

stigmas of dysembryogenesis, skeletal anomalies (funnel chest, short neck, spina bifida, articular contractions, hypoplasia and deformity of the hands and feet, defects in the development of fingers, congenital dislocation of the hip). Also congenital dislocations of the hip (tetrad of Fallot, coarctation of the aorta, heart septal defects, pulmonary valve stenosis, pyloric stenosis, hydronephrosis, horseshoe kidney, polycystic, gastroesophageal reflux, incomplete bowel rotation, as well as hypospadias, scrotal hypoplasia, bicornuate uterus). Appearance features are common, such as thin fused eyebrows, long curled eyelashes, a thin upper lip, marbled skin, hypertrichosis, and short stature. Possible delay in sexual development. Due to imperfections in the airways, there is a high likelihood of frequent recurrent respiratory diseases.

In the clinical picture of the syndrome, various disorders of the neurological status are revealed, manifested by a delay in neuropsychic development and pathologies of the sensory organs. Visual impairment in the form of myopia, strabismus, astigmatism, atrophy of the optic nerves, coloboma of the optic nerve, as well as hearing impairment — bilateral sensorineural hearing loss, conductive hearing loss, or their combination are likely. Such children are characterized by episodic convulsive readiness, muscle dystonia, and stereotypic hand movements. Higher nervous activity also suffers, auto-aggression is possible, mental retardation of varying degrees, up to imbecility;

In addition to the systemic examination, full genome sequencing of the proband is required to make a diagnosis.

No specific treatment has been developed. Neurometabolic, nootropic drugs, vitamins, speech therapy and psychological correction are used symptomatically.

Life expectancy depends on the severity of the defects of vital organs, on the quality of medical care, as well as the care of a sick child.

PURPOSE OF THE STUDY

Using the example of a clinical case, demonstrate the characteristic features of the clinical picture, namely the phenotype and deviations of the neurological status, in Cornelia de Lange syndrome.

MATERIALS AND METHODS

Girl M., born in 2018, at the age of 1 year 11 months turned to the Center for Pediatric Neurology and Medical Rehabilitation of GBUZ KDB № 2 in Tver. Her mother complained, the child does not walk independently, stands with legs, does not speak, obsessive movements (*crossed out* hand movement, waves his arms, puts his right hand behind the body, shakes

objects in the mouth area), lags behind in development, does not differentiate significant adults, does not speak, there is no pointing gesture.

Inpatient examination and treatment was carried out at the Center for Pediatric Neurology and Medical Rehabilitation.

RESULTS AND DISCUSSIONS

From the history of the patient's life, it is known that the girl was born from the 7th pregnancy, proceeding with the threat of termination of pregnancy, edema, high blood pressure, toxicosis, weight loss by 20 kg. Childbirth 3rd, at 37 weeks, urgent in breech presentation, by cesarean section, with an umbilical cord entwined around the neck and intrauterine fetal hypoxia. Body weight at birth 3480 g. Length 52 cm. Score on the Apgar scale 7/9 points. Discharged home on the 5th day.

Delayed neuropsychic and motor development was noted throughout life. Problems with humming, babbling, emotions from 6 months (according to the mother), motor development with a delay: he holds his head from 4 months, turns over from 6–8 months. Was observed by a neurologist irregularly from 3 months: PGIP of the central nervous system, syndrome of motor disorders (at 3 months — adductor spasm, delayed motor development). A course of exercise therapy and massage was carried out. Consultation with a neurologist at 11.5 months: PHIP of the central nervous system, grade 2, movement disorders syndrome, they refused inpatient treatment and examination, underwent an outpatient course of treatment. At the age of 1, the diagnosis was made: delayed motor development, syndrome of motor disorders. The treatment took place on an outpatient basis. According to neurosonography data: MPSH 4 mm, PRBZH 6 mm each, III ventricle 3.7 mm. Abdominal ultrasound was without pathology.

At 1 year 3 months, the child was again consulted by a neurologist about the delay in physical development, in the neurological status, muscle hypotonia, NRD: sits for a short time, staggering with a fall on his back, moves by jumping *like a frog*. Recommended examination — MRI of the brain, ENGM to exclude muscular dystrophy.

At 1 year 11 months, the diagnosis was made: Organic lesion of the central nervous system, delayed psychoverbal and motor development (genetically unverified form). Sent for inpatient examination and treatment at the Center for Pediatric Neurology and Medical Rehabilitation.

On admission to the hospital, somatically — a phenotype characteristic of Cornelia de Lange's syndrome. Height 76 cm (<5 percentile), weight 10.3

kg (<5 percentile), MG 47 cm. BMI = 17.8. Multiple stigmas of dysembryogenesis: microcephaly, deformity of the hands of both hands (flat scapular hands with clinodactyly of the little fingers, thumbs located proximally), varus-valgus deformity of the right and left foot, high palate, conical teeth, short neck, hypertrichosis of the whole body. The skin is clean, pale with a marble tint. The mucous membranes are pale pink, clean, moist, the tongue is coated with a white coating. Breathing is puerile. BH 30 times per minute. Heart sounds are sonorous, rhythmic. HELL 100/65 mm Hg Heart rate 140 beats per minute. The abdomen is soft and painless. The liver and spleen are not enlarged. The defecation is mushy, up to 3 times a day. Diuresis is not impaired.

From the side of the neurological status, there was a significant delay in CPR. Consciousness is clear. There are no general cerebral, meningeal symptoms. Partially accessible to verbal contact. Does not follow instructions. The head is microcephalic, in the sphere of cranial innervation: the sense of smell is preserved, the palpebral fissures are D = S, the pupils are round D = S, the reaction of the pupils to light is direct and friendly, the movement of the eyeballs is in full volume, the sensitivity on the face is preserved, the points of exit of the trigeminal nerve are painless. The face is symmetrical, nasolabial folds D = S, no nystagmus, increased pharyngeal reflex, phonation is not disturbed, head rotation and shoulder elevation are not disturbed, the soft palate does not sag, the tongue is in the midline. Tendon reflexes of the upper extremities of medium vivacity D = S, knee reflexes are reduced D = S, reflexes of the lower extremities are *flaccid* D = S, Achilles of medium vivacity D = S. There are no pathological reflexes. Dystonic muscle tone. Movement stereotypes: *crossed out* hand movement, waving his hands, waving his right hand behind the body, shaking objects in the mouth area, fingering fingers, *pinching*. Holds the head in the midline. Sits unstable, stands up with support, stands briefly with legs wide apart. Intelligence is reduced, understanding of active speech is incomplete, does not distinguish between significant adults, there is no active speech. Passive speech is selective. Emotionally labile.

The results of the examinations: ECG: no pathology. Standard EEG: there is a slowdown in the formation of the main cortical rhythms. Typical forms of epic activity have not been registered. TNSG: PRBZH on the right 4 mm, on the left 4 mm. III ventricle 3 mm. MRI of the brain: data for the presence of additional formations, foci of a pathological signal in the cerebral parenchyma were not obtained. Local expansion of the retrocerebellar subarachnoid space of the PCF. Ultrasound of the genitourinary system: horseshoe kidney.

Genealogical history: not burdened. The parents' marriage is unrelated.

Clinical blood test: no features

Biochemical blood test: alkaline phosphatase 431 U/L, AST 52 U/L, ALT 21 U/L, urea 4.4 mmol/L, lactate 2.56 mmol/L, otherwise no peculiarities

General urine analysis: no pathology.

Ophthalmologist's consultation: the optic discs are pale pink, the boundaries are clear. Arteries of normal caliber, veins are somewhat dilated.

Orthopedic consultation: equino-varus deformity of the right foot. Hallux valgus of the left foot. Deformation of the hands of both hands (flat, spatulate hands with clinodactyly of the little fingers, thumbs located proximally).

Speech therapist consultation: speech development dysphasia. Sensorimotor alalia.

Psychiatric consultation: delayed neuropsychic development.

Endocrinologist consultation: lag in physical development threatened by iodine deficiency. Short stature.

Consultation with an audiologist: bilateral sensorineural hearing loss, I–II degree.

Consultation with a geneticist: undifferentiated genetic pathology, karyotype 46, XX. Direction for whole genome sequencing.

Whole genome sequencing: a previously undescribed heterozygous mutation in exon 28 of the NIPBL gene was identified, leading to an amino acid substitution at position 1805 of the protein. Heterozygous mutations in the NIPBL gene have been described in patients with Cornelia de Lange syndrome, type 1.

Based on the examinations, the following diagnosis was established: Cornelia de Lange syndrome, type 1. Delayed physical, static-motor and mental development. Short stature. Congenital kidney anomaly: horseshoe kidney. Sensorineural hearing loss I–II degree

The priority areas in this case are improving the patient's quality of life, stimulating the development of the mental and motor spheres, socialization of the child in the children's society.

CONCLUSION

This clinical case demonstrates the need for early diagnosis of genetic disorders in order to build the correct social and medical rehabilitation of children with these clinical manifestations. Confirmation of genetic analysis leads to predicting the developmental lines of these children in order to develop rehabilitation measures, including the need for coordinated work of such specialists as defectologists, speech therapist,

neuropsychologist, and ergotherapist. It is also required to consult pregnant women about the presence of various orphan diseases, their manifestations and consequences for the formation of the correct social strategy in society.

REFERENCES

1. **ZHIVILO L.M.** Cornelia de Lange syndrome / L.M. Zhivilo, T.I. Tkachuk // *International neurological journal* 2016 – No 2 (80). – pp. 167–168.
2. **NAZARENKO L.P.** Federal clinical guidelines for the diagnosis and treatment of Cornelia de Lange syndrome / L.P. Nazarenko. – Moscow, 2015 – 27 p.
3. **RUSSEL J.** Cornelia de Lange Syndrom / J. Russel, R. Cohn // Bookvika publishing, 2012 – 176 p.
4. **MUNDLOS S., HORN D.** Cornelia de Lange Syndrome. // *Limb Malformations*. – 2014. – P.215–216. doi: 10.1007/978-3-540-95928-1
5. Clinical observation of a deeply premature baby with Cornelia de Lange syndrome / Nikitina IV, Ionov OV et al. // *Neonatology: News. Opinions. Education*. – 2018.
6. **SCHRIER S. A. ET AL.** Causes of death and autopsy findings in a large study cohort of individuals with Cornelia de Lange syndrome and review of the literature // *American Journal of Medical Genetics Part A*. – 2011. – Vol. 155. – No 12. – C. 3007–3024. DOI: 10.1002/ajmg.a.34329
7. **CORDIER, J. F.** Orphan Lung Diseases / J. F. Cordier, S. R. Johnson // *Eur. Respir. Mon.* – 2011. – Vol. 54. – P. 46–83.
8. **AIKARDI J., BUCKS M., GILLBERG K.** Diseases of the nervous system in children (Translated from English under the editorship of AA Skoromets). – Moscow: Panfilov Publishing House, BINOM, 2013, 1036 p.

<http://dx.doi.org/10.35630/2199-885X/2022/12/2.18>

EVALUATION OF THE PROGNOSTIC VALUE OF URINARY CREATININE LEVEL IN PATIENTS HOSPITALIZED WITH THE DIAGNOSIS OF CHRONIC SYSTOLIC HEART FAILURE IN SEYED AL-SHOHADA HOSPITAL IN URMIA, IRAN

Received 01 January 2022;
Received in revised form 18 February 2022;
Accepted 21 February 2022

Saeed Abkhiz¹ , Mojgan Hajahmadi-Pourrafsanjani ,
Alireza Rostamzadeh² , Soma Elhami³,
Roghayeh Afsargharehbagh² 

¹ Azarbaijan Hospital, Urmia University of Medical Sciences, Urmia;

² Department of Cardiology, Seyyed-al-Shohada Heart Center, Urmia University of Medical Science, Urmia;

³ Department of Cardiology, Urmia University of Medical Sciences, Urmia;

⁴ Faculty of Medicine, Urmia University of Medical Sciences, Urmia, Iran

✉ arzzr.4891@gmail.com

ABSTRACT — **INTRODUCTION:** Heart failure patients have frequent hospitalization leading to decreased quality of life and life expectancy. The purpose of this study was to evaluate the prognostic value of urinary creatinine test in immune-compromised patients with systolic heart failure.

MATERIAL AND METHODS: This study was conducted on 122 patients hospitalized in Urmia. The inclusion criterion was according to cardiac EF obtained from echocardiography and patients with EF less than 45% were considered. In the morning, urine samples were taken from them and the amount of urinary creatinine and other parameters were registered. **RESULTS:** According to the Pearson correlation test, there was no significant relationship between body weight, height, and body mass index with urinary creatinine, but there was no significant relationship between urinary creatinine and serum creatinine ($p > 0.05$). There is a positive and significant relationship between urinary creatinine level and GFR. There is also a significant relationship between diastolic blood pressure and urinary creatinine.

CONCLUSION: The results of the present study indicate the importance of paying attention to urinary creatinine as an effective underlying factor in predicting the symptoms of heart failure.

KEYWORDS — Urinary creatinine, Serum creatinine, Ventricular ejection fraction, Urinary albumin, GFR.

INTRODUCTION

Today, heart failure is one of the most common heart problems worldwide. According to the latest statistics, more than 26 million people in the world have heart failure. There are more than 6.2 million

people in the United States alone, which will increase to more than 8 million by 2030. Chronic heart failure causes mental and physical problems including fatigue, anxiety, depression and anemia. Heart failure eventually leads to increased hospitalization, lower quality of life, and lower life expectancy. The latest meta-analysis results show that most heart failure patients have moderate and poor quality of life. In Iran, over one million people suffer from heart failure (1–3).

Heart failure is associated with various symptoms such as shortness of breath, swollen ankles and fatigue. Symptoms of heart failure are often nonspecific and do not help differentiate heart failure from other problems. Identifying and interpreting signs and symptoms may be particularly difficult in obese, elderly, and patients with chronic lung disease (5). Some diagnostic tests include echocardiography and electrocardiography. Another test is the use of serum B-type natriuretic peptide.

The kidney is important in renal failure because the kidney controls fluid volume and sodium homeostasis, and progressive renal dysfunction often limits aggressive treatment. Despite this, in addition to measuring urine volume in response to prescribed diuretics, less attention has been paid to urinalysis in patients with heart failure. Recent advances in a large number of urinary biomarkers that can predict acute kidney damage in the days before elevated serum creatinine levels have led to the addition of urine samples to laboratory data collected in clinical trials.

However, it seems that the value of urine samples in patients with heart failure has not been well understood so far and their use has been limited to the measurement of urinary creatinine, which as a statistical finding has received little attention. Used solely as a measure of protein and biomarker ratios to calculate differences in urine concentration and volume. Ter Maaten and colleagues evaluated the prognostic value of urinary creatinine and its association with clinical variables and concluded that low urinary creatinine measured in the morning urine test in patients with heart failure, with lower renal function, was smaller.

Body size, more severe heart failure, and is independently associated with an increased risk of death (for all causes) and hospitalization (11).

Chronic heart failure is associated with treatment failure and high complications. In order to choose an effective and targeted treatment path and assess the prognosis of patients' clinical condition, simple and accurate prognosis models are needed. This model should be such that it is relatively widely available and has a high predictive value. Measurement of urinary creatinine can be considered as an available and inexpensive test. Therefore, the aim of this study was to evaluate the prognostic value of urinary creatinine test in patients with systolic heart failure.

METHODS AND MATERIALS

Design and participants

This cross-sectional study was performed on 134 patients suffering from chronic systolic heart failure from February 1 to December 10, 2020, in an educational hospital (Seyed Al-Shohada) in northwest Iran (Urmia). Patients were selected through the available sampling method. The required information was collected in the first visit and followed up one month later and three months later. The inclusion criterion was according to cardiac EF obtained from echocardiography and patients with EF less than 45% were considered. Suffer patients to chronic kidney failure in stages 4 and 5, as well as patients with normal serum creatinine who underwent dialysis and patients who did not consent to participate in this research project were excluded from the study. (Patients with GFR 30 and more are present in the study). The final study score of each patient was equal to the mortality due to the complications of this disease. The number of participants was calculated using Cochran's formula with an error of 0.05, which was appropriate for 178 participants.

Data collection

Data collection checklist included demographic characteristics (age, sex (male / female)), BMI, serum and urine creatinine level (mg/dL), EF (%), serum urea, serum and urine albumen (mg/dL) Deciliters), GFR, period of hospital stay and mortality. After obtaining the license and concordance with the hospital, the study purposes were first explained to the participants. Patients willing to participate in the study were considered in the study. Then, at the first visit of the patient, blood and urine tests were taken and the results were entered in the checklist.

Ethical Considerations

This study has been approved in the ethics committee of Urmia University of Medical Sciences with

the ethics code IR.UMSU.REC.1398.427 and the dissertation number: 3019-32-09-96. Before the start of the study, all participants gave written consent. Participants were assured that their information would be kept confidential. The STROBE checklist was used to report the study.

Data analysis

The collected data were entered into SPSS V21 software for analysis. Descriptive (mean, percentage, frequency) and analytical (Pearson correlation) tests were used to analyze the data. Pearson correlation test was used to determine the relationship between urinary creatinine and quantitative outcomes. Significance level was considered less than 0.05.

Results

In the present study, data of 122 participants was assessed in the final analysis. The mean age of participants was 67.36 years, weight 75.52, height 166.08, and BMI was 27.11. Most participants were male ($n=68$). (Table 1)

The results of Pearson correlation test show that there is no significant relationship between weight, height and body mass index with urinary creatinine ($p < 0.05$). The results also showed that there was no significant relationship between serum creatinine and urinary creatinine ($p < 0.05$). Also, independent t-test showed that there was no statistically significant relationship between fraction ejection and urinary creatinine ($P = 0.915$). Regarding the relationship between mortality and urinary creatinine, analysis of variance showed a non-significant relationship. Pearson correlation coefficient showed that there is a positive and significant relationship between GFR and urinary creatinine, so that with decreasing GFR level, urinary creatinine level also decreases. According to Pearson correlation coefficient, the results showed that there is a significant positive relationship between diastolic blood pressure and urinary creatinine. But there is no significant relationship between systolic blood pressure and heart rate with urinary creatinine (Table 2).

DISCUSSION

Edema of the wrists and feet is a major manifestation in patients with heart failure. However, there are several non-cardiac causes for this symptom. In general, right heart failure may present with edema, right hypochondriac pain (liver distance), abdominal swelling (ascites), and loss of appetite. In general, peripheral edema has a sensitivity of 10% and a specificity of 93% in the diagnosis of heart failure (18). In general, pulmonary crackles are heard in elderly patients with asymptomatic cardiovascular disease, even in the ab-

Table 1. Demographic characteristics of participants

		Mean or N(%)	Variable
		67.36	Age (y)
		27.11	BMI
		75.52	Weight
		166.08	Height
N (%)	Variables	68	Gender
		54	Male Female
68(55.7%) 54(44.3%)	Blood pressure Yes No	12(9,8) 25(20.5) 85(69..7)	NYHA class I II III IV
44(36.1%) 78(63.9%)	Diabetes Yes No	34(27.9%) 88(72.1)	EF 31-45% >30%
44(36.1%) 78(63.9%)	COPD Yes No	92(75.4%)	Ascites Yes No
6(4.9%) 116(95.1%)	CVA/TIA YES NO	38(31.1%) 84(68.9%)	Smoking Yes No
62(50.8%) 68(55.7%) 73(59.8%) 34(27.9%)	Consumption of HF drugs ARB or ACEI Beta-blockers Furosemide Spironolactone	57(46.7%) 65(53.3%)	History of MI Yes No
21 101	Mortality Yes No	98	History of hospitalization Yes No
49.82	GFR	85.11	HR
12.43	HB	1.50	Creatinine (serum)
106.52	T.G	57.13	Urea

sence of overt heart disease or associated lung disease (20, 19). In a study by Kataoka et al. The incidence of pulmonary crackles in patients with heart failure was 42% (21); In our study, this amount was reported more; This is probably due to the average age of most of the people we studied compared to the above study.

In present study the mean urinary creatinine level was 81.19 ± 50.01 mg / dl, There was no significant relationship between weight, height, body mass index, functional class, mortality, in-hospital or out-of-hospital mortality with urinary creatinine. Also, in this study, mean urinary creatinine level in patients was lower with class 4 compared to classes 3 and 2 (75.89 vs. 93.72) but this relationship was not significant and also in our study the mean urinary creatinine level in patients with a history of 3 hospitalizations was higher than other patients. But no significant relationship was observed between hospitalization rate and

urinary creatinine level. In this study, the mean urinary creatinine level in EF was less than 30 and between 31 and 45 were 81.50 50 50.80 and 80.42 48 48.65 mg / dl, respectively, and also there was a significant relationship between urinary creatinine level and EF.

In the study by Ter Maaten et al., 2130 patients with heart failure were included in the study. They reported that there was no significant relationship between body mass index and cardiac ejection fraction with urinary creatinine level, which is consistent with the results of our study, but there is a significant relationship between height, weight, serum creatinine level, functional class, which is in line with our study. Although in our study there was also a weak correlation between serum and urinary creatinine levels; As the serum creatinine level increases, the urinary level decreases.

Also, the mean urinary creatinine level in our study was lower in patients with higher functional

Table 2. Relationship between urinary creatinine and study indicators

	Correlation coefficient	Pvalue
Urinary creatinine with weight	-03/0	68/0
Urinary creatinine with weight	07.0	43.0
Urinary creatinine with body mass index	07.0	38.0
Urinary creatinine with serum creatinine	-17.0	0.06
EF <30 31-45	81.50±5.41 80.42±8.34	0.915
Has no history hospitalization First times Two times three times	76.47±44.50 88.42±59.66 83.17±41.27 127.87±115.78	0.73
Mortality situation alive Death while hospitalization Mortality in follow-up after a month Mortality in follow-up after three month	83.61±50.72 63.50±46.50 65.43±16.27 76.75±132.25	0.65
GFR with urinary creatinine	0.31	0.0001
Blood pressure Systolic blood pressure Diastolic blood pressure Heart rate	0.22 0.14 0.008	0.01 0.14 0.008

class; Which is in line with the results of the above study. The findings of our study showed a positive and significant relationship between urinary creatinine level and GFR, so we expect that with decreasing GFR, urinary creatinine level will also decrease, which is a significant relationship between Maaten et al. Urinary creatinine levels and renal function achieved are correlated. On the other hand, the results of our study showed that the mean level of urinary creatinine in patients with and without spironolactone was not different from the results of Maaten et al. In this study, we also found a significant relationship between diastolic blood pressure and urinary creatinine.

Different studies in different patients have shown that lower 24-hour urinary creatinine excretion is associated with all causes of mortality and major cardiovascular events (22–24). A small cohort study of patients with chronic heart failure found that lower 24-hour creatinine excretion was associated with a higher risk of clinical side effects (mortality, heart transplantation, myocardial infarction, or readmission) (25). The prognostic value of urinary creatinine has been studied in two community-based groups. In a cohort study conducted by Carter and colleagues on 2,627 population-based individuals; They reported that low urinary creatinine concentration was associated with an increased risk of cardiovascular complications (26). In another recent

study by Carter et al. In 6770 population-based individuals; Reported that there was no significant relationship between urinary creatinine level and cardiovascular complications (27). The results also showed that the level of urinary creatinine in patients was not significantly related to the number of hospitalizations, which is in line with the results of the Carter study.

CONCLUSION

The results showed that low urinary creatinine levels in patients with heart failure were not associated with high functional levels and readmission. Also, no relationship was found between urinary creatinine and weight, height, body mass index, functional class, mortality, in-hospital or out-of-hospital mortality rate, functional level, readmission and EF. But urinary creatinine level has a positive and significant relationship with GFR and diastolic blood pressure. The results of the present study indicate the importance of paying attention to urinary creatinine as an effective underlying factor in predicting the symptoms of heart failure.

Ethics approval and consent to participate

This study has been registered in the ethics committee of Urmia University of Medical Sciences with the ethics code IR.UMSU.REC.1398.427, and written consent was taken from each subject.

Competing interests

No conflict of interest.

Authors' contributions

SA, MHAPR, AR: Concept and design, SE: Data collection, RAG: Revision of the manuscript, SA, MHAPR, AR: Data collection and drafting of initial manuscript, AR: data interpretation, AR: Statistical analysis and critical revision of the manuscript. All authors have read and approved the manuscript.

REFERENCES

1. LONGO DL, FAUCI AS, KASPER DL, HAUSER SL, JAMESON JL, LOSCALZO J. Harrison's Principles of Internal Medicine 18E Vol 2 EB. McGraw Hill Professional; 2012 Nov 8.
2. AMBROSY AP, FONAROW GC, BUTLER J, CHIONCEL O, GREENE SJ, VADUGANATHAN M, ET AL. The global health and economic burden of hospitalizations for heart failure: lessons learned from hospitalized heart failure registries. *J Am Coll Cardiol*. 2014;63(12):1123–33.
3. MOMENI M, KHOSHTARASH M, GHANBARI KHANGHAH A, SALEHZADEH A, RAHMAT-

- POUR P.** Self-care behaviors and related factors in patients with heart failure referring to medical & educational center of heart in Rasht.. *J Holist Nurs Midwifery*. 2013; 23 (1) :22–29
4. **LINDEN B.** ESC guidelines on acute and chronic heart failure. *Brit J Cardiac Nur*. 2012;7(10):490–1.
 5. **PONIKOWSKI P, VOORS AA, ANKER SD, BUENO H, CLELAND JG, COATS AJ, ET AL.** ESC Guidelines for the diagnosis and treatment of acute and chronic heart failure: The Task Force for the diagnosis and treatment of acute and chronic heart failure of the European Society of Cardiology (ESC) Developed with the special contribution of the Heart Failure Association (HFA) of the ESC. *Europ Heart J*. 2016;37(27):2129–2200.
 6. **YANCY CW, JESSUP M, BOZKURT B, BUTLER J, CASEY DE, DRAZNER MH, ET AL.** ACCF/AHA guideline for the management of heart failure. *Circulation*. 2013 J CIR-0b013e31829e8776.
 7. **McKELVIE RS, MOE GW, EZEKOWITZ JA, HECKMAN GA, COSTIGAN J, DUCHARME A, ET AL** The 2012 Canadian Cardiovascular Society heart failure management guidelines update: focus on acute and chronic heart failure. *C J C*. 2013;29(2):168–81.
 8. **KING M, KINGERY J, CASEY B.** Diagnosis and evaluation of heart failure. *Am Fam Physician*. 2012;85(12):1161–8.
 9. **KRUM H, DRISCOLL A.** Management of heart failure. *Med J Aust*. 2013; 199(5):334–9.
 10. **BRISCO-BACIK MA.** Prognostication on the spot! The evolving importance of urinary creatinine in heart failure. *Am Heart J*. 2017;188:186–188.
 11. **TER MAATEN JM, MAGGIONI AP, LATINI R, MASSON S, TOGNONI G, TAVAZZI L, SIGNORINI S, ET AL.** Clinical and prognostic value of spot urinary creatinine in chronic heart failure – An analysis from GISSI-HE. *Am Heart J*. 2017;188:189–95.
 12. **MASSON S, LATINI R, MILANI V, MORETTI L, ROSSI MG, CARBONIERI E, ET AL.** Prevalence and prognostic value of elevated urinary albumin excretion in patients with chronic heart failure. Data from the GISSI-Heart Failure trial. *Circ Heart Fail*. 2010;3(1):65–72.
 13. **JACKSON CE, SOLOMON SD, GERSTEIN HC, ZETTERSTRAND S, OLOFSSON B, MICHELSON EL, ET AL.** Albuminuria in chronic heart failure: prevalence and prognostic importance. *Lancet*. 2009;374(9689):543–50.
 14. **MIURA M, SHIBA N, NOCHIOKA K, TAKADA T, TAKAHASHI J, KOHNO H, ET AL.** Urinary albumin excretion in heart failure with preserved ejection fraction: an interim analysis of the CHART 2 study. *Eu J Heart Fail*. 2012;14(4):367–76.
 15. **SPOELSTRA-DE MAN AM, BROUWER CB, STEHOUWER CD, SMULDERS YM.** Rapid progression of albumin excretion is an independent predictor of cardiovascular mortality in patients with type 2 diabetes and microalbuminuria. *Diabetes Care*. 2001;24(12):2097–101.
 16. **VILLACORTA H, FERRADAES PD, MESQUITA ET,**
 - NÓBREGA AC.** Microalbuminuria is an independent prognostic marker in patients with chronic heart failure. *Arq Bras Cardiol*. 2012;98(1):62–9.
 17. **VAN DE WAL RM, ASSELBERGS FW, PLOKKER HT, SMILDE TD, LOK D, VAN VELDHUISEN DJ, ET AL.** High prevalence of microalbuminuria in chronic heart failure patients. *J Car Fail*. 2005;11(8):602–6.
 18. **WATSON R, GIBBS C, LIP G.** Clinical features and complications. *BMJ*. 2000;320(7229):236–9.
 19. **HUSS J, BRYANT, LM.** Branch Library News. 1914;1:122.
 20. **THACKER RE, KRAMAN SS.** The prevalence of auscultatory crackles in subjects without lung disease. *Chest*. 1982;8672(4): 672–4.
 21. **KATAOKA H, MATSUNO O.** Age-related pulmonary crackles (rales) in asymptomatic cardiovascular patients. *Ann Fam Med*. 2008;6(3):239–45.
 22. **OTERDOOM LH, GANSEVOORT RT, SCHOUTEN JP, DE JONG PE, GANS RO, BAKKER SJ.** Urinary creatinine excretion, an indirect measure of muscle mass, is an independent predictor of cardiovascular disease and mortality in the general population. *Atherosclerosis*. 2009;207(2):534–40.
 23. **SINKELER SJ, KWAKERNAK AJ, BAKKER SJ, SHAHINFAR S, ESMATJES E, DE ZEEUW D, ET AL.** Creatinine excretion rate and mortality in type 2 diabetes and nephropathy. *Diabetets Care*. 2013;36(6): 1489–94.
 24. **IX JH, DE BOER IH, WASSEL CL, CRIQUI MH, SHLIPAK MG, WHOOLEY MA.** Urinary creatinine excretion rate and mortality in persons with coronary artery disease: the Heart and Soul Study. *Circulation*. 2010;121(11):1295.
 25. **TER MAATEN JM, DAMMAN K, HILLEGE HL, BAKKER SJ, ANKER SD, NAVIS G, ET AL.** Creatinine excretion rate, a marker of muscle mass, is related to clinical outcome in patients with chronic systolic heart failure. *Clinl Res Cardiol*. 2014;103(12):976–83.
 26. **CARTER CE, GANSEVOORT RT, SCHEVEN L, HEERSPINK HJL, SHLIPAK MG, DE JONG PE, ET AL.** Influence of urine creatinine on the relationship between the albumin-to-creatinine ratio and cardiovascular events. *Clin J e Am Soci Nephrol*. 2012;7(4):595–603.
 27. **CARTER CE, KATZ R, KRAMER H, DE BOER IH, KESTENBAUM BR, PERALTA CA, ET AL.** Influence of urine creatinine concentrations on the relation of albumin-creatinine ratio with cardiovascular disease events: the Multi-Ethnic Study of Atherosclerosis (MESA). *Am J Kidney Diseases*. 2013;62(4):722–9.

<http://dx.doi.org/10.35630/2199-885X/2022/12/2.19>

EFFECT OF BIOACTIVE GLASS-BASED COMPOSITE AND LOW ENERGY LASER ON BONE REGENERATION IN AN EXPERIMENTALLY INDUCED BONE DEFECT

Received 11 February 2022;
Received in revised form 10 March 2022;
Accepted 11 march 2022

**Sergey Konovalenko¹✉, Volodymyr Protsenko² ,
Yevgen Solonitsyn² , Taras Osadchuk²,
Volodymyr Konovalenko¹, Taras Omelchenko³ **

¹ *RE Kavetsky Institute of Experimental Pathology, Oncology and Radiobiology, National Academy of Sciences of Ukraine, Kyiv, Ukraine*

² *State Institute of Traumatology and Orthopaedics, National Academy of Sciences of Ukraine, Kyiv, Ukraine*

³ *Bogomolets National Medical University, Kyiv, Ukraine*

✉ ip15@ukr.net

ABSTRACT — In vivo experimental study was conducted to investigate the effect of bone regeneration under the use of a bioactive glass-based composite as well as the use of laser irradiation in the presence of the bioactive glass-based composite. In 16 white non-inbred rats, with a body weight of 300–350 g the bioactive glass-based composite was implanted into the tibial metaphysis. Besides, 90 female rats of the Wistar line weighing 250–270 g underwent laser irradiation on an artificially created tibial bone defect filled with the bioactive glass-based composite. The period of observation lasted respectively 2 and 4 weeks. It was found that application of the bioactive glass promotes bone regeneration, which is noticeably enhanced with the use of low energy laser. The combining effect leads to a significant increase in bone regeneration and the expression of bone tissue metabolic markers: osteocalcin and alkaline phosphatase. The most pronounced effect of the laser on bone regeneration occurred at a wavelength of 810 nm, which opens up prospects for the use of this technique in clinical practice.

KEYWORDS — bone regeneration, bioactive glass (BG)-based composite, low energy laser, osteocalcin (OC), alkaline phosphatase (ALP), bone tumor.

INTRODUCTION

The problem of filling in bone defects due to tumor excision and specific diseases, and the search for optimal materials for this purpose, is a topical issue in orthopaedics, traumatology, oncology, maxillo-facial surgery and neurosurgery [11]. Current stage of development in reconstructive surgery raises the urgent task of designing materials that can function as a framework for the regeneration of a damaged bone, whilst being gradually split and replaced by the patient's own

tissue, thus stimulating osteogenesis. At the same time, there are still many unclear issues related to the effects of biomaterials on osteogenesis [12]. Implant materials and structures should be biocompatible, osteoinductive, and, preferably, osteoconductive without causing toxic reactions, suppuration, rejection, and metallosis [16]. Among implantation materials, bioactive glass biocomposites and their modifications are widely used [17]. Bioactive glass biocomposites are completely replaceable by bone tissue without the formation of a fibrous layer. They actively stimulate bone formation and significantly enhance reparative processes in damaged tissues, which contributes to rapid bone fusion and restoration of the bone structure [17]. When applied, such biocomposites can firmly bond to the recipient's bone tissue due to the formation of a hydroxycarbonate-apatite layer, promote the activation and proliferation of osteogenic cells, and vascularisation due to the release of three biologically active ions (silicon, calcium and phosphates) in the physiological environment. The introduction of calcium-phosphate compounds into the composition of a bioglass makes it possible to obtain a material with specific properties that satisfy its use in skeletal regions under stress [14, 15]. Various techniques for intensifying repair processes in damaged tissues, including those in bone tissue, are reported in the literature [5]. One of the techniques of intensification of repair processes of damaged tissues, which is actively studied in the world today, is the effect of low energy laser radiation (LLLT — low level laser therapy) [5]. Light in the red to near infra-red range of 600–1,070 nm has the greatest influence on the biochemical activity of different cells [1]. There is also a substantial amount of data on the effectiveness of light energy in the treatment of cancer pathology: from surgery using high-power lasers to safer and, most importantly, organ-saving photodynamic therapy using photosensitizers and photobiomodulation [2, 3, 4, 13]. Due to its proven biostimulatory effects, LLLT at different wavelengths (660, 810, 940 nm) has been successfully used to improve cell proliferation and healing in bone tissue [6, 7, 8, 9]. Enhancement of osteogenesis occurs due to the increased activity of osteoblasts induced by

laser exposure: in cultured human hypoxic osteoblasts LLLT enhances the expression of bone morphogenic protein-2 (BMP-2), which acts as a transforming growth factor- β (TGF- β) for osteocalcin, type I collagen and alkaline phosphatase [10]. Considering the above, we proceeded with a series of experimental works to study the combined application of a bioactive glass-based composite and laser radiation on bone regeneration.

Aim:

to study the effect of photobiomodulation on bone regeneration in the context of bone formation markers: osteocalcin and alkaline phosphatase.

MATERIALS AND METHODS

The research was carried out in accordance with international requirements for the humane treatment of laboratory animals in the framework of the "European Convention for the Protection of Vertebrate Animals used for Experimental and Other Scientific Purposes" (Strasbourg, 1986) and the Law of Ukraine No. 3447-IV of 21.02.2006 "On protection of animals against cruel treatment".

The experiment was conducted on 16 animals (white non-inbred rats, with body mass of 300–350 g) obtained from the vivarium (RE Kavetsky Institute of Experimental Pathology, Oncology and Radiobiology, Ukraine). We evaluated porous samples (pellets) of a bioactive glass biocomposite when implanted into the metaphysis of the tibia.

The bioactive glass-based composite ("Biocomposite synthetic bone") was synthesised in laboratory of Prof. V. Dubok at Institute of Materials Research, National Academy of Sciences of Ukraine). The composition of the bioactive glass-based composite: bioactive glass 50–65%, hydroxyapatite 14–17%, tricalcium phosphate — 14–17 %, wollastonite — 7–9%.

The introduction of animals into the experiment, surgical intervention and withdrawal from the experiment was performed under general thiopental anaesthesia. The period of observation was determined by the objectives of the respective study (2 and 4 weeks). 16 rats underwent surgery on a section of the proximal cnemis (proximal area of the tibia), a scalpel was used to cut through the skin on the inner surface of the cnemis above the metaphysis of the tibia, the soft tissues were crossed, the periosteum was debrided with a raspator, then the bone was marked with an awl and a 2 mm drill was used to drill the bone plate to the medullary canal, the marrow in the area of the hole was exhumed with the Folkman spoon, then the bone cavity in the area of the trepanation hole was filled with the BG-based composite pellets, the soft tissues

were tightly sutured over the hole, the skin was sutured and the surgical suture was treated with brilliant green or iodine.

On the 2nd and 4th weeks after the surgery, the laboratory animals were withdrawn from the study to investigate the intensity of bone tissue regeneration at the site of BG implantation by means of light and electronic microscopy.

For morphological studies with a light microscope, a segment or a whole rat tibia with the implanted bioglass composite was removed and fixed in 10% neutral formalin solution, decalcified in 4% nitric acid solution, dehydrated in alcohol of increasing concentration and immersed in paraffin. Serial histological slices with a thickness of 7–9 μ m were made on a microtome and stained with Weigert's iron haematoxylin and eosin as well as with Van Gasson's pyrofuchsin. The stained slices were analysed using an Olympus BX-63 microscope.

A fragment of the rat tibia with the implanted BG-based composite was removed for morphological studies using an electron microscope. Samples were fixed in 10% formalin solution (phosphate buffer, pH=7.4). Decalcification was performed in Osteofast 2 solution (BioGnost, Croatia). After decalcification, bone fragments were excised at the defect level. The samples were then dehydrated in isopropanol and embedded in paraffin (Leica Surgipath Paraplast Regular, Leica Biosystems, Germany). Slices of 7–8 μ m thickness were obtained from paraffin blocks on a Thermo Microm HM 360 microtome (Thermo Fisher, USA). After deparaffinisation, the microslides were stained with haematoxylin and eosin and encased under coverslips in balsam (Merck, Germany). Microslides were examined and microphotographs were taken using an Olympus BX-51 microscope (Japan).

In addition 90 female rats of the Wistar line with a weight of 250–270 g were treated with laser irradiation on an artificially created tibial bone defect filled with the bioactive glass-based composite. Animals were allocated into 5 groups: "Control" (N=15), "Bio Glass" (N=15), "Laser 660" (N=15), "Laser 810" (N=15), "Bio Glass+Laser 660" (N=15), "Bio Glass+Laser 810" (N=15). "Lika Surgeon" and "Lika therapist M" lasers manufactured by "Fotonika Plus" company (Cherkasy, Ukraine) were used in the experiment. Irradiation of the rat tibial defect filled with the pellets of the bioactive glass biocomposite (3–5 mg) was performed with the laser at wavelength of 660 and 810 nm, 50 mW power and 5 minutes exposure. Levels of osteocalcin and alkaline phosphatase in the blood serum were measured the next day after the intervention, as well as on the 22nd day. The second control point was not chosen by chance because the highest

levels of serum markers of osteogenesis after bone injury are usually observed on the 14th day [9, 10]. Therefore it was decided to postpone the analysis by 7 days to make the measurement results more relevant.

RESULTS AND DISCUSSION

The morphological examination of bone tissue microslides in experimental animals after the implantation of pellets of the BG-based composite into the bone cavity using a light microscope detected: in the areas where biocomposite pellets had got into lacunes of cancellous bone, active osteogenesis was observed around this material (Fig. 1 a, b.). The biocomposite was partially surrounded by a connective tissue, mostly by bone tissue. Morphogenesis corresponded to the formation of lamellar bone tissue. There was isolation of the biocomposite from the surrounding bone marrow.

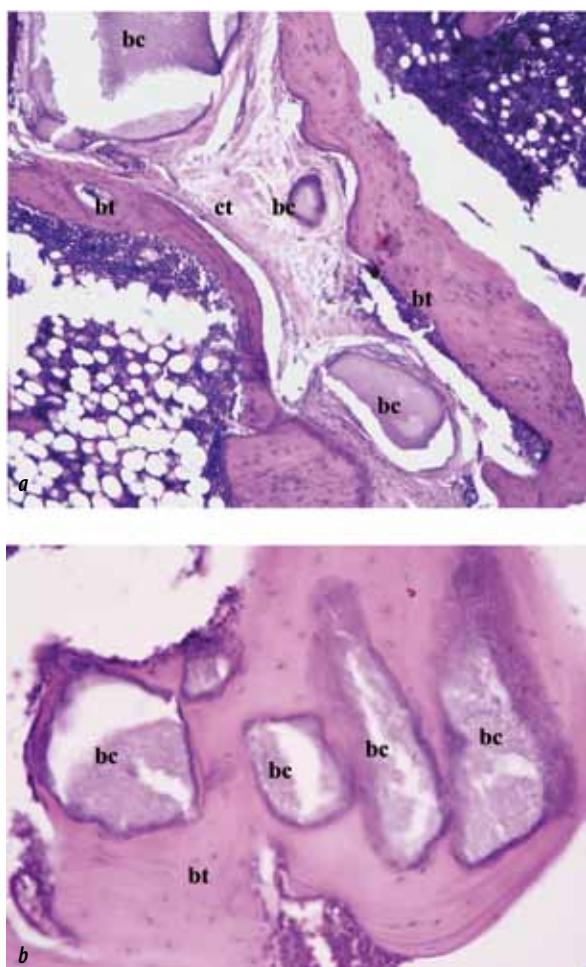


Fig. 1. (a, b) Active osteogenesis around the biocomposite. Notes: bc — biocomposite; ct — connective tissue; bt — bone tissue. Hematoxylin-eosin, a: $\times 100$; b: $\times 200$

Thus, active osteogenesis was observed around the BG-based composite, which was surrounded by newly formed bone tissue.

Morphological examination of bone tissue microslides in experimental animals after implantation of BG-based composite pellets into the bone cavity using an electron microscope revealed heterogeneous ultrastructural changes in selected samples. The examined samples were dominated by areas of heterogeneous cell populations, among which there were osteoblasts and fibroreticular cells, with far fewer macrophages. The extracellular matrix contained few fibrous components, only single bundles of collagen fibres. There were also small non-cellular areas with no signs of osteogenesis (see Fig. 2). The formation of a new bone matrix was detected only in individual small loci, in the form of trabeculae. Clusters of activated osteoblasts are concentrated along the contour of these trabeculae (see Fig. 3). The bone matrix contained dense clusters of fibrous elements and was electron-dense, which indicates its mineralization. In some loci, lacunas with osteocytes were found that had a well-developed endoplasmic reticulum and euchromatin dominated in the nucleus (see Fig. 4). Such ultrastructural characteristics of osteocytes indicate a functional state, i.e. their continued involvement in the formation of the bone matrix.

Thus, a weak reparative osteogenesis was detected around the BG-based composite, and areas of cellular organization contain activated osteoblasts as well as fibroreticular cells. Overall, the changes can be assessed as an initiatory stage of osteogenesis.

The following osteocalcin (OC) (see Table 1) levels were obtained in laboratory animals treated with laser irradiation on an artificially created tibial bone defect filled with the BG-based composite.

Analysis of osteocalcin expression at the control points indicates that both the BG-based composite and laser irradiation have a positive effect on bone regeneration: in comparison to the control group, where the index was 67.9 ng/ml on day 22, in animals treated only with the BG-based composite — osteocalcin expression was 74.6 ng/ml; the photobiomodulatory effect of the $\lambda 660$ nm laser stimulated osteocalcin level up to 67.1 ng/ml and the $\lambda 810$ nm laser up to 69.9 ng/ml.

However, it should be emphasised that the highest level of osteocalcin expression in the second control point was observed with the combination of the bioactive glass with the photobiomodulatory exposure to the light at a wavelength of 810 nm: 84.4 ng/ml, whereas in the “Bioglass+Laser 660” group the figure amounted to 79.9 ng/ml. (see Fig. 5).

We also observed positive effects using both bioactive glass and laser irradiation on the expression level of alkaline phosphatase (AP) (see Table 2).

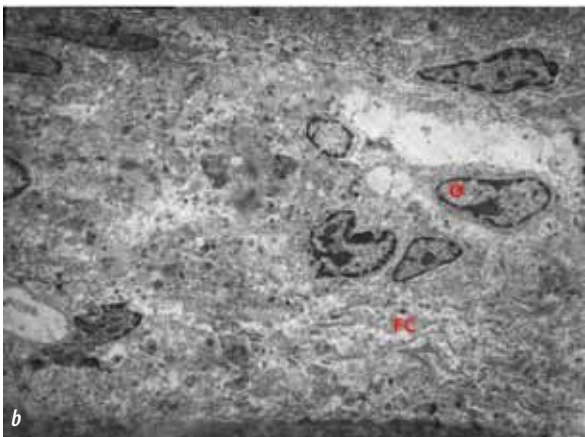
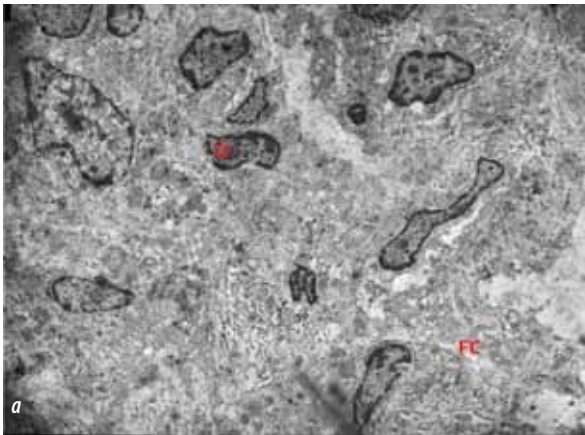


Fig. 2. (a, b) Section of cellular reorganisation around the site of application of the BG composite. Accumulation of osteocytes (O) and single fibroreticular cells (FC). Electrophotogram, $\times 2400$

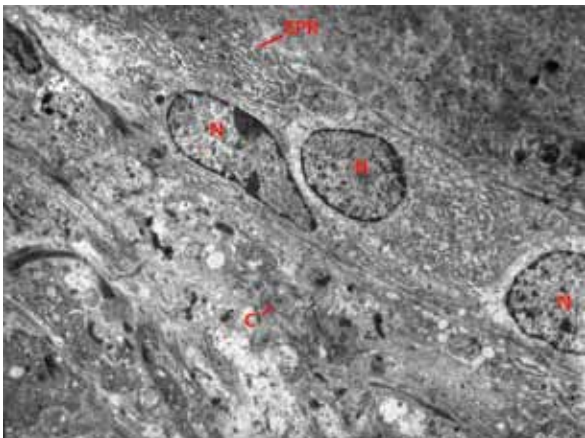


Fig. 3. Accumulation of osteocytes with a developed endoplasmic reticulum (EPR) and a dominance of euchromatin in the nuclei (N). Bundles of collagen fibres (C) are present in the extracellular matrix. Electrophotogram, $\times 2400$

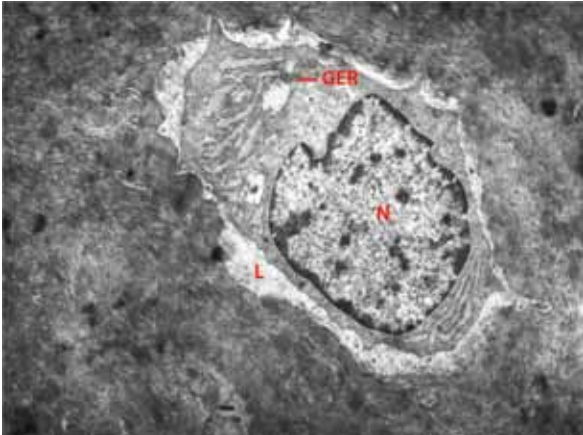


Fig. 4. Osteocyte in the lacuna (L) of the bone tissue after application of the bioactive glass-based composite. A developed granular endoplasmic reticulum (GER) and nucleus (N) with euchromatin dominance indicates an active functional (synthetic) state. The bone matrix (BM) contains fibrous structural elements. Electrophotogram, $\times 4000$

Table 1. Levels of osteocalcin and the dynamics of osteocalcin at the control points of the experiment

Group	Deadline	Osteocalcin, ng/ml			
		day 1	day 22	Δ abs	Δ %
Control		61,4	67,9	+6,5	+10,6%
Bioglass		66,2	74,6	+8,4	+12,7%
Laser 660		61,5	67,1	+5,6	+9,1%
Laser 810		63,4	69,9	+6,5	+10,3%
Bioglass + Laser 660		62,2	79,9	+17,7	+28,5%
Bioglass + Laser 810		61,9	84,4	+22,5	+36,3%

Table 2. Level of alkaline phosphatase and its dynamics at the control points of the experiment

Group	Deadline	Alkaline phosphatase, units/l			
		day 1	day 22	Δ abs	Δ %
Control		97,7	102,2	+4,5	+4,6%
Bioglass		100,2	114	+13,8	+13,8%
Laser 660		96,6	109,3	+12,7	+13,1%
Laser 810		100,7	122,2	+21,5	+21,4%
Bioglass + Laser 660		99,3	116	+16,7	+16,8%
Bioglass + Laser 810		95,5	144,4	+48,9	+51,2%

The results of the analysis of AP expression indicate that both the bioactive glass and laser irradiation demonstrated a stimulating effect on bone

regeneration in comparison with the control group of animals which were treated only with the bioactive glass, where alkaline phosphatase expression index was 114.0 units/l. The effect of $\lambda 660$ nm laser stimulated alkaline phosphatase level to 109.3 units/l, while at $\lambda 810$ nm laser alkaline phosphatase reached 122.2 units/l (see Fig. 6).

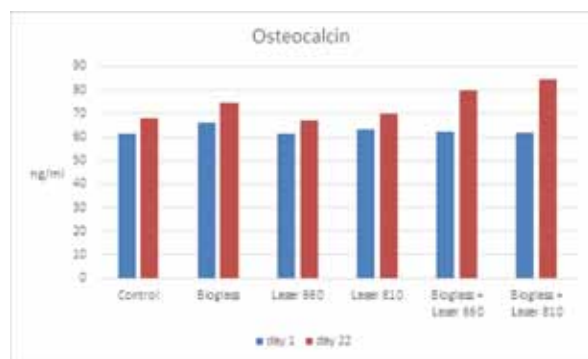


Fig. 5. Level of osteocalcin (OC) in different groups at day 1 and day 22 of the experiment

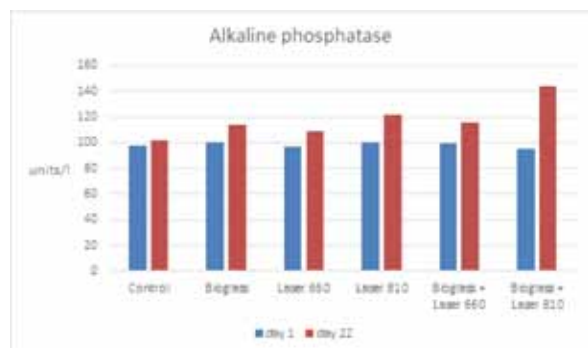


Fig. 6. Level of alkaline phosphatase (AP) in the test groups at day 1 and day 22 of the experiment

Similar to the increase in OC level, the highest LF expression rate on the day 22 of the observation was recorded when the bioactive glass was combined with the photobiomodulatory effect of 810 nm wavelength light: 144.4 units/l, while in the Bioglass+Laser 660 group its level was 116.0 ng/ml.

Similar data have also been observed by other researchers [4-10], since the infrared light has greater penetrating power and results in increased biochemical activity of cells, particularly during proliferation period, which, at the same time, is safer.

CONCLUSION

1. The experimental data show that the use of the bioactive glass-based composite stimulates bone regeneration and creates conditions for bone regeneration and repair.

2. Our results confirm the use of low level laser therapy with a wavelength of 810 nm as an effective photobiomodulatory factor, which in the presence of the bioactive glass significantly increases serum markers, namely OC and AF, indicating a positive effect on bone regeneration.

3. To ensure timely introduction of this method into clinical practice, the study of LLLT on bone regeneration needs to be continued in new experimental models and according to the principles of translational medicine.

REFERENCES

1. **TSAI SR, HAMBLIN MR.** Biological effects and medical applications of infrared radiation. *J Photochem Photobiol B.* 2017;170:197-207. DOI: 10.1016/j.jphotobiol.2017.04.014
2. **DEL VECCHIO, ALESSANDRO ET AL.** "Laser Photobiomodulation (PBM)-A Possible New Frontier for the Treatment of Oral Cancer: A Review of In Vitro and In Vivo Studies." *Healthcare (Basel, Switzerland)* vol. 9,2 134. 29 Jan. 2021, <https://doi.org/10.3390/healthcare9020134>
3. **CHEKHUN V.F.** Priority results of R. E. Kavetskyi Institute of Experimental Pathology and Oncology and Radiobiology of the National Academy of Sciences of Ukraine // *Science and Scientology.* - 2014. - No 1. - p. 46-57.
4. **WANG K, YU B, PATHAK JL.** An update in clinical utilization of photodynamic therapy for lung cancer. *J Cancer.* 2021;12(4):1154-1160. doi: 10.7150/jca.51537
5. **OLIVEIRA GJPL, PINOTTI FE, ARONI MAT, MARCANTONIO E JR, MARCANTONIO RAC.** Effect of different low-level intensity laser therapy (LLL) irradiation protocols on the osseointegration of implants placed in grafted areas. *J Appl Oral Sci.* 2021; 29:e20200647. Published 2021 Apr 14. DOI: 10.1590/1678-7757-2020-0647
6. **WANG L, LIU C, WU F.** Low-level laser irradiation enhances the proliferation and osteogenic differentiation of PDLSCs via BMP signalling. *Lasers Med Sci.* 2021 Jul 10. doi: 10.1007/s10103-021-03338-6. Epub ahead of print. PMID: 34247314.
7. **BAI J, LI L, KOU N, BAI Y, ZHANG Y, LU Y, GAO L, WANG F.** Low level laser therapy promotes bone regeneration by coupling angiogenesis and osteogenesis. *Stem Cell Res Ther.* 2021 Aug 3;12(1):432. DOI: 10.1186/s13287-021-02493-5. PMID: 34344474; PMCID: PMC8330075.
8. **SARMADI S, TANBAKUCHI B, HESAM AREFI A, CHINIFORUSH N.** The Effect of Photobiomodula-

- tion on Distraction Osteogenesis. *J Lasers Med Sci*. 2019;10(4):330-337. DOI: 10.15171/jlms.2019.53
9. **JAWAD MM, HUSEIN A, AZLINA A, ALAM MK, HASSAN R, SHAARI R.** Effect of 940 nm low-level laser therapy on osteogenesis in vitro. *J Biomed Opt*. 2013 Dec;18(12):128001. DOI: 10.1117/1.JBO.18.12.128001. PMID: 24337495.
 10. **MATYS J, ŚWIDER K, GRZECH-LEŚNIAK K, DOMINIAK M, ROMEO U.** Photobiomodulation by a 635nm Diode Laser on Peri-Implant Bone: Primary and Secondary Stability and Bone Density Analysis-A Randomized Clinical Trial. *Biomed Res Int*. 2019 Apr 22; 2019:2785302. <https://doi.org/10.1155/2019/2785302> PMID: 31143771;
 11. **ELIAZ N, METOKI N.** Calcium Phosphate Bioceramics: A Review of Their History, Structure, Properties, Coating Technologies and Biomedical Applications. *Materials (Basel)*. 2017 Mar; p. 334. <https://doi.org/10.3390/ma10040334> PMCID: PMC6501257.
 12. **PAVLOV S.A.** Study of osteogenesis markers of regenerative tissue of jaws after implantation of osteoplastic materials, Ph.D. thesis, 14.01.14, 2011, 135 p.
 13. **MAGRI AMP, FERNANDES KR, KIDO HW, FERNANDES GS, FERMINO SS, GABBAI-ARMELIN PR, BRAGA FJC, GÓES CP, PRADO JLDS, NEVES GRANITO R, RENNÓ ACM.** Bioglass/PLGA associated to photobiomodulation: effects on the healing process in an experimental model of calvarial bone defect. *J Mater Sci Mater Med*. 2019 Sep 7; 30(9):105. DOI: 10.1007/s10856-019-6307-x PMID: 31494718.
 14. **BRITO AF, ANTUNES B, DOS SANTOS F, FERNANDES HR, FERREIRA JMF.** Osteogenic capacity of alkali-free bioactive glasses. In vitro studies. *J Biomed Mater Res B Appl Biomater*. 2017 Nov; 105(8):2360-2365. <https://doi.org/10.1002/jbm.b.33771>. Epub 2016 Aug 16. PMID: 27526955.
 15. **BARGAVI P, CHITRA S, DURGALAKSHMI D, RAJASHREE P, BALAKUMAR S.** Effect of Titania Concentration in Bioglass/TiO₂ Nanostructures and Its In Vitro Biological Property Assessment. *J Nanosci Nanotechnol*. 2018 Jul 1; 18(7):4746-4754. 10.1166/jnn.2018.15340. PMID: 29442653.
 16. **KORZH N.A.** Implant materials and osteogenesis. Role of optimization and stimulation for bone reconstruction / N.A. Korzh, L.A. Kladchenko, S.V. Malyshkina // *Orthopaedics, Traumatology and Prosthetics*. – 2008. – No. 4. – p. 5–14.
 17. New approaches to treatment of patients with giant-cellular bone tumour (experimental and clinical study): abstract, Ph.D. thesis: 14.01.07/ V.V. Protsenko; R. E. Kavetsky Institute of Experimental Pathology, Oncology and Radiobiology of NAS of Ukraine. – K., 2010. – 38 p.

<http://dx.doi.org/10.35630/2199-885X/2022/12/2.20>

A UNIQUE CASE OF NODULAR FASCIITIS IN THE SUBMANDIBULAR GLAND MIMICKING PLEOMORPHIC ADENOMA

Received 15 January 2022;
Received in revised form 25 January 2022;
Accepted 27 January 2022

Itay Chen¹ , Attal Pierr¹,
Daria Kozlova², Jean-Yves Sichel¹ 

¹ Department of Otolaryngology, Head and Neck Surgery, Shaare Zedek Medical Center, Jerusalem, Israel

² Pathology Institute, Shaare Zedek Medical Center, Jerusalem, Israel

✉ chenitay2@gmail.com

Acknowledgments

Department of Radiology, Shaare Zedek Medical Center, Jerusalem, Israel

** All authors have no financial interests or relationships to disclose

** The authors declare that there is no conflict of interest

ABSTRACT — AIM: Nodular fasciitis (NF) is a rare entity responsible for 0.0025% of tumors in the head and neck, to our knowledge; there has been no report in the literature of NF infiltrating the submandibular gland. Through a case of a 29-year-old woman we will discuss the histology and imaging of NF in the submandibular gland and its resemblance to pleomorphic adenoma (PA).

CASE DESCRIPTION: Our patient presented with rapid growth of the right submandibular gland over a 6-month period. Fine Needle Aspiration Cytology suggested PA, nonetheless, mesenchymal origin could not be excluded. MRI strengthened the diagnosis of PA wherein the lesion appeared hyper-intense on T2, hypo-intense on T1 and enhanced with gadolinium. Right submandibulectomy was performed and the histopathological report compatible with NF

CONCLUSION: NF is a self-limited benign process that does not always require surgical removal while PA is a benign tumor treated with surgical resection. Differentiating between these two pathologies is important since surgery can be avoided with a diagnosis of NF. Currently, there is no non-invasive modality that can provide a definite diagnosis of NF in salivary glands. It is important to exhaust our diagnostic possibilities and regard scarcer etiologies in order to achieve the most favorable outcome for the patients.

KEYWORDS — Nodular Fasciitis, Submandibular gland, Pleomorphic adenoma, Salivary gland.

INTRODUCTION

Nodular fasciitis (NF) is a rare, self-limiting benign tumor consisting of fibroblasts and myofibroblasts. It can occur anywhere in the body with the highest incidence in the extremities followed by the

head and neck region with an incidence of 20% (1). Trauma or infection is thought to be the trigger of the fibroblast proliferation although the exact pathogenesis is still unknown. It Usually presents as a painless rapidly growing mass that spreads along the muscular fascia into the subcutaneous tissue and sometimes into the underlying muscle. Due to its rapid growth, its high mitotic activity and pleomorphic picture NF can be easily mistaken for a malignant tumor. Perioperative fine needle aspiration cytology (FNAC) and imaging such as CT and especially MRI can help in making a presumptive diagnosis (2, 3).

CASE REPORT

A 29 year-old generally healthy women was admitted to our department with a 6-month history of a rapidly growing mass in the right submandibular area. The mass was not painful, there was no history of trauma or infection and no history of smoking or alcohol use. The patient did not report fever, weight loss or pain with swallowing. On physical examination a 2 cm, smooth, firm, non-tender mass was palpated at the posterior aspect of the right submandibular triangle with no palpable lymph nodes. Laboratory studies were normal.

Neck ultrasonography revealed a 13X20X23 mm solid tumor within the right submandibular gland as well as benign appearing cervical lymph nodes. FNAC was then performed. The first attempt was non diagnostic. In the second FNAC specimen (alcohol fixation) blood and small amount of hyaline material with a few spindle cells were seen. This was read by the cytopathologist as suspicious for pleomorphic adenoma, although a mesenchymal origin could not be ruled out.

Prior to surgery an MRI of the neck with contrast was obtained. This showed a well- demarcated mass measuring 2.4X2.0X1.1 cm in the right submandibular gland, accompanied by mild enlargement of the gland. The mass was hyper-intense in T2 weighted image, relative to skeletal muscle (Fig 1A) and was hypo-intense on T1 weighted image (Fig 1B). It showed homogeneous enhancement following gadolinium injection (Fig 1C) and hyper-intensity in apparent diffusion coefficient (ADC) map relative to the normal gland. This MRI pattern was consistent with pleomorphic adenoma.

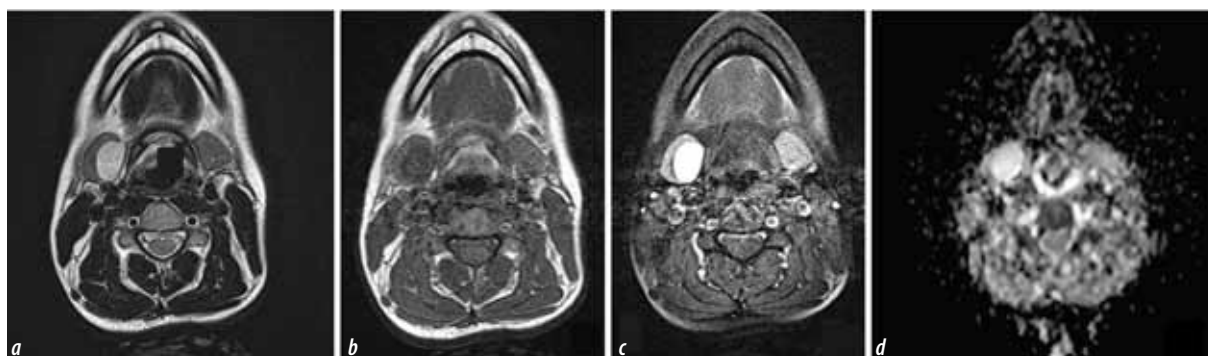


Fig. 1 MRI axial section of the neck showing NF in the right submandibular gland with similar features of PA:

Fig. 1A — T2 weighted image showing hyper intensity of the tumor within the right submandibular gland, Fig. 1B — T1 weighted image showing hypo-intensity of the tumor, Fig. 1C — a well demarcated hyper-intensity of the tumor Post Gadolinium Injection, Fig. 1D — ADC map showing hyper-intensity compared with the normal submandibular gland on the left side

Both the cytology and MRI were in concordance with the probable diagnosis of pleomorphic adenoma. A right submandibulectomy was performed. The surgery was uneventful.

The pathology report established the diagnosis of NF within the submandibular gland. The histology showed plump, immature-appearing fibroblasts and myofibroblasts (Fig. 2A). The cells were arranged in short, irregular bundles and fascicles with scattered lymphoid cells and extravasated erythrocytes (Fig. 2B). The specimen stained positive with alpha actin showing a sub-membranous "tram track" pattern that is characteristic for myofibroblasts (Fig. 2C). While the submandibular gland stained with S-100 the lesion did not (Fig. 2D).

DISCUSSION

NF is a benign self-limiting tumor which can arise anywhere in the body. The most common areas are found in the upper extremity with an incidence of nearly 46%, followed by the head and neck with a 20% incidence and the trunk and lower extremities with an incidence of 18–16% (1). A complete spontaneous resolution of the tumor had been described (4). NF is very rare within the salivary glands with majority of the cases found in the parotid gland (5–7). To our knowledge, NF arising from submandibular gland has not been documented before. Although one case report had been published entitled "NF in the submandibular gland" the text revealed that the tumor was located in parotid gland (8).

FNAC is a widely accepted diagnostic tool used in the workup of salivary gland masses differentiating between benign and malignant tumors due to its accuracy and its minimally invasive quality. The diagnostic accuracy of FNAC is reported to be between 86–98%, sensitivity of 62–97.6% and specificity of 94.3–100% (9, 10).

Pleomorphic adenoma is the most common major salivary tumor but on FNAC it can be mistaken for a variety of tumors due to its histologic variability (9). There are many similarities between NF and pleomorphic adenoma on FNAC. Both tumors may demonstrate bipolar spindle cells with central nuclei, loosely dispersed uniform plasmacytoid cells with round/ovoid eccentric nuclei and eosinophilic cytoplasm. Furthermore myxoid background and tufts of fibrillar intercellular material may be seen in both cases (5). In our case the FNAC favored the diagnosis of pleomorphic adenoma but emphasized that other mesenchymal tumors could not be ruled out.

Although MRI is a well-accepted modality for the diagnosis of salivary gland lesions,

very little is described regarding the MRI image of NF in salivary glands in general and within the submandibular gland in particular. MR images of NF in the skeletal system generally appear hyper-intense to skeletal muscle on T2-weighted and iso/hypo-intense on T1-weighted MR images. The vast majority of the lesions are hyper-intense following gadolinium administration (11).

Diffusion-weighted imaging (DWI) is an important tool used mostly in the examination of central nervous system pathology. DWI relies on water diffusion characteristics of the tissue, therefore cellularity and cell wall barrier are major factors in the differentiation between different tumors. The impedance of water molecule diffusion can be quantitatively assessed using the apparent diffusion coefficient (ADC) value (12).

The MRI characteristics of pleomorphic adenoma show hypo-intensity in T1 weighted image,

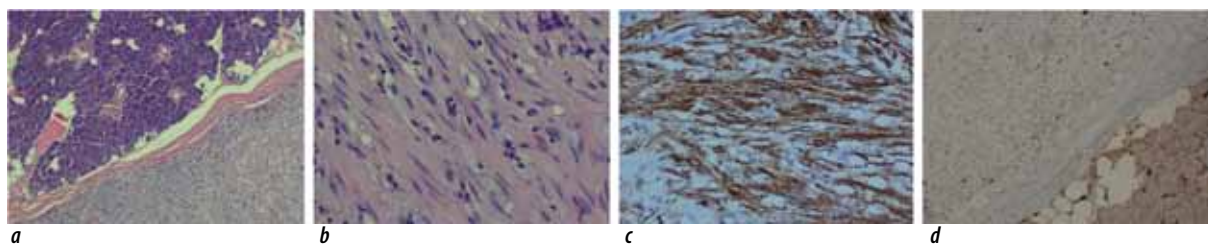


Fig. 2. Histologic slides of specimen post right submandibulectomy:

Fig. 2A. 4X magnification (H&E): left upper field — submandibular gland, right lower field — nodular fasciitis. Fig. 2B. 20X magnification (H&E) of the NF tumor showing immature fibroblasts and myofibroblasts. Fig. 2C. 'Tram track' pattern with alpha actin stain of the NF tumor. Fig. 2D. 5-100 does not stain NF (left upper field) but stains submandibular gland (right lower field)

hyper-intensity in T2 weighted image, enhancement upon gadolinium injection and relatively high values on ADC map (13, 14). It has been published that the presence of high ADC value in salivary gland tumors can differentiate benign from malignant tumors (15).

The MRI picture seen in our patient is similar both to the general image of NF in the skeletal system mentioned above and to the characteristics of pleomorphic adenoma on MRI. So like cytology, the MRI pattern of NF is similar to that of pleomorphic adenoma (PA).

A previous publication (16) compared MRI and FNAC in differentiating between benign and malignant parotid masses, the combination of MRI and diffused weighted image (DWI) with ADC calculation had similar diagnostic values for determining the specific histological types of common parotid masses as FNAC.

CONCLUSION

In conclusion, we have describes the first documented case, to our knowledge, of NF within the submandibular gland. Work up prior to surgery included FNAC and MRI. The FNAC was consistent with but not conclusive for the diagnosis of PA since it did not differentiate clear cut between PA and tumor of mesenchymal origin. NF is a self-limited benign process that does not always require surgical removal while PA is a benign tumor treated with surgical extirpation. Differentiating between these two pathologies is important since NF can spontaneously regress and surgery can be avoided. Currently there is no non-invasive modality that can provide a definite diagnosis of NF in salivary glands. Open biopsy is not a standard of practice in salivary gland tumor diagnosis due to

exacerbation of local spreading and its invasive nature. Core biopsy as a minimal invasive technique can aid us in the final diagnosis and in deciding the necessity of surgery. Thus it is important to exhaust our diagnostic possibilities and also regard the less common etiologies in order to achieve the most favorable outcome for the patients.

REFERENCES

1. GOLDBLUM JR, FOLPE AL, WEISS SW, ENZINGER FM, WEISS SW. *Enzinger and Weiss's soft tissue tumors*. 6th ed. Philadelphia, PA: Saunders/Elsevier; 2014. xiv, 1155 pp.
2. REN SX, ZHANG Y. Nodular fasciitis in the orofacial region: a report of three cases. *Chin J Dent Res*. 2012;15(1):55–9.
3. BORUMANDI F, CASCARINI L, MALLAWARACHCHI R, SANDISON A. The chameleon in the neck: Nodular fasciitis mimicking malignant neck mass of unknown primary. *Int J Surg Case Rep*. 2012;3(10):501-3. <https://doi.org/10.1016/j.ijscr.2012.05.018>
4. DUNCAN SF, ATHANASIAN EA, ANTONESCU CR, ROBERTS CC. Resolution of Nodular Fasciitis in the Upper Arm. *Radiol Case Rep*. 2006;1(1):17–20.
5. SAAD RS, TAKEI H, LIPSCOMB J, RUIZ B. Nodular fasciitis of parotid region: a pitfall in the diagnosis of pleomorphic adenomas on fine-needle aspiration cytology. *Diagn Cytopathol*. 2005;33(3):191-4.
6. HWANG CS, LEE CH, KIM A, SHIN N, PARK WY, PARK MG, ET AL. Nodular fasciitis of the parotid gland, masquerading as pleomorphic adenoma. *Korean J Pathol*. 2014;48(5):366–70. 10.4132/KoreanJPathol.2014.48.5.366
7. GIBSON TC, BISHOP JA, THOMPSON LD. Parotid Gland Nodular Fasciitis: A Clinicopathologic Series of 12 Cases with a Review of 18 Cases from the Literature. *Head Neck Pathol*. 2015;9(3):334-44. 10.1007/s12105-014-0594-9
8. JANG EJ, PARK TI, NAM SC, PARK JY. Nodular fasciitis in the submandibular gland. *Diagn Cytopathol*. 2008;36(11):805–8. DOI: 10.1002/dc.20914
9. ZHANG S, BAO R, BAGBY J, ABREO F. Fine needle aspiration of salivary glands: 5-year experience from a single academic center. *Acta Cytol*. 2009;53(4):375-82. <https://doi.org/10.1159/000325336>
10. RAJWANSHI A, GUPTA K, GUPTA N, SHUKLA R, SRINIVASAN R, NIJHAWAN R, ET AL. Fine-needle

- aspiration cytology of salivary glands: diagnostic pitfalls-revisited. *Diagn Cytopathol.* 2006;34(8):580-4.
11. COYLE J, WHITE LM, DICKSON B, FERGUSON P, WUNDER J, NARAGHI A. MRI characteristics of nodular fasciitis of the musculoskeletal system. *Skeletal Radiol.* 2013;42(7):975-82. DOI: 10.1007/s00256-013-1620-9
 12. EL KADY RM, CHOUDHARY AK, TAPPOUNI R. Accuracy of apparent diffusion coefficient value measurement on PACS workstation: A comparative analysis. *AJR Am J Roentgenol.* 2011;196(3):W280-4. DOI: 10.2214/AJR.10.4706
 13. TARTAGLIONE T, BOTTO A, SCIANDRA M, GAUDINO S, DANIELI L, PARRILLA C, ET AL. Differential diagnosis of parotid gland tumours: which magnetic resonance findings should be taken in account? *Acta Otorhinolaryngol Ital.* 2015;35(5):314-20. doi: 10.14639/0392-100X-693
 14. HABERMANN CR, ARNDT C, GRAESSNER J, DIESTEL L, PETERSEN KU, REITMEIER F, ET AL. Diffusion-weighted echo-planar MR imaging of primary parotid gland tumors: is a prediction of different histologic subtypes possible? *AJNR Am J Neuroradiol.* 2009;30(3):591-6. DOI: 10.3174/ajnr.A1412
 15. EIDA S, SUMI M, SAKIHAMA N, TAKAHASHI H, NAKAMURA T. Apparent diffusion coefficient mapping of salivary gland tumors: prediction of the benignancy and malignancy. *AJNR Am J Neuroradiol.* 2007;28(1):116-21.
 16. YERLI H, AYDIN E, HABERAL N, HARMAN A, KASKATI T, ALIBEK S. Diagnosing common parotid tumours with magnetic resonance imaging including diffusion-weighted imaging vs fine-needle aspiration cytology: a comparative study. *Dentomaxillofac Radiol.* 2010;39(6):349-55. 10.1259/dmfr/15047967

<http://dx.doi.org/10.35630/2199-885X/2022/12/2.21>

ESTIMATION OF THE POSSIBILITY FOR LEFT VENTRICULAR REMODELLING AFTER RESTORATION OF THE SINUS RHYTHM IN PATIENTS WITH PERSISTENT FORM OF ATRIAL FIBRILLATION

Received 25 January 2022;
Received in revised form 17 February 2022;
Accepted 21 February 2022

Stanislav Romanenko¹ , Yuriy Kostyamin¹ ,
Gleb Malgin¹, Elena Kurochka¹,
Vyacheslav Mykhaylichenko² 

¹ M. Gorky Donetsk National Medical University, Donetsk, Ukraine

² S.I. Georgievsky Medical Academy, Simferopol, Ukraine

✉ stas.romanenko1999@gmail.com

ABSTRACT — Atrial fibrillation is one of the most urgent rhythm disturbances leading to permanent disability of the population. Therefore, the aim of this study was to investigate the possibility of left ventricular remodelling after restoration of sinus rhythm. The results of treatment in 821 patients were analyzed, each of them was assigned to one of 4 groups depending on the tactics of surgical intervention: group 1 — electrical cardioversion was performed, group 2 — pacemaker implantation (DDD) and pharmacological cardioversion; 3rd group — electrical cardioversion and pacemaker implantation; and the 4th group — RFA was performed. After the treatment, a decrease in EDV was revealed by 18.7% in the 1st group, 13.7% in the 2nd group, 19.65% in the 3rd group and 11.3% in the 4th group. An increase in the SD was observed: by 14% in the 1st group, 5.6% in the 2nd group, 10.9% in the 3rd group and by 3.65% in the 4th group, as well as an increase in EF by 48% in the 1st group, 17.5% in group 2, 29.76% in group 3 and 4.5% in group 4. Thus, left ventricular remodelling is feasible after restoration of sinus rhythm after persistent atrial fibrillation.

KEYWORDS — atrial fibrillation (AF), LV remodelling, restoration of sinus rhythm, antiarrhythmic drugs.

INTRODUCTION

Atrial fibrillation (AF) is one of the most common rhythm disorders with a number of complications including stroke, left ventricular dysfunction, heart failure, impaired cognitive function and vascular dementia, which also significantly increases admission rates and affects quality of life [1, 2, 3]. An important issue in the treatment of long-term progressive AF is the maintenance of the restored rhythm. A factor contributing to the subsequent recurrence of AF is an increase in the size of the left chambers of the heart as a result of development of atrial dilatation and mitral re-

gurgitation (MR). It was established that 1/3 of patients with AF have valvular pathology that is detected only by echocardiography. Concomitant valvular pathology causes deterioration of the AF, leads to volume and pressure overload with the development of tachycardiomyopathy. The wave-like contraction of the atria leads to their dilation, and subsequent dilation of the LV cavity and mitral annulus with the development of MR. This dilation of the heart chambers also reduces the likelihood of subsequent restoration of sinus rhythm and leads to a sharp deterioration in the patient's general condition [4, 5, 6].

Purpose:

To analyse the outcomes and assess the possibility of left ventricular remodelling after restoration of sinus rhythm after treatment with antiarrhythmic drugs in combination with various invasive treatment methods.

MATERIAL AND METHODS

A retrospective analysis of the outcomes in 821 patients with AF at the DCTMC and Gusak IERS over the period since 2014 to 2020. Mean patient age was 69 ± 0.54 years (range: 31 to 93). Men — 528 (64.3%), women — 168 (35.7%). In all patients, AF duration exceeded 4 months, and drug therapy was ineffective for sinus rhythm maintenance. In 312 (38%) patients, persistent bradycardia (up to the episodes of light-headedness) occurred after attempts to maintain sinus rhythm. The patients were divided into several groups depending on the applied treatment methods: 1st — 418 (50%) patients who underwent electrical cardioversion; 2nd — 287 (35%) patients who underwent pacemaker implantation (DDD) and chemical cardioversion; 3rd — 62 (7.5%) patients who underwent electrical cardioversion and subsequent pacemaker implantation; 4th — 54 (6.5%) patients who underwent radiofrequency ablation: pulmonary veins isolation using Carto3 and/or Biotok system. Subsequently antiarrhythmic therapy was prescribed to all patients in the form of amiodarone tablets at a maintenance dose of 200 mg/day. Baseline data of the patients are presented in Table 1.

Table 1. Patients' baseline data.

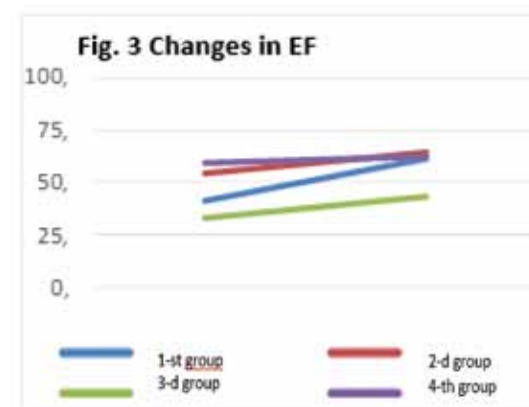
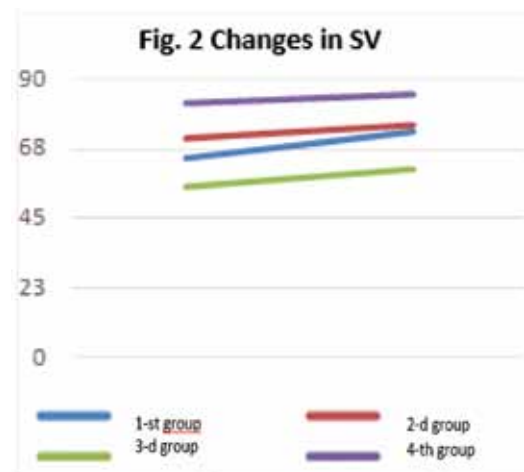
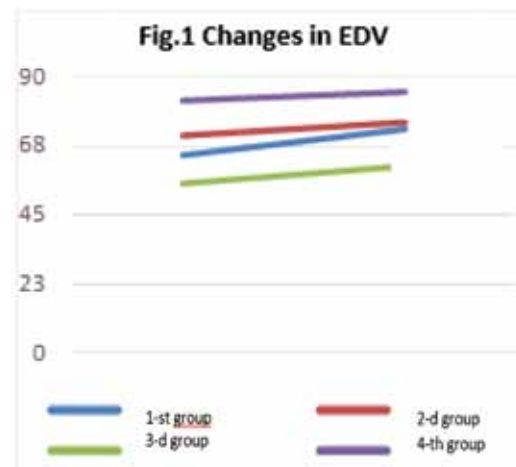
Parameter	Group 1	Group 2	Group 3	Group 4
EDV, ml	150±14	138±18	173±21	141±12
SV, ml	64±9	71±12	55±17	82±7
EF, %	41.3±4.8	54.8±3.2	33.6±2.1	59.4±1.8
Left atrium dimensions, cm	4.3*4.1*4.4	4.3*4.1*4.4	5.2*4.9*6.4	4.2*4.1*4.0
Right atrium dimensions, cm	4.2*4.1*4.9	4.2*4.1*4.9	6.2*4.9*5.8	4.1*3.9*3.9
Vena contracta, mm	4.3	3.7	5.1	2.4

RESULTS

In all patients, sinus rhythm was restored (in the 2nd and 3rd groups, the pacemaker DDD rhythm was maintained). Within 12 months AF recurrence occurred in 197 (24%) patients. There were 149 patients from the 1st group (18.15%), 25 (3.05%) from the second group, 4 (0.49%) from the 3rd group and 19 (2.31%) from the 4th group. These patients underwent repeated electrical cardioversion, the sinus rhythm was restored. Intensive antiarrhythmic treatment was prescribed with Amiodarone (solution for injections) 600 mg, IV drip, followed by a transition to a tablet form at a reduced dose of 200 mg/day. Echocardiographic data after 12 months are presented in Table 2. In the 1st, 2nd, 3rd and 4th groups, statistically significant differences ($p < 0.05$) in the echocardiographic indicators of the dimensions of the heart chambers were noted. In particular, in the 1st group, EDV reduced by 18.7%, SV increased by 14%, EF increased by 48%, vena contracta reduced by 40.5%. In groups 2, 3 and 4 the corresponding changes were 13.7%, 5.6%, 17.5%, 40.5%; 19.65%, 10.9%, 29.76%, 31.4%, and 11.3%, 3.65%, 4.5%, 25%, respectively. 4 patients died within 12 months: one due to the acute myocardial infarction, 2 due to oncological diseases, 1 due to the ischemic stroke (Table 2).

Table 2. Follow-up data after 12 months

Parameter	Group 1	Group 2	Group 3	Group 4
EDV, ml	122±9	119±7	139±11	125±10
SV, ml	73±4	75±11	61±57	85±9
EF, %	61.2±2.7	64.4±1.9	43.6±2.4	62.1±2.4
Left atrium dimensions, cm	4.1*4.4*5.3	3.9*3.8*4.1	4.2*4.1*4.4	4.0*4.0*3.9
Right atrium dimensions, cm	4.2*3.8*4.0	3.8*4.0*4.2	4.2*4.0*4.1	4.1*4.0*3.9
Vena contracta, mm	1.4	2.2	3.5	1.8



CONCLUSION

Analysis of the outcomes of combined treatment of AF using drug therapy and surgical methods showed that after sinus rhythm restoration, the best

results were observed in groups 2 and 3, however, in the short term, even in group 1. There were beneficial changes in echocardiography data, provided that the patients complied with all treatment recommendations. Thus, after more than 12-months follow-up in these groups of patients, left ventricular remodelling develops, which is manifested by a significant reduction in the mitral regurgitation grade, a reduction in EDV and an increase in EF.

of the working groups on cardiac pacing, arrhythmias, and cardiac cellular electrophysiology of the European Society of Cardiology, 21(6), 871–878. <https://doi.org/10.1093/europace/euz013>

REFERENCES

1. CAMM, A. J., SIMANTIRAKIS, E., GOETTE, A., LIP, G. Y., VARDAS, P., CALVERT, M., CHLOUVERAKIS, G., DIENER, H. C., & KIRCHHOF, P. (2017). Atrial high-rate episodes and stroke prevention. *Europace : European pacing, arrhythmias, and cardiac electrophysiology : journal of the working groups on cardiac pacing, arrhythmias, and cardiac cellular electrophysiology of the European Society of Cardiology*, 19(2), 169–179. <https://doi.org/10.1093/europace/euw279>
2. CHARITOS, E. I., STIERLE, U., ZIEGLER, P. D., BALDEWIG, M., ROBINSON, D. R., SIEVERS, H. H., & HANKE, T. (2012). A comprehensive evaluation of rhythm monitoring strategies for the detection of atrial fibrillation recurrence: insights from 647 continuously monitored patients and implications for monitoring after therapeutic interventions. *Circulation*, 126(7), 806–814. DOI: 10.1161/CIRCULATIONAHA.112.098079
3. STEINBERG, J. S., O'CONNELL, H., LI, S., & ZIEGLER, P. D. (2018). Thirty-Second Gold Standard Definition of Atrial Fibrillation and Its Relationship With Subsequent Arrhythmia Patterns: Analysis of a Large Prospective Device Database. *Circulation. Arrhythmia and electrophysiology*, 11(7), e006274. DOI: 10.1161/CIRCEP.118.006274
4. MIYAZAKI, S., KUWAHARA, T., KOBORI, A., TAKAHASHI, Y., TAKEI, A., SATO, A., ISOBE, M., & TAKAHASHI, A. (2011). Preprocedural predictors of atrial fibrillation recurrence following pulmonary vein antrum isolation in patients with paroxysmal atrial fibrillation: long-term follow-up results. *Journal of cardiovascular electrophysiology*, 22(6), 621–625. <https://doi.org/10.1111/j.1540-8167.2010.01984.x>
5. DEN UIJL, D. W., DELGADO, V., BERTINI, M., TOPS, L. F., TRINES, S. A., VAN DE VEIRE, N. R., ZEPPENFELD, K., SCHALIJ, M. J., & BAX, J. J. (2011). Impact of left atrial fibrosis and left atrial size on the outcome of catheter ablation for atrial fibrillation. *Heart (British Cardiac Society)*, 97(22), 1847–1851. DOI: 10.1136/hrt.2010.215335
6. MÜLLER-EDENBORN, B., MINNERS, J., ALLGEIER, J., BURKHARDT, T., LEHRMANN, H., RUILE, P., MERZ, S., ALLGEIER, M., NEUMANN, F. J., ARENTZ, T., JADIDI, A., & JANDER, N. (2019). Rapid improvement in left ventricular function after sinus rhythm restoration in patients with idiopathic cardiomyopathy and atrial fibrillation. *Europace : European pacing, arrhythmias, and cardiac electrophysiology : journal*

<http://dx.doi.org/10.35630/2199-885X/2022/12/2.22>

RARE INTRAOPERATIVE FIND — ADENOCARCINOMA OF THE APPENDIX: CLINICAL CASE

Received 13 February 2022;
Received in revised form 17 March 2022;
Accepted 21 March 2022

Lina Ancupova , Artem Morozov ,
Elshad Askerov, Alexey Sergeev ,
Maria Belyak , Lydia Pototskaya 

Tver State Medical University, Tver, Russia

 ammorozovv@gmail.com

RELEVANCE

Despite the fact that all over the world there is a significant increase in the indicators of the level and quality of population's life, and also an improving access to modern medical support, the problem of timely diagnosis of oncological diseases still remains. Malignant neoplasms constitute one of the nosological groups. They account for a significant part in the structure of morbidity, disability and mortality. Neoplasms of the large bowel are one of the most common diseases among all malignant neoplasms of the gastrointestinal tract. The predominant localization is the rectosigmoid junction. The rarest disease is a neoplasm of the appendix. It is found in 0.4% of all types of malignant neoplasms of the gastrointestinal tract [1].

The annual incidence of appendix cancer is 0.12 cases per 1 million people, according to the United States National Cancer Institute, Surveillance, Epidemiology and End Results (SEER) program. It should be noted that appendicular epithelial tumors are diagnosed in 0.9-1.4% during appendectomy with a histological assessment of a surgical tissue sample. The development of the appendix neoplasm in most cases proceeds without pronounced clinical symptoms or has a clinic of acute appendicitis due to blockage of the appendix lumen [2].

The appendix is most commonly the site of neuroendocrine tumors, called carcinoids. A carcinoid tumor can cause carcinoid syndrome. There are other histological types of tumors associated with the appendix. They are mainly tumors with epithelial structure. Some of them can cause pseudomyxoma of the peritoneum. The classification of these tumors in the literature is rather heterogeneous and based on many factors. The treatment options differ depending on the histological type and stage of the disease (from simple

ABSTRACT — **RELEVANCE:** Neoplasms of the large bowel are one of the most common diseases among all malignant neoplasms of the gastrointestinal tract. The predominant localization is the rectosigmoid junction. The rarest disease is a neoplasm of the appendix.

PURPOSE: Diagnosis of the neoplasm of the appendix with extension into cecum cupula and into the anterior abdominal wall and description of the results on the example of a clinical case.

MATERIALS: We present a case of patient I., male, 34 years old. He is a hypersthenic overweight person, essential hypertension stage I, rate III, risk 3.

RESULTS: Patient I. was first admitted in a private clinic (Tver, Russia) in September 2020 after the 1 day of onset. A clinical presentation complies with appendicitis. He was sent to the emergency surgery department after the examination by the surgeon. There he underwent a diagnostic laparoscopy, conversion, laparotomy with preservation of the appendix, and draining of the abdominal cavity. The second visit to a private clinic was in May 2021. The CT scan of the abdominal organs was performed and an infiltrate was detected in the cecum cupula with a small area of suppurative complication. Then the patient was hospitalized in the surgery department, where he was prescribed antibiotic therapy for periappendiceal mass and recommended a planned appendectomy. In September 2021, the patient turned to the surgery department at the place of residence due to the deterioration. He underwent a laparotomy in the right iliac region, viscerolysis, median laparotomy, right-sided hemicolectomy for adenocarcinoma of the appendix, ileotransverse anastomosis by the side-to-side method, drainage of the abdominal cavity.

CONCLUSION: Acute appendicitis remains a challenge for practicing surgeons despite being common and well-studied. Acute appendicitis is characterized by pronounced clinical symptoms. But it also has many hidden forms that mimicked other diseases. That's why the establishment of this diagnosis is difficult even for experienced clinicians. This clinical case demonstrates certain difficulties in the timely diagnosis of the appendix neoplasm. This is because the development of most appendix tumors is asymptomatic or resembles the clinic of acute appendicitis. The tumors are detected by chance, or during visualization, or during appendectomy. Only early diagnosis of the disease, knowledge of the treatment strategy and timely initiation of appropriate therapy can improve the prognosis of patients, reduce the risk of disability and death. It is undoubtedly important in clinical practice.

KEYWORDS — appendicitis, neoplasm, appendix, adenocarcinoma.

appendectomy with celioscopy to full cytoreduction with intraperitoneal hyperthermic chemotherapy and/or systemic chemotherapy). It requires a specialized

examination and consultation of a surgeon specializing in the treatment of rare tumors of the peritoneal cavity for the right treatment strategy suitable for each patient. It is necessary to know that in the case of the development of an oncological neoplasm, the decision on treatment is discussed at an interdisciplinary consultation meeting. It ensures the most optimal and adequate treatment with the help of the recommendations of several experts. The early detection is critical. Delayed diagnosis can result in worse outcomes, including death [3, 4].

Purpose of the study:

to diagnose a neoplasm of the appendix with extension into cecum cupula and into the anterior abdominal wall and describe the outcomes on the example of a clinical case.

MATERIALS AND METHODS

We present a case of a 34 years old patient I., male, with the hypersthenic body type and overweight, essential hypertension stage I, rate III, risk 3.

RESULTS AND DISCUSSIONS

Patient I. was first admitted a private clinic (the city of Tver, Russia) in September 2020 after the 1st day of onset. A clinical presentation complies with appendicitis. The main complaints were pain in the right side of the abdomen and a temperature increase up to 37.5° C. The patient was sent to the emergency surgery department after the examination by the surgeon. According to the results of the abdominal ultrasound, an infiltrative mass was revealed in the right iliac region. Based on the data of the anamnesis, examination and physical examinations surgery was indicated. It was carried out with the consent of the patient. The operation was carried out with endotracheal anesthesia. After surgical d-bridement, a laparoscope was inserted through the incision. The caecum cupula was determined above the entrance to the small pelvis. Additionally, 5 mm and 12 mm trocars were placed in the right hypochondrium and suprapubic region. A periappendicular mass was determined in the right iliac region. It included the caecum cupula, a loop of the small intestine, a section of the parietal peritoneum, and a scanty serous exudate with fibrin. It was not possible to separate the mass. A responsible surgeon on duty was invited for a consultation during the operation. It was decided to perform the conversion. After surgical d-bridement, the abdominal cavity was opened on the right by the Volkovich-Dyakonov access. A dense infiltrate was determined, consisting of the caecum cupula, parietal peritoneum, and a section of the ileum. Probably, the appendix went retroperitoneally through the lateral canal into the small pelvis.

During the separation of the infiltrate in a blunt way, about 5 ml of purulent discharge was released. The caecum cupula was brought into the wound. After this the appendix cut out on the base. The caecum caecum was infiltrated. The base of the appendix was obturated with a fecal stone. There was no discharge from the intestine. The appendix remained in the mass. The organ left retroperitoneally into the small pelvis. The surgeon on duty was re-invited to the consultation. It was decided to drain the abdominal cavity with glove drains. The small pelvis was drained with tumpers, glove drains were installed. This was followed by layer-by-layer suturing of the wound and the application of an aseptic dressing. In this connection combined antibiotic therapy was prescribed. After the end of the therapy, the patient was discharged in a satisfactory condition under supervision of a local surgeon.

The second visit to the private clinic was in May 2021. The patient had complaints of minor pain in the right iliac region and subfebrile temperature for 3 days. We made the CT scan of the abdominal organs and detected an infiltrate in the caecum cupula with a small area of suppurative complication. Then the patient was hospitalized in the surgery department, where he was prescribed antibiotic therapy for periappendiceal mass. based on physical examination and laboratory tests there were no indications for emergency surgery. The patient was discharged after the end of antibiotic therapy in a satisfactory condition under supervision of a local surgeon with a recommendation for a planned appendectomy.

In September 2021, the patient began to notice aching pains in the right iliac region, an increase in the volume of the abdomen after eating, predominant on the right side and an increase in body temperature up to 38° C. This condition lasted for 2 weeks. The patient turned to the emergency department of the hospital at the place of residence in connection with the deterioration of his condition. He was hospitalized in the surgical department after examining by the surgeons. Status localis: the tongue is dry, covered with a whitish coating. The abdomen is not swollen, symmetrical, and participates in the act of breathing. In the right iliac region there is a hypertrophic scar up to 5 cm. During palpation, the abdomen is soft, painful, tense in the right iliac region, where a dense infiltrate up to 7–8 cm in size is palpated. Blumberg's sign is doubtful. According to the ultrasound results, an infiltrate of 52×42 mm is visualized in the right iliac region, the appendix is thickened to 34 mm. Laboratory data: general urine analysis: color — yellow, transparent, acid reaction, specific gravity — 1010 g/l, protein — 0.1 g/l, sugar — absent, according to microscopy: squamous epithelium 1–3, leukocytes 4–6–8; erythrocytes 1–2; mucus

11. Blood test: Hb — 130 g/l; leukocytes — $8.9 \cdot 10^9$ /l; erythrocytes $4.4 \cdot 10^{12}$ /l; platelets - $156 \cdot 10^9$ /l; Ht — 41.4%. A diagnosis of acute appendicitis, periappendiceal mass with abscess was established on the basis of clinical and anamnestic data and US-results. Surgery was offered. It was carried out with the consent of the patient. The operation was with general anesthesia. A laparotomy was performed in the right iliac region with excision of the old scar, a dense infiltrate was detected. The part of the adhesions was divided, the caecum cupula with a dense, thickened appendix was isolated. When the appendix was isolated, its lumen was visible, filled with cartilaginous tissue of a dull gray color. Further revision revealed a dense tumor infiltrate consisting of the appendix and the caecum cupula with invasion into the anterior abdominal wall. It was performed the right-sided hemicolectomy with the imposition of anastomosis by the side-to-side method with a single-row polypropylene suture. There was a control for hemostasis, it was dry. Drainage was installed into the small pelvis through a separate puncture. The sutures were placed on the aponeurosis and skin. The wound area was treated with an antiseptic preparation. An aseptic dressing was applied. Macroscopic data: the right half of the colon had a tumor; there were fragments of the appendix tumor. The main final clinical diagnosis was formulated: Neoplasm of the appendix with germination in the caecum cupula and in the anterior abdominal wall. The patient was transferred to the intensive care unit due to the severity of the surgical intervention. All appointments were also agreed. After stabilization of the patient's condition, the patient was transferred to the surgical ward in a state of moderate severity. The macro- and microscopic examination of the biopsy material enabled to identify an adenocarcinoma of the appendix,

patients and reduce the risk of disability and death. It is undoubtedly important in clinical practice.

REFERENCES

1. **STEIN S, RAYMOND D O B.** Appendiceal Adenocarcinoma Presenting As Perforated Appendicitis. *Cureus*. 2021 Feb 26;13(2):e13578. doi: 10.7759/cureus.13578
2. **HATCH QM, GILBERT EW.** Appendiceal Neoplasms. *Clin Colon Rectal Surg*. 2018 Sep;31(5):278–287. doi: 10.1055/s-0038-1642051, Epub 2018 Sep 4
3. **VAN DE MOORTELE M, DE HERTOOGH G, SAGAERT X, VAN CUTSEM E.** Appendiceal cancer: a review of the literature. *Acta Gastroenterol Belg*. 2020 Jul-Sep;83(3):441–448. PMID: 33094592
4. **VALASEK MA, PAI RK.** An Update on the Diagnosis, Grading, and Staging of Appendiceal Mucinous Neoplasms. *Adv Anat Pathol*. 2018 Jan;25(1):38–60. doi: 10.1097/PAP.0000000000000178




CONCLUSION

Acute appendicitis remains a challenge for practicing surgeons despite being a common and well-studied disease. Acute appendicitis is characterized by pronounced clinical symptoms. But it also has many hidden forms that mimicked other diseases. That is why the establishment of this diagnosis is difficult even for experienced clinicians. Our clinical case demonstrates certain difficulties in the timely diagnosis of the appendix neoplasm. This is attributed to the fact that development of most appendix tumors is asymptomatic or resembles the clinic of acute appendicitis. The tumors are detected by chance, or during visualization, or during appendectomy. Although appendicular tumors are rare, only their early diagnosis, knowledge of the treatment strategy and timely initiation of appropriate therapy can improve prognosis of the

<http://dx.doi.org/10.35630/2199-885X/2022/12/2.23>

INTESTINAL ALKALINE PHOSPHATASE — A BIOMARKER OF THE DEGREE OF ACUTE ENTERAL INSUFFICIENCY IN URGENT SURGERY

Received 21 February 2022;
Received in revised form 21 March 2022;
Accepted 23 March 2022

Mikhail Topchiev¹ , Dmitry Parshin^{1✉} ,
Misrikhan Misrikhanov¹, Stanislav Pyatakov²,
Lev Brusnev³ , Marat Chotchaev³ 

¹ Astrakhan State Medical University, Astrakhan;

² City Hospital No. 4, Sochi;

³ Stavropol State Medical University, Stavropol, Russia

✉ parshin.doc@gmail.com

ABSTRACT — The diagnostic significance for levels of alkaline phosphatase (ALP) and intestinal alkaline phosphatase (IAP) and their ratio in blood serum and intestinal contents were compared to assess the degree of acute enteral insufficiency in urgent surgical pathology complicated by peritonitis. The results of examination of 112 patients with acute surgical pathology complicated by peritonitis were retrospectively analyzed. Biochemical data were compared with clinical and instrumental data obtained by ultrasonography and Doppler flowmetry. The main statistical indicator was Spearman's rank correlation coefficient, which showed a moderate direct correlation in patients with stage I and II enteral insufficiency ($r=0.63$ at $p \leq 0.05$), and in the group with st. III it showed a direct correlation with a high closeness of association ($r=0.71$ at $p \leq 0.05$). The IAP/ALP ratio makes it possible to objectively assess the severity of acute intestinal failure in urgent surgery.

KEYWORDS — peritonitis, acute intestinal failure, biomarkers, intestinal alkaline phosphatase, intestinal homeostasis.

RELEVANCE

Acute enteral insufficiency (AEI) is the most common clinical syndrome in acute surgical pathology and peritonitis. The frequency of AEI according to different authors ranges from 30 to 94%. The severity of AEI is diagnosed intraoperatively, as well as using rather expensive devices that assess the degree of morpho-functional dysfunction of the small intestine [1, 2]. Currently, there are no rapid biochemical tests to assess the degree of AEI in the preoperative and postoperative periods.

Alkaline phosphatases (ALPs) are a group of isoenzymes located on the outer layer of the cell membrane; they catalyze the hydrolysis of organic

phosphate esters present in the extracellular space. Intestinal alkaline phosphatase (IAP) is a multifunctional protein that has been shown to primarily protect the intestinal mucosa [3, 4, 5, 6]. The role of IAP in maintaining intestinal homeostasis is highlighted by the observation that IAP expression is impaired in many gastrointestinal disorders such as inflammatory bowel disease, necrotizing enterocolitis, and metabolic syndrome. Besides, exogenous IAP supplementation improves outcomes associated with these disorders [7, 8, 9, 10]. A recently identified new function of IAP is the induction of autophagy [11, 12]. Due to its critical role in gastrointestinal physiology and excellent safety profile, IAP has been used in clinical trials to treat many critical conditions, including those associated with sepsis [13, 14, 15].

The aim of the work

was to compare the diagnostic significance of the levels of alkaline ALP and IAP and their ratio in blood serum and intestinal contents for estimation of the degree of AEI in urgent surgical pathology complicated by peritonitis.

MATERIAL AND METHODS

A retrospective analysis of the results of examination of 112 patients with acute surgical pathology of the abdominal organs complicated by peritonitis and varying degrees of AEI was carried out. 26 patients were diagnosed with stage I AEI, 38 had stage II, and 48 — stage III decompensated AEI. The total ALP (U/l), its isoform IAP (U/l), as well as their IAP/ALP ratio (%) in blood serum and intestinal contents were determined using the enzyme immunoassay method and the Cobas e411 apparatus (Switzerland). Studies were carried out before surgery, on days 1–3 and 5–7. In order to summarize and compare the data we collected, the stage of AEI was subsequently assessed visually and intraoperatively, by calculating the enteral morpho-functional coefficient (EMFC), as well as data obtained using enteral laser Doppler flowmetry (ELDF).

EMFC was assessed after ultrasonography by the formula: $EMFC = Tst(k) \times D(k) / FPD$ in 1 minute,

where: Tst(k) — thickness of the intestinal wall (mm); D(k) - intestine diameter (mm); FPV — the frequency of peristaltic movement of the intestine in 1 minute. With a value of up to 5 points, it was defined as the stage I of compensation. From 5 to 25 points, stage II of subcompensation was detected, and with an EMFC value above 25 points, stage III of decompensation was diagnosed.

ELDF was performed with the analyzer of microcirculation and microlymph flow "Lasma MTs-1" (Russia). Investigated: percentage of microcirculation (PM; p.u.); standard deviation (SD; σ , p.u.), as well as the coefficient of variation (CV; %). The obtained results were compared with the reference values of abdominal microcirculation obtained in patients during elective operations for non-inflammatory diseases of the abdominal organs.

In order to identify and evaluate the tightness of the relationship between quantitative indicators, the Spearman rank correlation coefficient was calculated, which allowed to check the heteroscedasticity of random errors in the regression model. To determine the significance of p differences between groups, Student's t test and one-way analysis of variance with Fisher's F test were used. Differences were considered statistically significant at $p \leq 0.05$.

RESULTS AND DISCUSSION

At stage I AEI, the level of ALP in the blood serum was 213 ± 29.2 U/l, in the intestinal chyme - 38 ± 9.2 U/l; IAP was 1.18 ± 0.74 U/l and 1.24 ± 0.19 U/l, IAP/ALP ratio was $0.55 \pm 0.27\%$ and $3.26 \pm 0.27\%$, respectively. At stage II, ALP in serum was 295 ± 28.4 U/l, in chyme — 95 ± 13.4 U/l, IAP values were 1.87 ± 0.46 U/l and 3.86 ± 0.93 U/l, and the IAP/ALP ratio was $0.63 \pm 0.29\%$ and $4.06 \pm 0.29\%$, respectively. At stage III, the total serum ALP was 341 ± 33.3 U/l, in the intestinal contents — 141 ± 17.3 U/l, the IAP values were 2.29 ± 0.53 U/l and 4.31 ± 1.49 U/l, IAP/ALP were $0.67 \pm 0.15\%$ and $6.05 \pm 0.15\%$, respectively.

Thus, as AEI progressed, there was an increase in the levels of ALP and IAP in the blood serum and intestinal chyme. These data correlated with those obtained with EMFC and ELDF. With stage I AEI, the average score for EMFC calculation was 4.7 ± 0.3 , with stage II — 16.6 ± 1.2 , and with stage III — 27.4 ± 2.2 points. ELDF indices indicated a progressive increase in pre- and post-capillary resistance, arteriolo-venular shunting, which ultimately led to severe perfusion disorders of the intestinal wall (Table 1).

With the ratio of the obtained clinical-instrumental and biochemical data, it turned out that the most informative biochemical indicator was the IAP/ALP ratio. Spearman's rank correlation coefficient for

this indicator showed a moderate direct correlation in patients with stage I and II. AEI ($r=0.63$ at $p \leq 0.05$). In the group with stage III AEI score IAP/ALP showed a direct correlation with a high closeness of association ($r=0.71$ at $p \leq 0.05$).

CONCLUSIONS

The biochemical indicator IAP/ALP allows an objective assessment of the stage of AEI in patients with acute diseases of the abdominal organs complicated by peritonitis. This hypothesis was confirmed by clinical and instrumental data obtained with EMFC and ELDF. Biochemical monitoring of the IAP/ALP ratio allows diagnosing the stage of AEI both in the preoperative and postoperative periods, assessing the effectiveness of therapy and making timely corrections to the treatment.

REFERENCES

1. PARSHIN D. S., TOPCHIEV M. S., BRUSNEV L., EMKUZHEV K. Proinflammatory and antiapoptotic markers of the stages of acute enteral insufficiency. *Archiv EuroMedica*. 2020;10(4):90–93. doi: 10.35630/2199-885X/2020/10/4.22
2. TOPCHIEV M. A., PARSHIN D. S., BRUSNEV L. A., CHOTCHAEV M. K. Possibilities of drug experimental simulation of dynamic intestinal obstruction. *Medical News of North Caucasus*. 2020;15(3):373–376. 10.14300/mnnc.2021.16022
3. RADER B. A. Alkaline Phosphatase, an Unconventional Immune Protein. *Front. Immunol*. 2017;8:897. DOI: 10.3389/fimmu.2017.00897
4. SINGH S.B., LIN H.C. Role of Intestinal Alkaline Phosphatase in Innate Immunity. *Biomolecules*. 2021;11(12):1784. <https://doi.org/10.3390/biom11121784>
5. WHITEHOUSE J.S., RIGGLE K.M., PURPI D.P., MAYER A.N., PRITCHARD K.A., JR., OLDHAM K.T., GOURLAY D.M. The protective role of intestinal alkaline phosphatase in necrotizing enterocolitis. *J. Surg. Res*. 2010;163:79–85. DOI: 10.1016/j.jss.2010.04.048
6. WANG W., CHEN S.W., ZHU J., ZUO S., MA Y.Y. Intestinal Alkaline Phosphatase Inhibits the Translocation of Bacteria of Gut-Origin in Mice with Peritonitis: Mechanism of Action Intestinal Alkaline Phosphatase Inhibits the Translocation of Bacteria of Gut-Origin in Mice with Peritonitis: Mechanism of Action. *PLOS ONE*. 2015;10(5): e0124835. doi:10.1371/journal.pone.0124835. <https://doi.org/10.1371/journal.pone.0124835>
7. PLAEKE P., DE MAN J.G., SMET A., MALHOTRA-KUMAR S., PINTELON I., TIMMERMANS J.P., NULLENS S., JORENS P.G., HUBENS G., DE WINTER B.Y. Effects of intestinal alkaline phosphatase on intestinal barrier function in a cecal ligation and puncture (CLP)-induced mouse model for sepsis.

Table 1. Biochemical and clinical-instrumental parameters in patients with peritonitis depending on the degree of acute intestinal failure ($M \pm m$; abs)

AEI stage (n=112)	Object of study	ALP (ЕД/л)	IAP (ЕД/л)	IAP/ALP (%)	EMFC (points)	ELDF: (PM (p.u.) ; SD(p.u.); CV (%))
I (n=26)	serum	213±29,2	1,18±0,74	0,55±0,27*	4,7±0,3	32,21±1,18
	intestinal chyme	38±9,2	1,24±0,19	3,26±0,27*		5,42±0,33
II (n=38)	serum	295±28,4	1,86±0,46	0,63±0,29*	16,6±1,2	12,64±1,50
	intestinal chyme	95±13,4	3,86±0,90	4,06±0,29*		23,3±1,83
III (n=48)	serum	341±33,3	2,29±0,53	0,67±0,15*	27,4±2,2	3,69±0,15
	intestinal chyme	141±17,3	4,31±1,49	6,05*±0,15*		11,34±4,04
						17,6±1,55
						2,03±0,19
						6,03±3,79

Note: * — indicators at $p \leq 0.05$

- Neurogastroenterol Motil. 2020;32: e13754. <https://doi.org/10.1111/nmo.13754>
8. **FAWLEY J., GOURLAY D. M.** Intestinal alkaline phosphatase: a summary of its role in clinical disease. *Journal of Surgical Research*. 2016;202(1):225–234. doi: 10.1016/j.jss.2015.12.008.
9. **GRONDIN J.A., KWON Y.H., FAR P.M., HAQ S., KHAN W.I.** Mucins in Intestinal Mucosal Defense and Inflammation: Learning From Clinical and Experimental Studies. *Front. Immunol*. 2020;11:2054. doi: 10.3389/fimmu.2020.02054
10. **FANG J., WANG H., ZHOU Y., ZHANG H., ZHOU H., ZHANG X.** Slimy partners: the mucus barrier and gut microbiome in ulcerative colitis. *Exp Mol Med*. 2021;53(5):772–787. doi: 10.1038/s12276-021-00617-8
11. **JEAN-PAUL LALLÈS.** Intestinal alkaline phosphatase: novel functions and protective effects. *Nutrition Reviews*. 2014;72(2):82–94. doi: 10.1111/nure.12082
12. **SINGH S.B., CARROLL-PORTILLO A., COFFMAN C.** Intestinal Alkaline Phosphatase Exerts Anti-Inflammatory Effects Against Lipopolysaccharide by Inducing Autophagy. *Sci Rep*. 2020;10:3107. doi: 10.1038/s41598-020-59474-6
13. **LOWE D., SANVICTORES T., JOHN S.** Alkaline Phosphatase. 2021 Aug 11. In: StatPearls [Internet]. Treasure Island (FL): StatPearls Publishing; 2022 Jan–. PMID: 29083622 Bookshelf ID: NBK459201
14. **SHARMA U., PAL D., PRASAD R.** Alkaline phosphatase: an overview. *Indian J Clin Biochem*. 2014;29(3):269–78. doi: 10.1007/s12291-013-0408-y
15. **BILSKI J., MAZUR-BIALY A., WOJCIC D., ZAHRADNIK-BILSKA J., BRZOWSKI B., MAGIEROWSKI M., MACH T., MAGIEROWSKA K., BRZOWSKI T.** The Role of Intestinal Alkaline Phosphatase in Inflammatory Disorders of Gastrointestinal Tract. *Mediators of Inflammation*. 2017: 9074601. doi: 10.1155/2017/9074601

<http://dx.doi.org/10.35630/2199-885X/2022/12/2.25>

SURGICAL OPTIONS FOR THE TREATMENT OF PATIENTS WITH CENTRAL DIABETES INSIPIDUS

Received 17 December 2021;
Received in revised form 20 February 2022;
Accepted 23 February 2022

Yulia Artemova , Anna Plotnikova ,
Danil Naumov , Daria Asatryan ,
Zinfira Kaitova , Sergey Ryzhakin 

General Medicine, Medical Institute. Peoples' Friendship University of Russia, Moscow, Russia

✉ asterdasha@mail.ru

ABSTRACT — AIM: to study the results of surgical treatment of central diabetes insipidus and panhypopituitarism.

MATERIALS AND METHODS: The medical records of patients operated on at the Clinical Center for Andrology and Endocrine Organ Transplantation were studied. All patients underwent allotransplantation of the pituitary gland or hypothalamic-pituitary complex on vascular connections. The maximum follow-up period of patients was 18 years.

RESULTS: In all patients in the postoperative period, positive dynamics was noted, manifested in a decrease in thirst and diuresis, an improvement in general condition with an increase in the specific gravity of urine.

CONCLUSIONS: As a result of the study, it was once again confirmed that in the absence of the effect of conservative therapy, patients with central diabetes insipidus and panhypopituitarism are recommended for transplantation of pituitary gland or hypothalamic-pituitary complex on vascular connections. In the postoperative period, all patients should be prescribed immunosuppressive therapy and local X-ray irradiation.

KEYWORDS — centric diabetes insipidus, vasopressin, desmopressin, pituitary gland, pituitary gland transplantation, allotransplantation, hypothalamic-pituitary complex, diuresis, transplantation.

INTRODUCTION

Treatment of CDI is recommended with a synthetic vasopressin analog, desmopressin [6, 9, 2]. Sometimes natriuretic drugs (thiazide diuretics, indapamide, and others) may be used to treat central diabetes insipidus [1]. Today, desmopressin is the preferred treatment for central diabetes insipidus in the Russian Federation [7, 4]. However, surgical method has not been sufficiently studied to determine how transplantation affects performance of pituitary gland or hypothalamic-pituitary complex, as well as there are not so many medical records for rehabilitation processes and results of transplantation. It is also important

to determine how this method is going to affect key indices for treating CDI — urine specific gravity and what are pros and cons comparing to treatment with desmopressin.

Materials and methods of research

The medical records of patients who underwent surgery at the Clinical Center for Andrology and Endocrine Organ Transplantation were studied. A total of 14 people, including 7 women and 7 men. The average age was 20–35 years. All patients underwent pituitary or hypothalamic-pituitary complex allografts on vascular connections. The maximum follow-up period is 18 years.

RESULTS AND DISCUSSION

The median age of the patients was 20–35 years. All patients with this disease complained of general weakness, dry skin. During the day, they used to drink 12–25 liters of liquid with the need to urinate up to 25–27 times a day. The specific gravity of urine was 1001–1005. All patients underwent allograft of pituitary or hypothalamic-pituitary complex on vascular connections. The operation of transplantation of the pituitary gland or hypothalamic-pituitary complex on the arteriovenous pedicle (in Russia, this method is named after its developer, I. D. Kirpatovsky) consists of 3 stages: 1) pituitary graft collection from a donor, 2) preparation of the graft and its vascular pedicle for transplantation and 3) transplantation of the pituitary gland [8]. The transplant is taken from young people who have died from causes unrelated to craniocerebral pathology. In addition to the pituitary gland and its funnel, the graft includes cavernous sinuses with dura mater, the intersection of the optic nerves, as well as segments of the right and left internal carotid arteries with the anterior and middle arteries of the brain. In order not to dislocate the numerous vascular anastomoses of the upper and lower pituitary arteries while getting the graft, the pituitary body is taken from a corpse with the bones of a Turkish saddle. During the preparation of the graft for transplantation, bone fragments are removed. The graft is transplanted either to the hip with connection to the deep artery of thigh and the great saphenous vein, or to the anterior abdominal wall in the area of lower epigastric veins. When choosing a transplant placement, on the hip

or anterior abdominal wall, doctors are guided by the recipient's age and his constitutional features. With a normal physique and well-developed vessels, the graft was connected to the lower epigastric vessels. For patients with insufficient development of blood vessels, as well as for children, the graft was connected to the deep femoral artery. A dissection is made on the anteromedial surface of the thigh and the fascial bed of the adductors is opened, when graft is transplanted to a deep femoral artery. For venous outflow in this case, it is favorable to use a great saphenous vein.

In the postoperative period, all patients received immunosuppressive therapy, including prednisone, chorionic gonadotropin, heparin, and local X-Ray radiation exposure. All patients underwent immunological monitoring. Three patients developed a rejection crisis in the postoperative period. Two of them occurred in the first week after surgery and was successfully stopped by amplifying immunosuppressive therapy and additional local X-ray irradiation of the graft area. The graft function was not impaired after X-ray irradiation.

We recorded improvements for all patients in the postoperative period, which resulted in a decrease in thirst and urine output, an improvement in general condition with an increase in the urine specific gravity. With a smooth flow of the postoperative period, after 2-3 weeks, the amount of liquid consumed decreased to 4–6 liters, the urinary frequency decreased to 9–10 times a day.

By the time of discharge and in the long-term period, patients consumed 2–3.5 liters of liquid per day with a frequency of urination 6–7 times a day. The specific gravity of urine in the immediate postoperative period (before discharge from the hospital) increased to 1008-1010, and in a more distant period – to 1010–1020.

During the first year of follow-up, 11 out of 12 patients showed persistent normalization of diuresis (up to 2–4 liters per day with complete cancellation of hormone replacement therapy). Only 1 patient developed an irreversible rejection episode that led to a relapse of diabetes insipidus, which required the reinitiation of hormone therapy at the same dose as before the operation. 8 patients were examined and 7 of them retained normal diuresis in observation period from 1 to 5 years. 6 patients were observed for period from 6 to 10 years. Completely normal diuresis was recorded for 2 patients, while 4 patients took small doses of hormonal drugs to normalize diuresis. The maximum follow-up period after allotransplantation was 18 years (Table 1).

In the long-term observation period from 11 to 18 years after allotransplantation, 3 patients were ex-

amined. It was recorded that 2 of them took hormone preparations in a lower dose than before the operation, whereas 1 patient had to take hormones in full volume [3]. After 8 years of normal functioning of the hypothalamic-pituitary graft after suffering severe influenza virus infection, 1 patient had a relapse of diabetes insipidus without signs of its rejection, apparently due to viral damage to the nuclei in the hypothalamus of the transplanted complex. After additional evaluation, this patient underwent a successful repeated heterotopic transplantation of the hypothalamic-pituitary complex with the complete disappearance of the symptoms of central diabetes insipidus. The repeated graft has been functioning in accordance with standards for more than 2 years [3].

CONCLUSIONS

1. As a result of the study, it was once again confirmed, that in the absence of an effect from conservative therapy in patients with central diabetes insipidus and panhypopituitarism surgery is recommended. Specifically, these are transplantation of the pituitary or hypothalamic-pituitary complex on vascular connections due to its efficiency.

2. After allotransplantation, all patients should be prescribed immunosuppressive therapy, including prednisone, chorionic gonadotropin, heparin, as well as local X-ray radiation.

3. A one-year follow-up after allotransplantation is necessary for normalization of diuresis.

REFERENCES

1. **AL NOFAL A.** THIAZIDE Diuretics in the Management of Young Children with Central Diabetes Insipidus. *The Journal of Pediatrics*. Lteif A, 2015.167(3):658-661. DOI: 10.1016/j.jpeds.2015.06.002
2. **CHANSON P., SALENAY S.** Treatment of neurogenic diabetes insipidus. *Ann, Endocrinol Paris*. 2011, 72(6):496-499. 10.1016/j.ando.2011.09.001
3. **KHARCHENKO M. A., LICHENKO A.G., KAITOVA Z.S.** Female transsexualism - the problem of gender identification. *Zdorov'e i obrazovanie v XXI veke – Health and education in the XXI century*. Moscow, 2016, pp. 70-71.
4. **KIRPATOVSKY I.D., KIRPATOVSKY V. I.** Neuroendocrine transplantation. 2018, p.86.
5. **MAZERKINA N. A.** The drug vasomyrin in the treatment of central diabetes insipidus in children. *Farmateka - Pharmateca*. 2014, pp. 86-90.
6. **PIGAROVA E.A.** Central diabetes insipidus: pathogenetic and prognostic aspects, differential diagnosis. Dissertation for the degree of Candidate of Medical Sciences. Moscow. 2009, p.203.

Table 1. Long-term results of allotransplantation of the hypothalamic-pituitary complex in a patient with diabetes insipidus and panhypopituitarism

Terms of observation	Number of observations	Hormone therapy			Without a rejection crisis	Relief crisis	The crisis is not stopped
		Canceled	Dosage reduced price	The dose is not reduced			
Up to 1 year	12	11	0	1	10	1	1
1–5 years old	8	7	1	0	8	0	0
6–10 years old	6	2	4	0	6	0	0
11–18 years old	3	0	2	1	3	0	0

7. **PIGAROVA E. A., MIKHAILOVA D. S., DZERANOVA L.K., ROZHINSKAYA L. YA. AND OTHERS.** Central diabetes insipidus in the outcome of transsphenoidal treatment of tumors of the hypothalamic-pituitary region. Treatment and prevention. 2014, pp.14-40.
8. **SAIFAN S., NASR R., MEHTA S. ET AL.** Diabetes insipidus: A complex diagnosis using new medical treatment methods. Nephrology ISRN. 2013: 1-7.
9. **VANDE WALLE J., STOCKNER M, RAES A, NORGAARD J.** Desmopressin 30 Years in Clinical Use: A Safety Review. Current Drug Safety. 2007, 2(3):232-238. DOI: 10.2174/157488607781668891

<http://dx.doi.org/10.35630/2199-885X/2022/12/2.26>

THE STRUCTURE OF SYNCHRONOUS MULTIPLE PRIMARY COLORECTAL CANCER

Received 23 January 2022;
Received in revised form 20 February 2022;
Accepted 22 February 2022

Oleg Krashenkov¹ , Igor Ivanikov¹ ,
Oleg Kononov² , Mikhail Ryabov³ ,
Ruslan Absalyamov¹ , Asan Kashurnikov⁴ ,
Nikolai Sturov² , Alexander Tolkachev⁵ ,
Sergej Ryzhakin²

¹ Central clinical hospital and polyclinic, Moscow;

² Peoples' Friendship University of Russia (RUDN University), Moscow;

³ Yaroslavl State Medical University, Yaroslavl;

⁴ Research Institute for Healthcare and Medical Management of Moscow Healthcare Department, Moscow;

⁵ P.A. Hertsen Moscow Oncology Research Center, Moscow, Russia

✉ kononov_oe@mail.ru

ABSTRACT — One of the problems of modern oncology is the lack of timely diagnosis of synchronous forms of colorectal cancer. Therefore, the AIM OF THIS STUDY was to evaluate the structure of synchronous primary multiple forms of colorectal cancer. **METHODS:** We analyzed the results of colorectal cancer diagnostics ($n = 583$) in the period 2010–2019. We did not include patients with metachronous colorectal cancer in the study. The average age of all patients was 71.6 ± 7.4 years. There were 1.5 times more men than women. **RESULTS:** Synchronous colorectal cancer was detected in 171 (29.3%) patients. With synchronous primary multiple forms of colorectal cancer, 2 tumors were diagnosed in every second patient. In synchronous colorectal cancer, tumors were localized twice as often in the colon ($n = 118$) than in the rectum ($n = 53$). **CONCLUSIONS:** In patients with colorectal cancer, synchronous tumors occur in every third case. Synchronous colorectal cancer is more common in men. In the majority of patients (59.1%), synchronous colorectal cancer was detected within 6 months after imaging of the primary tumor.

KEYWORDS — colorectal cancer, synchronous carcinoma, multiple primary cancers, survival, diagnosis.

INTRODUCTION

With an increase in the overall survival of oncology patients, including patients with colorectal cancer (CRC), the incidence of multiple primary forms increases [1]. The proportion of CRC in the total amount of multiple primary tumors of various localization equals 17% [2]. It was found that 6% of radically cured patients with colorectal cancer subsequently develop new primary tumors [3]. In this case, the success of the treatment of multiple primary tumors depends

on the moment of detection of the second and subsequent tumor foci [4]. The complexity of the diagnosis of multiple primary malignant neoplasms also lies in the absence of a characteristic clinical picture. In some cases, signs of synchronous tumors are masked either by pronounced manifestations of one of them, or by concomitant non-tumor pathology.

Aim:

To assess the structure of synchronous primary multiple forms of colorectal cancer.

METHODS

This work was based on the analysis of the results of colorectal cancer treatment in the period 2010–2019. We analyzed the results of examination and treatment in 583 patients with colorectal cancer. There were no age restrictions for patients. The average age of all patients was 71.6 ± 7.4 years. In all patients, we evaluated the time of diagnosis, the number of detected tumors, and the anatomical location of the tumor. Exclusion criteria were metachronous tumors.

The statistical analysis was performed using spreadsheets “EXCEL” and “STATISTICA 8.0”. The significance of differences between quantitative indicators was assessed using the Mann–Whitney test. Differences were considered significant at $p < 0.05$.

RESULTS

Among all detected cases of colorectal cancer ($n = 583$), synchronous tumors were detected in 171 (29.3%) patients. We observed that the largest number of patients was simultaneously with two tumors of colorectal cancer — 164 (95.9%) (Table 1). There were 21.6% more men with synchronous colorectal cancer than women. Among patients with two carcinomas, men also significantly prevailed over women ($p < 0.05$) (Table 1). However, we did not find a significant difference between men and women in the presence of three tumor nodes ($p > 0.05$). There were no patients with five or more synchronous colorectal tumors in our study.

We found a direct relationship between the patient's age and the number of synchronous colorectal cancer tumors (Fig. 1) ($p < 0.05$, CI 65.5–77.5).

In 70 (40.9%) patients, synchronous primary multiple colorectal cancer was detected during revi-

Table 1. Distribution of patients depending on the number of detected tumors in synchronous primary multiple colorectal cancer

Number of tumors	Total(n=171)			
	men		women	
	n	%	n	%
Two tumors	99	57,8	65	38,0
Three tumors	3	1,7	2	1,1
Four tumors	2	1,1	—	—
Total	104	60,8	67	39,2

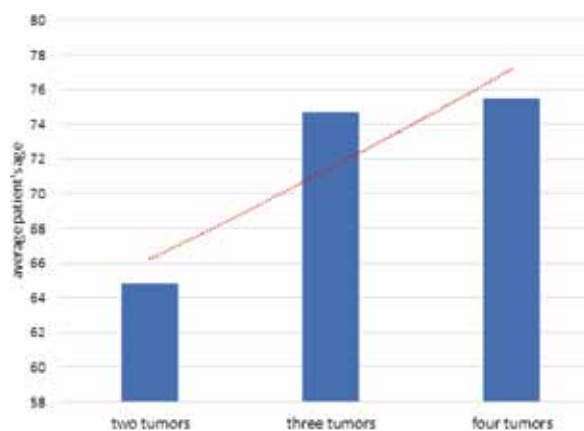


Fig. 1. Dependence of the number of synchronous colorectal cancer tumors on the patient's age

sion of the abdominal cavity during surgical treatment of the disease. In the remaining patients ($n = 101$ (59.1%)), this disease was detected within 6 months after surgery.

The most frequent localization of synchronous primary multiple colorectal cancer was in the colon ($n = 118$ (69.0%). In other cases, $n = 53$ (31%) tumors were localized in the rectum.

DISCUSSION

Synchronous colorectal cancer is multiple (two or more) malignant colorectal tumors that occur simultaneously in the same anatomical region. With synchronous and metachronous neoplasms localized in the gastrointestinal tract, the second tumor is untimely detected in more than 30% of observations: 16% of synchronous neoplasms are diagnosed during surgery, $\frac{2}{3}$ of them at stages III and IV of the disease [1]. Multiple primary colorectal cancer can develop in every 5th patient with familial adenomatous polyposis and ulcerative colitis [4]. In this regard, in addition to primary screening, diagnosis of multiple primary forms of colorectal cancer is relevant today. The main

methods are clinical data, X-ray and endoscopic examination.

Synchronous colorectal cancer is rare. So, according to Zhang C. et al. the overall incidence of multiple primary colorectal cancers was 2.8% [4]. With about the same frequency, this form of cancer is detected in Germany: out of a cohort of 3,714 patients, 103 (2.7%) people were diagnosed with Multiple primary colorectal cancers [5]. In Denmark, synchronous colorectal cancer is even less common and was diagnosed in 1.3% of the cases [6]. As the results of the study by De Rosa M. et al. showed that during surgery, or in the postoperative period within 6 months from the date of the initial diagnosis, synchronous colorectal cancer was detected in 8% of cases [7]. Vitko N.K. et al. over ten years of follow-up, 238 cases of primary multiple forms of the colorectal cancer were identified [3]. Our study showed that synchronous colorectal cancer was detected in 171 (29.3%) patients. Perhaps such high rates are due to the fact that we took into account only patients with tumors of the colorectal zone.

Synchronous colorectal cancer manifests itself not only at the time of diagnosis before surgery, but also several months after removal of the primary tumor. Perhaps such high incidence rates of synchronous colorectal cancer are due to the fact that we took into account only patients with tumors of the colorectal zone only.

CONCLUSIONS

Synchronous colorectal cancer occurs in almost $\frac{1}{3}$ of cases among malignant neoplasms of the colon. Synchronous primary multiple forms of colorectal cancer are more common in men. In almost $\frac{2}{3}$ of patients, synchronous primary multiple colorectal cancer is visualized within 6 months after removal of the primary tumor. Consequently, this group of patients needs not only rehabilitation, but also prolonged follow-up by specialists.

REFERENCES

1. KIT O.I., DZHENKOVA E.A., MIRZOYAN E.A., GEVORKYAN YU.A., SAGAKYANTS A.B., TIMOSHKINA N.N., KAYMAKCHI O.YU., KAYMAKCHI D.O., TOLMAKH R.E., DASHKOV A.V., KOLESNIKOV V.E., MILAKIN A.G., POLUEKTOV S.I. Molecular genetic classification of colorectal cancer subtypes: current state of the problem. South Russian Journal of Cancer. 2021;2(2):50–56. <https://doi.org/10.37748/2686-9039-2021-2-2-6>
2. GONCHARENKO G.V. Primary multiple malignant tumors most common localizations cancer – cancer study clinics. Research and Practical Medicine Journal. 2015;2(4):59–65. (In Russ.) <https://doi.org/10.17709/2409-2231-2015-2-4-59-65>

3. **VITKO N.K., ODINTSOV S.V., MOROZOV S.P., VINOGRADOVA N.N.** Diagnostics of the primary multiple forms of the colorectal cancer. *Khirurgiya. Zhurnal im. N.I. Pirogova*. 2013; 8: 49–55.
4. **ZHANG C, CUI M, XING J, YANG H, YAO Z, ZHANG N, SU X.** Clinicopathologic features and prognosis of synchronous and metachronous multiple primary colorectal cancer. *Clinical & translational oncology*. 2020; 23(2): 335–343. DOI: 10.1007/s12094-020-02426-3
5. **BARZ C, STOSS C, NEUMANN PA, WILHELM D, JANSSEN KP, FRIESS H, NITSCHKE, U.** Retrospective study of prognosis of patients with multiple colorectal carcinomas: synchronous versus metachronous makes the difference. *International journal of colorectal disease*. 2021; 36(7): 1487–1498. DOI: 10.1007/s00384-021-03926-6
6. **LINDBERG LJ, LADELUND S, BERNSTEIN I, THERKILDSSEN C, NILBERT M.** Risk of Synchronous and Metachronous Colorectal Cancer: Population-Based Estimates in Denmark with Focus on Non-Hereditary Cases Diagnosed After Age 50. *Scandinavian journal of surgery*. 2019; 108(2): 152–158. DOI: 10.1177/1457496918798212
7. **DE ROSA M, RONDELLI F, STELLA P, BONI M, ERMILI F, CECCARELLI G.** Triple synchronous colorectal carcinoma. *ANZ Journal of Surgery*. 2019; 89(7–8): 329–330. DOI:10.1111/ans.14452

<http://dx.doi.org/10.35630/2199-885X/2022/12/2.27>

THE ASSOCIATION BETWEEN INTRAUTERINE GROWTH RETARDATION AND MATERNAL THROMBOPHILIA

Received 18 February 2022;
Received in revised form 15 March 2022;
Accepted 17 March 2022

Nart Faruk Kunesko[✉] , Vasilina Golomazova ,
Olga Pitirimova 

¹ Faculty of Obstetrics and Gynecology, Sklifosovsky Research Institute, Moscow;

² Faculty of Obstetrics and Gynecology, Sechenov First Moscow State Medical University, Moscow;

³ National Scientific and Practical Center of Cardiovascular Surgery, Moscow, Russia

✉ dmartfaruk@mail.ru

ABSTRACT — Intrauterine growth retardation (IUGR) contributes to fetal morbidity and mortality, but its etiology is unknown in most cases. Our aim was to indicate the association between thrombophilia (genetic and acquired) and IUGR. A case-control study of 185 pregnant women with compensated and decompensated forms of placental insufficiency and IUGR has been conducted, with a control group (n=50) consisted of women who had normal growth fetuses. This case-controlled study demonstrated significantly higher prevalence of genetic and acquired thrombophilia in women with IUGR compared to women with normal pregnancies. However, further studies which employ randomized controlled trials and determine the preventive effect of the administration of LMWH (Low-molecular-weight heparin) and/or low-dose aspirin on women in risk groups for thrombophilia are required for a establishing a definitive relationship. Pregnant women with genetic or acquired thrombophilia belong to a high-risk group for the onset of intrauterine growth restriction syndrome. Our study included a small number of patients. To evaluate a more accurate relationship it is required to perform randomized controlled trials and determine potential benefits of administration of LMWH and/or low-dose aspirin in order to provide prophylaxis of IUGR in risk groups with genetic and acquired thrombophilia.

KEYWORDS — IUGR, FGR, FWA, thrombophilia, placental insufficiency, case-control, hemotrophic phase.

ABBREVIATIONS AND ACRONYMS:

IUGR — Intrauterine growth retardation
LMWH — Low-molecular-weight heparin
FGR — Fetal growth retardation
FWA — Fetal weight gain
HC — Head circumference
BPD — Biparietal head size
FAC — Fetometric abdominal circumference
FL — Femur length
FMP — Fetal movement profile
SGA — Small-for-gestational age

INTRODUCTION

Fetal growth retardation (FGR) is a term that describes a pathologically small fetus that has not reached its growth potential and has a high risk of perinatal complications (a slowed anticipated fetal weight gain (FWA) and/or abdominal circumference (AUC) <10th percentile, combined with abnormal blood flow as measured by US Doppler or FWA values <3rd percentile).

Causes leading to the development of PPH can be divided into 4 groups: maternal, placental, fetal and genetic. Although their pathophysiology is different, they all ultimately lead to the same result: decreased uterine-placental perfusion and fetal nutrition.

Fetal growth (fetal physical development) is a dynamic process and its evaluation requires multiple observations of fetal size throughout pregnancy. Fetal size is determined by measuring the head circumference (HC), biparietal head size (BPD), FAC (fetometric abdominal circumference), femur length (FL), and/or FMP (fetal movement profile) calculated by various formulas during ultrasound. These CRs use the terminology to describe fetal growth/developmental abnormalities shown in Table 1 (Table 1). Identification of FGR is often difficult because fetal growth cannot be assessed by a single measurement of fetal size and growth potential is a hypothetical concept.

Despite low sensitivity and specificity, the determination of growth-mass indices and uterine floor height (UFH) are the only routinely available physical examination methods. The UFH should be measured and entered into individual charts, or gravidograms; suboptimal fetal growth should be diagnosed by applying the MacDonald rule when the uterine floor height is less than ≥ 3 cm of gestational age in weeks.

It is recommended to conduct UFN measurement starting from 22nd week of gestation to detect fetal growth deficiencies.

Intrauterine growth retardation (IUGR), which is also referred to as fetal growth retardation (FGR) in medical literature, is a term which describes a condition in which a fetus experiences reduced growth compared to the expected rate. A widely used definition suggests that IUGR is present when the weight of a fetus lies below the 10th percentile for its gestational age; however, other parameters should be also em-

ployed to differentiate between IUGR and small-for-gestational age (SGA) condition.

IUGR contributes to fetal morbidity and mortality and is associated with higher chances of premature conditions and certain non-communicable diseases in adulthood, but its etiology is unknown in most cases.

Studies suggest such causes of IUGR as certain chronic and infectious diseases in mothers (diabetes, cardiovascular disease, etc), genetic disorders, placental insufficiencies, abnormal placentation, malnutrition and others. Our aim was to indicate the association between thrombophilia (genetic and acquired) and IUGR.

METHODS

As the main method of this study, we selected a case-control study of 185 pregnant women with compensated and decompensated forms of placental insufficiency and IUGR with a control group of women ($n=50$) who had normal growth fetuses. All women were tested in the third trimester for the following parameters: factor V Leiden, prothrombin gene (G20210A), MTHFR (C677T) and PAI-1 polymorphism and circulation of APA (LA, Cardiolipin Antibodies, Beta-2 Glycoprotein I Antibodies, Prothrombin Antibodies). We then compared the occurrence of IUGR

RESULTS

There were discovered no significant associations between mutations in prothrombin gene G2021A (0.16 percent points difference of occurrence between case group and control group for homozygote pattern and 1.03 percent points difference for heterozygote pattern) and Factor V Leiden thrombophilias (1.08 percent points difference for homozygote and about 0.5 percent points difference for heterozygote patterns) and IUGR in either of the groups.

Strongly significantly higher odds for IUGR are present in patients with PAI, MTHFR gene mutation (heterozygote and homozygote pattern) and circulation of antiphospholipid antibodies (Table 2). Patients with IUGR were found to be almost 4 times more likely to have plasminogen activator inhibitor caused thrombophilia than patients with normal pregnancies. MTHFR gene mutation caused thrombophilia chances are more than two times higher for women with IUGR (2.3 times higher for both homozygote and heterozygote pattern). The difference of occurrence thrombophilia caused by circulation of aPL antibodies in patients with IUGR differs from 3.9 times higher chances for cardiolipin antibodies to 7.3 times higher prothrombin antibodies.

We also discovered a higher occurrence of multigenic (5.5 times more often) and combined (7.7 times

more often) thrombophilias in women with IUGR.

DISCUSSION

This case-controlled study demonstrated significantly higher prevalence of genetic and acquired thrombophilia in women with IUGR compared to women with normal pregnancies. Furthermore, strongly significant associations between PAI and MTHFR thrombophilias and IUGR are demonstrated. The associations between IUGR and circulation of aPL antibodies differ for different antibodies type; however, it is, in principle, significantly high. Our study showed a higher prevalence of multigenic (33%) and combined thrombophilia (30,8%) in IUGR pregnancies compared with 6% and 4% in the control group. The association between IUGR and FV Leiden and Prothrombin gene G20210A mutations are controversial: no significant difference in occurrence of these phenomena has been found between case group and control group.

CONCLUSION

Our study suggests an association between genetic and acquired thrombophilias in pregnant women and intrauterine growth retardation. However, the occurrence of different variations of thrombophilia in women with IUGR is not heterogeneous.

The key role of thrombophilia in the pathogenesis of obstetric complications is as follows: microthrombosis of the vessels of the placental bed and, accordingly, a violation of uteroplacental blood flow occur. Implantation, invasion of trophoblast in the presence of genetic defects of coagulation is disrupted. It should be noted that in thrombophilia not only the early (avascular) implantation phase, but also the later stages of implantation (hemotrophic phase) and placentation suffer. Antiphospholipid antibodies are able to disrupt the process of trophoblast differentiation, which is manifested in changes in the embryo's adhesiveness, syncytium fusion disturbance, the depth of trophoblast invasion, a decrease in the production of chorionic gonadotropic hormone, and an increase in thrombotic tendencies. All of the above trends contribute significantly to the development of IUGR. Thus, pregnant women with genetic or acquired thrombophilia belong to a high-risk group for the onset of intrauterine growth restriction syndrome.

Our study included a small number of patients. To evaluate a more accurate relationship it is required to perform randomized controlled trials and determine potential benefits of administration of LMWH and/or low-dose aspirin in order to provide prophylaxis of IUGR in risk groups with genetic and acquired thrombophilia.

Table 1. (IUGR)

Title	Define
IUGR	Slow anticipated fetal weight gain (FWG) and/or abdominal circumference gain (ACG) or FWG and/or ACG values < 10 th percentile combined with abnormal blood flow as measured by ultrasound Doppler; or FWG and/or ACG values < 3 rd percentile
Congenital IUGR	Estimated fetal weight is less < 3 rd percentile

REFERENCES

1. COSTA S.L., PROCTOR L., DODD J.M., TOAL M., OKUN N., JOHNSON J.-A., ET AL. Screening for placental insufficiency in high-risk pregnancies: is earlier better? Placenta. 2008.
2. LAURINI R., LAURIN J., MARSÁL K. Placental histology and fetal blood flow in intrauterine growth retardation. Acta Obstet Gynecol Scand. 1994
3. SALAFIA C.M., MINIOR V.K., PEZZULLO J.C., POPEK E.J., ROSENKRANTZ T.S., VINTZILEOS A.M. Intrauterine growth restriction in infants of less than thirty-two weeks' gestation: associated placental pathologic features. Am J Obstet Gynecol. 1995;
4. ABALOS E., DULEY L., STEYN D.W., GIALDINI C. Antihypertensive drug therapy for mild to moderate hypertension during pregnancy. Cochrane database Syst Rev. 2018.
5. LANG J.M., LIEBERMAN E., COHEN A. A comparison of risk factors for preterm labor and term small-for-gestational-age birth. Epidemiology. 1996;
6. KEHL S., DÖTSCH J., HECHER K., SCHLEMBACH D., SCHMITZ D., STEPAN H., ET AL. Intrauterine Growth Restriction. Guideline of the German Society of Gynecology and Obstetrics (S2k-Level, AWMF Registry No. 015/080, October 2016). Geburtshilfe Frauenheilkd. 2017.
7. ANANTH C. V, PELTIER M.R., CHAVEZ M.R., KIRBY R.S., GETAHUN D., VINTZILEOS A.M. Recurrence of ischemic placental disease. Obstet Gynecol. 2007.
8. KRAMER M.S., PLATT R., YANG H., MCNAMARA H., USHER R.H. Are all growth-restricted newborns created equal(ly)? Pediatrics. 1999;
9. LERUEZ-VILLE M., VILLE Y. Fetal cytomegalovirus infection. Best Pract Res Clin Obstet Gynaecol. 2017;
10. Royal College of Obstetricians and Gynaecologists. Green-Top Guideline 31: The Investigation and Management of the Small-for-Gestational-Age Fetus. RCOG Green-top Guidel No 31. 2014.
11. Society for Maternal-Fetal Medicine (SMFM),

Table 2. Prevalence of thrombophilia in the two groups

Factor	Cases (n=185)		Control (n=50)	
FV Leiden homozyg	2	1,08%	0	0,00%
FV Leiden heterozyg	12	6,49%	3	6,00
Prothrombin homozyg	4	2,16%	1	2,00%
Prothrombin heterozyg	13	7,03%	3	6,00
MTHFR homozyg	17	9,19%	2	4,00
MTHFR heterozyg	51	27,57%	6	12,00
PAI	64	34,59%	4	8,00
Multigenic	61	32,97%	3	6,00
LA	21	11,35%	1	2,00
Cardiolipin AB	43	23,24%	3	6,00
B2Gpla AB	72	38,92%	4	8,00
Prothrombin AB	54	29,19%	2	4,00
Combined thrombophilia	57	30,81%	2	4,00

Martins J.G., Biggio J.R., Abuhamad A. Society for Maternal-Fetal Medicine Consult Series #52: Diagnosis and management of fetal growth restriction: (Replaces Clinical Guideline Number 3, April 2012). Am J Obstet Gynecol. 2020.

12. ALBU A.R., ANCA A.F., HORHOIANU V. V, HORHOIANU I.A. Predictive factors for intrauterine growth restriction. J Med Life. 2014. PMC4197512
13. PARKER S.E., WERLER M.M. Epidemiology of ischemic placental disease: a focus on preterm gestations. Semin Perinatol. 2014;
14. BERLIT S., NICKOL J., WEISS C., TUSCHY B., TEMERINAC D., MAYER J., ET AL. Zervixdilatation und Kürettage während eines primären Kaiserschnitts – eine retrospektive Analyse. Z Geburtshilfe Neonatol. 2013.
15. LEVINE T.A., GRUNAU R.E., MCAULIFFE F.M., PINNAMANENI R., FORAN A., ALDERDICE F.A. Early childhood neurodevelopment after intrauterine growth restriction: a systematic review. Pediatrics. 2015. DOI: 10.1542/peds.2014-1143
16. GORBAN T.S., DEGTEREVA M.V., BOBAK O.A. Fetal abnormalities in low weight preterms with intrauterine growth restriction. Issues of Practical Pediatrics. 2011;
17. MORAITIS A.A., WOOD A.M., FLEMING M., SMITH G.C.S. Birth weight percentile and the risk of term perinatal death. Obstet Gynecol. 2014
18. VASAK B., KOENEN S. V, KOSTER M.P.H., HUKKELHOVEN C.W.P.M., FRANX A., HANSON M.A., ET AL. Human fetal growth is constrained below optimal for perinatal survival. Ultrasound Obstet Gynecol. 2015; DOI: 10.1002/uog.14644
19. MCINTIRE D.D., BLOOM S.L., CASEY B.M., LEVENO K.J. Birth weight in relation to morbidity and mortality among newborn infants. N Engl J Med. 1999;

20. GARDOSI J., MADURASINGHE V., WILLIAMS M., MALIK A., FRANCIS A. Maternal and fetal risk factors for stillbirth: population based study. *BMJ*. 2013;
21. FLOOD K., UNTERSCHIEDER J., DALY S., GEARY M.P., KENNELLY M.M., MCAULIFFE F.M., ET AL. The role of brain sparing in the prediction of adverse outcomes in intrauterine growth restriction: results of the multicenter PORTO Study. *Am J Obstet Gynecol*. 2014;
22. POON L.C.Y., TAN M.Y., YERLIKAYA G., SYNGELAKI A., NICOLAIDES K.H. Birth weight in live births and stillbirths. *Ultrasound Obstet Gynecol*. 2016; DOI: 10.1002/uog.17287
23. PRIOR T., PARAMASIVAM G., BENNETT P., KUMAR S. Are fetuses that fail to achieve their growth potential at increased risk of intrapartum compromise? *Ultrasound Obstet Gynecol*. 2015 DOI: 10.1002/uog.14758
24. SHERRELL H., DUNN L., CLIFTON V., KUMAR S. Systematic review of maternal Placental Growth Factor levels in late pregnancy as a predictor of adverse intrapartum and perinatal outcomes. *Eur J Obstet Gynecol Reprod Biol*. 2018; DOI: 10.1016/j.ejogrb.2018.03.059
25. GARDENER G., WELLER M., WALLACE E., EAST C., OATS J., ELLWOOD D., ET AL. PSANZ. Position Statement: Detection and Management of Fetal Growth Restriction in Singleton Pregnancies. In *Perinat Soc Aust new Zealand/Stillbirth Cent Res Excell*. 2018;
26. CRIMMINS S., DESAI A., BLOCK-ABRAHAM D., BERG C., GEMBRUCH U., BASCHAT A.A. A comparison of Doppler and biophysical findings between liveborn and stillborn growth- restricted fetuses. *Am J Obstet Gynecol*. 2014. DOI: 10.1016/j.ajog.2014.06.022
27. SAYCHEV S., FIGUERAS F., SANZ-CORTES M., CRUZ-LEMINI M., TRIUNFO S., BOTET F., ET AL. Evaluation of an optimal gestational age cut-off for the definition of early- and late-onset fetal growth restriction. *Fetal Diagn Ther*. 2014; DOI: 10.1159/000355525
28. MIFSUD W., SEBIRE N.J. Placental pathology in early-onset and late-onset fetal growth restriction. *Fetal Diagn Ther*. 2014; DOI: 10.1159/000359969
29. FIGUERAS F., GRATACOS E. Stage-based approach to the management of fetal growth restriction. *Prenat Diagn*. 2014 DOI: 10.1002/pd.4412
30. GORDIJN S.J., BEUNE I.M., THILAGANATHAN B., PAPAGEORGHIOU A., BASCHAT A.A., BAKER P.N., ET AL. Consensus definition of fetal growth restriction: a Delphi procedure. *Ultrasound Obstet Gynecol*. 2016; DOI: 10.1002/uog.15884
31. LEES C.C., STAMPALJA T., BASCHAT A., DA SILVA COSTA F., FERRAZZI E., FIGUERAS F., ET AL. ISUOG Practice Guidelines: diagnosis and management of small-for-gestational-age fetus and fetal growth restriction. *Ultrasound Obstet Gynecol*. 2020; DOI: 10.1002/uog.22134
32. SALOMON L.J., ALFIREVIC Z., DA SILVA COSTA F., DETER R.L., FIGUERAS F., GHI T., ET AL. ISUOG Practice Guidelines: ultrasound assessment of fetal biometry and growth. *Ultrasound Obstet Gynecol*. 2019; <https://doi.org/10.1002/uog.20272>
33. MCCOWAN L.M., FIGUERAS F., ANDERSON N.H. Evidence-based national guidelines for the management of suspected fetal growth restriction: comparison, consensus, and controversy. *Am J Obstet Gynecol*. 2018 DOI: 10.1016/j.ajog.2017.12.004
34. MOLINA L.C.G., ODIBO L., ZIENTARA S., OBIČAN S.G., RODRIGUEZ A., STOUT M., ET AL. Validation of Delphi procedure consensus criteria for defining fetal growth restriction. *Ultrasound Obstet Gynecol*. 2020; DOI: 10.1002/uog.20854
35. ALLEN V.M., JOSEPH K., MURPHY K.E., MAGEE L.A., OHLSSON A. The effect of hypertensive disorders in pregnancy on small for gestational age and stillbirth: a population based study. *BMC Pregnancy Childbirth*. 2004;
36. KENNY L.C., BLACK M.A., POSTON L., TAYLOR R., MYERS J.E., BAKER P.N., ET AL. Early pregnancy prediction of preeclampsia in nulliparous women, combining clinical risk and biomarkers: the Screening for Pregnancy Endpoints (SCOPE) international cohort study. *Hypertens (Dallas, Tex 1979)*. 2014; DOI: 10.1161/HYPERTENSIONAHA.114.03578
37. BLIGH L.N., FLATLEY C.J., KUMAR S. Reduced growth velocity at term is associated with adverse neonatal outcomes in non-small for gestational age infants. *Eur J Obstet Gynecol Reprod Biol*. 2019; DOI: 10.1016/j.ejogrb.2019.06.026
38. MORALES-ROSELLÓ J., KHALIL A., MORLANDO M., PAPAGEORGHIOU A., BHIDE A., THILAGANATHAN B. Changes in fetal Doppler indices as a marker of failure to reach growth potential at term. *Ultrasound Obstet Gynecol*. 2014; DOI: 10.1002/uog.13319
39. PAPAGEORGHIOU A.T., OHUMA E.O., GRAVETT M.G., HIRST J., DA SILVEIRA M.F., LAMBERT A., ET AL. International standards for symphysis-fundal height based on serial measurements from the Fetal Growth Longitudinal Study of the INTERGROWTH-21st Project: prospective cohort study in eight countries. *BMJ*. 2016; DOI: 10.1136/bmj.i5662
40. GRIFFIN M., SEED P.T., WEBSTER L., MYERS J., MACKILLOP L., SIMPSON N., ET AL. Diagnostic accuracy of placental growth factor and ultrasound parameters to predict the small-for-gestational-age infant in women presenting with reduced symphysis-fundus height. *Ultrasound Obstet Gynecol*. 2015; DOI: 10.1002/uog.14860
41. AGDH: Pregnancy Care Guidelines: Fetal growth restriction and well-being. *Aust Gov Dep Heal*. 2019;

<http://dx.doi.org/10.35630/2199-885X/2022/12/2.28>

IMPROVEMENT OF AUTOFLUORESCENCE IMAGING METHOD IN DETECTION OF CANCEROUS LESIONS OF THE ORAL MUCOSA

Received 04 February 2022;
Received in revised form 22 February 2022;
Accepted 24 February 2022

Ekaterina Gorbatova[✉] , **Marina Kozlova** ,
Larisa Dzikovitskaya , **Tamara Glybina** 

Central State Medical Academy, Department of President Affairs, Moscow, Russia

✉ Gorbatova_k@mail.ru

ABSTRACT — PURPOSE: to optimize the diagnostic method for detecting neoplasms of the oral mucosa.

MATERIALS AND METHODS: The study group included 32 people with lesions of the oral mucosa: lichen planus — 17; chronic mechanical injury (decubital ulcer) — 15. The authors have proposed a method for diagnosing erosive and ulcerative elements of the oral mucosa, which consists in staining pathological foci with a 1% solution of toluidine blue followed by autofluorescence imaging. The effectiveness of autofluorescence imaging by «AFS» stomatoscope, staining and a combination of two methods in visualizing the boundaries of precancerous lesions of the oral mucosa was determined.

RESULTS AND DISCUSSION: The technique of autofluorescence imaging by «AFS» stomatoscope, in 63.7% incorrectly diagnosed patients with cancer of the oral mucosa, in addition, 27.3% did not reveal malignant neoplasms. Marking the lesion elements with a 1% toluidine blue solution and their illumination with autofluorescence imaging, made it possible to establish a dark glow zone in those cases (27.3%) when imaging did not identify the pathological focus as an area without fluorescence. In all patients with malignant neoplasms of the oral mucosa diagnosed by autofluorescence imaging with staining, a truly positive result was confirmed by morphometric data.

CONCLUSION: Autofluorescence imaging with staining has a high sensitivity and specificity of 100%, and is 2 times more effective than autofluorescence imaging in the diagnosis of dysplasia of erosive and ulcerative elements of the oral mucosa.

KEYWORDS — autofluorescence imaging, optical diagnostic method, diagnosis for cancerous oral lesions.

INTRODUCTION

According to the literature, precancerous lesions of the oral mucosa range from 15.2 to 84.9% of all nosologies [1, 2]. This pathology of the mucous membranes of the oral cavity with the potential for the development of dysplasia, based on the classifica-

tion of A. L. Mashkillayson (1970) and other authors [3], includes: long-term non-healing ulcers, erosive-ulcerative forms of lichen planus, leukoplakia. Timely diagnosis of such conditions and neoplasms is the key to a favorable prognosis of the disease [4–6].

Detection of malignancy of precancerous conditions by standard methods is difficult due to the variability of the pathological process, expressed in a variety of morphological and morphometric disorders of the mucosa [7].

Studies conducted by A.E. Pursanova and co-authors (2015) showed that 42.8% of specialists differentiate early manifestations of cancer of the oral mucosa [8]. A.M. Avanesov and co-authors (2017) found that in 65% of cases, the dentist may suspect the presence of malignant neoplasms only on the third visit of the patient [9]. In the initial period, during the clinical examination of the oral mucosa, good visibility of the lesion elements does not give advantages therefore additional methods should be used [8–11].

To date, modern diagnostic tests that help primary care physicians to establish a disease of the oral mucosa and suspect the development of carcinogenesis include: autofluorescence imaging, luminescent imaging, staining with toluidine solution [3, 10–15].

The autofluorescence imaging technique is based on differences in the spectral composition and intensity of endogenous radiation of healthy tissues and lesions. As a result of disruption of metabolic processes, endogenous porphyrin (fluorophore) accumulates in tissues, due to this, when exposed to a light beam of the blue spectrum on the inflammatory zones, a red or maroon glow appears, the absence of a glow (dark spot) indicates malignization [10–15]. In dental practice today, this method is widely used to detect oncological diseases of the oral cavity that have manifestations in the form of erosive and ulcerative elements. According to a number of authors, the disadvantage of the method is low specificity according to the stated diagnostic criteria [14, 15].

In international practice, marking of lesion elements with a 1% toluidine blue solution is used to assess the size of a pathological focus. The principle of operation of the technique is based on the retention of

the dye in the intercellular space of damaged cells with impaired metabolic processes; binding to negatively charged mitochondrial membranes, affinity for DNA and sulfated mucopolysaccharides [3]. Sol Silverman et al., (2010) claimed a high (90%) accuracy of this diagnostic method.

Thus, the autofluorescence imaging methodology has disadvantages, and needs additional refinement. The test that involves staining with a 1% solution of toluidine elements of the lesion, despite its availability and high percentage of reliability, has not been widely used in practical dentistry.

The aim of the study

is to optimize the method for diagnosis of oral cavity neoplasms

MATERIALS AND METHODS

In 2019–2021, 67 patients aged 35 to 87 years with diseases of the oral mucosa were examined at the Department of Dentistry, Central State Medical Academy (Moscow, Russia)

Inclusion criteria:

- erosive and ulcerative forms of lichen planus;
- individual elements of the lesion — erosion, ulcer, due to chronic mechanical trauma.

Exclusion criteria patients with diseases of the oral mucosa:

- infectious;
- allergic;
- benign tumors;
- keratoses.

Thus, the study group included 32 people (men — 13, women — 22) older than 45 years with the following lesions of the oral mucosa: lichen planus — 17; chronic mechanical injury (decubital ulcer) — 15.

The clinical examination consisted of standard methods: a survey, anamnesis collection, examination of the external status with mandatory palpation of the lymph nodes of the regional region. The examination of the mouth included a description of the condition of the mucous membrane of the lips, cheeks, hard and soft palate, gums, teeth, dentition, identification of factors of chronic mechanical trauma (dystopian teeth, sharp edges of teeth, fillings, orthopedic structures, the presence of dissimilar metals). The lesions of the oral mucosa were analyzed in detail according to the following scheme:

1. Appearance: type, localization; size; shape of edges; condition of surrounding tissues;
2. Palpation: painful/painless; consistency (soft-elastic/ tight-elastic), the presence of a seal;
3. Autofluorescence imaging is performed by a

fluorescent stomatoscope "AFS", the manufacturer "Polironik" (Russia) (Fig. 1 a, b).

With this device, it is possible to detect the localization of pathological processes due to the excitation of tissue fluorophores by light. In the light of a wave of a blue light beam, a healthy mucosa has a green or blue glow, foci of inflammation are red or maroon (due to endogenous porphyrins - waste products of pathogenic microflora), suspicious areas of the oral cavity will emit their own light with a longer wavelength, have a darker color and an uneven surface compared to other areas, which indicates the fact of accumulation of a large number of cells with enlarged nuclei in one place.

To visualize the size and boundaries of erosive and ulcerative elements of the lesion of the oral mucosa during biopsy, a method was patented (Gorbatova, E., Kozlova M., Ryabov, V. 2019 Visualization of oral lesions using autofluorescence imaging with staining in biopsy, 2722766. Rospatent, Russia):

1. The mouth is rinsed with water.
2. The staining of the lesion element of the oral mucosa (erosion or ulcers) is performed 1% toluidine blue solution with a sterile cotton swab, for 15 seconds.
3. The mouth is rinsed with water.
4. A 1% solution of acetic acid is applied to the lesion element of the oral mucosa with a sterile cotton swab, for 15 seconds.
5. The oral cavity is rinsed with water.
6. In natural light autofluorescence imaging Staining with subsequent autofluorescence imaging by "AFS" stomatoscope changes the intensity of fluorescence of pathological foci and gives a clear topography of the site of sampling of biological material, which ensures the reliability of histological examination.

For the final diagnosis, the lesions of the oral mucosa were taken for biopsy. Histological samples were examined in the Pathoanatomical Department of the Herzen Moscow State Medical Institute and Blokhin Russian Cancer Research Center (Moscow; Russia)

To evaluate the proposed method, a comparison of autofluorescence imaging using "AFS" stomatoscope, or autofluorescence imaging with staining with 1% toluidine blue solution and without staining was performed. The effectiveness was calculated using sensitivity and specificity.

Sensitivity (Sen.) was calculated by the formula:

$$\text{Sen.} = \frac{\text{truly positive}}{\text{true positive} + \text{false negative}} \times 100\%$$

Specificity (Sp.) was calculated:

$$Sp. = \frac{\text{truly negative}}{\text{false positive} + \text{truly negative}} \times 100\%$$

The values of the morphological conclusion were taken as an indisputable criterion for the diagnosis of cancer and the exclusion of false positive/negative results.

The obtained results were processed by the method of descriptive statistics, the method of variance analysis (Student's t-test). The differences were considered significant in cases when the probability of belonging to one of the communities did not exceed $p = 0.023$.

RESULTS AND DISCUSSION

Analysis of the dental status of all patients showed that in 95% of all cases, the local cause of the occurrence or exacerbation of the existing disease of the oral mucosa was a permanent injury of various origins, mainly sharp edges of destroyed and dystopian teeth, orthopedic structures.

During autofluorescence imaging by "AFS" stomatoscope, in 32 patients with erosive and ulcerative changes of the oral mucosa in 36.4% of cases, a "false positive" identification of the development of carcinogenesis occurred, a positive result was confirmed in 27.3%, a false negative response — 27.3%, a true negative — 9.0%.

Thus, when conducting the autofluorescence imaging technique in 63.7%, the test did not have reliable information regarding the diagnosis of patients with oral mucosal cancer, the same percentage of detection (27.3%) and non-detection (27.3%) of this pathology was also established. Otherwise, half of the patients with suspected possible malignancy of the lesion elements were not detected.

Marking the lesion elements with a 1% toluidine blue solution and their illumination with an «AFS» stomatoscope revealed a zone of dark glow in those cases (27.3%) whereas only autofluorescence imaging failed to identify the pathological focus as an area without fluorescence.

All erosive and ulcerative lesions that intensively absorbed the dye and had a black halo of glow were subsequently confirmed as malignant neoplasms according to morphometric studies. (Fig. 2 (a, b, c, d)).

All patients who were diagnosed with the condition of the oral mucosa by the autofluorescence imaging method with staining had truly positive results of the presence of malignant neoplasms, confirmed by histological results. In addition, the identification of the sampling site for the biopsy took place, which was an important advantage of this method.

Analyzing the results obtained, it should be noted that autofluorescence imaging method with staining

has a high sensitivity of 100%, 2 times more effective than autofluorescence imaging in detecting dysplasia of erosive and ulcerative elements of the oral mucosa. The specificity of the diagnostic autofluorescence test was 25%, with staining — 100% ($p=0.023$).

The difficulty of interpreting the results of the diagnosis of autofluorescence imaging is due to the fact that the presence of porphyrins is also characteristic of inflammatory processes. A number of experimental and clinical studies have confirmed the fact that fluorophores were present in areas of ischemia and hypoxia of tissues, while morphologically altered cells characteristic of malignant or benign neoplasms were not detected [16]. This method can determine the prevalence of a pathological focus and it is impossible to analyze the depth of the lesion.

Autofluorescence imaging can be recommended as a diagnostic test to identify the presence of pathology of the mucous membranes of the oral cavity.

Autofluorescence imaging by "AFS" stomatoscope with marking of elements with 1% toluidine blue solution more effectively visualizes the zone of altered fluorescence and determines the site for biopsy. The described methods should be used by general dentists in case of suspected malignancy of the oral mucosa as a first opinion. At the second level of examination, the results of autofluorescence must be confirmed by morphometric examination of the pathological focus.

CONCLUSIONS

1. The proposed method of topography of erosive and ulcerative lesions of the oral mucosa with subsequent autofluorescence imaging by "AFS" stomatoscope allows us to clearly visualize the zones of altered fluorescence, the boundaries of the pathological focus and intact tissue for biopsy, which ensures a reliable result of histological examination.

2. The diagnostic technique of autofluorescence imaging with staining is 2 times more effective than autofluorescence imaging in determining neoplastic changes in the tissues of the oral mucosa.

REFERENCES

1. GILEVA O. S. ET AL. Precancerous diseases in the structure of pathology of the oral mucosa // Problems of dentistry. – 2013. – No. 2. – p. 1–9.
2. ISKAKOVA M. K., ZARKUMOVA A. E., NUR-MUKHAMBETOVA G. K. The proportion of diseases of the oral mucosa among common dental diseases // Bulletin of the Kazakh National Medical University. – 2017. – No. 3. – p. 163–167.
3. SILVERMAN S., EVERSOLE L.R., TRUELOVE E.L. Essentials of Oral Medicine, 2010, 467 p.
4. ZAZULEVSKAYA L. YA., RUSANOV V. P., VALOV

- K. M. Oncological alertness of dentists-the key to preventing cancer of the oral mucosa // Bulletin of the Kazakh National Medical University. – 2012. – No. 1. – p. 201–204.
5. ZYKOVA E. A. Oncological alertness in diseases of the oral mucosa // Healthcare of Ugra: experience and innovations. – 2016. – No. 3. – p. 49–55.
 6. AMKHADOVA M. A., SOYHER M. I., CHUYANOVA E. YU. Onconastentiveness in the practice of a dentist // Medical alphabet. – 2016. – Vol. 2. – No. 9. – p. 6–9.
 7. TKACHENKO T. B., GAIKOVA O. N. Features of the oral mucosa in various age periods of human life (morphological study) // Institute of Dentistry. – 2008. – Vol. 3. – No. 40. – p. 70–73.
 8. PURSANOVA A. E. ET AL. Evaluation of the effectiveness of therapy of precancerous diseases of the oral mucosa using autofluorescence diagnostics // Modern problems of science and education. – 2018. – No. 4. – p. 151–151.
 9. AVANESOV A. M., GVOZDIKOVA E. N. Determination of dental risk groups for radiation mucositis in patients with squamous cell carcinoma of the oropharyngeal region on the background of radiation therapy // Radiation diagnostics and therapy. – 2017. – No. 2. – p. 66–66.
 10. GAZHVA S. I. ET AL. Direct visualization of autofluorescence of tissues as a method of early diagnosis of pathological conditions of the oral mucosa // Modern problems of science and education. – 2014. – No. 6. – p. 1237–1237.
 11. SHKAREDNAYA O. V. ET AL. Optimization of early diagnosis of pathological conditions of the oral mucosa // Modern technologies in medicine. – 2017. – Vol. 9. – No. 3. – P. 119–125.
 12. BULGAKOVA N. N., VOLKOV E. A., POZDNYAKOVA T. I. Autofluorescence stomatoscopy as a method of oncoscreening of diseases of the oral mucosa // Russian Dental Journal. – 2015. – Vol. 19. – No. 1. – p. 27–30.
 13. KRIKHELI N. I. ET AL. Results of autofluorescence stomatoscopy of lichen planus as a screening method for detecting precancerous and cancerous changes in the oral mucosa // Russian dentistry. – 2016. – Vol. 9. – No. 4. – p. 13–17.
 14. NAGI R., REDDY-KANTHARAJ Y., RAKESH N., JANARDHAN-REDDY S., SAHU S. Efficacy of light based detection systems for early detection of oral cancer and oral potentially malignant disorders: Systematic review // Med Oral Patol Oral Cir Bucal. – 2016. – V. 21. – No 4. P. 447–455. 10.4317/medoral.21104
 15. NALLAN C. S. ET AL. A Meta-analysis on efficacy of auto fluorescence in detecting the early dysplastic changes of oral cavity. Chaitanya K., Sunanda Chavva, Elizabeth Surekha, Vedula Priyanka, Mule Akhila, Hari Kiran Ponnuru, and Charan Kumar Reddy // South Asian J Cancer. – 2019. – V. 8. – No 4. P. 233–236. doi: 10.4103/sajc.sajc_336_18
 16. LITVINOVA K. S., ROGATKIN D. A. Catalogue of spectral characteristics of the main fluorophores of human and animal tissues // Collection of materi-



a) visualization pathological foci of oral mucosa

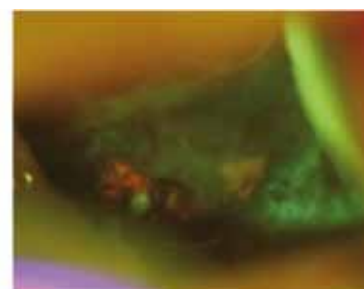


b) Stomatoscope "AFS"

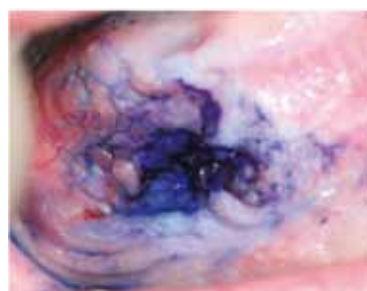
Fig. 1. Visualization of pathological foci of oral mucosa by stomatoscope "AFS", "Polironik" (Russia)



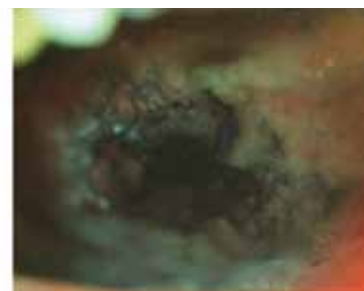
a) an ulcer on the lateral surface of the tongue on the right



b) autofluorescence imaging showed fluorescence of red, maroon glow and a dark zone



c) visualization of the ulcer boundaries after staining with 1% toluidine blue solution



d) there is no fluorescence in the pathological focus after staining and autofluorescence imaging. In a morphometric study, neoplastic changes of cells were established, on the basis of the histological examination (No. 1532/2019), the final diagnosis was made – "squamous cell carcinoma"

Fig. 2. Clinical picture, patient B., 81. Autofluorescence imaging (a, b), autofluorescence imaging with staining (c, d)

als of the III Eurasian Congress on Medical Physics and Engineering "Medical Physics-2010". Moscow: Publishing House of Moscow State University. – 2010. – pp. 141–143.

<http://dx.doi.org/10.35630/2199-885X/2022/12/2.29>

IMPLEMENTATION OF NEUROMUSCULAR DENTISTRY PRINCIPLES IN REHABILITATION OF PATIENTS WITH COMPLETE ADENTIA

Received 30 December 2021;
Received in revised form 26 January 2022;
Accepted 27 January 2022

**Dmitry Domenyuk^{1,7} , Taisiya Kochkonyan² ,
Maria Rozhkova³ , Sergey Fischev³,
Alexandr Lepilin⁴ , Arkady Sevastyanov³,
Irina Orlova³, Margarita Puzdyreva³ ,
Roman Subbotin³ , Sergei Dmitrienko⁵ ,
Stanislav Domenyuk⁶ **

¹ Stavropol State Medical University, Stavropol;

² Kuban State Medical University, Krasnodar;

³ St. Petersburg State Pediatric Medical University, St. Petersburg;

⁴ Saratov State Medical University, Saratov;

⁵ Volgograd State Medical University, Volgograd;

⁶ North Caucasus Federal University, Stavropol;

⁷ Pyatigorsk Medical and Pharmaceutical Institute — Branch of the Volgograd State Medical University, Pyatigorsk, Russia

✉ domenyukda@mail.ru

ABSTRACT — According to World Health Organization about 15% of the world's adult population suffer from complete adentia, with a steady growth in the number of patients affecting not only the elderly which is accounted for by an increase in life expectancy, yet also among people in their working age. Apart from disturbed chewing and speech functions, complete adentia leads to altered anatomical and topographic proportions of the face and facial skeleton, progressive atrophy and osteoporosis of the jaws, masticatory and mimic muscle atrophy, as well as to dysfunction affecting these muscles and temporomandibular joints. Due to lack of proper nutrition, changed exterior, issues in interaction with others, this group of patients develop a whole set of psychosomatic reactions finally causing social withdrawal. Rehabilitation of patients with complete loss of teeth is an urgent issue. However, the effectiveness of prosthetic treatment depends not only on the denture manufacturing technology, but on the quality of functioning involving the maxillofacial organs in combination with the respective orthopedic appliances. Whereas precise and reliable assessment of the maxillofacial neuromuscular balance enables to predict immediate and long-term outcomes of orthopedic treatment. Employing the principles of neuromuscular dentistry allows us to assess reliably the changes in the reflex mechanisms of muscular apparatus. This was carried out throughout all the stages of prosthetic treatment in patients with complete adentia with intraosseous implants with fixed bridges and conditionally removable dentures.

KEYWORDS — neuromuscular dentistry, complete adentia, masticatory muscles functional activity, electromyography, occlusion computer analysis, dental implants.

INTRODUCTION

Loss of teeth entails serious changes affecting the masticatory system, which involves the bones, mucous membranes and muscles. The alveolar process bone tends to resorb, the development of a new bone slows down, the covering mucosa features a decrease in the number of receptors, thus resulting in reduced afferent pulsation. Sensitive receptors, such as neuromuscular spindles, periodontal and intradental pressure receptors, have a strong effect on the activity of motor neurons, and thereby — on muscle control. Most of the sensitive impulse connections with the motor impulse generated in the central nervous system occur at the level of premotoneurons located in the nucleus reticularis parvocellularis, in the trigeminal nerve medullary nucleus, and in the adjacent nuclei. Many cells in these nuclei have receptor fields in mucous membrane and respond to the pressure experienced by the teeth, as well as to extension of the masticatory muscles [15, 43].

Loss of teeth entails serious changes affecting the masticatory system, which involves the bones, mucous membranes and muscles. The alveolar process bone tends to resorb, the development of a new bone slows down, the covering mucosa features a decrease in the number of receptors, thus resulting in reduced afferent pulsation. Sensitive receptors, such as neuromuscular spindles, periodontal and intradental pressure receptors, have a strong effect on the activity of motor neurons, and thereby — on muscle control. Most of the sensitive impulse connections with the motor impulse generated in the central nervous system occur at the level of premotoneurons located in the nucleus reticularis parvocellularis, in the trigeminal nerve medullary nucleus, and in the adjacent nuclei. Many cells in these nuclei have receptor fields in mucous membrane and respond to the pressure experienced by the teeth, as well as to extension of the masticatory muscles [15, 43].

Rehabilitation of patients with complete adentia is not only an urgent interdisciplinary issue faced by orthopedic and surgical dentistry, yet also a social one. The rehabilitation objectives in this case include the following: restored chewing and speech function; jaw atrophy and osteoporosis prevention; shorter terms of functional adjustment to dentures; developing conditions for effective social adjustment of patients with complete adentia [7–10, 13, 19, 22–26, 30, 38, 42].

The issues above-mentioned can be resolved only taking in view of the pathogenesis of the dental system morphological and functional changes, which are due to complete loss of teeth. The prevention of progressive atrophy, jaw osteoporosis and change affecting the topographic and anatomical maxillofacial proportions in case of complete adentia rely on the preservation of blood supply, microcirculation and recovery of bioelectric activity in the jaw bone tissue [2, 12, 16, 29, 32, 37, 41].

The authors have proven that the mandible resting position in patients with complete adentia changes due to loss of function of proprioceptive receptors located in the periodontium. The factors affecting the mandible resting position include physiological reasons (volitional control over the jaw position, the emotional status, fatigue, parafunctions of the masticatory muscles) and pathological conditions of the maxillofacial area organs (diseases of muscles, joints, nervous regulation disorders) [1, 34].

Currently, the treatment of patients with complete adentia relies on prosthetic treatment with completely removable dentures, as well as on combined treatment, which involves surgical approaches for correcting topographic and anatomical conditions for removable prosthetics and endoprosthetics (implantation) for removable and non-removable prosthetics [4, 11, 20, 31, 40].

Intraosseous implants used to fix dentures adds to the stability of orthopedic structures, promotes improvement of the temporomandibular function, activates metabolism in the surrounding tissues, ensures uniform load distribution on the prosthetic bed tissues and multiple occlusal contacts of artificial teeth in case of a complicated jaw ratio, thus allowing arriving at high functional and aesthetic results [3, 18, 27, 33, 39]. The main advantage of dental implantation is the maximum preservation of the alveolar bone. The stress and tension on the bone tissue lead to an increase in the bone trabeculation, which enhances its density, so there is no pronounced atrophy of the jaw bone tissue. The authors claim that, from the stance of recovering the lost functions, prevention of jaw atrophy and osteoporosis, as well as in view of social well-being, implantation can be considered one of the most acceptable rehabilitation ways for patients with complete adentia [5, 17, 21, 28, 35].

Despite the available research data on changes affecting masticatory muscle function in case of complete adentia, the data concerning the status of the motor and tonic activity in the masticatory muscles in case of employing various rehabilitation methods when dealing with patients featuring complete loss of teeth, remains incomplete and lacks systematic arrangement.

Aim of study:

to evaluate the effectiveness of fixed and conditionally removable prosthetics based on the analysis of the functional activity in the masticatory muscles and the occlusion balance in patients with complete adentia.

MATERIALS AND METHODS

The study involved 11 patients (4 males, 7 females; median age — 56.2 ± 4.3) with complete aden-

tia, whose orthopedic rehabilitation relied on bridge-shaped metal-ceramic prostheses with cement fixation (Group 1; $n = 2$) and conditionally removable prostheses with beam fixation (Group 2; $n = 9$). The exclusion criteria were hemorheological, mental, oncological diseases, as well as general somatic diseases in their decompensation stage. The patients had titanium screw implants installed: Touareg (ADIN Dental implant systems Ltd, Israel) — 3 patients, 30 implants; SPI (Alpha-Bio.Tec. Ltd, Israel) — 8 patients, 70 implants. The installation of intraosseous dental implants was performed subject to the traditional two-stage technique with delayed loading. In the first week following the surgery, a provision structure was made. 3–6 months after the surgery and the end of implant engraftment, there were abutments attached to them. After the gum contour was shaped, with full-fledged osteointegration (objective stability of implants following the Periostest method — 3.7 ± 1.6) and upon checking the correctness of the central point's location and the axes of implants, patients with complete adentia underwent clinical and laboratory stages required to manufacture dental prosthetic structures. The final load, therefore, was applied 3–6 months after the plantation.

Two patients of Group 1 had bridge-shaped metal-ceramic prostheses made for them with cement fixation supported by 8 implants for the upper jaw, and 6 implants — for the lower jaw (Fig. 1).

The 9 patients of Group 2, following the All-on-4 implantation surgical protocol (Palo Malo), had four implants installed in the following positions: two implants were installed in the bulk of the available bone tissue in the frontal part of the jaw, with another two implants installed more distally at an angle of up to 45° , not affecting the maxillary sinus inner wall in the upper jaw, the mandibular canal and the mental opening in the lower jaw (sinus lifting and lateralization of the mandibular nerve are excluded). The primary stabilization of the implants through the surgery was $30\text{--}35\text{ N/cm}^2$, which allowed having direct loading on the implants. Subject to the All-on-4 implantation protocol, the sutures were removed on the 10th day following the surgery. The beams were made by milling by CAD/CAM (Fig. 2).

The study of the masticatory muscles functional status was carried out through the bioelectric activity of the proper masticatory muscles and the anterior part of the temporal ones were recorded simultaneously on both sides during the functional state of rest of the lower jaw as well as during a chewing test (0.8g of almonds). The electromyograms were evaluated by the shape, amplitude and duration of the bioelectric activity phases corresponding to muscle contraction. The analysis of the bioelectric activity and bioelec-

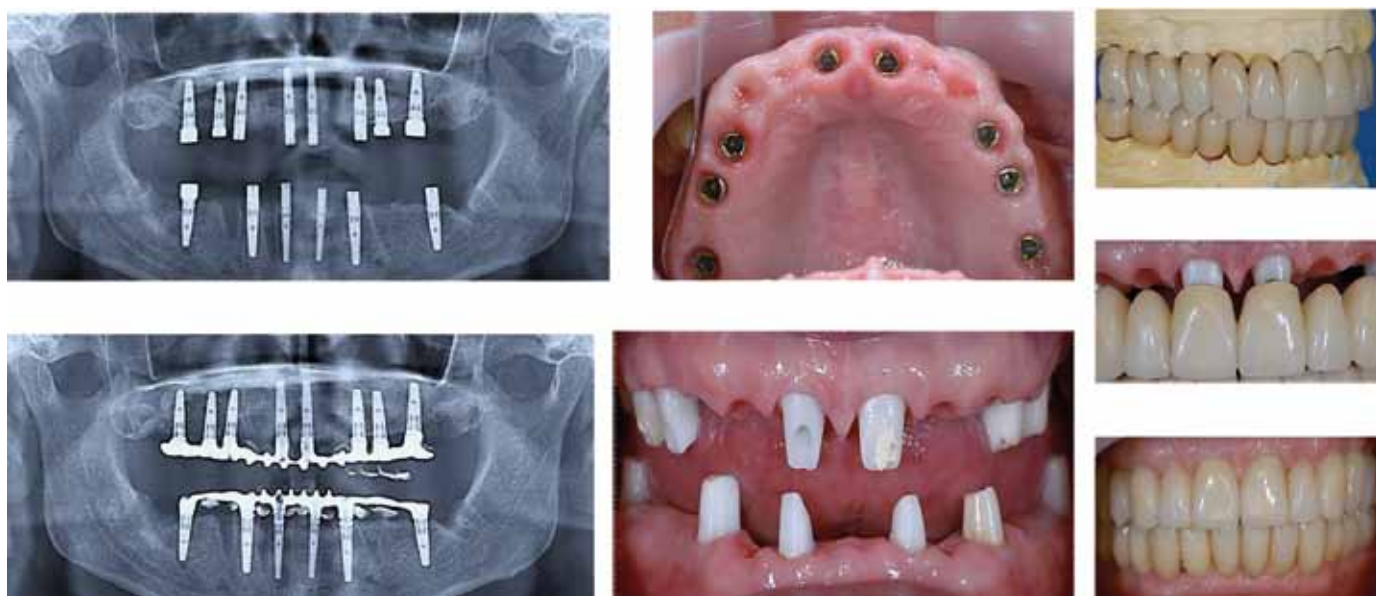


Fig. 1. Installed (a) and osteointegrated (b, c) dental implants on the upper and lower jaws; individual full-ceramic Procera abutments on dental implants (d); metal-ceramic structures in the articulator (e) and in the oral cavity (f, g)

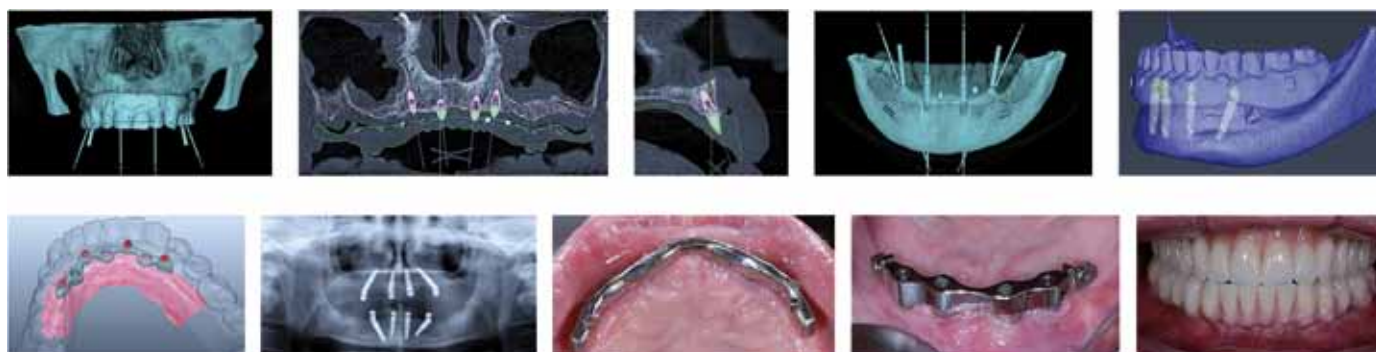


Fig. 2. Planning of dental implantation in the frontal part of the upper and lower jaw (a–f); osteointegrated (g) dental implants on the upper and lower jaws; installed beam structures on dental implants on the upper (h) and lower (i) jaws; conditionally removable dentures in the oral cavity (k)

tronic rest duration offers an idea of the excitation and torsion process, as well as of the muscle endurance. Matching of electromyograms of the muscles on the right and left sides allows identifying the side of chewing, its type, and the coordination of the muscles of both sides. When processing electromyograms, the following was detected: A_{ch} — the average amplitude of biopotentials in the phase of bioelectric activity of the muscles through chewing the nuts (microvolts); A_{avch} — the average amplitude of biopotentials in the phase of bioelectric activity of the muscles during the maximal jaw compression (microvolts); T_a — the time of bioelectric activity of the muscles during excitation through the phase of one chewing movement (sec); T_r

— the time of bioelectric muscle activity during rest in the phase of one chewing movement (sec); coefficient K ($K = T_a / T_r$); the time of one chewing movement ($T_a + T_r$) (sec).

Occlusion analysis was done employing the T-scan III system, which real-time-recorded the sequence of occlusal contacts, their localization, time, the portion of each tooth and the resulting strength of the total occlusal load. In each record, there was detection made for the period of the first occlusal contact occurrence and its location, the presence or lack of contacts between all teeth, as well as the percentage distribution of the balance of forces between the left and right sides at the time of multiple occlusion.

To study the tone of the masticatory muscles (that of proper masticatory and temporal ones), a SZIRMA myotometer (METRIMPEX, Hungary) was used. The device is equipped with a scale calibrated in grams, and a probe with a contact pad. When immersing the probe in the motor point (the most convex part of the muscle), the moment the restrictive area touched the skin, the readings on the scale were taken using light indication. The measurements were taken both at resting (T_r) and at stressed (T_s) condition of the masticatory muscles. Myofunctional studies and T-scan studies were carried out on the day the fixation was applied, one month and six months following the installation of permanent prosthetic structures. The statistical analysis of the study outcomes was done with the Statistica 12.0 software (StatSoft Inc., USA).

RESULTS AND DISCUSSION

The results obtained through the electromyographic (EMG) studies of M. masseter and M. temporalis in Group 1 on the right (dexter, D) and on the left (sinister, S) featured no statistically meaningful differences, which allowed them to be combined (Table 1, 2).

The difference in electromyographic (EMG) studies of M. masseter and M. temporalis in Group 2 patients on the right (dexter, D) and on the left (sinister, S) featured no statistical differences, which allowed them to be combined (Table 3, 4).

Examining the results of the magnitude of the biopotentials average amplitude with the maximum reduction of M. masseter (D), M. masseter (S) and M. temporalis (D), M. temporalis (S) in the two groups, revealed that the values were most optimal one month after the introduction of dental prosthetic structures: Group 1 — $418.5 \pm 35.1 \mu V$ and $377.4 \pm 33.8 \mu V$, respectively; Group 2 — $314.7 \pm 26.8 \mu V$ and $284.4 \pm 23.1 \mu V$, respectively.

The maximum values of the biopotentials average amplitude of M. masseter (D), M. masseter (S), M. temporalis (D), and M. temporalis (S) during functional loading (0.8 g of nut chewing) in patients of both groups were observed six months after the application of prosthetic structures, namely, Group 1 — $363.3 \pm 28.1 \mu V$ and $345.7 \pm 24.8 \mu V$, respectively; Group 2 — $279.4 \pm 18.7 \mu V$ and $263.9 \pm 17.8 \mu V$, respectively.

The examination of the *excitation time* indicator in patients of both groups shows that the

Table 1. Functional characteristics of M. masseter (D) and M. masseter (S), Group 1, ($p > 0.05$)

EMG indicators	Terms of examination		
	On the application day	1 month	6 months
Chewing amplitude, μV	209.2 ± 18.9	351.8 ± 27.6	363.3 ± 28.1
Maximum compression amplitude, μV	256.4 ± 21.3	418.5 ± 35.1	421.6 ± 34.7
Rest time T_r , sec	0.43 ± 0.02	0.37 ± 0.03	0.36 ± 0.02
Excitation time T_a , sec	0.48 ± 0.02	0.41 ± 0.03	0.39 ± 0.03
$K = T_a/T_r$	1.12 ± 0.03	1.11 ± 0.02	1.08 ± 0.02
Time of one chewing movement $T_a + T_r$, sec	0.91 ± 0.02	0.78 ± 0.03	0.75 ± 0.02

Table 2. Functional characteristics of M. temporalis (D) and M. temporalis (S), Group 1, ($p > 0.05$)

EMG indicators	Terms of examination		
	On the application day	1 month	6 months
Chewing amplitude, μV	191.7 ± 17.6	339.2 ± 25.9	345.7 ± 24.8
Maximum compression amplitude, μV	239.1 ± 20.2	377.4 ± 33.8	375.8 ± 32.3
Rest time T_r , sec	0.35 ± 0.03	0.31 ± 0.02	0.29 ± 0.02
Excitation time T_a , sec	0.42 ± 0.03	0.35 ± 0.02	0.32 ± 0.03
$K = T_a/T_r$	1.20 ± 0.02	1.13 ± 0.03	1.10 ± 0.02
Time of one chewing movement $T_a + T_r$, sec	0.77 ± 0.03	0.66 ± 0.02	0.61 ± 0.02

Table 3. Functional characteristics of *M. masseter (D)* and *M. masseter (S)*, Group 2, ($p>0.05$)

EMG indicators	Terms of examination		
	On the application day	1 month	6 months
Chewing amplitude, μV	157.8 ± 17.4	268.3 ± 19.1	279.4 ± 18.7
Maximum compression amplitude, μV	194.1 ± 21.3	314.7 ± 26.8	318.8 ± 25.6
Rest time T_r , sec	0.49 ± 0.04	0.45 ± 0.02	0.43 ± 0.03
Excitation time T_a , sec	0.54 ± 0.03	0.46 ± 0.04	0.45 ± 0.02
$K = T_a/T_r$	1.10 ± 0.02	1.02 ± 0.03	1.05 ± 0.02
Time of one chewing movement $T_a + T_r$, sec	1.03 ± 0.03	0.91 ± 0.02	0.88 ± 0.03

Table 4. Functional characteristics of *M. temporalis (D)* and *M. temporalis (S)*, Group 2, ($p>0.05$)

EMG indicators	Terms of examination		
	On the application day	1 month	6 months
Chewing amplitude, μV	146.2 ± 16.3	257.9 ± 18.4	263.9 ± 17.8
Maximum compression amplitude, μV	181.6 ± 20.4	284.4 ± 23.1	282.5 ± 22.7
Rest time T_r , sec	0.43 ± 0.03	0.42 ± 0.02	0.38 ± 0.03
Excitation time T_a , sec	0.51 ± 0.02	0.43 ± 0.03	0.42 ± 0.02
$K = T_a/T_r$	1.19 ± 0.03	1.02 ± 0.02	1.11 ± 0.03
Time of one chewing movement $T_a + T_r$, sec	0.94 ± 0.02	0.85 ± 0.03	0.80 ± 0.02

maximum values were obtained on the day the dental structures were applied (Group 1 — 0.48 ± 0.02 sec and 0.42 ± 0.03 sec, respectively; Group 2 — 0.54 ± 0.03 sec and 0.51 ± 0.02 sec, respectively). The minimum parameters of the active period through one chewing movement the phase were identified six months following the introduction of the prostheses (Group 1 — 0.39 ± 0.03 sec and 0.32 ± 0.03 sec respectively; Group 2 — 0.45 ± 0.02 sec and 0.42 ± 0.02 sec, respectively).

Studying the *rest time* indicator allows stating that in both groups the maximum values were obtained on the day of applying the prosthetic structures (Group 1 — 0.43 ± 0.02 sec and 0.35 ± 0.03 sec, respectively; Group 2 — 0.49 ± 0.04 sec and 0.43 ± 0.03 sec, respectively). The lowest values of the passive period in one chewing movement phase were to be observed six months after the application of the prostheses (Group 1 — 0.36 ± 0.02 sec and 0.29 ± 0.02 sec, respectively; Group 2 patients — 0.43 ± 0.03 sec and 0.38 ± 0.03 sec, respectively), which points at a gradual proper recovery of the tone and bio-electrical activity in the muscle fibers after loading.

An analysis of the *K* coefficient revealed that on the day the dental structures were installed (Group 1 — 1.12 ± 0.03 and 1.20 ± 0.02 , respectively; Group 2 — 1.10 ± 0.02 and 1.19 ± 0.03 , respectively), its value was maximum, which is to be accounted for by a sig-

nificant predominance of the bioelectric activity time over the bioelectric rest time and the initial phases of adjustment to the dental structures. Further on, the *K* coefficient value decreased following six months the installation of the dentures, reaching 1.08 ± 0.02 and 1.10 ± 0.02 , respectively, in Group 1, and 1.05 ± 0.02 and 1.11 ± 0.03 , respectively, in Group 2. The nearly full balance between the bioelectric excitation time and the bioelectric rest time six months after the prosthetic structures were installed, combined with a reduction in the one chewing movement time in both groups, means the completion of adjustment to new occlusal relationships after applying the prosthesis and the restructuring the masticatory muscles coordination ratios.

Qualitative assessment of the obtained electromyograms showed that in both groups, after the prosthetic structures were installed, the vibration amplification assumes some typical Spindle-shaped appearance, with clarity appearing in the rotation between biopotential impulses and rest periods, as well as there was some synchronicity and symmetry identified in the function of the examined muscles, with no chaotic bursts in biopotentials (Fig. 3).

Occlusiogram analysis in Groups 1 and 2 following the installation of the prosthetic structures showed that all cases featured occlusion issues: uneven distribution of occlusal load between the left and the

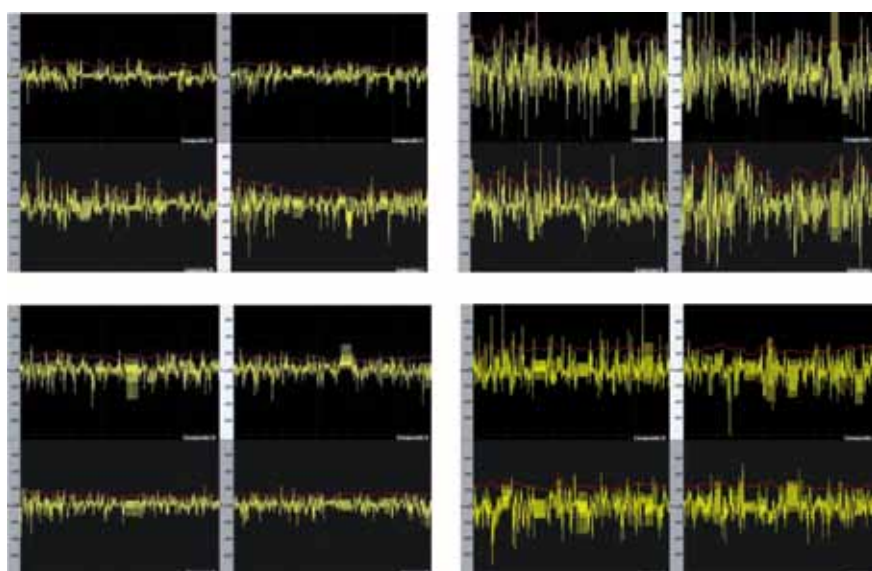


Fig. 3. Electromyograms of the biopotential dynamics in the M. temporalis and M. masseter performance at the stages of adjustment: on the day of the dentures were applied (a — Group 1, b — Group 2); 6 months after the dentures were applied (c — Group 1, d — Group 2)

right dentition sides; an increase in the time required to arrive at the maximum inter-tubercular contact (in Group 1 — up to 2.7 sec; in Group 2 — up to 4.3 sec); displaced total vector. As computer occlusiography (T-Scan device) showed, all patients (100%) of both groups were found to have: occlusive issues manifesting as premature contacts; supercontacts; displaced total vector of occlusive load; disturbed occlusion balance between the left and the right sides; unequal distribution of contacts over the area. We believe that the similarity of signs for the occlusion issues in the two groups developed due to lengthy lack of teeth and adaptive-compensatory restructuring of the maxillary system (Fig. 4).

6 months following the installation of dentures in Group 1, there was a more effective recovery of occlusive balance observed (50/50 balance was observed in 100% of patients), whereas in Group 2, a 50/50 balance was to be seen in 67% of cases (n=6). The time required to arrive at the maximum inter-tubercular contact decreased, reaching 0.23 ± 0.01 sec in Group 1, and 1.02 ± 0.01 sec — in Group 2. A recovered trajectory of the relative straightness of the occlusal load total vector was found in all the patients of Group 1 and in 88% of the patients (n=8) in Group 2 (Fig. 5).

The dynamics of changes in the M. masseter (D, S) and M. temporalis (D, S) tone in Groups 1 and 2 can be seen in Table 5, 6.

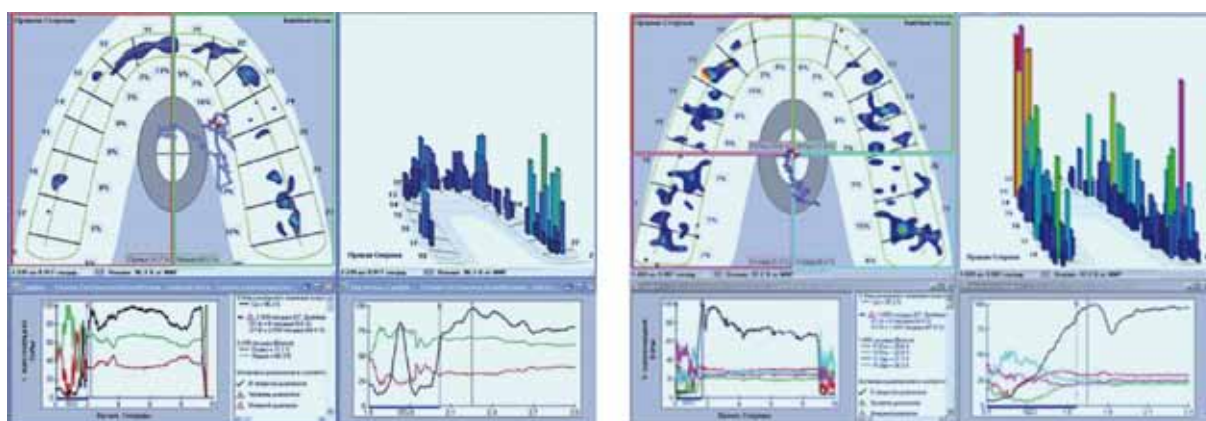


Fig. 4. Computer analysis of the occlusion following the fixation of dentures at maximum closure. Imbalanced occlusal load between the left and the right sides of the dentition (a — Group 1, b — Group 2)

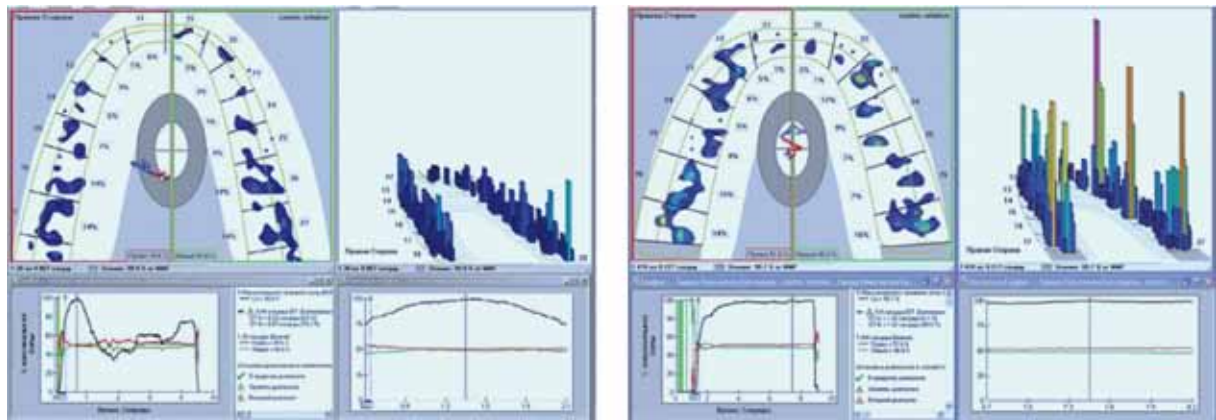


Fig. 5. Computer analysis of occlusion following 6 months from the date the dentures were applied at maximum closure (a – Group 1, b – Group 2)

Table 5. Tone indicators for *M. masseter* (D, S) and *M. temporalis* (D, S), Group 1, (g), ($p>0.05$)

Tone indicators	Terms of examination		
	On the application day	1 month	6 months
<i>M. masseter</i> (D, S)			
Resting tone, Tr	27.9 ± 7.4	47.8 ± 5.1	49.3 ± 5.6
Stress tone, Ts	81.6 ± 14.2	162.7 ± 10.6	167.3 ± 9.2
<i>M. temporalis</i> (D, S)			
Resting tone, Tr	30.4 ± 6.8	45.4 ± 5.9	48.1 ± 8.1
Stress tone, Ts	89.1 ± 8.4	150.2 ± 9.3	156.9 ± 9.7

Table 6. Tone indicators for *M. masseter* (D, S) and *M. temporalis* (D, S), Group 2, (g), ($p>0.05$)

Tone indicators	Terms of examination		
	On the application day	1 month	6 months
<i>M. masseter</i> (D, S)			
Resting tone, Tr	22.1 ± 7.7	37.2 ± 6.3	38.5 ± 5.1
Stress tone, Ts	64.2 ± 11.9	126.9 ± 8.8	129.4 ± 7.8
<i>M. temporalis</i> (D, S)			
Resting tone, Tr	24.5 ± 6.9	35.0 ± 6.6	36.9 ± 7.5
Stress tone, Ts	69.7 ± 7.2	114.9 ± 7.6	117.4 ± 9.1

The resting tone indicators for *M. temporalis* in patients of the groups exceeded the similar parameters of *M. masseter*, on average by 3.1 ± 0.6 grams, while the stress tone indicators of *M. temporalis* exceeded similar values of *M. masseter*, on average by 8.6 ± 4.7 grams through all the stages of functional status recovery in the chewing muscles in case of using prosthetics to treat patients with complete adentia.

The growth rates of masticatory muscle tone indicators by month 6 following the installation of prosthetic structures in Group 1 (*M. masseter*: resting

tone — $76.7 \pm 5.4\%$, stress tone — $105.0 \pm 8.7\%$; *M. temporalis*: resting tone — $58.2 \pm 4.7\%$, stress tone — $76.1 \pm 7.3\%$) exceeded the increase dynamics in functional indicators of Group 2 (*M. masseter*: resting tone — $74.2 \pm 4.6\%$, tension tone — $101.6 \pm 7.9\%$; *M. temporalis*: resting tone — $50.6 \pm 4.1\%$, tension tone — $68.4 \pm 5.9\%$).

The above shows that in almost all patients, within 3–6 months following the installation of fixed and conditionally removable dentures relying on intra-osseous implants, there was proper recovery observed

in the masticatory and phonetic function. Besides, prevention of jaw atrophy and osteoporosis, improved functional adjustment to the dentures, all this should contribute to the patient's better overall health status and higher quality of life.

CONCLUSIONS

1. The results of our functional studies show that employing fixed and conditionally removable prosthetics relying on intraosseous implants in patients with complete adentia leads by the 6th month after installation of prosthetic structures to improved position of the lower jaw and optimal spatial ratio of TMJ elements. We also observed an improved functional status of the masticatory muscles due to improved bioelectric activity, elimination of occlusal imbalance, restored coordination between M. masseter (D, S) and M. temporalis (D, S).

2. Electromyography data, 6 months after the installation of the prostheses revealed symmetric involvement of the temporal and masticatory muscles observed in the jaws closing, which basically matched the conventional values typical of the normal indicators. The balance between the bioelectric excitation time and the bioelectric rest time in combination with a reduction in the one chewing movement time, as well as a significant decrease in the spontaneous activity of M. masseter (D, S) and M. temporalis (D, S) in both groups down to the upper limits of the normal values could be attributed to the emergence of uniform occlusive contacts in the position of central occlusion on the teeth of the right and left sides after prosthetic treatment. This is a tendency towards completion of the adjustment process and compensatory restructuring of the dental system in view of the new occlusive balance.

3. As computer occlusiograms and electromyograms show, higher indicators of the clinical and functional effectiveness of orthopedic treatment offered to patients with complete adentia, using fixed bridges relying on intraosseous implants, in contrast to prosthetics with conditionally removable dentures, are due to reduced time of the occlusal balance improvement (50/50); reduced time required to achieve maximum inter-tubercular contact (below 0.3 seconds); recovered trajectory of relative straightness of the occlusal load total vector; basically complete balance between the bioelectric excitation time and the bioelectric rest time after six months from the moment the prosthetic structures were installed, combined with a reduction in the one chewing movement time in both groups.

4. Electromyography, as a basic method for functional research, allows studying the coordination of the antagonist and synergist muscles operation prior

to, and through, surgical treatment, while comparative electromyography helps identify the degree and the type of chewing in a particular clinical case. Electromyography results can serve as an objective indicator pointing at the masticatory muscles functional status, as well as at the effectiveness of orthopedic treatment.

5. Interdisciplinary studies should be part of the entire set of comprehensive diagnostics and examination administered to patients with complete adentia and seeking a complete reconstruction of the dentition. Such examination should include assessment of the musculoskeletal condition, neurological and psychological status, the patient's quality of life, as well as consultations of respective specialists.

6. The tone in the masticatory muscles does not increase in strict proportion to the developed force of masticatory contractions. The interdependence between the tone of the masticatory muscles and the compression force is subject to individual fluctuations, with no direct relationship between the increase rate in the masticatory muscle tone and the compression force.

REFERENCES

1. **ASH M.M.** Wheeler's dental anatomy, physiology and occlusion. Philadelphia: WB Saunders; 2003.
2. **BOUCHER S.** Prosthodontic Treatment for Edentulous Patients / S. Boucher, G. A. Zarb, C. L. Bolender, G. E. Carlsson. – Mosby, 1997. – 558 p.
3. **BAIRIKOV I.M., GAIVORONSKAYA T.V., DEDIKOV D.** Reconstruction of mandibular defects using individual vascularized autografts combined with macroporous titanium fiber material // *Archiv EuroMedica*. 2021. Vol. 11. № 1. P. 147-159. <https://doi.org/10.35630/2199-885X/2021/11/1.32>
4. **BARONE A, CORNELINI R, CIAGLIA R, COVANI U.** Implant placement in fresh extraction sockets and simultaneous osteotome sinus floor elevation: a case series. *International Journal of Periodontics and Restorative Dentistry*, 2008, 28:283-289.
5. **CRISTACHE C.M., ILIESCU A.A., CRISTACHEET G. ET AL.** Four-years evaluation of different retention systems for implant-supported overdentures. *Clin. Oral Implants Res.* 2011; 22(9): 984-5.
6. **CHAN, C.A.** Common myths of neuromuscular dentistry and the five basic principals of neuromuscular occlusion. *Sept./Oct. Vol.2, Number 5. LV1 Dental Vision*; 2002:10-11.
7. **DMITRIENKO S.V.** Analytical approach within cephalometric studies assessment in people with various somatotypes. *Archiv EuroMedica*. 2019. Vol. 9; 3: 103-111. <https://doi.org/10.35630/2199-885X/2019/9/3.29>
8. **DMITRIENKO S.V.** Enhancement of research method for spatial location of temporomandibular elements and maxillary and mandibular medial incisors. *Archiv*

- EuroMedica. 2019. Vol. 9. № 1. P. 38–44. <https://doi.org/10.35630/2199-885X/2019/9/1/38>
9. **DOMENYUK D.** Structural arrangement of the temporomandibular joint in view of the constitutional anatomy. *Archiv EuroMedica*. 2020. Vol. 10. № 1. P. 126–136. <https://doi.org/10.35630/2199-885X/2020/10/37>
 10. **FISCHEV S.B., PUZDYRYOVA M.N.** Morphological features of dentofacial area in peoples with dental arch issues combined with occlusion anomalies // *Archiv EuroMedica*. 2019. Vol. 9; 1: 162–163. <https://doi.org/10.35630/2199-885X/2019/9/1/162>
 11. **FOMIN I.V., IVANOV S.Yu.** Efficiency of osseointegration properties manifestation in dental implants with hydroxyapatite plasma coating // *Archiv EuroMedica*. 2019. Vol. 9; 1: 138–139. <https://doi.org/10.35630/2199-885X/2019/9/2/138>
 12. **GHAMDAN AL.H.** A method for modeling artificial dentures in patients with adentia based on individual sizes of alveolar arches and constitution type. *Archiv EuroMedica*. 2021. Vol. 11; 1: 109–115. <https://doi.org/10.35630/2199-885X/2021/11/1.25>
 13. **GROSS, M. D.** Occlusion in Restorative Dentistry / M. D. Gross. Mathews. Churchill Livingstone, Edinburgh, London, Melbourne and New York, 1982. 169 p.
 14. **GUYTON A.C.** Human Physiology and Mechanisms of Disease. 6th ed. Philadelphia: WB Saunders Co. – 1997. – 737p.
 15. **FULLER J.L., DENEHY G.E., SCHULEIN T.M.** Concise Dental Anatomy and Morphology. 4th ed. USA: Univ of Iowa Office of State; 2001.
 16. **HAYAKAWA I.** Principles and Practices of Complete Dentures / I. Hayakawa. – Tokyo, 2001. – 255 p.
 17. **KARPYUK V.B., PEROVA M.D., GILEVICH I.V., SEVOSTYANOV I.A.** Cell-potentiated regenerative technologies for restoring jaw bone tissues in case of odontogenic inflammatory & destructive process // *Archiv EuroMedica*. 2019. Vol. 9. № 2. P. 140–146. <https://doi.org/10.35630/2199-885X/2019/9/2/140>
 18. **KARPYUK V.B., PEROVA M.D.** Innovation-based approach in reconstruction of reduced jaw alveolar ridge bone using cell regeneration technologies // *Archiv EuroMedica*. 2019. Vol. 9. № 2. P. 147–155. <https://doi.org/10.35630/2199-885X/2019/9/2/147>
 19. **IVANYUTA O.P., AL-HARASI G.** Modification of the dental arch shape using graphic reproduction method and its clinical effectiveness in patients with occlusion anomalies // *Archiv EuroMedica*. 2020. Vol. 10; 4: 181–190. <https://dx.doi.org/10.35630/2199-885X/2020/10/4.42>
 20. **KARABUDA C, YALTIRIK M, BAYRAKTAR M.** A clinical comparison of prosthetic complications of implant-supported overdentures with different attachment systems. *Implant Dent*. 2008;17:74–81. DOI: 10.1097 / ID.0b013e318166d88b.
 21. **KOBZEVA Yu.A., OSTROVSKAYA L.Yu.** The impact of osteoplastic compositions on remodeling of bone tissue in immunodeficient animals: experimental study. *Archiv EuroMedica*. 2020. Vol. 10; 2: 26–29. <https://dx.doi.org/10.35630/2199-885X/2020/10/2.7>
 22. **KOCHKONYAN T.S., AL-HARAZI G.** Specific features of variant anatomy and morphometric characteristics of the palatal vault in adults with different gnathic and dental types of arches. *Archiv EuroMedica*. 2021. Vol. 11; 3: 54–60. <https://dx.doi.org/10.35630/2199-885X/2021/11/3/14>
 23. **KOCHKONYAN T.S., AL-HARAZI G.** Morphometric patterns of maxillary apical base variability in people with various dental arches at physiological occlusion. *Archiv EuroMedica*. 2021. Vol. 11; 4: 123–129. <https://dx.doi.org/10.35630/2199-885X/2021/11/4.29>
 24. **KONDRATYEVA T.** Methodological approaches to dental arch morphology studying. *Archiv EuroMedica*. 2020. Vol. 10; 2: 95–100. <https://dx.doi.org/10.35630/2199-885X/2020/10/2.25>
 25. **KONDRATYUK A., SUBBOTIN R., PUZDYREVA M., FISCHEV S., LEPILIN A.V.** Dependence of facial morphometric parameters from masticatory muscles tone in people with horizontal type of increased dental abrasion. *Archiv EuroMedica*. 2019. Vol. 9; 3: 91–96. <https://dx.doi.org/10.35630/2199-885X/2019/9/3.26>
 26. **KOROBKEEV A. A.** Morphological features of the maxillofacial region in patients with full secondary adentia and variations of the constitution. *Medical News of North Caucasus*. 2020;15(4):539–543. DOI – <https://doi.org/10.14300/mnnc.2020.15127> (In Russ.)
 27. **KUPRYAKHIN S.V., LEPILIN A.V., KUPRYAKHIN V.A.** Optimization of dental implantation combined with closed sinus lift in patients with low maxillary sinus floor // *Archiv EuroMedica*. 2019. Vol. 9; 2: 117–121. <https://doi.org/10.35630/2199-885X/2019/9/2/117>
 28. **KUPRYAKHIN S.V., LEPILIN A.V., KUPRYAKHIN V.A., POSTNIKOV M.A.** Potential introduction of cell technologies to improve dental implant surface preparing // *Archiv EuroMedica*. 2019. Vol. 9; 2: 122–129. <https://doi.org/10.35630/2199-885X/2019/9/2/122>
 29. **LEPILIN A.V., PUZDYRYOVA M.N., SUBBOTIN R.S.** Dependence of stress strain of dental hard tissues and periodontal on horizontal deformation degree // *Archiv EuroMedica*. 2019. Vol. 9; 1: 173–174. <https://doi.org/10.35630/2199-885X/2019/9/1/173>
 30. **LEPILIN A.V.** A biometric approach to diagnosis and management of morphological changes in the dental structure. *Archiv EuroMedica*. 2020. Vol. 10; 3: 118–126. <https://dx.doi.org/10.35630/2199-885X/2020/10/3.30>
 31. **MALO P.** Short implants placed one-stage in maxillae and mandibles: a retrospective clinical study with 1 to 9 years of follow-up / P. Malo, M. de Araujo Nobre, B. Rangert // *Clin. Implant Dent. Relat. Res*. 2007. Vol. 9, № 1. – P. 15–21. DOI: 10.1111 / j.1708-8208.2006.00027.x

32. **MAZHAROV V. N.** Peculiarities of the orientation of the occlusion plane in people with different types of the gnathic part of the face. *Medical News of North Caucasus*. 2021;16(1):42-46. DOI – <https://doi.org/10.14300/mnnc.2021.16011> (In Russ.)
33. **MISCH C.M.** Dental Implant Prosthetics. // St.Louis: Mosby-Year Book. 2005. – 567 p.
34. **NELSON S.J.** Wheeler's dental anatomy, physiology, and occlusion [Text] / S.J. Nelson. – London: Second Edition. – 2015 – 350 s. – ISBN: 978-0-323-26323-8
35. **PALARIE V.** Three years follow-up study of egg-shaped Dolder bar and ball anchors retention devices for implant-supported overdentures. *Clin. Oral Implants Res.* 2011; 22(9): 999–1000.
36. **RASHMI G.S.** Textbook of Dental Anatomy, Physiology and Occlusion. 1st ed. New Delhi: Jaypee Brothers Medical Publishers Ltd; 2014. DOI: 10.5005 / jp / books / 11841
37. **SADYKOV M.I., NESTEROV A.M., ERTESYAN A.R., KONNOV V.V., MATROSOV V.** Biomechanical evaluation of stress -strain condition of restorative ceramic pin structures and dental roots. *Archiv EuroMedica*. 2020. Vol. 10. № 2. P. 115–120. <https://doi.org/10.35630/2199-885X/2020/10/2.29>
38. **SADYKOV M.I., NESTEROV A.M., ERTESYAN A.R., KONNOV V.V., SINEV I.I.** Biomechanical assessment of the stress-strain status of splinting structures and teeth periodontium in case of chronic periodontitis // *Archiv EuroMedica*. 2020. Vol. 10; 4: 149–155. <http://dx.doi.org/10.35630/2199-885X/2020/10/4.34>
39. **STOKER G.T., WISMEIJER D., VAN WAAS M.A.** An eight-year follow-up to a randomized clinical trial of aftercare and cost-analysis with three types of mandibular implant-retained overdentures. *J. Dent. Res.* 2007; 86 (3): 276-80. DOI: 10.1177 / 154405910708600315
40. **SLOT W., RAGHOEBAR G.M., VISSINK A., HUDDELESTON SLATER J.J., MEIJER H.J.** A systematic review of implant-supported maxillary overdentures after a mean observation period of at least 1 year. *J Clin Periodontol.* 2010;37:98–110. DOI: 10.1111 / j.1600-051X.2009.01493.x.
41. **SHKARIN V.V., KOCHKONYAN T.S., GHAMDAN AL.H.** Occlusal plane orientation in patients with dentofacial anomalies based on morphometric craniofacial measurements. *Archiv EuroMedica*. 2021. Vol. 11; 1: 116–121. <https://doi.org/10.35630/2199-885X/2021/11/1.26>
42. **ZARB, G. A.** Boucher's prosthodontic treatment for edentulous patients / G. A. Zarb, C. L. Bolender, G. E. Carlsson. Mosby, Inc., 1997. 135 p.
43. **WILE D.R.** Muscle, Studies in Biology. 2nd ed. London: A Edward Ltd; 1979.

<http://dx.doi.org/10.35630/2199-885X/2022/12/2.30>

EFFECTIVENESS OF DENTAL IMPLANTATION WITH IMMEDIATE LOADING WHEN REPLACING FRONTAL DENTITION DEFECTS

Received 02 January 2022;
Received in revised form 01 February 2022;
Accepted 03 February 2022

Alexandr Lepilin¹ , Maria Shalina¹,
Nadezhda Erokhina¹, Natalia Zakharova¹,
Sergey Fischev², Arkady Sevastyanov²,
Yana Chernenko¹ , Dmitry Domenyuk^{3,4} 

¹ Saratov State Medical University, Saratov;

² St. Petersburg State Pediatric Medical University, St. Petersburg;

³ Stavropol State Medical University, Stavropol;

⁴ Pyatigorsk Medical and Pharmaceutical Institute — Branch of the Volgograd State Medical University, Pyatigorsk, Russia

✉ lepilins@mail.ru

ABSTRACT — Dental implantation, viewed as an independent research-based method used to treat patients with partial and complete adentia, has a special place among the major dental specialties. There are surgical algorithms and established methods for using dental implants available. The classical two-stage implantation protocol with delayed loading is considered the most reliable and predictable, featuring the lowest complication rate. The increased interest in direct dental implantation with immediate loading can be accounted for by psycho-emotional factors, accelerated implant osseointegration, better functional and aesthetic results, prevention of alveolar process bone atrophy, as well as reduced volume of surgical and orthopedic interventions. The stability of dental implants after direct implantation and immediate loading has been found to match the stability of implants after employing a two-stage technique. The primary stability of dental implants installed directly into the hole of the removed tooth on the anterior mandible is due to a small volume of spongy substance at a significantly thick cortical layer, possible installation of an implant with a length exceeding the length of the tooth root, the availability of a proper keratinized gum zone, as well as the removal from occlusion temporary structures on implants.

KEYWORDS — dental implantation, immediate loading, osseointegration, frontal mandible.

INTRODUCTION

Prosthetics on dental implants is currently considered as one of the most common orthopedic methods used to treat dentition defects of various lengths [3, 4, 20–22].

The standard two-stage implantation protocol takes 3–6 months right before prosthetics, which has a

significant negative impact on the patient's life quality at the treatment stages. Direct prosthetics implying the installation of implants in the hole of a removed tooth or in the area of a long-missing tooth has been proven effective by positive clinical outcomes [6, 9].

The idea of im-mediate prosthetics involves the fixation of abutments and temporary crowns straight after the im-plants are installed. The requirements for direct prosthetics include good quality of the bone tissue (Type DI, DII type); possible installation of 10–16 mm long implants; available duly keratinized gum zone; possible removal from occlusion of the temporary prosthesis on implants. Single-stage implantation and direct prosthetics allow installing the implant in the hole right after the respective tooth was extracted, while achieving the stability of the implant will require its length exceeding the roots of the teeth, thus improving the intra- vs. extra-bone part ratio of the structure. The authors claim that the specifics of dental implantation in the chin part of the mandible are due not to lack of anatomical structures that complicate the installation, yet also to the lack of bone tissue required for implantation [5, 6, 9].

Arriving at a positive outcome of dental implantation will take considering the respective anatomical and topographic features [5], a thorough surgery plan, studying all possible ways to measure the implant stability [6], and due examination of the gingival sulcus cytokine profile at the installed implants [1, 2, 7, 8, 12–18]. Additional treatment, including medication, following dental implantation surgery, plays a significant role, too [6, 9–11].

The subject of the study focusing on the reliability of implants in case of direct installation in the upper jaw (palatine installation) and lower jaw (lingual installation) after removal of single-root teeth was the size, the topography of the installed implants, the stability, and the absence of pain and inflammation. As the authors found, direct implantation can offer predictable anatomical, functional and aesthetic results, regardless of the implant size and location, whereas their survival rate reaches 96% [19].

According to the reference literature the effectiveness of dental implantation in the frontal mandible

underlying various installation protocols has not been studied well enough.

Aim of the study:

to develop a surgical treatment algorithm forecasting possible immediate load on dental implants for improved dental implantation in the anterior mandible

MATERIALS AND METHODS

The study involved 83 patients (42 males and 41 females) aged 20–50, with anterior mandible dentition issues. The patients were divided into groups as follows: Group 1 — patients (n=12, 14.5%) who had undergone orthopedic treatment with no dental implants used; Group 2 — patients (n=25, 30.0%) who had dental implants installed 5–6 following the teeth removal (comparison group), while the load on the installed implants was applied 3–6 months later (Fig. 1);

Impro, AnyRidge, AnyOne, Osstem MS; diameter — 2.5–3.3 mm; length — 10 mm) were installed in the frontal mandible.

To identify the stability and osseointegration, a MEGA ISQ device was used, the performance of that based on the registration of resonant electromagnetic vibrations of the implant and of the surrounding bone. MEGA IQ identifies the implant stabilization via calculating the difference in the resonant frequencies between the test pin screwed onto the implant and the analyzing unit. The magnet on the pin is exposed to electromagnetic impulses, with the vibrations further evaluated on a 0 to 100 scale. A value exceeding 70 units points at a high primary stabilization of the implant. Radiofrequency analysis can help quantify the stabilization of the implant as well as its changes over time, such as the force of fixation of the implant in the bone.



Fig. 1. Two-stage dentition defect implantation in the anterior mandible with delayed loading (a-h)

Group 3 — patients (n=28, 34.0%) who had dental implant installed straight into the replaced tooth's hole with immediate load applied on the implants, whereas they were administered medication treatment following the surgery (with no Imudon® lozenge administered); Group 4 — patients (n=18, 21.5%) who had undergone an implantation surgery with the implant installed right into the hole of the removed tooth, with immediate load on the implants and further administration of Imudon® lozenges within the post-surgery period (daily dosage — 6 lozenges; course duration — 10 days) (Fig. 2).

The cone-beam computed tomograms (CBCT) of the 83 patients with dentition issues were performed on a PointNix Combi 500 computer tomography device. 110 implants of various systems (Alpha BIO,

The object of the immunological study was the crevicular fluid. The cytokine content was examined 7 days and 1 month following the implants installation. The substances identified in the vascular fluid by solid-phase enzyme immunoassay (using Vector Best reagent kits; Novosibirsk, Russia) were interleukin-8 (IL-8), interleukin-1 receptor antagonist (IL-1RA), monocyte chemoattractant protein (MCP-1), tumor necrosis factor alpha (TNFα). The effectiveness of the reparation and osseointegration was done through the repair index:

$$(RI). RI = IL-1RA / (IL-8 + MCP-1 + TNF\alpha).$$

The statistical processing of the data was performed using the Statistica 6.0 software for Windows.



Fig. 2. One-stage implantation and direct prosthetics of a dentition defect in the frontal mandible (a-i)

RESULTS AND DISCUSSION

Prior to the surgery, each patient was offered full information regarding the upcoming intervention, treatment plan, expected results and associated risks. The preoperative examination included a thorough collection of a personal medical history, as well as clinical and radiological data. The quality and the quantity of the alveolar bone tissue in the anterior mandible were evaluated, too. As the CBCT data shows, the 1st type of bone tissue with a compact layer predominating was found in 10.1% of the cases ($n=9$); the 2nd type of bone tissue — a combination of a spongy and compact layer (1:1 ratio) was to be observed in 35.5% of the cases ($n=29$), the 3rd type of bone tissue — the spongy layer predominating, with a typical network of thin trabeculae, was found in 47% of the cases ($n=39$), while the 4th type of bone tissue, featuring a 4:1 spongy VS. compact layer ratio, was detected in 7.4% of the cases ($n=6$) (Fig. 3).

The height of the anterior mandible measured from the ridge top to the lower edge of the mandible

in 77 (93%) patients was 15 mm or above. Anatomical and topographic measurements were carried out at a point located on the vertex of the alveolar ridge and every 5 mm to the lower edge of the jaw. When examining the area of the 42nd tooth (removed previously), the average width at the first point (the alveolar ridge tip) was 2.2 ± 0.01 mm; at the second — 3.8 ± 0.01 m; at the third — 4.9 ± 0.01 mm, and at the fourth — 5 ± 0.02 mm. The area of the 41st previously removed tooth could be described as follows: at the first point — 2.2 ± 0.01 mm; at the second — 4.2 ± 0.01 mm; at the third — 5.6 ± 0.02 mm, at the fourth — 6 ± 0.02 mm. The area of the 31st previously extracted tooth: at the first point — 2.2 ± 0.01 mm; at the second point — 4.2 ± 0.01 mm; at the third point — 5.9 ± 0.01 mm; at the fourth — 5.6 ± 0.02 mm. The area of the 32nd previously removed tooth: at the first point — 1.6 ± 0.01 mm; at the second — 3.1 ± 0.01 mm; at the third — 4.4 ± 0.01 mm, and at the fourth — 6.1 ± 0.02 mm. surgical treatment was initiated once the structure of the bone tissue was studied completely.

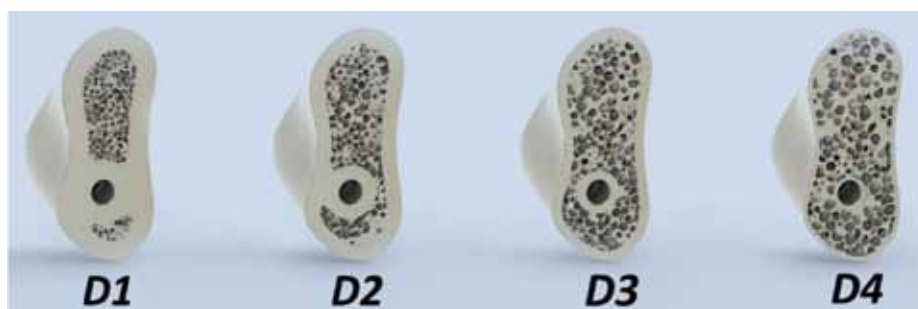


Fig. 3. Bone density classification (C.E. Misch, 1990)

When installing an implant in the respective hole, ensuring high primary stability of the implant is of importance. There was a dependence identified between the bone tissue density and the primary stability indicator. The stability figures for implants installed in Type 1 bone tissue fell within the range of 78 to 90 units, for implants installed in Type 2 bone tissue — from 76 to 90 units.

The primary stability values for implants embedded in Type 3 bone tissue were much lower, ranging from 65 to 70 units. As for as Type 4 bone tissue is concerned, the primary stability of the implanted implants was under 60 units. Out of all the implants loaded directly on the day the surgery was done, 12 (32.4%) implants were installed in Type 1 bone tissue (primary stability on the MEGA ISQ device ranging from 88 to 90 units); 20 (54.1%) implants were installed in Type 2 bone tissue (primary stability — 85–88 units) and 5 (13.5%) implants in Type 3 bone tissue (primary stability — from 78 to 79 units). The next examination of the stability featured by the implants with immediate loading was carried out 1 month after surgical treatment. At this point, the plan was to replace the temporary orthopedic structure with a permanent one. A measurement of the stability of the implant (MEGA ISQ device) installed in the bone tissue of Type 1 and 2, which was done 1 month following the surgery, revealed no decrease in the stability values. One of the 5 implants installed in Type 3 bone tissue and loaded on the day of surgery showed a stability decrease down to 65 units.

Once the implant is installed, the top important task is to identify and early postoperative complications. During the first 7 days, and a month following delayed installation of implants, and immediate installation of implants right into the hole of the extracted tooth, there is a change in the content of pro- and anti-inflammatory cytokines in the crevicular fluid. Inflammation at the lesion comes along with predominating activity of pro-inflammatory interleukins-IL-8, MCP-1, TNF α synthesis. In the postoperative period, on Day 7 and a month following the installation of the implants, patients who underwent delayed implantation, as well as those who underwent immediate implantation, had the level of IL-1RA at 35–36.7% of the level of Group 1 ($p<0.001$) and 33.6–36.9% ($p<0.001$). The TNF α content was 88.2% on the 7th day and 78.9% — a month later, from the level of Group 1 indicators 1 ($p<0.01$), in patients who underwent delayed implantation, and in patients who underwent immediate implantation — 73.7% of Group 1 indicators ($p<0.01$). The content of IL-8 in the gingival fluid on Day 7 day and a month following the installation of implants in patients who underwent delayed implanta-

tion went down to 23.4% and 23.0–32.9% of Group 1 levels ($p<0.01$); in Group 3 after immediate implantation — 23.7% and 14.8–26.5% of Group 1 levels ($p<0.01$). In the postoperative period, on Day 7 and a month later, only the MSR-1 content was growing. The content of MCP-1 in the gingival fluid, during that, was observed to be increasing only in patients who had undergone delayed implantation — up to 113.5–121.2% of Group 1 levels ($p<0.05$); in those who had had immediate implantation, it fell to 77.8% of Group 1 levels ($p<0.01$) (Table 1).

A local imbalance in cytokine production, therefore, accounts for the development of chronic inflammation, which requires immune medication treatment that will affect the cytokine status. We found that against the background of treatment with Imudon[®], there were changes in the balance of pro- and anti-inflammatory cytokines typical of the two groups of patients described above (with delayed and with immediate installation of implants). In the postoperative period, the decrease in the IL-1RA levels on day 7 was up to 73.8% ($p<0.05$), whereas following one month its content recovered almost to Group 1 levels. The decrease in pro- and anti-inflammatory cytokines in the postoperative period in patients taking the Imudon[®] occurred was going on not so significantly, i.e. a mechanism was triggered, which promoted bone regeneration.

For evaluating the effectiveness of reparation and osseointegration, as well as possible complications of dental implantation in the early postoperative period, there was the ratio index calculated for pro- and anti-inflammatory cytokines. The RI calculation showed that in the postoperative period, patients in groups with delayed and immediate implantation had the indicator — on Day 7 and a month later — went down to 24.7 and 26.8 units, and to 29 and 31.2 units ($p<0.05$). The decrease in RI in these groups of patients points at a high activity of the postoperative inflammation, which is accompanied by the development of pain syndrome, and a postoperative edema followed with loss of bone tissue around the implant. Decreasing pro- and pro-inflammatory cytokine pools in the postoperative period in patients taking Imudon[®] was less pronounced, which means that after immediate implantation into the extracted tooth's hole, the mechanism was triggered, which was responsible for cytokine regulation of processes promoting bone tissue reparative regeneration. A typical feature of this was a significant increase in RI — 110.50 units after 7 days, and 134.95 units — after a month ($p<0.01$).

CONCLUSIONS

1. As cone-beam computed tomography data shows, identifying the stability and osseointegration,

Table 1. The cytokine level in the gingival fluid after the installation of dental implants in the early postoperative period (mean value and quartile range)

Study groups	MCP-1 (pg / ml)	IL-1RA (pg / ml)	IL-8 (pg / ml)	TNF α (pg / ml)	RI (units)
Group 1 (Control group)	28,9 (26,6;32,1)	4279,50 (3655,0;4951,0)	69,50 (13,85;96,02)	7,60 (5,87;9,50)	42,60 (36,55;53,51)
Group 2 (Comparison group)					
7 days later	32,80 (29,35;45,20)	1498,00 (1367,00;1836,00)	16,20 (13,70;17,80)	6,7 (5,50;8,45)	24,70 (22,45;30,90)
30 days later	32,75 (28,68;37,33)	1568,50 (1454,25;1604,00)	16,00 (13,30;16,50)	6,70 (5,90;7,00)	26,80 (23,70;28,34)
Group 3 (Immediate implantation)					
7 days later	22,30 (15,25;30,73)	1437,30 (1314,08;1518,23)	16,05 (13,75;20,53)	5,60 (5,30;6,30)	29,55 (25,40;31,90)
30 days later	28,9 (26,65;32,15)	1498,00 (1367,00;1836,00)	10,30 (9,75;23,55)	4,60 (4,20;4,75)	31,20 (29,30;40,70)
Group 4 (Immediate implantation + Imudon®)					
7 days later	4,89 (3,45; 8,26)	3160,00 (2995,00;3860,00)	32,27 (17,80;46,80)	2,12 (1,83;2,85)	110,50 (88,47;116,60)
30 days later	6,46 (4,45; 8,04)	4570,00 (3733,00;4800,00)	19,50 (11,80;44,70)	2,07 (1,63;2,75)	134,95 (78,90;215,01)

restoring anterior mandible dentition defects can be done during dental implantation performed subject to the delayed and immediate installation protocol.

2. Direct prosthetics on implants with immediate functional load offers a good alternative to the standard treatment protocol, also featuring the following advantages: a low degree of surgical intervention; a short treatment period; the capacity to maintain the height and width of the alveolar bone at a stable level; accelerated bone regeneration. Reduced treatment course down to one month is possible in case of the right selection of patients who feature good quality of bone tissue, mucous membrane, as well as the right height and width of the alveolar process.

3. The bone tissue structure and density, with Type 1, 2 and 3 of bone tissue, allows primary stability of implants in the anterior mandible that is enough to carry out immediate loading involving removable and/or non-removable dentures.

4. The implant stability of 75 units and above (as measured on a MEGA ICQ device) allows predicting a guaranteed stable outcome with immediate loading applied to dental implants.

5. The administration of the Imudon® drug in the postoperative period is an effective treatment and prevention measure that can be employed for the rehabilitation of patients after dental implantation, the measure in question reducing the risk of inflammation-induced complications.

6. One of the advantages to be gained through immediate implantation is nearly complete absence of

atrophic changes at the surgery area, while it requires atraumatic tooth extraction along with preserving all the bone walls of the hole; in case any defects occur, the method of directed bone and tissue regeneration should be employed. Achieving primary stability of the implant installed in the hole of the extracted tooth will take its maximum contact with the bone walls in the hole as well as possible further early loading.

7. In case of one-stage implantation and direct prosthetics, implants should be installed inside the holes of teeth that have no an acute or chronic inflammation, while this method should be used carefully in cases featuring periodontal issues. When an implant is installed immediately into a single-root tooth's hole, it would be reasonable to ensure maximum match between the implant shape and the dental alveolus anatomical shape.

REFERENCES

1. **DOLGUSHIN I.I., LATYUSHINA L., PIOTROVICH A.V., NIKUSHKINA K.V.** Effect of local immunocorrection on saliva cytokine profile during the "closed" sinus lifting and simultaneous implantation // Cytokines and inflammation. 2016;2:198–203. <http://www.cytokines.ru/russian/2016/2/Art12.php>.
2. **EROKINA N. L., LEPILIN A. V., ZAKHAROVA N. B.** Profile of cytokines in the content of periodontal pockets in patients with fractures of the mandible with periodontitis. Clin.lab. diagnostics 2011;9:6–7.
3. **LEPILIN A.V., SMIRNOV D.A., MOSTOVAYA O.S., ZHILKINA O.V.** Questioning results of dental clinic patients on the use of the dental implantation method.

- Scientific and practical journal "Dentistry". MediaSfera, 2013;3;Vol.92:112–113.
4. **LEPILIN A.V., EROKINA N.L., SAVELYEVA S.S., AGEEV A.B.** Features of the use of domestic dental implants. *Dental Forum*, 2016;4:50.
 5. **LEPILIN A.V., SHALINA M. YU., HALTURINA V. G., MARTYNOVA M. I.** the Use of cone-beam computed tomography to study the anatomical and topographic structure of the alveolar part of the chin of the lower jaw. *Dental Forum*, 2017;4(67):47–48. <https://elibrary.ru/item.asp?id=30504296>.
 6. **LEPILIN A.V., SHALINA M.Y., SAVEL'eva S.S., MUKHINA N.M., NOZDRACHEV V.G.** Predicting the possibility of immediate dental implants loading by frequency-resonance analysis. *Clinical Dentistry*, 2018;2(86):50–53.
 7. **LEPILIN A. V., ZAKHAROVA N. B., FISHCHEV S. B., SHALIN M. Y.** Peculiarities of the dynamics of the cytokine profile of angiogenesis in the gingival fluid of patients with the installation of dental implants. *Periodontology*, 2018; 1:26–29. DOI: 10.25636/PMP.1.2018.1.6.
 8. **LEPILIN A. V., OSTROVSKAYA L. YU., ZAKHAROVA N. B., EROKINA N. L.** Modern technologies and substantiation of pathogenetic treatment of periodontal diseases. – Saratov: Publ., SGMU, 2015. – 138p.
 9. **LEPILIN A.V., MOSTOVAYA O.S., KONNOV V. V., MASLENNIKOV D. N.** Directly installation of a dental implant in the hole of a removed tooth // *Dental implantology and surgery*. 2015. №4 (21). P. 36–38. <https://elibrary.ru/item.asp?id=29299839>
 10. **LEPILIN A.V., RAYGORODSKY YU.M., EROKINA N.L., SMIRNOV D.A., LISTOPADOV M.A.** Rationale for the use of physiotherapy after dental implantation. *Periodontology*, 2010; Vol.15;2(55):62–64.
 11. **LEPILIN A.V., RAYGORODSKY YU.M., EROKINA N.L., BULKIN V.A., PROKOFIEVA O.V., SMIRNOV D.A.** Application of physiotherapeutic techniques for the improvement of the efficacy of dental implantation. *Questions of balneology, physiotherapy and physiotherapy*, 2010;4: 15–16. <https://elibrary.ru/item.asp?id=15271445>.
 12. **LEPILIN A.V., EROKINA N.L., TITORENKO V.A., OSTROVSKAYA L.YU., BISULTANOV H.U.** The condition of periodontal tissues in patients with mandibular fractures in combination with inflammatory diseases of periodontium in dynamics of treatment. *Saratov Journal of Medical Scientific Research*, 2008; Vol. 4;1: 115–118.
 13. **RABINOVICH I. M., RABINOVICH O. F.** Experience of clinical use of Imudon in the treatment of diseases of the oral mucosa. *Clinical dentistry*. 2000; 66(3): 64–65.
 14. **TSEPOV L.M., OREKHOVA L.YU., NIKOLAEV A.I., MIKHEEVA E.A.** Certain aspects of etiology and pathogenesis of chronic inflammatory periodontal diseases (review). Chapter I. *Periodontology*, 2005; 2 (35): 3–6.
 15. **A. DASANAYAKE.** Periodontal disease is related to local and systemic mediators of inflammation. *J Evid Based Dent Pract*. 2010;10(4):246–247. <https://doi.org/10.1016/j.jebdp.2010.09.006>.
 16. **T. R. FITZSIMMONS, A. E. SANDERS, P. M. BARTOLD, G. D. SLADE.** Local and systemic biomarkers in gingival crevicular fluid increase odds of periodontitis. *J Clin Periodontol*. 2010;37(1):30–36. <https://doi.org/10.1111/j.1600-051X.2009.01506.x>.
 17. **M. L. GEISINGER, B. S. MICHALOWICZ, W. HOU, E. SCHOENFELD, M. GELATO, S. P. ENGBRETSON, L. HYMAN.** Systemic inflammatory biomarkers and their association with periodontal and diabetes-related factors in the diabetes and periodontal therapy trial, a randomized controlled trial. *Journal of Periodontology*. 2016;87(8):900–913. <https://doi.org/10.1902/jop.2016.150727>.
 18. **T. SHIMIZU, T. KUBOTA, M. IWASAKI, T. MOROZUMI.** Changes in Biomarkers after Initial Periodontal Treatment in Gingival Crevicular Fluid from Patients with Chronic Periodontitis Presenting with Drug-Induced Gingival Overgrowth. *Open Journal of Stomatology*. 2016;6(2):64–72. <http://dx.doi.org/10.4236/ojst.2016.62008>.
 19. **S. RAMALINGAM, M. AL-HINDI, R. A. AL-EID, N. NOOH.** Clinical evaluation of implant survival based on size and site of placement: A retrospective study of immediate implants at single rooted teeth sites. *The Saudi Dental Journal*. 2015; Vol. 27; 2:105–111. DOI: 10.1016 / j.sdentj.2014.11.003
 20. **BAIRIKOV I.M., GAIVORONSKAYA T.V., DEDIKOV D.** Reconstruction of mandibular defects using individual vascularized autografts combined with macroporous titanium fiber material // *Archiv EuroMedica*. 2021. Vol. 11. № 1. P. 147–159. <https://doi.org/10.35630/2199-885X/2021/11/1.32>
 21. **KUPRYAKHIN S.V., LEPILIN A.V., KUPRYAKHIN V.A.** Optimization of dental implantation combined with closed sinus lift in patients with low maxillary sinus floor // *Archiv EuroMedica*. 2019. Vol. 9; 2: 117–121. <https://doi.org/10.35630/2199-885X/2019/9/2/117>
 22. **KUPRYAKHIN S.V., LEPILIN A.V., KUPRYAKHIN V.A., POSTNIKOV M.A.** Potential introduction of cell technologies to improve dental implant surface preparing // *Archiv EuroMedica*. 2019. Vol. 9; 2: 122–129. <https://doi.org/10.35630/2199-885X/2019/9/2/122>

<http://dx.doi.org/10.35630/2199-885X/2022/12/2.31>

THE EFFECT OF SILICA GEL TO THE ADHESIVE PROTOCOL STAGES IN THE TREATMENT OF CARIES AND ITS COMPLICATIONS

Received 21 January 2022;
Received in revised form 18 February 2022;
Accepted 21 February 2022

Zurab Khabadze[✉] , Sergey Ivanov,
Aleksandra Kotelnikova , Mikhail Protsky,
Ekaterina Shylyayeva , Darya Nazarova 

The Peoples' Friendship University of Russia; Moscow, Russia

✉ khabadze-zs@rudn.ru

ABSTRACT — The etching solution is used to remove the inert surface layer of the hard tissues of the tooth, change the wetting parameters and create conditions for micromechanical adhesion. The most commonly used gel is 37% orthophosphoric acid.

However, silicic acid as a thickener in the composition of etching gels, when interacting with hydroxyapatite of the tooth, gives a precipitate in the form of silicon oxide — silica.

Scanning electron microscopy makes it possible to see the accumulation of round silica nanoparticles, approximately 20–40 nm in diameter.

According to studies, the formation of silica particles does not affect the quality of restoration, so there is no need to remove them from the surface of demineralized dentin.

THE PURPOSE of this review article is to study scientific data on the formation of an insoluble precipitate after the interaction of inorganic acid in the form of a gel with components of the inorganic enamel matrix (hydroxyapatite), and its effect on the adhesion quality of the filling material.

MATERIALS AND METHODS: Electronic search of articles was carried out using search engines and databases Google Scholar, Pub Med. The articles are included, the content of which concerns the topic of determining the sediment formed when etching the tooth surface with orthophosphoric gel. The publication date criterion has been selected since 2011.

RESULTS: 69 articles were reviewed during the review process. After analyzing the literature according to the inclusion criteria, the total number was 20 publications.

CONCLUSION: When etching dentin with a solution of orthophosphoric acid in the form of a gel, a precipitate of silicon oxide is formed. This is due to the presence of a thickener in the gel in the form of silicic acid.

Silicic acid, or silica gel, reacts chemically with hydroxyapatite of the tooth. As a result, silica is formed, which remains on the surface of demineralized dentin in the form of round nanoparticles with a size of 20–40 nm.

According to studies, the formation of silica particles does not affect the quality of restoration, so there is no need to remove them from the surface of demineralized dentin.

KEYWORDS — orthophosphoric acid, silica gel, precipitate, enamel etching, hydroxyapatite.

INTRODUCTION

Composite materials for dental restoration are the youngest and developing class of materials in dentistry [1, 2]. However, despite many positive qualities, one of the disadvantages of composites is polymerization shrinkage [3, 4].

According to numerous studies, the amount of polymerization shrinkage of composites reaches 3–5% volume units [5, 6]. Shrinkage of the composite leads to the formation of a compressive force directed deep into the composite material and may exceed the force of adhesion to the walls of the cavity of the tooth being restored. As a result, an edge gap is formed, which leads to a color change at the border of the restoration, the penetration of microorganisms and the development of secondary caries. Therefore, adhesive systems are used to improve the edge fit of the seal to the walls of the prepared tooth cavity [7].

Despite the variety of dental adhesive systems currently being produced, the following general and fundamental components of their composition can be distinguished: etching solution, primer and adhesive.

The etching solution is used to remove the inert surface layer of the hard tissues of the tooth, change the wetting parameters and create conditions for micromechanical adhesion. The most commonly used gel is 37% orthophosphoric acid [8,9].

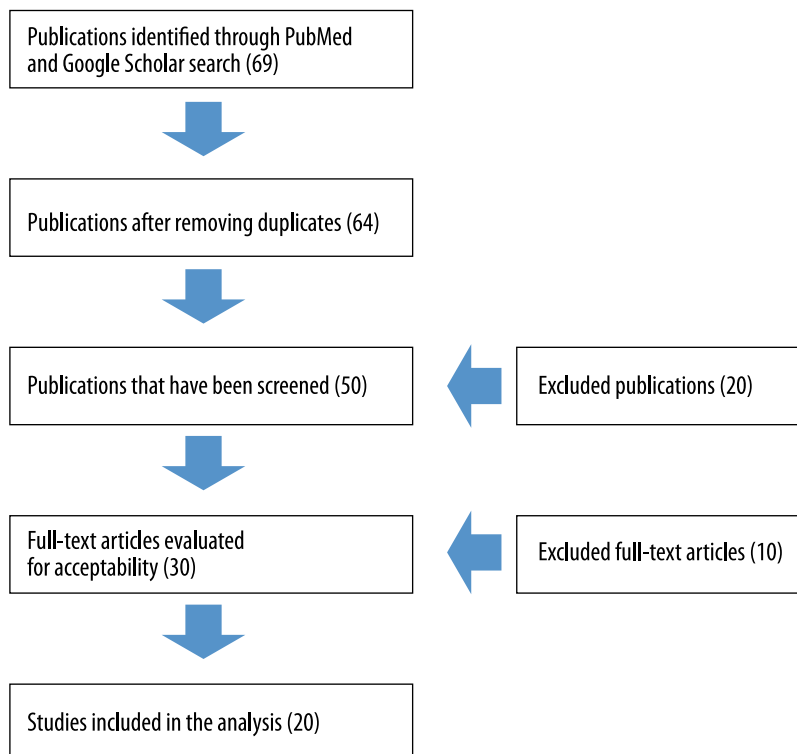
However, it is believed that the silica gel (silicic acid) contained in the gel, when interacting with hydroxyapatite of the tooth, gives a precipitate in the form of silicon oxide — silica [10].

The purpose of the study: to evaluate scientific data on the formation of insoluble precipitate after the interaction of inorganic acid in the form of a gel with the components of the inorganic enamel matrix (hydroxyapatite), and its effect on the adhesion quality of the filling material.

MATERIALS AND METHODS

Electronic search of articles was carried out using search engines and databases Google Scholar, PubMed. The articles are included, the content of which concerns the topic of determining the sediment formed when etching the tooth surface with orthophosphoric gel. The publication date criterion has been selected since 2011.

Table 1. Article selection process



Search terms included *orthophosphoric acid*, *silica gel*, *precipitate*, *enamel etching*, *hydroxyapatite*.

The studies were filtered and selected in several stages. Firstly, they were evaluated by name. Secondly, individual documents at the first stage were additionally evaluated by reading abstracts and full-text articles. The difference in choice was resolved by discussion. The selection of publications was also carried out according to the following inclusion criteria — the date of publication of the article no earlier than 2011, the subject of determining the sediment formed when etching the tooth surface with orthophosphoric gel.

The first exclusion criterion was the selection of publications dated earlier than 2011. Further, the review did not include works whose title and summary did not meet at least one of the submitted inclusion criteria. At the last stage, the content of the full-text versions of the selected articles was studied.

During the study of all the selected information, the possibility of a systematic error was considered. The Cochrane Collaboration system was used to determine the risk of the possibility of a systematic error during the study of the selected information [11]

The levels of systematic error were systematized as follows: low risk if all criteria were met; moderate risk when only one criterion was missing; high risk if two or more criteria were missing; and unclear risk if there were too few details to decide on a certain risk assessment.

Summing up the risk of bias for each study, most studies were classified as unclear risk. A number of studies have been found to have a low risk of bias. There were several limitations in the current review, including stud-

ies written only in English, which could lead to publication bias. In each study, there were different degrees of heterogeneity in the materials and methods of the study.

RESULTS

69 articles were reviewed, 49 of which were based on PubMed, 20 on Google Scholar. Having made the selection according to the exclusion criteria, the total number of works was 20. In the selected articles, current data on the inorganic sediment that is formed when etching the tooth surface with orthophosphoric gel were analyzed.

DISCUSSION

Orthophosphoric acid is used in dentistry for etching enamel and dentin [12].

The interaction of etching agents with dentin is limited by the buffering effect of hydroxyapatite and other dentin components. Acidic agents remove the smear layer and the upper and lower part of the dentin, open the dentine tubules, demineralize the dentin surface and increase the microporosity of the intertubular dentin. The penetration of acids occurs mainly through the tubules [13].

It is believed that the adhesion to dentin mainly depends on the micromechanical adhesion of hydrophilic resins in this demineralized microporous dentin, thus forming a mesh intertwined hybrid tissue consisting of collagen, residual mineral particles and resin [14].

Despite the fact that for many years they have been sold in the form of liquids, most modern etchants are currently gels of either thick or thin consistency. To make a gel from liquid phosphoric acid, it is necessary to use silicic acid as a thickener. Manufacturers add thickeners to their gels to facilitate processing. The advantages of gel forms are that a clinician can easily

control the spread of acid over the surface and visually determine the presence of acid [15].

The demineralizing effect is clinically observed when gas bubbles accumulate inside the gel. Pickling gels thickened with silica microparticles leave a precipitate in the form of particles on the dentin surface, which cannot be completely removed even with intensive rinsing [16].

As a result of acid etching of dentin, a layer of denatured collagen and particles of the residual smear layer may form on the dentin surface, which prevent the complete exposure of the collagen network. It has not been established whether the silica component of some etchants partially prevents the formation of this residual surface layer [17].

Studies using scanning electron microscopy demonstrate the demineralization of dentin. At a higher magnification, three zones are visible: the upper porous zone with a residual lubricated layer, denatured collagen and silica particles; the intermediate zone with randomly oriented collagen fibers; the lower zone with a submicron break, a small amount of collagen fibers and inclusions of hydroxyapatite [18].

A large magnification (100,000) showed the accumulation of round silica nanoparticles, approximately 20-40 nm in diameter, with needle-like apatite crystals on top of exposed collagen fibrils [19].

Silicic acid as a thickener in the composition of etching gels, although it gives a precipitate in the form of silica on the surface of dentin, but, according to research, does not affect the quality of restoration [13].

In addition, the use of gels is more practical in clinical settings, when the etching area can be precisely controlled using phosphoric acid gels, rather than liquids [12].

CONCLUSION

When etching dentin with a solution of orthophosphoric acid in the form of a gel, a precipitate of silicon oxide is formed [7]. This is due to the presence of a thickener in the gel in the form of silicic acid [16]. Silicic acid, or silica gel, reacts chemically with hydroxyapatite of the tooth. As a result, silica is formed, which remains on the surface of demineralized dentin in the form of round nanoparticles with a size of 20–40 nm [20]. According to studies, the formation of silica particles does not affect the quality of restoration, so there is no need to remove them from the surface of demineralized dentin [19].

REFERENCES

1. **ALTMAN D.G., GOTTSCHKE P.C., HIGGINS J.P.T., JÜNI P., MOHER D., OXMAN A.D., SAVOVIĆ J., SCHULZ K.F., STERNE J.A., WEEKS L.,** The Co-

chrane Collaboration's tool for assessing risk of bias in randomised trials. *BMJ*. 2011;343:d5928. DOI: 10.1136/bmj.d5928

2. **ARAÚJO IDT, BORGES BCD, FERREIRA IÁ, LOPES CP, SOARES RB.,** Influence of exposure to phosphoric and polyacrylic acids on selected microscopic and physical/chemical properties of calcium hydroxide cements. *Eur Oral Res*. 2020 May 1;54(2):69-76. DOI: 10.26650/eor.20200057
3. **BESINIS A, MARTIN N, VAN NOORT R.** Infiltration of demineralized dentin with silica and hydroxyapatite nanoparticles. *Dent Mater*. 2012 Sep;28(9):1012-23. DOI: 10.1016/j.dental.2012.05.007
4. **NAIK A., SHEPHERD DV., SHEPHERD JH, BEST SM, CAMERON RE.** The effect of the type of HA on the degradation of PLGA/HA composites. *Mater Sci Eng C Mater Biol Appl*. 2017 Jan 1;70(Pt 1):824-31. DOI: 10.1016/j.msec.2016.09.048
5. **BLATZ MB, OZER F.** Self-etch and etch-and-rinse adhesive systems in clinical dentistry. *Compend Contin Educ Dent*. 2013 Jan;34(1):12-4, 16, 18; quiz 20, 30.
6. **BORGES AFS, FURUSE AY, ISHIKIRIAMA SK, MENDONÇA G, MONDELLI RFL, RIZZANTE FAP.** Shrinkage stress and elastic modulus assessment of bulk-fill composites. *J Appl Oral Sci*. 2019 Jan 7;27:e20180132.
7. **BRESCHI L, CADENARO M, COMBA A, CUNHA SR, MARAVIC T, TJÄDERHANE L, ET AL.** Dentin bonding systems: From dentin collagen structure to bond preservation and clinical applications. *Dent Mater*. 2018 Jan;34(1):78-96. DOI: 10.1016/j.dental.2017.11.005
8. **CAMARENA F, JIMENEZ N, RODRIGUEZ-SENDRA J, SAURO S, TORRES I.,** Ultrasonic Monitoring of Dentin Demineralization. *IEEE Trans Ultrason Ferroelectr Freq Control*. 2021 03;68(3):570-8.
9. **CAMILLERI J.** Investigation of Biodentine as dentine replacement material. *J Dent*. 2013 Jul;41(7):60
10. **CARVALHO RM, HARNIRATTISAI C, MATSUMOTO M, SAIKAEW P, SANO H, SATTABANASUK V.** Ultra-morphological characteristics of dentin surfaces after different preparations and treatments. *Eur J Oral Sci*. 2020 06;128(3):246-54 DOI: 10.1111/eos.12698
11. **CENCI MS, COLLARES K, CORREA MB, DEMARCO FF, MORAES RR, OPDAM NJ.** Should my composite restorations last forever? Why are they failing. *Braz Oral Res*. 2017 Aug 28;31(suppl 1):e56. 10.1016/j.dental.2015.07.005
12. **CHEN WJ, KE JL, LEE HC, TSAI MT, WANG YL, YEH TW ET AL.** Early detection of enamel demineralization by optical coherence tomography. *Sci Rep*. 2019 11 20;9(1):17154. doi: 10.1038/s41598-019-53567-7
13. **CHESTERMAN J, GALLACHER A, JOWETT A, NIXON P.** Bulk-fill resin-based composite restorative materials: a review. *Br Dent J*. 2017 Mar 10;222(5):337-44. DOI: 10.1038/sj.bdj.2017.214

14. **DE MUNCK J, LISE DP, VAN ENDE A, VAN MEER-BEEK B.** Bulk-Fill Composites: A Review of the Current Literature. *J Adhes Dent.* 2017;19(2):95–109. DOI: 10.3290/j.jad.a38141
15. **DUARTE MAH, DUQUE JA, ISHIKIRIAMA SK, MENDONÇA G, MONDELLI RFL, RIZZANTE FAP.** Polymerization shrinkage, microhardness and depth of cure of bulk fill resin composites. *Dent Mater J.* 2019 Jun 1;38(3):403–10. DOI: 10.4012/dmj.2018-063
16. **GEZAWI ME, KAISARLY D.** Polymerization shrinkage assessment of dental resin composites: a literature review. *Odontology.* 2016 Sep;104(3):257–70. DOI: 10.1007/s10266-016-0264-3
17. **HÄGG U, MATINLINNA JP, TANG AT, ZHU JJ.,** Acid etching of human enamel in clinical applications: a systematic review. *J Prosthet Dent.* 2014 Aug;112(2):122–35. DOI: 10.1016/j.pros-dent.2013.08.024
18. **HOCH M, PETERSON J, RIZK M, WIEGAND A.** Bonding performance of self-adhesive flowable composites to enamel, dentin and a nano-hybrid composite. *Odontology.* 2018 Apr;106(2):171–80. DOI: 10.1007/s10266-017-0324-3
19. **KARAN K, WANG Y, XU C, YAO X.,** Chemical characterization of etched dentin in non-carious cervical lesions. *J Adhes Dent.* 2012 Aug;14(4):315–22. DOI: 10.3290/j.jad.a22766
20. **KLAUS P, LOPES GC, OLIVEIRA GM, THYS DG, WIDMER N.** Enamel acid etching: a review. *Compend Contin Educ Dent.* 2007 Jan;28(1):18-24; quiz 25, 42.

<http://dx.doi.org/10.35630/2199-885X/2022/12/2.32>

VARIANT ANATOMY OF TRANSITIONAL OCCLUSION DENTAL ARCH AT OPTIMAL OCCLUSAL RELATIONSHIPS

Received 29 January 2022;
Received in revised form 21 February 2022;
Accepted 22 February 2022

Taisiya Kochkonyan , Dmitry Domenyuk ,
Vladimir Shkarin , Sergei Dmitrienko ,
Stanislav Domenyuk 

¹ Kuban State Medical University, Krasnodar;

² Stavropol State Medical University, Stavropol;

³ Volgograd State Medical University, Volgograd;

⁴ North Caucasus Federal University, Stavropol, Russia

✉ domenyukda@mail.ru

ABSTRACT — Through the transitional bite period, the variability of the dental arch shape and size is due to the replacement of milk teeth with permanent ones, which feature different odontometric values. The aim of this study was to identify the main linear and angular parameters of dental arches, in view of the trusive position of the incisors with optimal functional occlusion. A stratified study was involved 76 children ages 8–12 years old, who were divided into three groups (protrusive, retrusive and mesotrusive dental arches). An analysis of cone-beam computed tomograms and plaster models of jaws was carried out, which was preceded by obtaining informed consents according to the Ethics Committee requirements. The study revealed certain features of the variant anatomy of transitional occlusion dental arch. The calculated factors allowed identifying the proportionality of the dental arch parameters to odontometric indicators. During that, the dental-diagonal factor (the ratio of the dental arch length to the incisor-molar diagonals) for the upper jaw was 1.06 ± 0.01 , for the lower arch being equal to 1.09 ± 0.01 , in all types of dental arches, which is a fact to be used in clinical orthography to predict the location of the dental arch incisor (central) point in case of shape anomalies, specifically in the anterior part. The angular parameters of the diagnostic dental pentagon will allow simulating the geometric and graphical construction of arches through the transitional occlusion period.

KEYWORDS — morphometry, odontometry, CBCT, plaster model biometry, physiological protrusion of teeth, transitional occlusion.

INTRODUCTION

Through the period of transitional occlusion, dental arches feature the greatest variability, while their parameters are dependent from numerous etiological factors due to replacement of milk teeth with permanent ones, pathologies of dental and periodontal hard tissues, and premature removal of milk teeth

[2, 5, 13, 19, 37, 40].

This age period is under special attention from orthodontists, while the treatment of anomalies is typically aimed at the jaw bone growth, taking into account the cranial morphology [4, 6, 9, 12, 23, 36, 42].

Speaking of permanent teeth occlusion period, the main differences in the shape of the human dental arch with physiological occlusion are known to be due to the specifics of sagittal, diagonal and transversal sizes that determine the arcade and dental types of the teeth system, as well as due to peculiarities of the teeth physiological rotation at different variants of dental arches [10, 14, 20, 24, 27, 30, 38, 45].

The calculated index values of the gnathic (arcanian) type, as well as differences in odontometric indicators determining the dental arch length, are currently employed in clinical orthodontics and orthopedic dentistry when treating patients through the period of permanent teeth occlusion [11, 15, 21, 25, 44].

Research has revealed certain sex- and race-bound features of the milk and permanent teeth, dental arches, dental segments, which allows identifying respective treatment methods and prevention measures, as well as to regulate the orthodontic load during the replacement of abnormally positioned teeth [17, 22, 26, 29].

Special importance in clinical orthodontics is attached to biometric studies through the transitional occlusion period, where the dental arch parameters change after the eruption of the next group of the second-generation teeth [3, 16, 35].

Until now, the protocol methods employed to study transversal arch sizes are Pont's and Linder-Harth methods, which differ in index values, which, in turn, often determines the difficulties related to their clinical implementation associated with the dental system featuring either the brachygnathic or the dolichognathic type [1, 18, 41].

Through the transitional occlusion period, such studies can be held only after the incisors cut out on both jaws, whereas the dimensions of such jaws correlate, to a certain extent, with the dental arch and craniofacial parameters. At the same time, the eruption of the first premolars is viewed as a necessary condition for measuring the anterior part parameters [39]. Within this period of the maxillary system

development, the mutual position of incisors can be used to measure the incisor angle of antagonists that determine the trusive type of the dental system. The X-ray methods of examination show that in case of the mesotrusive type, the incisor angle made up by the conditional median verticals of the medial upper incisors and their antagonists is an average of 120–140° degrees. A decrease in the angle is typical of physiological protrusion, provided the incisor overlap is optimal both vertically and horizontally. An increase in the angle is indicative of the retrusive position of the incisors in both jaws [7, 28]. As far as transversal dimensions of dental arches are concerned, most experts tend to believe that the most appropriate reference to be used when measuring them are points located not in the middle of the occlusal surface of the chewing teeth (as proposed by A. Pont (1909), G. Harth (1930), H. Linder (1931)) yet on the crown vestibular surface of the teeth located near the occlusal contour [34]. This can be accounted for by the fact that the shape of dental arches allows choose the size of metal dental arches of non-removable arch structures, which are widely used in clinical practice [8, 31–33, 43].

However, we found no data regarding the variants of biometric parameters and odontometric indicators in children through their transitional occlusion period, so the rational of this work as well as its aim can be explained by a brief review of respective literature that has been carried out.

Aim:

To identify the main dental arch parameters of the transitional occlusion in view of the variant anatomy of the intrusive position of the incisors with optimal functional occlusion.

MATERIALS AND METHODS

The study involved 76 children who were divided into three groups based on the trusion type, namely by the front teeth location, and the magnitude of the incisor angle of the antagonizing medial incisors, taking into account the recommendations offered by experts, where a value of 125–140° is typical of mesotrusion. An increase or a decrease in the angle points at the retrusive or protrusive types, respectively.

Group 1 included 32 children with incisors were located by the mesotrusive type; Group 2 were 26 patients with the protrusive type of incisor arrangement, and Group 3 included 18 children who featured the retrusive position of the incisors with an optimal amount of incisor overlap, both vertically and horizontally. The relationship of antagonists, in all pairs of jaw models, matched the signs of optimal functional occlusion, following the respective age characteristics (Fig. 1).

Odontometry implied only identifying the mesial-distal diameters of the teeth crowns and calculating the total length of the dental arch (DAL12 teeth) following the total sum component, while there was also the sum of the width of the 4 incisor crowns identified (CW4 incisors) of the upper and the lower jaw, which is a mandatory protocol measure in clinical orthodontics.

The transversal dimensions included an analysis of the dental arch width between the first permanent molars located on the 6th position in the dental arch (DAW6-6). The width of the anterior dental arch was measured between the contact points of the distal surfaces of the lateral incisors located the 2nd in the dental arch (IW2-2).

The size of the incisor-molar diagonal was measured from the interincisal point (the first position of the teeth in the arch) to the distal vestibular tubercle of the sixth tooth (IMD1-6). In the anterior part, the incisor diagonal (ID1-2) was measured from the interincisal point to the distal contact point of the permanent lateral incisor with a milk canine and, actually, was close to the sum total component of the incisor crowns width in the examined part of the dental arch.

The depth of the anterior (incisal) part of the arch (IDep1-2) was measured sagittally from the interincisal point to the conditional line connecting the distal surfaces of the lateral incisors.

The obtained linear dimensions allowed using geometrical methods to design diagnostic dental pentagons, where the base was the dental arch molar width, whereas the height corresponded to the dental arch depth. The anterior part of the pentagon was shaped by an isosceles incisor triangle, the sides of that corresponding to the dimensions of the incisor diagonals, its base being the width between the incisors, while the height of the triangle corresponded to the incisor depth. The sides of the pentagon connected the lateral incisor distal point with the distal vestibular odontomer of the six-year molar (Fig. 2).

The main angles of the pentagon (incisor, canine and molar) were measured with the calculation of the sum total component for all the trusive variants of dental arches.

The statistical processing of the obtained data was performed with Microsoft Excel 2013 software as well as the SPSS Statistics (Version 22) statistical software package. The critical level of a possible null statistical hypothesis was set at 0.05.

RESULTS AND DISCUSSION

Table 1 offers a look at the analysis of the data obtained through measuring the jaw cast models within the period of the transitional occlusion in view of the



Fig. 1. Occlusion relationships through the transitional occlusion period (a, b) and identifying the incisor angle of antagonists on CBCT (c)

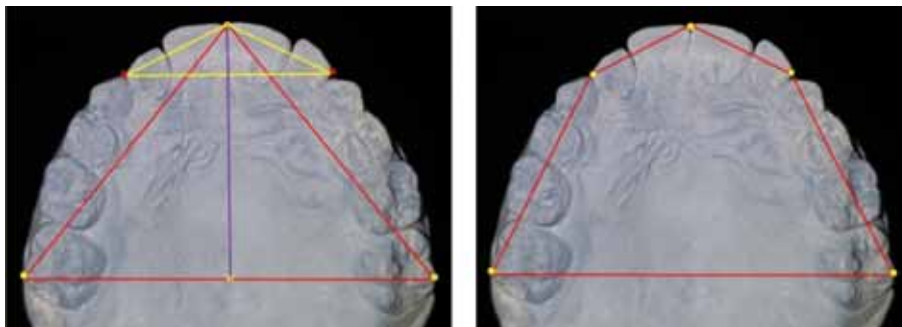


Fig. 2. Designing diagnostic triangles (a) and the dental arch pentagon (b) on jaw cast model photos featuring transitional occlusion, to measure the angles

dental arch trusion type, which served the basis for distributing the patients through the groups (Table 1).

the macrodont type of the dental system. A similar, and quite expected, situation was also seen in relation to such an indicator as the total width of the crowns of the 4 incisors in the upper jaw (CW4 incisors), which, upon analysis of the models within Group 2 was found

Table 1. Dental arch size in the three groups, (mm), ($M \pm m$) ($p \leq 0.05$)

Dental arch parameters	Dental arch size in studied groups					
	Group 1, on arch		Group 2, on arch		Group 3, on arch	
	upper	lower	upper	lower	upper	lower
DAL12 teeth	92.24 \pm 1.11	86.70 \pm 1.08	100.78 \pm 1.14	91.78 \pm 1.12	91.55 \pm 1.07	85.44 \pm 1.09
CW4 incisors	31.02 \pm 1.07	22.79 \pm 1.04	33.14 \pm 0.94	24.50 \pm 1.12	27.49 \pm 1.15	21.30 \pm 0.73
DAW6-6	57.97 \pm 1.54	52.28 \pm 1.61	60.91 \pm 1.49	55.11 \pm 1.55	54.13 \pm 1.39	48.68 \pm 1.42
IMD1-6	44.24 \pm 0.62	40.65 \pm 0.68	47.57 \pm 0.73	42.12 \pm 0.59	42.66 \pm 0.61	38.52 \pm 0.63
DAD1-6	33.42 \pm 0.81	31.01 \pm 0.73	36.54 \pm 0.84	33.93 \pm 0.66	31.56 \pm 0.59	29.61 \pm 0.68
ID1-2	15.51 \pm 0.58	11.39 \pm 0.47	16.57 \pm 0.44	12.25 \pm 0.53	14.62 \pm 0.56	11.03 \pm 0.32
IDep1-2	6.67 \pm 0.19	3.87 \pm 0.11	8.28 \pm 0.13	5.27 \pm 0.09	4.96 \pm 0.06	2.86 \pm 0.04
IW2-2	28.01 \pm 1.02	21.43 \pm 0.99	28.70 \pm 1.04	22.12 \pm 0.96	27.49 \pm 1.02	21.30 \pm 1.05

The patients within the groups revealed certain difference in odontometric indicators that determine the dental arch length (DAL12 teeth). The highest indicators of the parameter in question were to be observed in Group 2 with the protrusive type of dental systems — 100.78 \pm 1.14 mm on the upper jaw, and 91.78 \pm 1.12 mm — on the lower jaw, which lies within the opinion of experts pointing that with the protrusive type of arch is more commonly associated with

to be at 33.14 \pm 0.94 mm, this being above the respective indicators in Groups 1 and 2 (31.02 \pm 1.07 mm and 27.49 \pm 1.15 mm, respectively).

The transversal parameters, both in the molar (DAW6-6) and in the anterior part (IW2-2) of the dental arches were similar with no significant difference identified between the studied indicators.

A reliable difference ($p < 0.05$) was observed when analyzing the dental arch anterior part depth (ID1-2),

which was due to the trusive type of arches and the teeth inclination value in the anterior-posterior direction.

The obtained absolute values for transversal, diagonal and sagittal dimensions allowed identifying the index values. The ratio of the dental arch length to the sum total component (IMD1-6) of the incisor-molar diagonals (dental-diagonal factor) in the examined children, for instance, was 1.06 ± 0.01 for the upper jaw and 1.09 ± 0.01 for the lower arch, and the values now can be used in clinical practice to diagnosis of anomalies in the shape and size of dental arches, specifically in the sagittal and diagonal direction. Besides, the linear parameters of the dental arches allowed — as per each type of dental systems — building individual diagnostic dental pentagons and identifying the features of the major angles: incisor, canine and molar, which can be seen in Table 2.

specific features of the dental arch variant anatomy for the transitional occlusion.

2. The major linear parameters of dental arches within the transitional occlusion period were determined by the trusive types of dental arches as well as the vestibular-lingual inclination of the front teeth.

3. The proposed, explained and calculated index values, which take into account the transversal, the diagonal and the sagittal dimensions of the dental arches enabled to identify the proportion relationship between the odontometric indicators and the parameters of dental arches.

4. The dental-diagonal factor, taken as the ratio of the dental arch length to the incisor-molar diagonals, was 1.06 ± 0.01 for the upper jaw and 1.09 ± 0.01 for the lower jaw, regardless of the dental arch type. This knowledge can be used in clinical orthodontics to

Table 2. Dental pentagon angles in the groups examined within the study, ($^{\circ}$), ($M \pm m$) ($p \leq 0.05$)

Major parameters	Dental pentagon angle					
	Group 1, on arch		Group 2, on arch		Group 3, on arch	
	upper	lower	upper	lower	upper	lower
Incisor	131.1 ± 1.69	139.9 ± 1.75	120.7 ± 1.49	130.3 ± 1.53	139.8 ± 1.47	151.0 ± 1.58
Canine	139.6 ± 1.64	136.4 ± 1.59	145.7 ± 1.99	142.5 ± 1.87	132.4 ± 1.89	127.6 ± 1.78
Molar	65.2 ± 1.33	63.7 ± 1.72	64.7 ± 1.76	62.3 ± 1.67	66.4 ± 1.58	67.5 ± 1.49
Sum total	539.6 ± 2.98	540.2 ± 2.85	540.7 ± 2.77	539.7 ± 1.95	540.6 ± 2.09	540.0 ± 2.14

The lowest values for the incisor angle, measured both on the upper and lower dental arch, were obtained while studying models with the protrusive type of incisors (Group 2), whereas the said values were the largest in physiological variants of the retrusive position (Group 3). During that, the canine angles on each side, on the contrary, had a larger value in case of arches falling within the protrusive type — $145.7 \pm 1.99^{\circ}$ on the upper jaw, and $142.5 \pm 1.87^{\circ}$ on the lower arch. The lowest value of the pentagon canine angle was detected through the models in Group 3 groups — $132.4 \pm 1.89^{\circ}$ and $127.6 \pm 1.78^{\circ}$ on the upper and on the lower jaw, respectively,

Notable is the approximate equality of the molar angles of the pentagon — the analysis of these revealed no significant difference ($p < 0.05$). Given that, children going through the transitional occlusion period with optimal functional bite had the pentagon sum total value within an average of 540° .

CONCLUSIONS

1. The data obtained through clinical, radiological, and morphometric studies helped identify the

forecast the location of the incisor (central) point of the dental arch with shape anomalies, especially in the anterior part.

5. The angular parameters of the diagnostic dental pentagon might allow simulating the geo-metric and graphical construction of arches through the transitional occlusion period.

REFERENCES

1. ASH M.M. Wheeler's dental anatomy, physiology and occlusion. Philadelphia: WB Saunders; 2003.
2. AVANISYAN V., AL-HARAZI G. Morphology of facial skeleton in children with undifferentiated connective tissue dysplasia. Archiv EuroMedica. 2020. Vol. 10; 3: 130–141. <https://dx.doi.org/10.35630/2199-885X/2020/10/3.32>
3. BRAND R.W., ISSELHARD D.E. Anatomy of Oral structures. 7th ed. Mosby co. St. Louis; 2003.
4. DAVYDOV B.N., KONDRATYEVA T.A., HARUTYUNYAN YU.S. Cephalometric features of connective tissue dysplasia manifestation in children and adolescents. Pediatric dentistry and dental profilaxis. 2020;20(3):174–183. (In Russ.) <https://doi.org/10.33925/1683-3031-2020-20-3-174-183>

5. **DAVYDOV, B.N.** Improving diagnostics of periodontal diseases in children with connective tissue dysplasia based on X-ray morphometric and densitometric data. *Parodontologiya*. 2020; 25(4): 266–275. (in Russ.) <https://doi.org/10.33925/1683-3759-2020-25-4-266-275>.
6. **DAVYDOV B.N.** Morphological peculiarities of facial skelet structure and clinical and diagnostic approaches to the treatment of dental anomalies in children in the period of early change. *Pediatric dentistry and prophylaxis*. 2019; Vol. 19; 1 (69): 26–38. (In Russ.) DOI: 10.33925/1683-3031-2019-19-69-26-38.
7. **DEAN, J. A.** McDonald and Avery's dentistry for the child and adolescent, tenth edition [Text] / J.A. Dean // 2015. – ISBN: 978-0-323-28745-6 – 700 s.
8. **DMITRIENKO S.V.** Analytical approach within cephalometric studies assessment in people with various somatotypes. *Archiv EuroMedica*. 2019. Vol. 9; 3: 103–111. <https://doi.org/10.35630/2199-885X/2019/9/3.29>
9. **DMITRIENKO S.V., PORFIRIADIS M.P., DOMENYUK D.A.** Dentoalveolar specifics in children with cleft palate during primary occlusion period. *Archiv EuroMedica*. 2018. Vol. 8; 1: 33–34. <https://doi.org/10.35630/2199-885X/2018/8/1/33>
10. **DMITRIENKO T.D.** Connection between clinical and radiological torque of medial incisor at physiological occlusion. *Archiv EuroMedica*. 2019. Vol. 9. № 1. P. 29–37. <https://doi.org/10.35630/2199-885X/2019/9/1/29>
11. **GHAMDAN AL.H.** Occlusal plane orientation in patients with dentofacial anomalies based on morphometric cranio-facial measurements. *Archiv EuroMedica*. 2021. Vol. 11; 1: 116–121. <https://doi.org/10.35630/2199-885X/2021/11/1.26>
12. **DOMENYUK D.A., DAVYDOV B.N., DMITRIENKO S.V.** Changes of the morphological state of tissue of the paradontal complex in the dynamics of orthodontic transfer of teeth (experimental study). *Periodontology*. 2018; Vol. 23; 1–23(86): 69–78. DOI:10.25636/PMP.1.2018.1.15
13. **DOMENYUK D.A.** Contemporary methodological approaches to diagnosing bone tissue disturbances in children with type 1 diabetes. *Archiv EuroMedica*. 2018; 8(2): 71–81. <https://doi.org/10.35630/2199-885X/2018/8/2/71>
14. **DOMENYUK D.A., VEDESHINA E G., DMITRIENKO S.V.** Correlation of dental arch major linear parameters and odontometric indices given physiological occlusion of permanent teeth in various face types. *Archiv EuroMedica*. 2016. Vol. 6; 2: 18–22.
15. **DOMENYUK D.A.** Efficiency evaluation for integrated approach to choice of orthodontic and prosthetic treatments in patients with reduced gnathic region. *Archiv EuroMedica*. 2015. Vol. 5. № 2. P. 6–12.
16. **DOMENYUK D.A., LEPILIN A.V., FOMIN I.V.** Improving odontometric diagnostics at jaw stone model examination. *Archiv EuroMedica*. 2018. Vol. 8; 1: 34–35. <https://doi.org/10.35630/2199-885X/2018/8/1/34>
17. **DOMENYUK D.A.** Major telerehthengogram indicators in people with various growth types of facial area. *Archiv EuroMedica*. 2018. Vol. 8; 1: 19–24. <https://doi.org/10.35630/2199-885X/2018/8/1/19>
18. **DOMENYUK D.A., VEDESHINA E G., DMITRIENKO S.V.** Mistakes in Pont (Linder-Hart) method used for diagnosing abnormal dental arches in transversal plane. *Archiv EuroMedica*. 2016. Vol. 6; 2: 23–26.
19. **DOMENYUK D.A., ZELENSKY V.A., DMITRIENKO S.V.** Peculiarities of phosphorine calcium exchange in the pathogenesis of dental caries in children with diabetes of the first type. *Entomology and Applied Science Letters*. 2018. Vol. 5. № 4. P. 49–64.
20. **DOMENYUK D.** Structural arrangement of the temporomandibular joint in view of the constitutional anatomy. *Archiv EuroMedica*. 2020. Vol. 10. № 1. P. 126–136. <https://doi.org/10.35630/2199-885X/2020/10/37>
21. **FISCHEV S.B., PUZDYRYOVA M.N.** Morphological features of dentofacial area in peoples with dental arch issues combined with occlusion anomalies. *Archiv EuroMedica*. 2019. Vol. 9; 1: 162–163. <https://doi.org/10.35630/2199-885X/2019/9/1/162>
22. **FULLER J.L., DENEHY G.E., SCHULEIN T.M.** Concise Dental Anatomy and Morphology. 4th ed. USA: Univ of Iowa Office of State; 2001.
23. **HARUTYUNYAN YU.** Undifferentiated connective tissue dysplasia as a key factor in pathogenesis of maxillofacial disorders in children and adolescents. *Archiv EuroMedica*. 2020. Vol. 10; 2: 83–94. <https://dx.doi.org/10.35630/2199-885X/2020/10/2.24>
24. **IVANYUTA O.P., AL-HARASI G.** Modification of the dental arch shape using graphic reproduction method and its clinical effectiveness in patients with occlusion anomalies // *Archiv EuroMedica*. 2020. Vol. 10; 4: 181–190. <https://dx.doi.org/10.35630/2199-885X/2020/10/4.42>
25. **KOCHKONYAN T.S., AL-HARAZI G.** Specific features of variant anatomy and morphometric characteristics of the palatal vault in adults with different gnathic and dental types of arches. *Archiv EuroMedica*. 2021. Vol. 11; 3: 54–60. <https://dx.doi.org/10.35630/2199-885X/2021/11/3/14>
26. **KOCHKONYAN T.S., AL-HARAZI G.** Morphometric patterns of maxillary apical base variability in people with various dental arches at physiological. *Archiv EuroMedica*. 2021. Vol. 11; 4: 123–129. <https://dx.doi.org/10.35630/2199-885X/2021/11/4.29>
27. **KONDRATYEVA T.** Methodological approaches to dental arch morphology studying. *Archiv EuroMedica*. 2020. Vol. 10; 2: 95–100. <https://dx.doi.org/10.35630/2199-885X/2020/10/2.25>
28. **KOROBKEEV A. A.** Anatomical and topographical features of temporomandibular joints in various types of mandibular arches. *Medical News of North*

- Caucasus. 2019;14(2):363–367. DOI – <http://dx.doi.org/10.14300/mnnc.2019.14089> (In Russ.).
29. **KOROBKEEV A. A.** Variability of odontometric indices in the aspect of sexual dimorphism. *Medical News of North Caucasus*. 2019;14(1.1):103–107. DOI – <https://doi.org/10.14300/mnnc.2019.14062> (In Russ.).
 30. **KOROBKEEV A. A.** Anatomical features of the interdependence of the basic parameters of the dental arches of the upper and lower jaws of man. *Medical news of North Caucasus*. 2018. – Vol. 13. – № 1-1. – P. 66-69. (In Russ., English abstract). DOI – <https://doi.org/10.14300/mnnc.2018.13019>
 31. **LEPILIN A.V.** A biometric approach to diagnosis and management of morphological changes in the dental structure. *Archiv EuroMedica*. 2020. Vol. 10; 3: 118-126. <https://dx.doi.org/10.35630/2199-885X/2020/10/3.30>
 32. **LEPILIN A.V.** Dependence of stress strain of dental hard tissues and periodontal on horizontal deformation degree. *Archiv EuroMedica*. 2019. Vol. 9; 1: 173-174. <https://doi.org/10.35630/2199-885X/2019/9/1/173>
 33. **MAZHAROV V. N.** Peculiarities of the orientation of the occlusion plane in people with different types of the gnathic part of the face. *Medical News of North Caucasus*. 2021;16(1):42-46. DOI – <https://doi.org/10.14300/mnnc.2021.16011> (In Russ.)
 34. **McNAMARA J.A.** *Orthodontic and Dentofacial Orthopedics*. Needfarm Press. Inc., 1998. 555 p.
 35. **NANDA R.** *Esthetics and biomechanics in orthodontics* [Text] / R. Nanda. – Oxford University Press in the UK: CRC Press. – 2015 – 612 p. – ISBN: 978-1-4557-5085-6
 36. **NELSON S.J.** *Wheeler's dental anatomy, physiology, and occlusion* [Text] / S.J. Nelson. – London: Second Edition. – 2015 – 350 s. – ISBN: 978-0-323-26323-8
 37. **PHULARI, B.S.** *An atlas on cephalometric landmarks* [Text] / B. S. Phulari. – London: First Edition, 2013. – ISBN: 978-93-5090-324-7 – 213 s.
 38. **PORFIRIADIS M.P.** Mathematic simulation for upper dental arch in primary teeth occlusion. *Archiv EuroMedica*, 2018. Vol. 8. № 1. P. 36–37. <https://doi.org/10.35630/2199-885X/2018/8/1/36>
 39. **PROFFIT W.R., FIELDS H.W.** *Contemporary orthodontics*. – St. Louis: C.V. Mosby, 2000. – 768 p.
 40. **RASHMI G.S.** *Textbook of Dental Anatomy, Physiology and Occlusion*. 1st ed. New Delhi: Jaypee Brothers Medical Publishers Ltd; 2014. DOI: 10.5005/jp/books/11841
 41. **SCOTT J.H., SYMONS N.B.B.** *Introduction to Dental Anatomy*. 9th ed. New York: Buttler & Tanner Ltd; 1982. DOI: 10.1016/0030-4220(65)90026-5
 42. **SHKARIN V.V., DAVYDOV B.N.** Non-removable arch orthodontic appliances for treating children with congenital maxillofacial pathologies – efficiency evolution. *Archiv EuroMedica*. 2018. Vol. 8; 1: 97-98. <https://doi.org/10.35630/2199-885X/2018/8/1/97>
 43. **SHKARIN V.V., IVANOV S.YU.** Morphological specifics of craniofacial complex in people with various types of facial skeleton growth in case of transversal occlusion anomalies. *Archiv EuroMedica*. 2019. Vol. 9; 2: 5–16. <https://doi.org/10.35630/2199-885X/2019/9/2/5>
 44. **SHKARIN V.V., GRININ V.M., KHALFIN R.A.** Specific features of transversal and vertical parameters in lower molars crowns at various dental types of arches. *Archiv EuroMedica*. 2019. Vol. 9; 2: 174–181. <https://doi.org/10.35630/2199-885X/2019/9/2/174>
 45. **SHKARIN V.V., GRININ V.M., KHALFIN R.A.** Specific features of grinder teeth rotation at physiological occlusion of various gnathic dental arches. *Archiv EuroMedica*. 2019. Vol. 9; 2: 168–173. <https://doi.org/10.35630/2199-885X/2019/9/2/168>

<http://dx.doi.org/10.35630/2199-885X/2022/12/2.33>

MATHEMATICAL ANALYSIS BASED STUDY OF DENTAL IMPLANT BIOMECHANICS WITH OCCLUSAL LOAD ON BONE TISSUE

Received 31 January 2022;
Received in revised form 13 March 2022;
Accepted 14 March 2022

Vladimir Tlustenko[✉] , Elena Golovina ,
Valentina Tlustenko , Sergey Komlev ,
Vladimir Koshelev 

¹ Samara State Medical University, Samara, Russia

✉ vlastt@yandex.ru

ABSTRACT — The article contains theoretical studies aimed at identifying the load and detecting the factors that have a negative impact on implants. One of the reasons behind implant disintegration is bone tissue resorption, which is due to overload. Direct measurements of the oral cavity stresses affecting the tissues around the implants are basically impossible. The purpose here is to choose the optimal inclination of the implant in relation to the vertical axis in view of mismatch of the mandibular and maxillary alveolar arches. The study here employed the finite element method (FEM) relying on the universal FEM ANSYS package. Three patterns have been identified. First, the dependence of the destructive force on the bone tissue on the implant inclination angle (up to 5° — it is twice as low compared to the initial value, and above 20° — it becomes destructive). Second, the implant deviation in the transversal plane results in a greater decrease in strength, compared to its deviation in the sagittal plane. Third, the greatest destruction resulting from the stress-strain bone tissue status is observed in the cortical, and not in the spongy bone. The study allows proper selection of implants, their installation options, as well as scientifically reliable forecast of the respective long-term outcomes.

KEYWORDS — mathematical analysis, implantation, biomechanics of implant.

INTRODUCTION

Despite the current progress in the modern dentistry, the number of patients with complete adentia has not revealed any decrease [1, 6–8]. A number of patients who use full removable dentures complain of poor fixation. This makes them apply for dental implantation in order to replace removable orthopedic dentures with non-removable ones. In case of significant atrophy of the alveolar processes in the upper and lower jaws, the inter-jaw ratios change. Given a mismatch, when the lower jaw alveolar arch is narrower than that of the upper jaw, the need arises to have implants installed on the lower jaw with a certain decline. Here, certain mechanical deformations occur both in

the surrounding tissues and in the implant itself.

In case of a reasonable rational functional load, the endossal implant will stimulate osteogenesis after its introduction into the jaw bone through surgery. An increased occlusal load, which is not balanced in its strength, also being improper in its direction, will result in destroyed bone tissue at the respective area, as well as in the implant rejection. Given that, we are still facing the issue of objective evaluation of the bone tissue status at the periimplant zone thus aiming to prevent and treat pathologies affecting it.

The conducted studies allow, in each case, explaining and setting match as per each prosthetics scheme based on implants, with designing a proper mathematical model, including for situations of various prosthetic levels: in cases where several teeth are missing in a row with several free-standing implants to be installed, to cases of complete adentia where prosthetic bridges are to be installed relying on implants.

A high occlusive load is known to be one of the main reasons behind the implant disintegration. Rehabilitation to be offered to such patients appears a relevant issue that would enjoy a lot of demand. This scientific problem can be solved involving theoretical research in the field of mechanics of deformable bodies and structures. Given the advanced orthopedic treatment technologies relying on implants, it will take new mathematical approaches to make respective calculations, ensure the implant stability, as well as the strength of dentures.

Aim:

to study dental implant of biomechanics in the lower jaw involving bone tissue, in view of occlusal load, involving mathematical analysis.

MATERIALS AND METHODS

The study was carried out employing the finite element method (FEM), which is currently the main calculation tool when it comes to studying the strength of various structures [2–5]. During that, the universal FEM ANSYS package was used.

The study involved the method of calculating bone tissue stresses under various loads on the implant, with a mathematical model for calculating the stress-strain status of the mandibular bone tissue

designed, which was done subject to the generally accepted method. To identify the maximum loads that the implant works on the bone tissue, a volumetric model of the lower jaw was taken. The initial data were accepted as follows: the implant (titanium) — diameter $D = 3$ mm; elasticity modulus $E = 1.1 \cdot 10^5$ MPa; Poisson ratio $\mu = 0.3$. Cortical bone tissue: $E = 1.35 \cdot 10^4$ MPa; $\mu = 0.3$; tensile strength $q_{\text{cort}} = 40$ MPa. Spongy bone: $E = 1.35 \cdot 10^3$ MPa; $\mu = 0.3$; $q_{\text{lip}} = 20$ MPa. In order to idealize the implant-bone system, isoparametric volumetric elements of a second-order tetrahedral shape with ten nodes (SOLID92) were used. The analysis of the stress-strain status, which corresponds to the specified scheme of the implant loading, allowed identifying 6 main internal decisive force factors: stress along the implant (vertical load); stress in the sagittal plane (horizontal load); stress in the transversal plane (horizontal load); stress from the bending moment in the sagittal plane, respectively; stress from the bending moment in the transversal plane, respectively; stress from the torque.

RESULTS AND DISCUSSION

Nowadays, various prosthetics techniques involving the installation of dentures on implants are associated with bone resorption in the upper and lower jaw structures. A specific feature of resorption is the individual nature of load perception revealed by each patient, while it all depends on the type of the prosthetic biomechanical structures on implants.

Research focused on the stress-strain status shows that the destructive force is defined here as the lowest load at which equivalent stresses affecting the bone tissue reach the strength limit. The conducted studies allow, in each case, explaining and setting match as per each prosthetics scheme based on implants, with designing a proper mathematical model, including for situations of various prosthetic levels: in cases where several teeth are missing in a row with several free-standing implants to be installed, to cases of complete adentia where prosthetic bridges are to be installed relying on implants.

The mathematical analysis revealed that in case the implant deviation angle is 0° , there is only compression stress that occurs in the bone. It has no negative effect on the peri-implant area tissues. When the implant deviates from the vertical axis, there is an additional bending moment that occurs at the spot where the implant is planted in the bone, i.e., the cervical area. The amount of additional stresses affecting the bone features a linear increase along with an increase in the implant inclination angle. The calculations allowed identifying the following pattern: in case there was no implant deviation from the vertical, the implant could

resist a vertical load of 200 N, while at an implant inclination angle of 5° , it would go down to 100 N (half the initial value); when the angle is 10° only 72.5 N could be resisted, i.e., the destructive vertical forces went on increasing. In case of an inclination ranging within 10° – 20° , the bone strength limit decreases proportionately to the increase in the implant inclination angle.

Beyond 20° , the tensile strength drops sharply, the implant being able to cope with a load of no more than 40 N. the degree of biomechanical risk, therefore, increases dramatically once the implant is tilted more than 10° , whereas after 20° it becomes destructive. The results of the calculations revealed another pattern. Comparing the implant inclination degree in the sagittal and transversal planes, reliable data were obtained showing that the implant deviation in the transversal plane will lead to a slightly greater decrease in strength than the deviation in the sagittal plane. (Fig.1, 2)

Moreover, the use of prostheses can lead, over time, to changes affecting the soft and bone tissue of the jaw supporting arches, which is due to the effect of loads from implants, also depending on the type of structures installed on them.

When the implant is tilted in the transversal plane, therefore, the degree of biomechanical risk is higher. In these cases, we would recommend plastic surgery of the alveolar process in order to increase it, so that further on the implant inclination degree could be reduced. Besides, there is certain interest in a comparative evaluation of the stress-strain status in the cortical and spongy bone.

We took the initial value of the most commonly seen implant inclination angle as equal to 10° . In case of the vertical force of 72.5 N applied in the transversal plane at the point where the implant contacts the cortical bone tissue, the stress is found to reach a strength limit of 40 MPa. The stresses in the spongy bone, however, are significantly below the destructive ones (20 MPa). A similar pattern was to be observed for the implant deviation in the longitudinal plane by an angle of 10° . The permissible destructive force, though, was slightly above in this case — 81.8 N in the cortical bone, while in the spongy bone it was 2 times as low. This means that there was a third pattern identified: the greatest destruction caused by the bone tissue stress-strain status in case of a deviated implant is to be observed in the cortical, and not in the spongy bone. This is in line with the clinical image of dental peri-implantitis obtained while following the respective dynamics. Bone resorption was found to begin in the cervical area of the installed implant. The overload first results in bone resorption with no inflammatory reaction reported, with a bone pocket developing, and then that is accompanied by the adjacent gum atrophy.

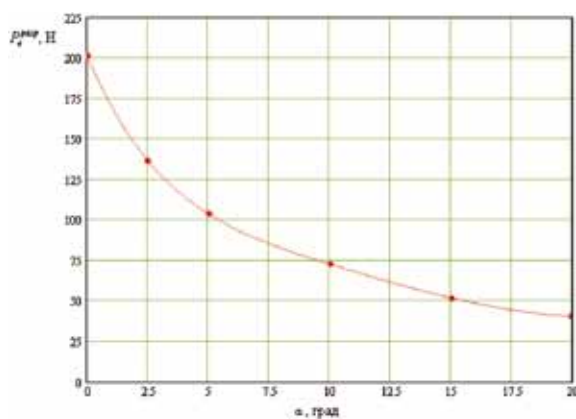


Fig. 1. Dependence of the vertical destructive force on the implant deviation angle in the transverse plane

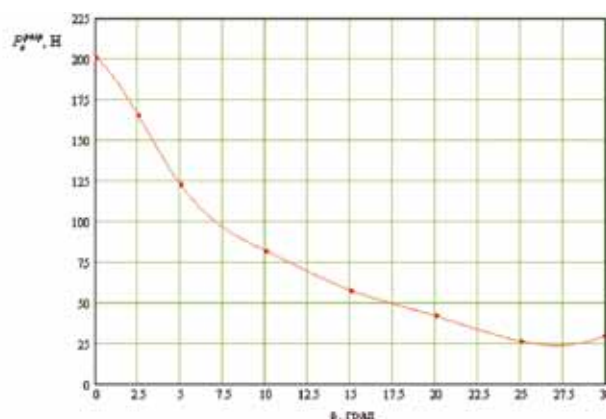


Fig. 2. Dependence of the vertical destructive force on the implant deviation angle in the longitudinal plane

Further on, along with an increase in the load, the bone tissue destruction increases, the entire process progresses, with inflammation joining it.

The developed methodology employed for mathematical modeling and investigation of the bone tissue stress-strain status will allow forecasting the likelihood of bone resorption in the real time mode as well as for future periods, depending on the implant design and on the types of their installation when subjected to average loads.

CONCLUSION

The mathematical analysis method employed for the implant-bone system allowed identifying the dependence of the effect that the implant inclination angle has on the bone tissue stress-strain status. The degree of biomechanical risk increases dramatically once the implant deviates more than 10°, whereas in the event the angle goes above 20°, the effect becomes destructive. Besides, the implant deviation in the transversal plane leads to a greater decrease in strength than sagittal deviation, while the greatest damage in case of a deviated implant is to be seen in the cortical and not in the spongy bone.

The modeling and research methods allow, beyond other, predicting possible injury to soft and bone tissues due to a mathematically designed calculation of both the number of implants to be installed and their size and structure. The proposed methods and theory employed to study the effect that implant load will have on soft and bone tissues based on mathematical modeling will serve the basis for further progress of methodologies of explanation and implantation in two stages, or, in some cases, offering the possibility of one-stage implantation.

This means that a clear understanding of the implant biomechanics would allow improving treatment

scheme for each patient thus aiming to reduce the risk of functional issues as well as the implant failure.

REFERENCES

1. MALO P., DE ARAUJO NOBRE M., LOPES A., MOSS S.M., MOLINA G.J. A longitudinal study of the survival of All-on-4 implants in the mandible with up to 10 Years of follow-up. *Journal of the American Dental Association*, 2011, vol.142, no.3, p.310–320. doi: 10.14219/jada.archive.2011.0170
2. ATIK F., ATAC M.S., ÖZKAN A., KILINC Y., ARSLAN M. Biomechanical analysis of titanium fixation plates and screws in mandibular angle fractures. *Niger J. Clin Pract.* 2016; 19 (3): 386–390. <https://doi.org/10.4103/1119-3077.179292>.
3. OLESOVA V. N., BRONSHTEIN D. A., UZUNJAN N. A., ZASLAVSKY R. S., LERNER A. JA., SHMATOV K. V. Biomechanics of implant retained fixed prosthesis in patient with edentulous upper jaw. *Stomatologiya*. 2018;97(6):53–56. 10.17116/stomat20189706153
4. SAFAROV M.T., TASHPULATOVA K.M., ASEMOVA S., VALIDJANOVA SH. Experience in applying mathematical modeling to predict the long-term effectiveness of prosthetics on dental implants. *Medicine and innovation*. 2021; 2: 95–98.
5. KULAKOV A.A, GVETADZE R.SH., BRAILOVSKAIA T.V., KHARKOVA A.A., DZIKOVITSKAYA L.S. Modern approaches to dental implants placement in deficient alveolar bone. *Stomatologiya*. 2017;96(1):43–45. 10.17116/stomat201796143-45
6. BAIRIKOV I.M., GAIVORONSKAYA T.V., DEDIKOV D. Reconstruction of mandibular defects using individual vascularized autografts combined with macroporous titanium fiber material. *Archiv Euro-Medica*. 2021. Vol. 11. № 1. P. 147–159. <https://doi.org/10.35630/2199-885X/2021/11/1.32>
7. TLUSTENKO V.S., TLUSTENKO V.P., GOLOVINA E.S. Comparative clinical and radiological assessment of acute and chronic peri-implant mucositis. *Archiv*

EuroMedica. 2021. Vol. 11. № 3. P. 71–74. <https://doi.org/10.35630/2199-885X/2021/11/3/17>

8. **GHAMDAN AL.H., SHKARIN V.V., KOCHKONYAN T.S.** A method for modeling artificial dentures in

patients with adentia based on individual sizes of alveolar arches and constitution type. *Archiv EuroMedica*. 2021. Vol. 11. № 1. P. 109–115. <https://doi.org/10.35630/2199-885X/2021/11/1.25>